Biosolids Minimization by Partial Ozonation of Return Activated Sludge: Model Development and Bacterial Population Dynamics

Siavash Isazadeh

Doctor of Philosophy

Department of Civil Engineering and Applied Mechanics

McGill University

Montreal, Quebec, Canada

August, 2014

A thesis submitted to McGill University in partial fulfillment of the requirements of the degree of Doctor of Philosophy

“There are only two ways to live your life. One is as though nothing is a miracle. The other is as though everything is a miracle.”

Albert Einstein

TABLE OF CONTENTS

LIST OF TABLES

LIST OF FIGURES

LIST OF ABBREVIATIONS AND SYMBOLS

The common list of abbreviations and symbols used in this thesis is presented here. The detail list of abbreviations is presented in the supplementary materials of each chapter.

Abbreviations

amoA	Ammonia monooxygenase gene
ANO	Autotrophic nitrifying organisms
AOA	Ammonia oxidizing archaea
AOB	Ammonia oxidizing bacteria
AOO-OUR	Ammonia oxidizing organisms oxygen uptake rate
ASP	Activated sludge process
AS-WWTP	Activated sludge wastewater treatment plant
ATP	Adenosine triphosphate
B	Biochemical parameter
BR	Biosolids reduction
BR-Efficiency	Biosolids reduction efficiency
COD	Chemical oxygen demand
DAPI	4',6-Diamidino-2-Phenylindole
DBPs	Disinfection by-products
Endogenous-OUR	Endogenous oxygen uptake rate
EPS	Exopolymeric substances
F/M	Food/microorganism
FISH	Fluorescence *in situ* hybridization
GAO	Glycogen accumulating organisms
GSA	Global sensitivity analysis
HRT	Hydraulic residence time
ISS	Inorganic suspended solids
IWA-ASM3	International water association - activated sludge model 3
LHS	Latin hypercube sampling
MBR	Membrane bioreactors
MLVSS	Mixed liquor volatile suspended solids
NOB	Nitrite oxidizing bacteria
NOM	Natural organic materials
NOO-OUR	Nitrite oxidizing organisms oxygen uptake rate
nxrB	Gene encoding subunit beta of nitrite oxidoreductase
OHO	Ordinary heterotrophic organisms
Op	Operational parameter
OSA	Oxic-settling anaerobic

Abbreviations	**List of abbreviations –continued**
OTUs	Operational taxonomic units
Oz	Ozone reaction parameter
PAO	Phosphorus accumulating organisms
PCNM	Principal coordinates of neighbour matrixes
PCoA	Principal coordinate analyses
PCR	Polymerase chain reaction
RAEBL	Régie de l'Assainissement des Eaux du Bassin LaPrairie
RAS	Return activated sludge
RDA	Redundancy analysis
SBR	Sequence batch reactor
SF	Safety factor
SF_{ANO}	Safety factor for ammonia nitrifying organism
SNA	Specific nitrification activity
SOUR	Specific Oxygen uptake rate
SRC	Standardized regression coefficient
SRT	Solid retention time
TKN	Total Kjeldahl Nitrogen
TSS	Total suspended solids
UV	Ultraviolet
VSS	Volatile suspended solids

Symbols for COD pools of ASM3

$f_{SB,Inf}$	Soluble biodegradable COD fraction in the influent
S_B	Soluble biodegradable COD
S_U	Soluble undegradable COD
X_{ANO}	Autotrophic nitrifying organism biomass COD
XC_B	Particulate/colloidal biodegradable COD
X_{OHO}	Ordinary heterotrophic organism biomass COD
X_{STO}	Storage compound COD in ordinary heterotrophic
X_U	organisms Particulate undegradable COD from the influent
X_{U_biolys}	Biomass debris

Symbols for model parameters of ASM3 used in the text

$K_{SB,OHO}$	Half saturation constant for soluble biodegradable COD
K_{NH4}	Half saturation constant for soluble ammonium

Symbols for model parameters describing ozone transformation of solids

Stoichiometric solids transformation and inactivation fractions

f_{Bio}	Fraction of biomass in particulate COD excluding storage
$f_{Bio,storage}$	Fraction of biomass in particulate COD including storage
$f_{mnr,O3}$	Fraction of transformed COD that is mineralized (mnr)
$f_{SB\_O3,inact}$	Soluble biodegradable COD fraction of inactivated biomass
$f_{SU\_O3,inact}$	Soluble undegradableCOD fraction of inactivated biomass
$f_{SB\_O3,trans}$	Soluble biodegradable COD fraction of transformed non-

Abbreviations	**List of abbreviations -continued**
	biomass
$f_{SU\_O3,trans}$	Soluble undegradableCOD fraction of transformed non-biomass

Transformation and inactivation rates and constants

$b_{Bio,O3,inact}$	Inactivation rate of biomass due to ozone
$q_{Xtot,O3,sol}$	Overall solids COD solubilization by ozone rate constant
COD_{sol}	Soluble COD increase through the ozone contactor
$q_{MLVSS\ treated}$	fraction of biosolids inventory exposed to ozone per day normalized to the aerated solids COD inventory
$q_{XU\_XCB,O3,trans}$	Non-biomass solids transformation rate due to ozone
$\eta_{Bio,O3,inact}$	first-order inactivation coefficient with respect to COD_{sol}

ABSTRACT

Although ozonation of return activated sludge (RAS) has been used for some time at full-scale biological wastewater treatment plants and a substantive body of literature exists with respect to biosolids minimization, little work has been done on the modeling of the process to predict biosolids reduction. Furthermore, the impact of RAS-ozonation on the microbial community composition in biological treatment systems has rarely been studied. Therefore, the first goal of this study was to develop a new model to predict biosolids reduction based on the International Water Association Activated Sludge Model 3 (IWA-ASM3). The second goal of this study was to investigate the bacterial community structure subjected to RAS-ozonation. To achieve these goals, two pilot-scale wastewater treatment reactors were operated over a three- year period: one control reactor and one RAS-ozonated reactor. The operational results were used to validate the model, and the population structures of ordinary heterotrophic organisms (OHO) and nitrifiers were determined by high-throughput pyrosequencing of 16S rRNA genes and two functional genes (*amoA* and *nxrB*) targeting autotrophic nitrifying organisms (ANO). Finally, additional laboratory-scale experiments were conducted to complement the pilot-scale study.

The proposed mathematical model of RAS-ozonation assumed that two groups of reactions occurred: (i) the *transformation/mineralization* of non-biomass solids (which includes direct oxidation of the solids chemical oxygen demand (COD) by ozone) and (ii) the *inactivation* of biomass. Laboratory-scale experiments were conducted to parameterize the biomass inactivation process during exposure to ozone. The experiments revealed that biomass inactivation occurred even at the lowest doses of ozone, but that it was not associated with extensive COD solubilization. Furthermore, the ozone inactivation rates of ANO were similar to those observed for OHO. Once the biomass inactivation was parameterized, the model accuracy was evaluated

by comparing the simulation predictions with observed data from the pilot-scale reactors. The model was calibrated against the data of Year 1 of the study, in which the reactors were only operated as conventional activated sludge systems and the ozone dosages were increased. Once calibrated, the model satisfactorily simulated the operational data from all three years of the study. The simulated data included: biosolids inventories, effluent soluble COD, and specific nitrification activities. This modeling success strongly supported the validity and the widespread uses of the model because, in Years 2 and 3, solids retention times (SRT) were varied and the system configurations were altered to test anoxic/oxic systems performing denitrification/nitrification.

After model validation, a global sensitivity analysis was performed to identify influential and non-influential parameters for biosolids reduction efficiency, change in specific nitrification activity, and alteration to expected nitrification stability. In general, the model outputs were sensitive to operational and ozone reaction parameters, but not to biochemical parameters. For operational parameters, mainly temperature and initial SRT influenced all model outputs. For biosolids reduction, an increase in the degradability of the influent COD decreased the reduction efficiency. For the specific nitrification activity, the changes were highly dependent on the influent total Kjeldahl nitrogen (TKN)/COD ratio. Our findings also imply that the stability of the nitrification process in ozonated systems should be enhanced at constant mixed liquor volatile suspended solids (MLVSS) for warm temperatures, but could be reduced at temperatures below 12 °C and aerated SRTs below 10 days.

With respect to the composition of the bacterial community, the results suggest that RAS-ozonation does not really influence the structure of the community. Instead, the parallel drifts and slight convergence of the two community structures (in the control and in the RAS-ozonated

reactors) during the first and third years indicate that other environmental factors such as influent wastewater composition, temperature, and reactor operation (configuration and SRT) may be more important environmental factors. This study also provides new insights on the importance of environmental variables on community structures of activated sludge systems.

To put the data obtained with the pilot-scale study in a more general context, the heterotrophic community assemblies at eight full-scale activated sludge wastewater treatment plants (AS-WWTPs) were also determined by high-throughput pyrosequencing of 16S rRNA genes. Observed differences in community compositions and structures were partitioned with respect to a range of key environmental variables, namely reactor size (pilot- vs. full-scale reactors), chemical stress induced by a higher mortality upon exposure to ozone (RAS-ozonated vs. non-ozonated control reactors), seasonal temperature variation (winter vs. summer), inter-annual variation, geographical locations, treatment process types (conventional, oxidation ditch, and sequence batch reactor (SBR)) and influent characteristics. The results suggest that, among the range of environmental variables assessed, influent composition and geographic location contributed approximately 26% of the observed differences in the activated sludge bacterial community structures. The remaining variation (74%) could not be explained by any of the factors that were considerd

RÉSUMÉ

Bien que l'ozonation des boues activées de retour (acronyme anglais : RAS) ait été utilisée pendant un certain temps par des usines de traitement biologique des eaux usées à pleine échelle et qu'une quantité substantielle de littérature existe sur la minimisation des biosolides, peu de travail a été réalisé sur la modélisation du procédé afin de prédire la performance de réduction des biosolides. De plus, l'impact de l'ozonation des RAS sur la composition de la communauté microbienne dans les systèmes de traitement biologique n'a été que rarement étudié. Par conséquent, le premier objectif de la présente étude était de développer un nouveau modèle pour prédire la réduction des biosolides en se basant sur le Modèle de boue activée #3 de l'International Water Association (acronyme anglais: IWA-ASM3). Le deuxième objectif de cette étude était d'investiguer la structure de la communauté bactérienne soumise à l'ozonation des RAS. Afin d'atteindre ces objectifs, deux réacteurs d'épuration des eaux usées à l'échelle pilote ont été opérés sur une période de trois années: un réacteur témoin et un réacteur avec RAS ozonées. Le structures des populations d'organismes hétérotrophes ordinaires (OHO) et organisme autotrophes nitrifiants (OAN) ont été déterminées par le séquençage metagénomique des gènes d'ARNr 16S et deux gènes fonctionnels (*amoA* et *nxrB*) ciblant deux populations de OAN. De plus, d'autres expériences à l'échelle de laboratoire ont été menées pour complémenter l'étude à l'échelle pilote.

Le modèle mathématique proposé de l'ozonation des RAS a supposé que deux groupes de réactions se produisent: (i) la transformation/minéralisation des matières solides autres que la biomasse (ce qui comprend l'oxydation directe de la demande chimique en oxygène (DCO) des matières solides par l'ozone) et (ii) l'inactivation de la biomasse. Des expériences en laboratoire ont été menées pour paramétrer le processus d'inactivation de la biomasse lors de l'exposition à

l'ozone. Les expériences ont démontré que l'inactivation de la biomasse avait lieu même aux doses les plus faibles, mais qu'elle n'était pas associée à une solubilisation importante de la DCO. De plus, les taux d'inactivation des OAN par l'ozone étaient similaires à ceux observés pour les OHO. Une fois l'inactivation de la biomasse paramétrée, la précision du modèle a été évaluée en comparant les prédictions de simulation avec les données observées des réacteurs à l'échelle pilote. Le modèle a été calibré par rapport aux données de la première année de l'étude, pendant laquelle les réacteurs n'ont été opérés que par les systèmes conventionnels de boues activées et les doses d'ozone ont été augmentées périodiquement. Une fois calibré, le modèle a simulé de manière satisfaisante les données d'opération des trois ans de l'étude. Les données simulées incluaient: les inventaires des biosolides, la DCO soluble des effluents, et les activités spécifiques de la nitrification. Ce succès de la modélisation soutient fortement la validité et l'utilisation généralisée du modèle parce que dans les deuxième et troisième années, les temps de rétention des boues ont été variés et les configurations du système ont été modifiées pour tester les systèmes anoxiques/oxiques performant la dénitrification/nitrification.

Après la validation du modèle, une analyse de sensibilité globale a été effectuée pour identifier les paramètres influents et non influents en matière d'efficacité de réduction des biosolides, le changement de l'activité spécifique de la nitrification, et l'altération de la stabilité de la nitrification. En général, les résultats du modèle étaient sensibles aux paramètres opérationnels et de réaction à l'ozone, mais pas à des paramètres biochimiques. Pour les paramètres opérationnels, c'est principalement la température et le temps de rétention des boues initial qui ont influencé tous les résultats du modèle. Pour la réduction des biosolides, l'augmentation de la dégradabilité de la DCO de l'affluent diminuait l'efficacité de la réduction. Pour l'activité spécifique de la nitrification, les changements ont été trouvé très dépendants du rapport azote

total Kjeldahl (NTK)/DCO de l'affluent. Nos résultats impliquent aussi que, si les concentrations de matières volatile en suspension (MVES) de la liqueur mixte étaient gardées constantes, la stabilité du processus de nitrification dans les systèmes ozonés devrait être améliorée à des températures chaudes, mais pourrait être réduite à des températures inférieures à 12 °C et des temps de rétention des boues aéré de moins de 10 jours.

En ce qui concerne la composition de la population bactérienne, les résultats suggèrent que l'ozonation des RAS n'influence pas réellement sa structure. Au lieu de cela, les dérives parallèles et une légère convergence des deux structures communautaires (dans le contrôle et dans le réacteur RAS ozonés) au cours des première et troisième années d'opération indiquent que d'autres facteurs environnementaux tels que la composition de l'affluent des eaux usées, la température et le fonctionnement du réacteur (configuration et temps de rétention des boues) peuvent être des facteurs environnementaux plus importants. Cette étude fournit également de nouvelles perspectives sur l'importance de variables environnementales sur les structures des communautaires microbiennes des systèmes de traitement par boues activées.

Pour mettre les données obtenues de l'étude à l'échelle pilote dans un contexte plus général, les assemblages des communautés hétérotrophes de huit usines de traitement des eaux usées par boues activées à pleine échelle a également été déterminé par le pyroséquençage metagénomique des gènes d'ARNr 16S. Les différences observées dans les compositions et les structures des communautés ont été répartis par rapport à une gamme de variables environnementales, à savoir la taille du réacteur (réacteurs à l'échelle pilote contre réacteurs à grande échelle), le stress chimique induit par une mortalité plus élevée lors de l'exposition à l'ozone (RAS-ozonée contre réacteur contrôle non-ozoné), la variation saisonnière de la température (hiver contre été), la variation inter annuelle, les lieux géographiques, les types de procédés de traitement

(conventionnel contre déphosphatation biologique) et les caractéristiques de l'affluent. Les résultats suggèrent que, parmi la gamme de variables environnementales évalués, la composition de l'affluent et la situation géographique ont contribué à environ 26% des différences observées dans les structures des communautés bactériennes des boues activées. Le reste de la variation observée (74%) ne pouvait s'expliquer par aucun des facteurs hypothétiques.

ACKNOWLEDGEMENTS

It has been a great privilege to be able to study for a PhD, and I am grateful to all those who have made it possible.

I would like to thank my supervisor, Prof. Dominic Frigon, for giving me the support and freedom to develop and explore my own ideas, always meeting these with enthusiasm and the necessary intellectual guidance. I would also like to thank Air Liquide Canada and the Régie de l'Assainissement des Eaux du Bassin LaPrairie (RAEBL), for funding this work. I would like to thank in particular Michel Épiney of Air Liquide Canada as well as Gilbert Samson and all the staff at RAEBL wastewater treatment plant who have enthusiastically accommodated the pilot scale reactor for far longer than expected.

I would like to thank all colleagues, staff and former members of the group, particularly: John Bartczak, Mauhamad Shamee Jauffur, Luis Enrique Urbina Rivas, Min Feng, Francesca Asfar, Wei Yi Kho, Peter Farrell, Yuan Ma, and Ji Zhuo Yang for their assistance during this study. I would also like to thank Dr. Pinar Ozcer in particular for her assistance during the second and third years of pilot operation.

As well as intellectual and financial support, I have also received much needed emotional and moral support during the course of this PhD. This has come from many of those listed above, but also from my family who have not only made my completing a PhD possible, but are also the reason why it has been worthwhile. I would like to thank my father, Mr. Shahbaz Isazadeh, for telling me what I am capable of and for inspiring me to pursue my dream and for believing that I have the talent to reach my goals. I also thank my mother, Mrs. Monyereh Hamedi, for her personality, for sharing her love of life, sense of humor, excitement for every experience, ability

to befriend a stranger, and courage to look fear directly in the face until it backs down. I would like to thank my lovely wife, Nayereh, for her incredible kindness, understanding and encouragement throughout these years. I would also like to thank my lovely brothers and sisters, Mina, Ali, Hamid, and Fatemeh, for their prolonged understanding, and non-stop support and encouragement during my life. Last but not least, I would like to thank my wonderful and kind uncle Mr. Mehdi Hamedi for his inspiration, emotional support and being available when I needed him the most.

PREFACE

In accordance with the "Guidelines for Thesis Preparation", this thesis is presented in a manuscript-based format. General introduction and literature review chapters precede the results section, which includes chapters 3-7. The final chapter presents a summary and the overall conclusions. Chapters 3-7 are manuscripts that are already published, submitted, or in preparation for submission to peer-reviewed journals. For all these manuscripts, the author of the current thesis is the primary author of the manuscripts. Below is a detailed description of each author's contributions to the manuscripts (the author of the thesis is underlined):

Isazadeh, S., Feng, M., Urbina Rivas, L.E., Frigon, D., 2014. New mechanistically based model for predicting reduction of biosolids waste by ozonation of return activated sludge. ***Journal of Hazardous Materials***, 270, 160-168.

Author's contributions:

S. Isazadeh: operated the pilot-scale reactors, performed a large number of the chemical tests, compiled and analysis the results, help supervised the execution and interpretation of the laboratory-scale solids-ozonation experiments, performed the overall model calibration and analysis, and was the primary author of the manuscript.

M. Feng: performed the complementary laboratory-scale solids-ozonation experiments, compiled the data for these experiments, and wrote the first version of the material and methods associated to these experiments.

L.E. Urbina Rivas: reviewed the model formulation, contributed to programming the numerical

solver of the model, and performed the first of several calibrations of the model.

D. Frigon: obtained the funding for the work, oversaw the operation of the pilot-scale reactors, supervised the research in general, and revised the manuscript.

Isazadeh, S., Urbina. L, Ozcer, P., and Frigon, D. Reduction of waste biosolids by RAS-ozonation: model validation and sensitivity analysis for biosolids reduction and nitrification. ***Environmental Modelling & Software*** *under revision*

Author's contributions:

S. Isazadeh: operated the pilot-scale reactors, performed a large number of the chemical tests, compiled and analysis the results, performed the scenario analysis for nitrification, performed the global sensitivity analyses for nitrification, help supervised the execution of the global sensitivity analysis for biosolids reduction, and was the primary author of the manuscript.

L. Urbina: contributed to programming the numerical solver of the model, and performed the biosolids global sensitivity analysis

P. Ozcer: operated the pilot-scale reactors and performed a number of chemical tests, and revised the manuscript

D. Frigon: obtained the funding for the work, oversaw the operation of the pilot-scale reactors, supervised the research in general, and revised the manuscript.

Isazadeh, S., Ozcer, P. and Frigon. D. "Microbial community structure of wastewater treatment subjected to high mortality rate due to ozonation of return activated sludge". ***Journal of Applied Microbiology*** 2014, 117 (2), 586-596.

Author's contributions:

S. Isazadeh: operated the pilot-scale reactors, performed the molecular assays and analysed the data, and was the primary author of the manuscript.

P. Ozcer: assisted with the molecular assays, and reviewed the manuscript.

D. Frigon: obtained the funding for the work, supervised the research in general, and revised the manuscript.

Isazadeh, S., Jauffur, M.S. and Frigon, D. "Bacterial community assembly in activated sludge: mapping beta diversity across ecological variables". ***ISME Journal****, to be submitted.*

Author's contributions:

S. Isazadeh: operated the pilot-scale reactors, performed the molecular assays, conducted the statistical analysis of the data, and was the primary author of the manuscript.

M.S. Jauffur: obtained some of the biomass samples of the full-scale WWTPs and performed the molecular assays on them, and reviewed the manuscript.

D. Frigon: obtained the funding for the work, supervised the sampling of WWTPs over several years, supervised the research in general, and revised the manuscript.

Isazadeh, S., Ozcer, P. and Frigon, D. "A comprehensive look to process modelling and bacterial population structure of nitrification under ozonation of return activated sludge". ***Journal of Bioresource Technology****, to be submitted.*

Author's contributions:

S. Isazadeh: operated the pilot-scale reactors, performed the molecular assays, conducted the statistical analysis of the data, and was the primary author of the manuscript.

P. Ozcer: operated the pilot-scale reactors and performed a number of chemical tests

D. Frigon: obtained the funding for the work, supervised the sampling of WWTPs over several years, supervised the research in general, and revised the manuscript.

CHAPTER 1:

Introduction

1.1. INTRODUCTION

Biosolids management cost is the major operational cost of activated sludge wastewater treatment plants (AS-WWTP) all over the world. Handling and disposal of excess biosolids is one of the bottlenecks in the wastewater treatment process, and it has important repercussions on the management of the facilities due to environmental, economic, social and legal factors (Pérez-Elvira et al. 2006). From an environmental perspective, there is a need to reduce landfill disposal of biosolids to safeguard ecosystems and reduce greenhouse gas emissions. The Government of Québec addressed this need in 2010 by a sharp increase in landfill disposal fees in the form of a green tax, fees that continue to increase and rose from $10.95 in 2010 to $19.50 per ton of dry solids in 2012 (CCME 2010). This increase translates into a large financial burden for municipalities. For instance, at the Régie de l'Assainissement des Eaux du Bassin LaPrairie (RAEBL, one of our main collaborators in the current project), the combination of new taxes and increased landfilling prices doubled the cost of biosolids disposal from $1 to $2 million in ten years. This has left biosolids management as the largest operational budget item in this plant (Gilbert Samson, RAEBL, pers. comm). As a result of the increased burden on municipal tax payers, wastewater treatment facilities are looking to evaluate a series of options including physical, chemical, and biological processes to minimize biosolids production (Chu et al. 2009).

Chemical oxidation of biosolids by ozone has received attention as it can not only deliver biosolids reduction up to 100% in ideal conditions, but also can be used to oxidize other emerging contaminants such as pharmaceutical products and other micro pollutants present in municipal wastewater. Ozone can also be used for effluent disinfection. As such, ozonation could

be a process of choice to generate synergistic applications and simultaneously solve several concerns of plant operators . Although partial ozonation of activated sludge has been practiced successfully at full-scale WWTPs in Europe and Asia (Böhler and Siegrist 2004, Egemen 2001, Fabiyi , Kamiya 1998, Sakai 1997, Yasui and Shibata 1994), there is no full-scale installation of this technology in North America. One reason for this is the lower cost of biosolids disposal in North America than elsewhere in the world, but the recent increases of landfilling costs in Québec and other parts of Canada is making the process economically feasible for these regions. Another reason for the lack of full-scale installations in North America is that the economic performance predictions for the process remain imprecise without expensive pilot-scale studies, which reduces the interest of potential adopters of the technology.

Precise prediction of biosolids reduction by ozone without using pilot-scale studies requires a strong modelling approach. A good model would ideally need to consider both biological treatment processes and biosolids reactions with ozone. From the wastewater practitioner's perspective, an effective model should be simple, rely on only a few modelling parameters to calibrate, and be applicable for most of WWTPs with a variety of treatment processes. All of these goals should be met without increasing the uncertainty of the modeling predictions. In addition to providing reliable predictions, an ideal mathematical model of the biosolids minimization process by partial RAS-ozonation should provide guidance in the development and the optimization of the technology by answering the following questions as examples: How much biosolids reduction is possible in a certain treatment plant? How much do operational parameters such as SRT or influent characteristics influence the biosolids reduction? Will the technology affect the treatment performance with respect to other treatment goals such as biological nitrification? The last question is especially relevant because a portion of the biomass

in the treatment process is either killed or damaged during ozonation (Chu et al. 2009), which could compromise the efficiency of more fragile processes like nitrification in more extreme environments such as the colder Canadian climate.

Studies in the literature emphasize that the nitrification in wastewater treatment plants (WWTPs) can be easily affected by environmental conditions such as temperature, substrate concentrations (O_2, NH_3, and NO_2^-), and organic matter concentrations (Berent and Sperinado, 2009). It is known that the stability of nitrification can be altered by the presence of toxic chemicals or sudden arrival of high organic loads. In contrast to ordinary heterotrophic organisms, in general, autotrophic nitrifying organisms (ANO) are more fragile and vulnerable to environmental stresses and have much lower maximum growth rates. The higher sensitivity of nitrifying bacteria to the toxic and inhibitory effects of chemicals than ordinary heterotrophic organism makes nitrification the Achilles heel of WWTPs. Thus, increasing the mortality of nitrifiers by RAS-ozonation would potentially reduce the stability of the nitrification process. This is especially important if one considers that the activity of nitrifiers is now required, even at low temperatures (i.e., during winter), to meet the limiting ammonia discharge regulation imposed by the new Canadian Fisheries legislation (Fisheries and Oceans Canada 2012). Howerver ANO are organisms found in natural environments, they should have the ability to handle some environmental stresses. Therefore, one should question if they can adapt to RAS-ozonation through physiological (Schimel et al. 2007) or ecological (e.g., species selection) acclimation mechanisms. Details of such acclimation would help engineers to quantify the behaviour of microorganism and predict their activity based on different ecological conditions. Yet, only a few studies have described the impact of environmental stresses on the population of nitrifiers (e.g., Balser and Firestone 2005, Zak et al. 2003).

This thesis and the research work supporting it were divided into two parts. In the first part, a new mathematical model for the prediction of biosolids reduction by RAS-ozonation was developed, validated, and studied for the sensitivity of model outputs. The model was based on the description of activated sludge biological processes developed in the IWA-ASM3 model, and includes new processes describing the reactions of ozone with RAS solids. The model output accuracy was verified by comparison with experimental data obtained, through which the ozone doses and the WWTP configurations were varied. The validated model was then studied using a global sensitivity analysis to determine the sensitivity of model outputs such as biosolids reduction levels, specific nitrification rates, and nitrification stabilities to the changes in the input model parameters (biological, ozone reaction, and operational conditions).

In the second part of this thesis, the effects of ozone on the microbial populations of OHO and ANO were investigated by using high-throughput pyrosequencing of PCR amplicons from 16S rRNA, *amoA* (encoding the ammonia monooxygenase enzyme) and *nxrB (*encoding the beta subunit of the nitrite oxidoreductase enzyme) genes. In addition, the community assemblies of eight full-scale activated sludge systems were studied over same three-year period as above. This provided a baseline to interpret the results from the pilot-scale reactor study in the same context as the microbial diversity data at the AS-WWTPs.

In the rest of this chapter, the experimental set-up used in this study will be presented. Then, the thesis objectives and the organisation of the other chapters will be discussed.

1.2. EXPERIMENTAL SET-UP

Two pilot-scale reactors (RAS-ozonated and non-ozonated control) were operated to explore the objectives of this research. Reactors were constructed at a local wastewater treatment plant at the

Régie d'assainissement des eaux de basin LaPrairie (REABL) (the South shore of Montreal, Québec), and each reactor had a total volume of 1.7 m^3 (including the reactor tank and the secondary clarifier), (Fig. 1.1). Both reactors were fed with the same incoming raw municipal wastewater. The influent was pumped to an overflowing turbulent distribution tank with a hydraulic residence time (HRT) of a few minutes, and then re-pumped to each of the reactors with the flow passing through a 5-mm screen to reduce clogging of the peristaltic pumps. Reactors were equipped with online magnetic flow meters (Sika, NJ, USA), oxygen and temperature sensors (ABB, Gloucestershire, UK) to log the data every 5 min. Biosolids was wasted through timed pumps directly from the aeration tanks. Both clarifiers (cylindrical tanks with 45° conical bottoms) were equipped with rotating rakes to help evacuate the solids in the center of the tanks. Ozone contactor and generators were designed and provided by Air Liquide Canada (Montreal, Québec), and additional design and operation information is given in Chapter 3.

The pilot-scale study was conducted over three years, with experiments lasting 6-8 months each year (including the start-up periods). During the first year of the study (experiment conducted from September to December 2009), the reactors were only operated as conventional activated sludge systems (SRT≈6 days) and multiple ozone doses were applied to decrease biosolids production rates. During the second year of study (June to October 2010), treatment systems' operational conditions were kept similar to the first year, but the applied ozone doses were increased to the point of causing nitrification failure, determined by respirometry, in the RAS-ozonated reactor. Finally, during the third year of the study (May to November 2011), the ozone doses were kept constant throughout the experimental period, but treatment reactor configurations and operations were modified such that the nitrification/denitrification

configuration could be compared to the conventional activated sludge configuration, and that long total SRTs (~12 days) could be compared to short total SRTs (~6 days).

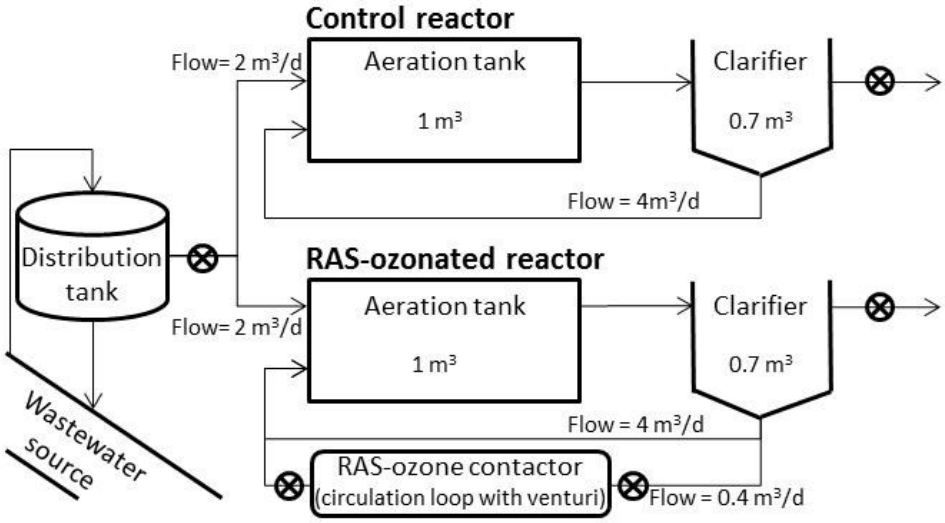

(a)

(b)

(c)

Fig. 1.1. Schematic of pilot-scale reactors used in this research. Target flow rates, size of the units, and the autosampler locations (⊗) are indicated (a). Control (left) and RAS-ozonated (right) reactors in picture (b) and provided ozone contactor and generator by Air Liquide Canada (c).

1.3. SPECIFIC RESEARCH OBJECTIVES AND RELEVANT TASKS

The first goal of the current study was to develop an accurate model to predict the biosolids reduction in RAS-ozonated AS-WWTPs. The second goal was to monitor the population structures of ordinary OHO and ANO populations, and to test the effects of RAS-ozonation and operational conditions, to understand the main factors shaping the bacterial community diversity in AS-WWTPs. To achieve these goals, the following specific objectives and tasks were pursued.

Objective 1: To develop a new mechanistic model for prediction of biosolids reduction by ozone (Chapter 3).

Task 1*:* Design and construction of two pilot-scale (control and RAS-ozonated) reactors.

Task 2*:* Operation of two reactors for 98 days (after 2-month start-up and troubleshooting) in 2009 with variable ozone dose to reach the targeted biosolids reduction.

Task 3*:* Performing an independent chemical oxygen demand (COD) solubilisation and biomass inactivation test to validate the model parameterization.

Task 4*:* Calibration of biological parameters and influent characteristics with observed data from non-ozonated (control) reactor, and calibration of ozone related operation parameters of the model with observed data from RAS-ozonated reactors and independent study.

Objective 2: To substantiate the model accuracy for nitrification activity predictions and determine the influence of input model parameters on: biosolids reduction levels, nitrification specific activity and nitrification safety which measures the relative expected process stability based on the absolute minimum solids retention time to maintain nitrifiers (described by Rittman and McCarty(2001) (Chapter 4).

Task 1: Operation of pilot-scale reactors for 120 days in 2010 to obtain necessary data for model validation, and simulation of the results (biomass inventory) with the calibration values obtained by fitting the 2009 pilot-scale reactor data.

Task 2: Validation of nitrification prediction through a scenario analysis by comparing specific nitrification activity observations compiled from literature and three years pilot-scale study

Task 3: Computational analysis of global sensitivity analysis with respect to biosolids reduction efficiency, nitrification specific activity, and nitrification stability

Objective 3: To evaluate the impact of high mortality rate due to RAS-ozonation on the microbial community structure during the 2009 experiment.

Task 1*:* DNA extraction and PCR amplification of 16S rRNA gene followed by high-throughput pyrosequencing analysis of gene amplicons.

Task 2*:* Comparison of community structures obtained from amplicon pyrosequencing and from quantitative fluorescence *in situ* hybridization (FISH) (the more common in the technique in the literature).

Task 3*:* Explanation of the presence of unusual population in the RAEBL WWTP bacterial community such as the methanol/nitrate consumer: *Methylotenera* genus.

Objective 4: To quantify the relative effect of RAS-ozonation and other operational conditions on the structure of the microbial community structure at AS-WWTPs.

Task 1: Determination the bacterial community structures of the RAEBL full-scale WWTP and of both pilot-scale reactors during the 2010 and 2011 experiments by 6S rRNA gene PCR amplicon pyrosequencing.

Task 2*:* Determination the bacterial community structures at 8 WWTPs located within a 65 km radius of Montreal during different seasons (winter vs. summer) and over two different years (2009 and 2013)

Task 3: Partitioning the observed variance in bacterial community structures (i.e., beta-diversity) between various environmental factors: RAS-ozonation process, reactor scale, influent characteristics, and operational parameters.

Objective 5: To determine the effects of RAS-ozonation and treatment reactor's configuration and operation on the population structure of ANO populations: ammonia oxidizing bacteria (AOB) and *Nitrospira*-related nitrite oxidizing bacteria (NOB).

Task 1*:* Operation of pilot-scale reactors for 200 days during 2011. For the experiment, the target is approximately 50% reduction in biosolids production and to vary the reactor configuration (nitrification/denitrification vs. conventional activated sludge) and the SRT.

Task 2*:* Simulation of experimental results with proposed model using the calibrated parameters obtained using the 2009 fitting exercise.

Task 3: Optimization of PCR reactions targeted at *amoA* genes (AOB) and *nxrB* genes (*Nitrospira*-related NOB); pyrosequencing of the amplicons, and bioinformatics analysis of sequence data.

1.4. DISSERTATION OUTLINE

This thesis comprises seven chapters beyond this introduction: a literature review, 5 chapters of novel research and a conclusion chapter.

Chapter 2 reviews the literature on biosolids minimization technologies, ozone properties and relevant reactions, ozone applications in water and wastewater treatment, the modelling of biosolids reduction processes, and ozone effects on the activated sludge microbial communities. Furthermore, the essential data pertaining to the phylogeny and physiology AOB and NOB is discussed.

Chapter 3 **(objective 1)** describes the new mathematical model proposed to predict the reduction of biosolids production by RAS-ozonation. Three ozone doses were tested during the pilot-scale study to provide a range of reduction levels. In addition, laboratory-scale experiments were conducted to ascertain the parameterization of the biomass inactivation process during exposure to ozone. The experiments revealed that biomass inactivation occurred even at the lowest doses, and that it was not associated with extensive COD solubilization. The model was used to simulate the temporal dynamics of the pilot-scale operational data (98 days), which showed that increasing the description accuracy of the inactivation process improved the precision of the model predictions.

Chapter 4 (**objective 2)** studies the model through a scenario analysis and a global sensitivity analysis of the biosolids reduction efficiency, of the specific nitrification activity, and of the nitrification stability. Generally, the model outputs were sensitive to treatment reactor operational parameters and to ozone reaction parameters, but not to biochemical parameters. For

operational parameters, mainly temperature and initial SRT influenced all model outputs. For biosolids reduction, increase in the degradability of the influent VSS decreased the reduction efficiency. For specific nitrification activity, the changes were highly dependent on the influent TKN/COD ratio. Finally, the stability of the nitrification process in ozonated systems was found to be generally enhanced at a constant MLVSS, but it was reduced for certain operational conditions at temperatures below 12 °C and at aerated SRTs below 10 days.

Chapter 5 **(objective 3)** describes the changes in microbial community structure in the two pilot-scale reactors (RAS-ozonated vs. Control) and compares the observed structure by 16S rRNA gene amplicon pyrosequencing with the ones FISH experiment. The results reveal that RAS-ozonation is not a main environmental factor structuring the community composition of ASP. Instead, the parallel drifts and slight convergence of the two community structures indicate that other environmental factors such as influent wastewater composition and temperature may be more important.

Chapter 6 (**objective 4)** describes the microbial community structures at eight full-scale WWTPs in addition to the one in the two pilot-scale reactors using 16S rRNA gene amplicon pyrosequencing over a period of 4 years. Partitioning of the variance in community structures (i.e., beta diversity) over several hypothesized ecological factors (reactor-scale, RAS-ozonation, season, sampling year, geographic location, and influent characteristics) suggests that only influent characteristics or geographic location contributed appreciably to the differences in structures. However, only 26% of structure variance could be explained, leaving the main portion of beta diversity (74%) unexplained by the hypothesized environmental factors.

Chapter 7 **(objective 5)** describes the nitrification process and nitrifiers' population in two pilot-scales activated sludge, for three years in various operational conditions. Operation results suggests that more nitrifiers were observed in RAS-ozonated reactor in Anoxic/Oxic (A/O) when it compared with Oxic (O) operation and nitrifiers inactivation rate with ozone is similar to ordinary heterotrophs organisms (OHO). RAS-ozonation did not create a major shift in population structure while changes in the operational conditions seemed more likely to affect these populations.

Chapter 8 summarizes of the work presented in the thesis, and presents general conclusions from this doctoral research.

1.5. CONTRIBUTIONS TO KNOWLEDGE

Minimization of biosolids production by partial ozonation of return activated sludge has been in place for many years (Chu et al. 2009, Yasui and Shibata 1994). However, a reliable tool to precisely simulate the biosolids reduction and the fate of nitrification process before the implementation of ozone still does not exist. Existing models are either too simplistic (Mines et al. 2008, Yasui and Shibata 1994) or too complex (Manterola et al. 2007). The first model tends to ignore the importance of influent COD fractionations (e.g., variations in non-degradable VSS), or variation of operational conditions such as SRT and temperature on the biosolids reduction efficiency. The second model includes all possible processes in the gas and liquid phases and makes it difficult to understand the process and reproduce the results. Additionally, the effects of RAS-ozonation the bacterial community structure have not been studied with sufficient depth. This thesis is a remedy to these deficiencies with the following specific contributions.

1. Development of a new mechanistic basis model for predicting the reduction of biosolids production and the nitrification activities process after the installation of new RAS-ozonation processes.
2. Validation of the model performance in predictions of biodolids reductions with obtained data from pilot-scale activated sludge reactors that were fed with actual municipal wastewater and were operated over a three-year period. The validation was extended to two activated sludge reactor configurations and two SRTs.
3. Validation of the model prediction for nitrification activities using data from pilot-scale activated sludge reactors and from a compilation of observations from the literature. A scenario analysis was used for the validation and to explain seemingly opposing observations from the literature.
4. Examination of the sensitivity of biosolids reduction, nitrification activity, and nitrification stability to changes in model input parameters. These sensitivity analyses provided additional insights on beneficial/detrimental WWTP process conditions, and pave the ways to optimize biosolids reduction.
5. Demonstration that RAS-ozonation did not cause a major shift in the bacterial community structures of both OHO and ANO populations.
6. Demonstration that bacterial community structures determined by 16S rRNA gene PCR amplicon pyrosequencing and fluorescence in situ hybridization (FISH) may differ due to different biases of the two methods.
7. Quantification of ecological factors contributions in shaping the bacterial community; and demonstration that influent characteristics and geographic locations were the most important factors.

8. Demonstration that the ecological factor data collected could only explain 26% of the variance in community structure, leaving most of the variance unexplained.

Finally, some of the work presented herein has already appeared in the published literature:

1. Isazadeh, S., Feng. M, Urbina. L, and Frigon, D. "New mechanistically-based model for predicting reduction of biosolids waste by ozonation of return activated sludge". *Journal of Hazardous Materials* 2014, 270 , 160-168. (Chapter 3)
2. Isazadeh, S., Ozcer, P. and Frigon. D. "Microbial community structure of wastewater treatment subjected to high mortality rate due to ozonation of return activated sludge". *Journal of Applied Microbiology*.2014, 117(2), 587-596. (Chapter 5)

1.6. REFERENCES

Balser, T.C., Firestone, M.K., 2005. Linking microbial community composition and soil processes in a California annual grassland and mixed-conifer forest. Biogeochemistry 73(2), 395-415.

Böhler, M., Siegrist, H., 2004. Partial ozonation of activated sludge to reduce excess sludge, improve denitrification and control scumming and bulking. Water Science and Technology 49(10), 41-49.

CCME, 2010. A Review of the current Canadian legislative framework for wastewater biosolids Canadian Council of Ministers of the Environment.

Chu, L., Yan, S., Xing, X.-H., Sun, X., Jurcik, B., 2009. Progress and perspectives of sludge ozonation as a powerful pretreatment method for minimization of excess sludge production. Water Research 43(7), 1811-1822.

Egemen, E., 2001. Evaluation of an ozonation system for reduced waste sludge generation. Water Science and Technology, 445-452.

Fabiyi, M., Full Scale Application of a Novel Sludge Ozonation Process for Achieving up to 80 Excess Sludge Reduction at a 25,000 m3day Municipal Wastewater Plant.

Fisheries and Oceans Canada, 2012. Wastewater systems effluent regulations, Government of Canada, Vol. 146, No. 15, Canada Gazette.

Kamiya, T., 1998. New combined system of biological process and intermittent ozonation for advanced wastewater treatment. Water Science and Technology 38(8), 145.

Manterola, G., Grau, P., Ayesa, E., Uriarte, I., Sanch, L., 2007. Mathematical modelling of sludge ozonation process for WWTP excess sludge reduction. Moving Forward Wastewater Biosolids Sustainability: Technical, Managerial, and Public Synergy, 287-294, Moncton, New Brunswick, Canada, June 24 – 27.

Mines, R.O., Northenor, C.B., Murchison, M., 2008. Oxidation and ozonation of waste activated sludge. Journal of Environmental Science and Health, Part A 43(6), 610-618.

Pérez-Elvira, S., Nieto Diez, P., Fdz-Polanco, F., 2006. Sludge minimisation technologies. Reviews in Environmental Science and Biotechnology 5(4), 375-398.

Sakai, Y., 1997. An activated sludge process without excess sludge production. Water Science and Technology, 163-170.

Schimel, J., Balser, T.C., Wallenstein, M., 2007. Microbial Stress-Response Physiology and Its Implications for Ecosystem Function. Ecology 88(6), 1386-1394.

Yasui, H., Shibata, M., 1994. An innovative approach to reduce excess sludge production in the activated sludge process. Water Science and Technology 30(9), 11-20.

Zak, D.R., Holmes, W.E., White, D.C., Peacock, A.D., Tilman, D., 2003. Plant diversity, soil microbial communities, and ecosystem function: are there any links? Ecology 84(8), 2042-2050.

Rittmann, B., McCarty, P.L., 2001. Environmental Biotechnology : Principles and Applications, McGraw-Hill Science Engineering, New Yourk.

CHAPTER 2:

LITERATURE REVIEW

Connecting text: In this chapter, the literature covering the applications of ozone in water and wastewater treatment is reviewed along with processes for reduction in biosolids production. In addition, the phylogeny and physiology of the two nitrifiers' populations (ammonia and nitrite oxidizing bacteria) are presented.

2.1. BIOSOLIDS MINIMIZATION

In a conventional activated sludge process, biosolids are comprised of accumulated solids stemming from incoming influent and residual solids as a result of biological processes (Fig. 2.1). In practice, measuring the total suspended solids (TSS) and its components, namely volatile or organic suspended solids (VSS) and non-volatile or inorganic suspended solids (ISS), is the general way of quantifying biosolids in wastewater treatment systems (Tchobanoglous et al. 2003). However, this approach not only does not provide a precise way to track the fate and transport of solids, especially the organic part, but also makes it difficult to accurately quantify and predict biosolids production in an activated sludge process (ASP). Therefore, detailed fractionation of biosolids with regards to influent solids is necessary. Since influent has been fractionated and the resulting components have been successfully applied in wastewater modeling (Gujer et al. 1999, M Henze 2000), biosolids fractionation can also follow the same concept. Influent wastewater encompasses soluble biodegradable ($S_{B,inf}$), soluble un-biodegradable ($S_{U,inf}$), particulate biodegradable ($X_{B,inf}$), particulate un-biodegradable ($X_{U,inf}$), and inorganic suspended solids (ISS_{inf}) (Fig. 2.2). Two of these components, namely ISS_{inf} and $X_{U,inf}$, end up directly in the biosolids fraction. Two other parts, $X_{B,inf}$ and $S_{B,inf}$, have to go through the biological process and are transferred to the active biomass (X_H) and biological residue (X_{UE}).

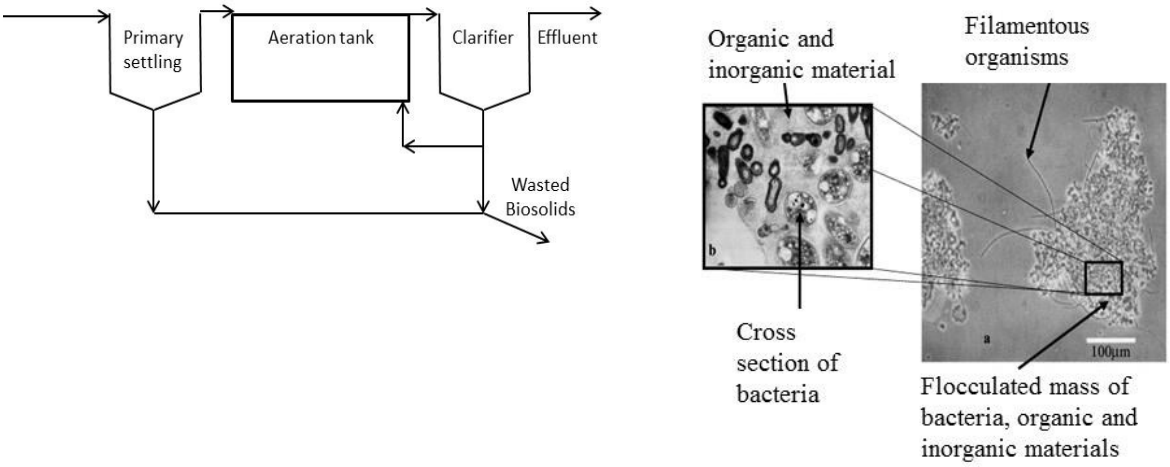

Fig. 2.1. Schematic of a conventional activated sludge system and sludge floc structure as viewed under light microscopy and TEM micrograph adapted from Jenkins et al. 2004 and Biggs et al. 1997.

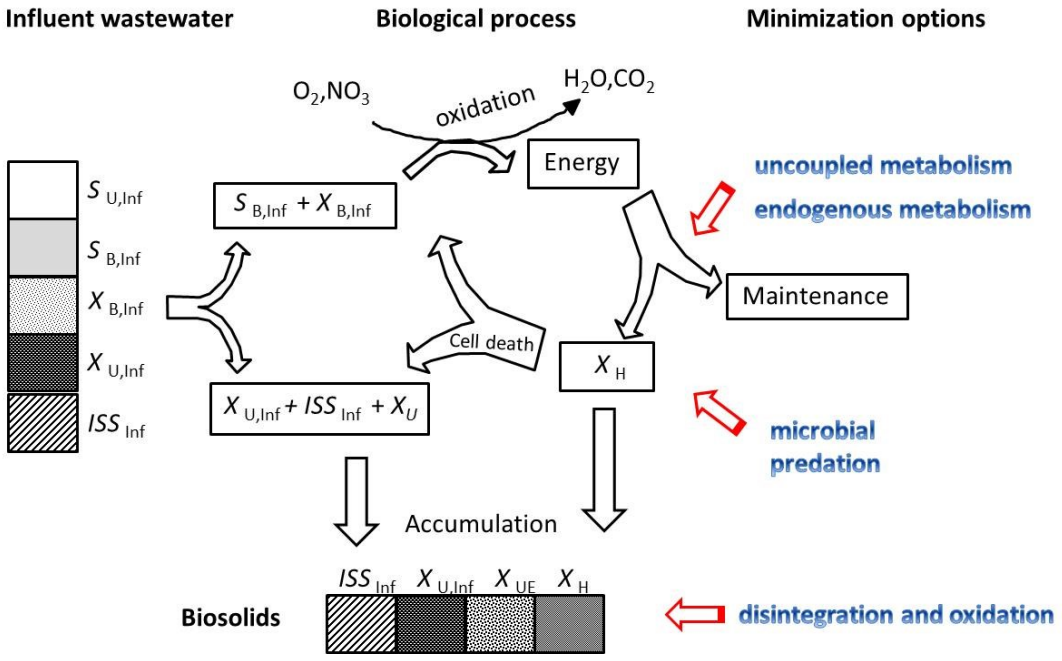

Fig. 2.2. Schematic representation of sludge fractionation in influent and biosolids along with possible biosolids minimization options (adapted from Paul et al. 2012)

Based on the biosolids composition, different options can be employed to minimize biosolids generated in ASP (Foladori et al. 2010, Paul et al. 2012, US-EPA 2006). One option is to directly influence the biological process by increasing the biomass decay or reducing the bacterial growth. This can be achieved by modifications in the operational conditions. Longer solids retention time (SRT) in extended aeration and membrane bioreactors (MBR), or the application of a process which requires lower biomass growth, like oxic-settling anaerobic (OSA) (e.g., Cannibal process), or managing the food supply chain to favour predation, are just a few examples of possible operational modifications. Another well-known option is to deter bacterial growth by using chemical uncouplers such as 2,4-dinitrophenol (*d*NP), *para*-nitrophenol (*p*NP) and pentachlorophenol (PCP).These chemicals prevent adenosine triphosphate (ATP) formation during catabolism and incur a discrepancy in energy (ATP) level between catabolism and anabolism and consequently limit energy supply available for biomass production in anabolism (Wei et al. 2003).

A second option is to return accumulated inert fractions of biosolids and reuse them in the biological process. Physical or chemical processes such as oxidation, enzymatic hydrolysis, thermal treatment, ultrasonication, and mechanical homogenization, can be applied to disintegrate these solids fractions. The application of each of these options has its own potentials and limits as summarized in Table 2.1 which displays the mechanism, targets and limits of these options as highlighted in the literature.

Chemical oxidation of biosolids by ozone is one of the technologies falling under the second option above and has received considerable attention due to its promising features and benefits. This option not only can achieve a biosolids reduction of up to 100%, but also can be used in oxidizing emerging contaminants of concern like pharmaceutical compounds or micro-pollutants

in wastewater effluent. Ozone also can be used for bacterial disinfection of wastewater effluent. Although partial ozonation of activated sludge has been successfully implemented in full-scale treatment plants in Europe and Asia (Böhler and Siegrist 2004, Egemen 2001, Fabiyi 2007 , Kamiya 1998, Sakai 1997, Yasui and Shibata 1994) the installation of such technology has not been established in North America.

Table 2.1. Summary of limits and potentials of techniques employed for biosolids minimization in activated sludge process (adapted from Paul et al. 2012)

Minimisation techniques	Mechanism of action	Solid fraction[a]	Reduction (%)	Limits of application	Reference
Biological					
Endogenous metabolism: *Longer SRT in MBR extended aeration*	increased biomass decay, slow hydrolysis	$X_{U,inf}$, X_H	5-40	size of the treatment plant	Laera et al. (2009)
Uncoupled metabolism: *2,4-dinitrophenol para-nitrophenol*	reduced bacterial growth yield	X_H, X_{UE}	40-77	partial or complete nitrification inhibition, reduced COD removal efficiency	Low et al. (2000), Yang et al. (2003),Liu (2000), Tian et al. (2013)
Oxic-settling-anaerobic: *Cannibal*	reduced bacterial growth yield	X_H, X_{UE}	38-54	increase in P in effluent	Goel and Noguera(2006), Chen et al. (2003), Quan et al. (2012)
Eco-manipulation: *Predation: protozoa, metazoan, worms*	increased bacterial decay by encouraging predators	X_H	12-75		Lee and Welander (1996), Wei et al. (2009)
Physical & Chemical					
Thermal treatment (40 to 80 °C)	increased biomass decay, improve biodegradability of inert compounds	$X_{U,inf}$, X_{UE}, X_H	up to 100	high energy requirement	Canales et al. (1994), Bougrier et al. (2008), Carrere et al. (2010)
Mechanical disintegration: *Homogenization Ultrasonication*	improved biodegradability of inert compounds	$X_{U,inf}$, X_{UE}	25-59	impaired settleability, high energy requirement	Camacho et al. (2002), Zhang et al. (2007), Hwang et al. (2010)
Oxidation and hydrolysis: *Ozone, chlorine, acid, H_2O_2, enzymes*	improve biodegradability of inert compounds	$X_{U,inf}$, X_{UE}, X_H	up to 100	Accumulation of inorganic materials in system, high energy requirement	Liu (2003), Li et al. (2008), Saby et al. (2002)

a: $X_{U,inf}$: Particulate un-biodegradable , X_H: active biomass , X_{UE}: biological residue

2.1.1 Ozone properties

Ozone gas is an unstable triatomic form of oxygen (O_3) with a molecular weight of 48 (Fig. 2.3a). At the stratospheric level, ozone creates a protective layer (i.e., ozone layer) against ultraviolet (UV) radiation of the sun. At the atmospheric level, it a powerful oxidant and therefore has a lot of industrially related applications. Naturally, ozone is produced from the reaction of oxygen with solar UV rays in the stratosphere. In the atmosphere, ozone can be produced in low concentrations by the high voltage lighting of thunderstorms or as photochemical smog during summer time. Commercially, ozone is produced in different ways depending on the required concentration. Corona-discharge, which essentially is a spark of high voltage electricity, can produce ozone with a concentration up to 22% (Fig. 2.3b). UV- light ozone generation, which is a photochemical way of ozone production, can produce ozone with a concentration up to 2%. Ozone cannot be stored or transported due to its relatively short half-life and subsequently requires on-site generation. Ozone generation facilities which use pure oxygen instead of ambient air can yield higher production rates.

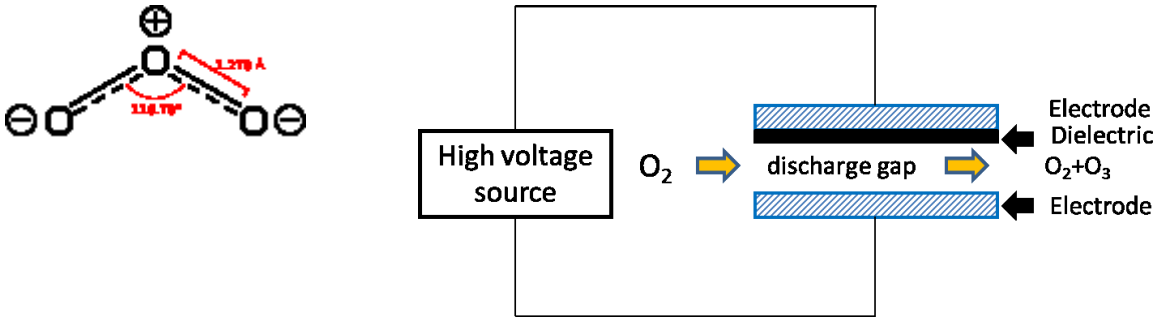

Fig. 2.3. Molecular shape of ozone on left and outline of corona-discharge generator on right adapted from (US-EPA 1999)

Ozone is highly corrosive and toxic and exposure can cause severe health problems. At low concentrations it can cause irritation of the eye, nose, throat and respiratory system, while at high concentrations it can cause lung damage, edema and hemorrhage (US-EPA 1999). The American conference of government industrial hygienists (ACGIH) recommends a maximum ozone level of 0.1 mg/L (by volume) for a normal eight hour work day, and a maximum concentration of 0.3 mg/L (by volume) for exposure of up to 15 minutes (US-EPA 1999).

Ozone has a wide range of applications in food, pulp and paper, and water and wastewater treatment. In the water and wastewater industry, ozone is known to be an excellent disinfectant and has widespread application throughout the world (von Gunten 2003a). The commendable features of ozone reside mainly in the fact that it can induce disinfection of pathogens and oxidation of organic materials with less harmful by-products. This has made it a very good candidate to replace the widely applied chlorine which presents a noticeable amount of disinfection by-products (DBPs). Ozone has also shown the capability to oxidize micro-pollutants, taste and odors, iron and manganese, and emerging contaminants in wastewater effluent along with its capacity to reduce biosolids production.

2.1.2 Ozone application in water

Ozone was first used for drinking water treatment in 1893 in the Netherlands (US-EPA 1999). Ozone is unstable in water and decomposes within seconds to hours (von Gunten 2003a). During the spontaneous decomposition it produces hydroxyl free radicals (OH°) which are among the most reactive materials with reaction rates of the order 10^{10} - 10^{13} M^{-1} s^{-1}(US-EPA 1999). Therefore, ozone can oxidize the existing compounds in water either directly or indirectly by ozone molecules and hydroxyl radicals respectively. Ozone demand for water treatment is

associated with the presence of natural organic materials (NOM), synthetic organic compounds and bicarbonates or carbonates which can scavenge both molecular ozone or hydroxyl radicals (von Gunten 2003a).

Ozone application in water treatment has been the subject of many research studies (Camel and Bermond 1998, von Gunten 2003a, b). Camel and Bermond tried to address ozone as a major disinfectant for microbial inactivation, while some focused on the oxidative property of ozone and von Gunten considered the kinetics and the rate of oxidation with inorganic and organic compounds. Ozone disrupts bacterial membrane integrity by targeting glycoproteins or glycolipids (Scott and Lesher 1963) or by attacking amino acids such as tryptophan (Goldstein and McDonagh 1975). Ozone can also react with cytoplasmic material and disrupt the enzymatic activity of bacteria. In viral inactivation, ozone attacks the capsid protein. The effects of ozone on protozoa (i.e., *Giardia* and *Cryptosporidium*) have also been reported but they appear to be more resistant to ozone as compared to vegetative bacteria (Labatiuk et al. 1992). Several research studies have shown that the inactivation of microorganisms by ozone follows the first order Chick-Watson model or its delayed version (Corona-Vasquez et al. 2002, Finch et al. 1993).

Ozone reaction rates with organic and inorganic compounds are well-documented in the water treatment literature (Hoigné and Bader 1983a, Hoigné et al. 1985). The kinetics of the reaction are typically second order, first order with ozone and first order with compounds (von Gunten 2003a). It seems that oxygen transfer is the main mechanism involved in the oxidation of inorganic compounds. Ammonia (NH_3/NH_4^+) has the lowest (0 to 20 $M^{-1}s^{-1}$) and nitrite (NO_2^-) has the highest (3.7×10^5 $M^{-1}s^{-1}$) reaction rate constant with ozone among nitrogen species. They both convert to nitrate (NO_3^-) after ozone exposure. Although in potable water treatment

processes NH_4^-/NH_3 is not oxidized significantly due to limited ozone concentrations, in municipal wastewater a significant amount of ozone can be consumed by the ammonical nitrogen (Hoigne and Bader 1978).

Ozone reaction with organic materials in water is highly selective and electrophilic (Hoigné and Bader 1983b). Ozone, depending on the structure of organic compounds, can form an oxyl radical which has an inherent capability of inserting into carbon chains and forming ring-shaped structures (von Gunten 2003a). Therefore, the potential for producing intermediary organic compounds in the chain of reactions is high and usually the pH of water and the dissociation of organic materials play crucial roles in the fate of ozonated organic compounds.

2.1.3 Ozone application in wastewater for biosolids reduction

The principle of using chemical hydrolysis to reduce biosolids was first described by Gaudy et al. (1971) in which he used acidic hydrolysis in an extended aeration system. Later, Van Leeuwen (1988), adopting the same concept, used ozone and reported simultaneous biosolids reduction and bulking control in a pilot-scale study. Yasui and Shibata (1994) operated an activated sludge system with zero sludge production. Since then, this chemical-assisted biosolids reduction strategy has been applied in both activated sludge and anaerobic digesters. Studies on activated sludge at laboratory-scale with synthetic wastewater (Dytczak et al. 2007, Richardson et al. 2009), at pilot- and full-scale with municipal and industrial wastewaters (Deleris et al. 2002, Mines et al. 2008, Sakai 1997, Salhi 2003), and in anaerobic digestion systems (Battimelli et al. 2003, Goel et al. 2004) have shown a biosolids reduction ranging from zero to one hundred percent. Details of reported sludge reduction and corresponding ozone dose in the literature have been documented by Foladori et al. (2010), Paul et al. (2012) and Chu et al. (2009b). Several

options have been designed to apply ozone in wastewater treatment facilities. The main point of ozone application is on settled sludge before recycling it to the aeration tank or anaerobic digester.

2.1.4 Modeling biosolids reduction in activated sludge by RAS-ozonatation

Yasui and Shibata (1994) were the first to employ a biosolids mass balance to simulate the ozone effects on active and inactive biomass by using global constants. Similarly, others (Mines et al. 2008, Wang et al. 2008) described the ozone effect as a pseudo or first order reaction, but this approach does not provide insights on how ozone efficiency may vary with changes in SRT and influent wastewater characteristics.

Linking the operational parameters and influent characteristics requires ASP models. The biosolids composition described before is similar to biosolids' definition in IWA-activated sludge models (ASM)(Henze, 2000). ASM models are mathematical models describing the fate and transport of carbon (C), nitrogen (N) and phosphorus (P) removal through biological processes in ASP. As a result of the existing link between the influent COD fractionation and biological processes such as growth and decay, it is accurate to combine ozone model with the ASM model series. Salhi (2003) was the first to explore this inherent feature. His model was based on the assumption that ozone, below the threshold value of 0.01g $O_3.g^{-1}$ COD, does not attack X_{OHO} and effect the non-viable fraction of biosolids (X_U, $X_{U,E}$). Manterola et al. (2007) developed an extension of the IWA-ASM1, in which the gas liquid transfer rate of ozone was included along with complex ozone reactions using a large number of new particulate and soluble COD pools. This comprehensive approach came at the cost of reduced clarity and predictability of the model, and model calibration suffered from a lack of necessary supporting

experimental data. As a result, the quality of the model fit was poor. Recently, Frigon and Isazadeh (2011) introduced an extension to the IWA-ASM3 model. Their modeling tested three approaches: (1) inactivation of active biomass only, (2) inactivation of biomass and transformation of non-biomass solids at the same rate, and (3) inactivation and transformation at different rates (Fig. 2.4). Relying on the steady-state fit of their model to MLVSS, ATP, and nitrification activity data, they concluded that the third approach was the most plausible, with the biomass inactivation rate due to ozone likely being higher than the non-biomass transformation rate.

Ozone effects on biosolids is also linked to the concept of "cryptic growth" (Dytczak et al. 2007, Fabiyi 2007, Huysmans et al. 2001, Kamiya 1998, Richardson et al. 2009, Yasui and Shibata 1994), which describe cell repairs and regrowth after cell lysis with the utilization of lysis products as food sources. In this approach, ozone simply induces cell lysis and cryptic growth by attacking live microorganisms in the sludge, and does not react significantly with other solids fractions. If true, the fraction of active biomass should be reduced after the addition of the ozonation process. This prediction, however, was not substantiated by Paul and Debellefontaine (2007a), who found that ozonation did not reduce the relative heterotrophic activity. On the other hand, Frigon and Isazadeh (2011), based on ozonated pilot-scale studies, found a reduction in the ATP content of sludge (proportional to heterotrophic biomass) and specific nitrification activity, both indicative of a reduction in active biomass. However, the cryptic growth concept was unable to explain the extent of sludge reduction observed in their pilot-scale experiment.

.

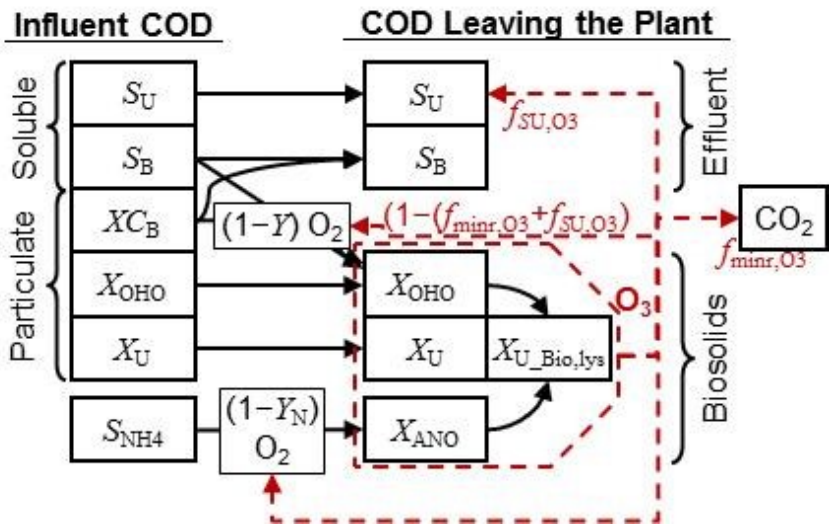

Fig. 2.4. COD flow in activated sludge subjected to RAS-ozonation according to the IWA-ASM3 model and the proposed extension describing ozone reactions with VSS. Solid lines represent IWA-ASM3 biochemical conversions, dashed lines represent conversions due to ozonation of RAS. COD pools: degradable (S_B) and undegradable (S_U) soluble COD, biodegradable (XC_B) and undegradable (X_U) particulate COD, heterotrophic (X_{OHO}) and nitrifying (X_{ANO}) biomass, biomass debris ($X_{U\_bio,lys}$), and ammonium (S_{NH4}). Ozone reaction fractions: undegradable soluble COD ($f_{SU,O3}$), and mineralized COD ($f_{minr,O3}$).

2.2. OZONE EFFECT on the ACTIVE BACTERIAL POPULATION

Bacteria can be categorized into several groups according to carbon, energy and reducing power (electron) sources that they need for growth (Seviour and Nielsen 2010). In ASP, two important groups of Chemoorganoheterotrophs and Chemolithoautotrophs are mainly involved in carrying out the bioremediation processes. The former obtains all carbon, energy, and reducing power from oxidisable organic compounds while the latter obtains the carbon from carbon dioxide or carbonate and the reduction power from oxidizable inorganic compounds. Most bacteria, Archaea, and protozoa are ordinary heterotrophic organisms (OHO) in ASP. They use available organic compounds (COD) and oxygen for respiration. Autotrophic nitrifying organisms (ANO), on the other hand, use CO_2 for cell carbon synthesis and their energy results from oxidation of

either ammonia (NH_3) or nitrite (NO_2) through the process of nitrification. Both the populations of OHO and ANO are component variables in the IWA-activated sludge model ASM3.

The vulnerability of OHO and ANO to partial RAS-ozonation of ASP was evaluated in two types of studies: (i) ozone inactivation studies (i.e., viability or activity decrease upon ozone exposure), and (ii) long-term monitoring of nitrification specific activity and process efficiency. Ozone inactivation studies have mainly been conducted for OHO. The techniques used to determine inactivation include heterotrophic plate counts, heterotrophic maximum oxygen uptake rates (OUR) with defined substrates, solids ATP concentrations and enzymatic (e.g., protease) activities (Chu et al. 2008, Chu et al. 2009a, Dziurla et al. 2005, Jarvik et al. 2010, Labelle et al. 2011, Lee et al. 2005, Paul and Debellefontaine 2007b, Yan et al. 2009, Yasui and Shibata 1994). Although most authors seem to agree that the ozone dosage should be normalized to the solids concentration, the literature is not clear on the shape of the inactivation curve, as linear (Chu et al. 2009b, Jarvik et al. 2010, Labelle et al. 2011), exponential (Chu et al. 2008, Dziurla et al. 2005, Yan et al. 2009, Yasui and Shibata 1994), and power (Paul and Debellefontaine 2007b) functions have been used for analysis. Furthermore, some reported data suggested dose thresholds before the onset of inactivation (Chu et al. 2009a, Dziurla et al. 2005, Paul and Debellefontaine 2007b), while this threshold was not observed in other data (Chu et al. 2008, Dziurla et al. 2005, Jarvik et al. 2010, Labelle et al. 2011, Yan et al. 2009, Yasui and Shibata 1994). It would be expected that the inactivation of ANO would follow similar trends as with the OHO. However, direct comparison based on empirical experimental data appears not to have been performed. Comparing reports of inactivation determined by plate counts for OHO and by most probable number for ANO for an ozone dose of 0.05 g-O_3/g-suspended solids (SS) suggest a certain protection level of ANO with an inactivation level of 80% (Kobayashi et al.

2001)Chu et al. 2009b), while the inactivation of heterotrophs ranges from 90-99.99% (Lee et al. 2005, Yan et al. 2009, Yasui and Shibata 1994).

Long-term monitoring of nitrification process efficiency (measured as the transformation of ammonia into nitrate through the bioreactor) showed that it is typically not affected by the RAS-ozonation process (Böhler and Siegrist 2004, Deleris et al. 2002, Dytczak et al. 2007, Sakai 1997). However, the nitrification specific activities (measured as the maximum activity per mixed liquor volatile suspended solids (MLVSS) in a batch test) were usually reduced with increasing reduction in biosolids (Böhler and Siegrist 2004, Dytczak et al. 2007, Vergine et al. 2007). This reduction seems to be dependent on the treatment process as less reduction was observed in anoxic/aerobic (pre-denitrification) processes than in fully aerobic ones (Dytczak et al. 2007). It has been speculated that the denser flocs found in anoxic/aerobic reactors compared to fully aerobic reactors could provide additional protection to the nitrifiers and explain the process dependency of the observed results (Böhler and Siegrist 2004, Deleris et al. 2002). Nevertheless, Dytczak et al. (2007) could not explain all their results by differences in floc structures between alternating anoxic/aerobic and fully aerobic reactors, and they hypothesized that there must be other unknown protection factors.

2.2.1 Assembly of bacterial community structure in activated sludge process

Activated sludge is an engineered bio-system designed to employ the bacterial community for the biodegradation of organic compounds. Although it has been in practice for nearly a century, most systems have been designed without a priori knowledge about the diversity and bacterial community structure of activated sludge (Pholchan et al. 2010). Existing biochemical activated sludge models (e.g., IWA-ASM series) do not address variation in the bacterial community

structure and consider them with the generic names OHO and ANO. It is well known that plenty of observed problems in ASP, such as in biosolids removal (e.g., bulking, rising sludge blanket, foaming), in biochemical removal (e.g. loss of bacterial population responsible for nitrification), and in system stability (e.g., reduction in final effluent quality), are all associated with the variation in the bacterial community structure (Graham and Smith 2004). Therefore, knowledge of bacterial community structures and the factors shaping them would shed light on understanding the activated process and pave the way to couple biochemical models with ecological models. Ecological models establish a link between diversity and performance relation and can help in the optimization of ecological conditions in view of exploiting the bacterial population capacity for degradation of organic compounds.

Ecological models are based on deterministic and/or stochastic concepts. The deterministic approach argues that competition and niche-specific variables have a major influence on shaping the community assembly. For instance, competitive strategies that species will eventually succeed depend on their ability to uptake maximum resource available and occupy the niche for long-term. The stochastic approach, on the other hand, considers the probability of bacterial dispersal by random events of colonization/extinction or unpredictable fluctuations in the chemical composition of the influent (McMahon et al. 2007). The random community assembly is based on neutral theories of macro-ecology (Hubbell 2001, MacArthur. RH and Wilson 1976). However, there are also efforts to reconcile these two concepts in order to appreciate the coexistence of these components in shaping bacterial structures (Curtis et al. 2003, Nemergut et al. 2013, Ofiţeru et al. 2010). Partitioning of beta diversity in a systematic experimental design can be a helpful tool to shed light on finding which one of these approaches are more appropriate in population assembly of ASP

2.2.2 Phylogeny of ordinary heterotrophic organisms in activated sludge

Based on 4', 6-Diamidino-2-Phenylindole (DAPI) staining it was estimated that there are 1-10^{12} bacteria per gram of VSS in an activated sludge system (Nielson and Neilson 2002). The advent of molecular methods, which relies on 16S rRNA analysis, has revolutionized the microbial ecology of activated sludge and has provided deeper insights into the population composition of OHO. While culture-dependent methods using nutrient rich media favour the growth of some specific subphyla like *Gammaproteobacteria* in conventional activated sludge plants, both Fluorescence *In Situ* Hybridization (FISH) and clone library data using 16s rRNA have confirmed the presence of 8 main phyla, *Proteobacteria (Alpha, Beta*, and *Gamma*), *Actinobacteria*, *Firmicutes*, *Bacteriodetes*, *Chloroflexi*, *Planctomycetes*, *Acidobacteria* and *Nitrospira* in activated sludge systems (Seviour and Nielsen 2010). Application of high throughput sequencing techniques and analysis of metagenomic data have shown a larger number of previously undescribed, phylogenetically diverse candidate phyla including *TM7*, *OP11*, and *OP7*.

Identification of OHO involved in ASP revealed more about the process and paved the way for establishing a link between the function and identity of phylotypes. For instance, the presence of denitrifying bacteria like *Azoracus*, *Thaura* or *Zoogloea spp* (Thomsen et al. 2007), polymer degrading bacteria, especially protein degraders, like TM7 and *Chloroflexi* belonging to the *Betaproteobacteria* group (Xia et al. 2007), iron bacteria like *Geobacter sulfurreducens* (Nielsen et al. 1997), sulfate reducing bacteria like *Desulfobacteriaceae* (Manz et al. 1998), PHA accumulation bacteria like glycogen accumulating organisms (GAO) and phosphorus accumulating organisms (PAO) (Seviour and Nielsen 2010), unveiled more about the physiology and process of activated sludge systems.

2.2.3 Phylogeny and physiology of ammonia and nitrite oxidizing bacteria in activated sludge

Nitrification is a two-step sequential process of oxidizing ammonia to nitrite and then to nitrate by microbial process. Ammonia oxidizing bacteria/or Archaea (AOB or AOA) are involved in the first step and nitrite oxidizing bacteria (NOB) carry out the second step. AOB and NOB are known to be chemolithoautotrophic microorganisms utilizing inorganic nitrogen, CO_2 and O_2 as their sole energy carbon and electron acceptor sources, respectively. Physiologically, AOB use oxygen as an electron acceptor to oxidize ammonia to nitrite in two sequential enzymatic reactions (Fig. 2.5). Ammonia is first oxidized to hydroxylamine (NH_2OH) with the help of the membrane-bound enzyme ammonia monooxygenase (AMO) (eq.2). This is an energy consuming step and requires two electrons. Electrons are recovered through the oxidation of hydroxylamine to nitrite by a periplasmic enzyme hydroxylamine oxidoreductase (HAO) (eq.3) (Chain et al. 2003) (Fig. 2.5). The alpha-subunit of AMO (*amoA*) provides a comprehensive and distinctive molecular marker (McTavish et al., 1993) for the detection of the AOB population.

$$\mathrm{NH_3} + O_2 \xrightarrow{AOB\ or\ AOA} NO_2^- + 3H^+ + 2e^- \qquad eq.1$$

$$\Delta \mathrm{G} = -65\ \mathrm{kcal}/mole$$

$$\mathrm{NH_3} + O_2 + 2H^+ + 2e^- \xrightarrow{AMO} NH_2OH + H_2O \qquad eq.2$$

$$NH_2OH + H_2O \xrightarrow{HAO} NO_2^- + 5H^+ + 4e^- \qquad eq.3$$

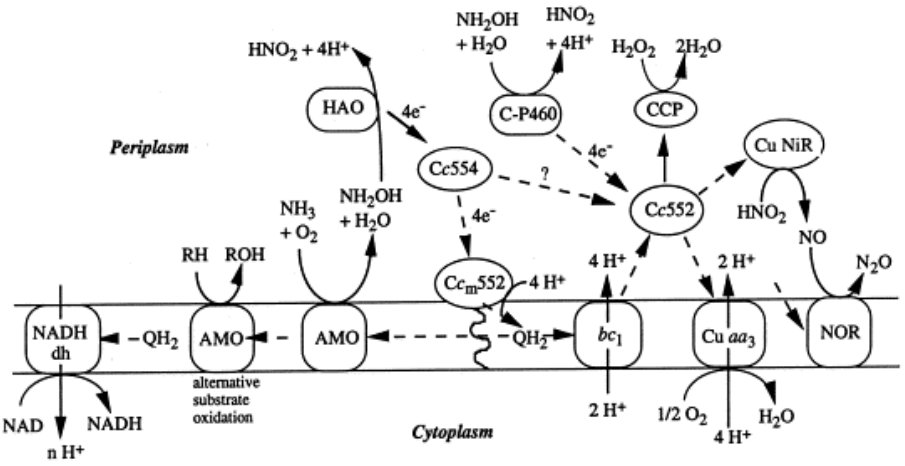

Fig. 2.5. Energy generation in AOB showing the two enzymes involved in this process (Whittaker et al. 2000).

The second step of nitrification is tightly coupled to the first step (eq.4). Nitrite produced from ammonia oxidation is further oxidized to nitrate (NO_3^-) by the membrane-associated enzyme nitrite oxidoreductase (*NXR*). Fig. 2.6 shows the conceptual model of NOB electron chain postulated by Lucker et al. (2010). *NxrB* encoding the beta subunit of nitrite oxidoreductase is the best biomarker for detection of nitrite oxidizing *Nitrospira* (Pester et al., 2013).

$$NO_2^- + H_2O \xrightarrow{NOB} NO_3^- + 2H^+ + 2e^- \qquad eq.4$$

$$\Delta G = -18\ \text{kcal}/mole$$

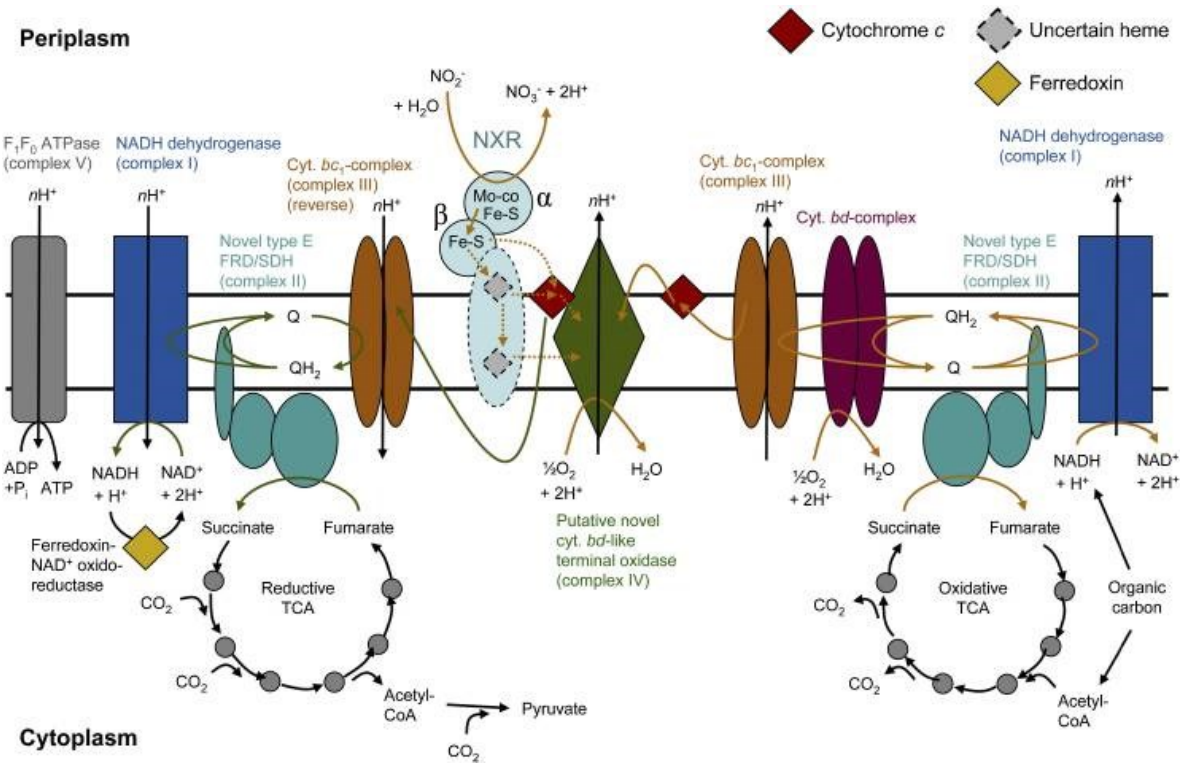

Fig. 2.6. Energy generation in NOB, showing *nxrβ* (Lücker et al. 2010)

AOB have been observed in a wide range of aquatic and terrestrial ecosystems. Phylogenetically they spread over four genera belonging to the *Betaproteobacteria* and *Gammaproteobacteria* of the *Proteobacteria* phylum while NOB has been classified under two phyla of bacteria. In the *Proteobacteria* phylum, they spread over the *Alphaproteobacteria*, *Gammaproteobacteria* and *Deltaproteobacteria* with genera like *Nitrobacter*, *Nitrococcus* and *Nitrospina,* respectively (Spieck et al. 2013). In the second phylum, which represents an exclusive phylum for NOB, so far the genus of *Nitrospira* (Ehrich et al., 1995; Spieck and Bock, 2001), new isolates from freshwater and marine habitats such as *Nitrospira marina* (Watson et al., 1986) and *Nitrospira moscoviensis* (Ehrich et al., 1995), as well as isolates from activated sludge like *Candidatus Nitrospira defluvii* (Spieck et al., 2006), have been observed.

AOB are extremely slow growing bacteria with generation times between eight hours to several days (Dworkin et al. 2006). NOB generates only two electrons during the oxidation of nitrite to nitrate, which is half than the final number of electrons produced by AOB during the ammonia oxidation. The biomass yield of NOB is therefore expected to be half that of AOB per unit of nitrogen (Winkler et al. 2012). This simply indicates that NOB/AOB prevail in activated sludge systems in a ratio of 0.5 (Aleem 1966, Ferguson 1982, Hagopian and Riley 1998). This ratio would be expected to be lower in the simultaneous nitrification/denitrification processes.

.

2.3. REFERENCES

Aleem, M.I., 1966. Generation of reducing power in chemosynthesis. II. Energy-linked reduction of pyridine nucleotides in the chemoautotroph, Nitrosomonas europaea. Biochimica et Biophysica Acta (BBA) - Bioenergetics 113(2), 216-224.

Battimelli, A., Millet, C., Delgenes, J.P., Moletta, R., 2003. Anaerobic digestion of waste activated sludge combined with ozone post-treatment and recycling. Water Science & Technology 48(4), 61-68.

Biggs, C.A., Keller, J., Newell, R.B., Lant, P.A., 1997. Modelling flocculation processes in activated sludge, Rotorua New Zealand.

Böhler, M., Siegrist, H., 2004. Partial ozonation of activated sludge to reduce excess sludge, improve denitrification and control scumming and bulking. Water Science and Technology 49(10), 41-49.

Bougrier, C., Delgenès, J.P., Carrère, H., 2008. Effects of thermal treatments on five different waste activated sludge samples solubilisation, physical properties and anaerobic digestion. Chemical Engineering Journal 139(2), 236-244.

Camacho, P., Geaugey, V., Ginestet, P., Paul, E., 2002. Feasibility study of mechanically disintegrated sludge and recycle in the activated-sludge process. Water Science & Technology 46(10), 97-104.

Camel, V., Bermond, A., 1998. The use of ozone and associated oxidation processes in drinking water treatment. Water Research 32(11), 3208-3222.

Canales, A., Pareilleux, A., Rols, J.L., Goma, G., Huyard, A., 1994. Decreased sludge production strategy for domestic wastewater treatment. Water Science and Technology 30(8), 97–106.

Carrère, H., Dumas, C., Battimelli, A., Batstone, D.J., Delgenès, J.P., Steyer, J.P., Ferrer, I., 2010. Pretreatment methods to improve sludge anaerobic degradability: A review. Journal of Hazardous Materials 183(1–3), 1-15.

Chen, G.H., An, K.J., Saby, S., Brois, E., Djafer, M., 2003. Possible cause of excess sludge reduction in an oxic-settling-anaerobic activated sludge process (OSA process). Water Research 37(16), 3855-3866.

Chu, L.-B., Yan, S.-T., Xing, X.-H., Yu, A.-F., Sun, X.-L., Jurcik, B., 2008. Enhanced sludge solubilization by microbubble ozonation. Chemosphere 72(2), 205-212.

Chu, L., Wang, J., Wang, B., Xing, X.-H., Yan, S., Sun, X., Jurcik, B., 2009a. Changes in biomass activity and characteristics of activated sludge exposed to low ozone dose. Chemosphere 77(2), 269-272.

Chu, L., Yan, S., Xing, X.-H., Sun, X., Jurcik, B., 2009b. Progress and perspectives of sludge ozonation as a powerful pretreatment method for minimization of excess sludge production. Water Research 43(7), 1811-1822.

Corona-Vasquez, B., Samuelson, A., Rennecker, J.L., Mariñas, B.J., 2002. Inactivation of Cryptosporidium parvum oocysts with ozone and free chlorine. Water Research 36(16), 4053-4063.

Curtis, T.P., HEAD, I.M., GRAHAM, D.W., 2003. Peer reviewed: Theoretical ecology for engineering biology. Environmental Science & Technology 37(3), 64A.

Deleris, S., Geauge, V., Camacho, P., Debelletontaine, H., Paul, E., 2002. Minimization of sludge production in biological processes: an alternative solution for the problem of sludge disposal. Water Science and Technology 46(10), 63-70.

Dworkin, M., Falkow, S., Rosenberg, E., Schleifer, K.H., 2006. The Prokaryotes: Vol. 2: Ecophysiology and Biochemistry, Springer.
Dytczak, M.A., Londry, K.L., Siegrist, H., Oleszkiewicz, J.A., 2007. Ozonation reduces sludge production and improves denitrification. Water Research 41(3), 543-550.
Dziurla, M.A., Salhi, M., Leroy, P., Paul, E., Ginestet, P., Block, J.C., 2005. Variations of respiratory activity and glutathione in activated sludges exposed to low ozone doses. Water Research 39(12), 2591-2598.
Egemen, E., 2001. Evaluation of an ozonation system for reduced waste sludge generation. Water Science and Technology, 445-452.
Fabiyi, M., 2008 Full Scale Application of a Novel Sludge Ozonation Process for Achieving up to 80 Excess Sludge Reduction at a 25,000 m3day Municipal Wastewater Plant.
Ferguson, S.J., 1982. Is a proton-pumping cytochrome oxidase essential for energy conservation in Nitrobacter? FEBS Letters 146(2), 239-243.
Finch, G.R., Black, E.K., Gyurek, L., Belosevic, M., 1993. Ozone inactivation of Cryptosporidium parvum in demand-free phosphate buffer determined by in vitro excystation and animal infectivity. Applied and Environmental Microbiology 59(12), 4203-4210.
Foladori, P., Andreottola, G., Ziglio, G., 2010. Sludge Reduction Technologies in Wastewater Treatment Plants, IWA Publishing, London, UK.
Frigon, D., Isazadeh, S., 2011. Evaluation of a new model for the reduction of excess sludge production by ozonation of return activated sludge: what solids COD fraction is affected? Water Science and Technology 63(1), 156-163.
Gaudy, A.F., Jr., Yang, P.Y., Obayashi, A.W., 1971. Studies on the Total Oxidation of Activated Sludge with and without Hydrolytic Pretreatment. Journal (Water Pollution Control Federation) 43(1), 40-54.
Goel, R., Komatsu, K., Yasui, H., Harada, H., 2004. Process performance and change in sludge characteristics during anaerobic digestion of sewage sludge with ozonation. Water Science & Technology 49(10), 105-113.
Goel, R., Noguera, D., 2006. Evaluation of Sludge Yield and Phosphorus Removal in a Cannibal Solids Reduction Process. Journal of Environmental Engineering 132(10), 1331-1337.
Goldstein, B.D., McDonagh, E.M., 1975. Effect of ozone on cell membrane protein fluorescence: I. In vitro studies utilizing the red cell membrane. Environmental Research 9(2), 179-186.
Graham, D.W., Smith, V.H., 2004. Designed Ecosystem Services: Application of Ecological Principles in Wastewater Treatment Engineering. Frontiers in Ecology and the Environment 2(4), 199-206.
Gujer, W., Henze, M., Mino, T., van Loosdrecht, M.C.M., 1999. Activated sludge model No. 3. Water Science and Technology 39(1), 183-193.
Hagopian, D.S., Riley, J.G., 1998. A closer look at the bacteriology of nitrification. Aquacultural Engineering 18(4), 223-244.
Hoigne, J., Bader, H., 1978. Ozonation of water: kinetics of oxidation of ammonia by ozone and hydroxyl radicals. Environmental Science & Technology 12(1), 79-84.
Hoigné, J., Bader, H., 1983a. Rate constants of reactions of ozone with organic and inorganic compounds in water—II: Dissociating organic compounds. Water Research 17(2), 185-194.

Hoigné, J., Bader, H., 1983b. Rate constants of reactions of ozone with organic and inorganic compounds in water—I: Non-dissociating organic compounds. Water Research 17(2), 173-183.
Hoigné, J., Bader, H., Haag, W.R., Staehelin, J., 1985. Rate constants of reactions of ozone with organic and inorganic compounds in water—III. Inorganic compounds and radicals. Water Research 19(8), 993-1004.
Hubbell, S.P., 2001. The Unified Neutral Theory of Biodiversity and Biogeography, Princeton University Press, NJ.
Huysmans, A., Weemaes, M., Fonseca, P A., Verstraete, W., 2001. Ozonation of activated sludge in the recycle stream. Journal of Chemical Technology and Biotechnology 76(3), 321-324.
Hwang, B.-K., Son, H.-S., Kim, J.-H., Ahn, C.H., Lee, C.-H., Song, J.-Y., Ra, Y.-H., 2010. Decomposition of excess sludge in a membrane bioreactor using a turbulent jet flow ozone contactor. Journal of Industrial and Engineering Chemistry 16(4), 602-608.
Jarvik , O., Kamenev, S., Kasemets, K., Kamenev, I., 2010. Effect of ozone on viability of activated sludge detected by oxygen uptake rate (OUR) and Adenosine-5'-triphosphate (ATP) measurement. Ozone: Science & Engineering 32(6), 408-416.
Jenkins, D., Richard, M.G., Daigger, G.T., 2004. Manual on the Causes and Control of Activated Sludge Bulking, Foaming, and Other Solids Seperation Problems, 3rd Edition, Lewis Publishers/CRC Press.
Kamiya, T., 1998. New combined system of biological process and intermittent ozonation for advanced wastewater treatment. Water Science and Technology 38(8), 145.
Kobayashi, T., Arakawa, K., Katu, Y., Tanaka, T., 2001. Study on sludge reduction and other factors by use of an ozonation process treatment., London.
Labatiuk, C.W., Belosevic, M., Finch, G.R., 1992. Factors influencing the infectivity of Giardia muris cysts following ozone inactivation in laboratory and natural waters. Water Research 26(6), 733-743.
Labelle, M.A., Ramdani, A., Deleris, S., Gadbois, A., Dold, P., Comeau, Y., 2011. Ozonation of endogenous residue and active biomass from a synthetic activated sludge. Water Science and Technology 63(2), 297-302.
Laera, G., Pollice, A., Saturno, D., Giordano, C., Sandulli, R., 2009. Influence of sludge retention time on biomass characteristics and cleaning requirements in a membrane bioreactor for municipal wastewater treatment. Desalination 236(1–3), 104-110.
Lee, J.W., Cha, H.Y., Park, K.Y., Song, K.G., Ahn, K.H., 2005. Operational strategies for an activated sludge process in conjunction with ozone oxidation for zero excess sludge production during winter season. Water Research 39(7), 1199-1204.
Lee, N., Welander, T., 1996. Use of protozoa and metazoa for decreasing sludge production in aerobic wastewater treatment. Biotechnology Letters 18(4), 429-434.
Leeuwen, J.V., 1988. Improved Sewage Treatment with Ozonated Activated Sludge. Water and Environment Journal 2(5), 493-499.
Li, H., Jin, Y., Mahar, R., Wang, Z., Nie, Y., 2008. Effects and model of alkaline waste activated sludge treatment. Bioresource Technology 99(11), 5140-5144.
Liu, Y., 2000. Effect of chemical uncoupler on the observed growth yield in batch culture of activated sludge. Water Research 34(7), 2025-2030.
Liu, Y., 2003. Chemically reduced excess sludge production in the activated sludge process. Chemosphere 50(1), 1-7.

Low, E.W., Chase, H.A., Milner, M.G., Curtis, T.P., 2000. Uncoupling of metabolism to reduce biomass production in the activated sludge process. Water Research 34(12), 3204-3212.
Lücker, S., Wagner, M., Maixner, F., Pelletier, E., Koch, H., Vacherie, B., Rattei, T., Damsté, J.S.S., Spieck, E., Le Paslier, D., Daims, H., 2010. A Nitrospira metagenome illuminates the physiology and evolution of globally important nitrite-oxidizing bacteria. Proceedings of the National Academy of Sciences 107(30), 13479-13484.
M Henze, W.G., T Mino, M van Loosedrecht 2000. Activated sludge models ASM1, ASM2, ASM2d and ASM3, London, UK.
MacArthur. RH, Wilson, E., 1976. The theory of island biogeography, Princeton University Press, NJ.
Manterola, G., Grau, P., Ayesa, E., Uriarte, I., Sanch, L., 2007. Mathematical modelling of sludge ozonation process for WWTP excess sludge reduction. Moving Forward Wastewater Biosolids Sustainability: Technical, Managerial, and Public Synergy, 287-294, Moncton, New Brunswick, Canada, June 24 – 27.
Manz, W., Eisenbrecher, M., Neu, T.R., Szewzyk, U., 1998. Abundance and spatial organization of Gram-negative sulfate-reducing bacteria in activated sludge investigated by in situ probing with specific 16S rRNA targeted oligonucleotides. FEMS Microbiology Ecology 25(1), 43-61.
McMahon, K.D., Martin, H.G., Hugenholtz, P., 2007. Integrating ecology into biotechnology. Current Opinion in Biotechnology 18(3), 287-292.
Mines, R.O., Northenor, C.B., Murchison, M., 2008. Oxidation and ozonation of waste activated sludge. Journal of Environmental Science and Health, Part A 43(6), 610-618.
Nemergut, D.R., Schmidt, S.K., Fukami, T., O'Neill, S.P., Bilinski, T.M., Stanish, L.F., Knelman, J.E., Darcy, J.L., Lynch, R.C., Wickey, P., Ferrenberg, S., 2013. Patterns and processes of microbial community assembly. Microbiology and Molecular Biology Reviews 77(3), 342-356.
Nielsen, P.H., Frølund, B., Spring, S., Caccavo Jr, F., 1997. Microbial Fe(III) Reduction in Activated Sludge. Systematic and Applied Microbiology 20(4), 645-651.
Ofiţeru, I.D., Lunn, M., Curtis, T.P., Wells, G.F., Criddle, C.S., Francis, C.A., Sloan, W.T., 2010. Combined niche and neutral effects in a microbial wastewater treatment community. Proceedings of the National Academy of Sciences 107(35), 15345-15350.
Paul, E., Debellefontaine, H., 2007a. Reduction of Excess Sludge Produced by Biological Treatment Processes: Effect of Ozonation on Biomass and on Sludge. Ozone: Science & Engineering: The Journal of the International Ozone Association 29(6), 415-427.
Paul, E., Debellefontaine, H., 2007b. Reduction of excess sludge produced by biological treatment processes: effect of ozonation on biomass and on sludge. Ozone-Science & Engineering 29(6), 415-427.
Paul, E., Liu, Q.-S., Liu, Y., 2012. Biological Sludge Minimization and Biomaterials/Bioenergy Recovery Technologies. Paul, E. and Liu, Y. (eds), p. 209, John Wiley & Sons, Inc, Hoboken, New Jersey.
Pholchan, M.K., Baptista Jde, C., Davenport, R.J., Curtis, T.P., 2010. Systematic study of the effect of operating variables on reactor performance and microbial diversity in laboratory-scale activated sludge reactors. Water Research 44(5), 1341-1352.
Quan, F., Anfeng, Y., Libing, C., Hongzhang, C., Xing, X.-H., 2012. Mechanistic study of on-site sludge reduction in a baffled bioreactor consisting of three series of alternating aerobic and anaerobic compartments. Biochemical Engineering Journal 67(0), 45-51.

Richardson, E.E., Hanson, A., Hernandez, J., 2009. Ozonation of continuous-flow activated sludge for reduction of waste solids. Ozone: Science & Engineering: The Journal of the International Ozone Association 31(3), 247-256.
Saby, S., Djafer, M., Chen, G.H., 2002. Feasibility of using a chlorination step to reduce excess sludge in activated sludge process. Water Research 36(3), 656-666.
Sakai, Y., 1997. An activated sludge process without excess sludge production. Water Science and Technology, 163-170.
Salhi, M., 2003. Procédés couplés boues activées - ozonation pour la réduction de la production de boues, Toulouse, INSA.
Scott, D.B., Lesher, E.C., 1963. EFFECT OF OZONE ON SURVIVAL AND PERMEABILITY OF ESCHERICHIA COLI. Journal of Bacteriology 85, 567-576.
Seviour, R.J., Nielsen, P.H., 2010. Microbial ecology of activated sludge, IWA Publishing, London, UK.
Tchobanoglous, G., Burton, F.L., Metcalf, Eddy, 2003. Wastewater Engineering : Treatment, Disposal, and Reuse, McGraw-Hill, New York.
Thomsen, T.R., Kong, Y., Nielsen, P.H., 2007. Ecophysiology of abundant denitrifying bacteria in activated sludge. FEMS Microbiology Ecology 60(3), 370-382.
Tian, Y., Zhang, J., Wu, D., Li, Z., Cui, Y., 2013. Distribution variation of a metabolic uncoupler, 2,6-dichlorophenol (2,6-DCP) in long-term sludge culture and their effects on sludge reduction and biological inhibition. Water Research 47(1), 279-288.
US-EPA, 1999. Alternative Disinfectants and Oxidants Guidance Manual, U.S. Environmental Protection Agency, Office of Water.
US-EPA, 2006. Emerging Technologies for Wastewater Biosolids Management, p. 133, U.S. Environmental Protection Agency, Office of Water.
Vergine, P., Menin, G., Canziani, R., Ficara, E., Fabiyi, M., Novak, R., Sandon, A., Bianchi, A., Bergna, G., 2007. Partial ozonation of activated sludge to reduce excess sludge production: evaluation of effects on biomass activity in a full scale demonstration test, pp. 295-302, Moncton, Canada.
von Gunten, U., 2003a. Ozonation of drinking water: Part I. Oxidation kinetics and product formation. Water Research 37(7), 1443-1467.
von Gunten, U., 2003b. Ozonation of drinking water: Part II. Disinfection and by-product formation in presence of bromide, iodide or chlorine. Water Research 37(7), 1469-1487.
Wang, Z., Wang, L., Wang, B.Z., Jiang, Y.F., Liu, S., 2008. Bench-scale study on zero excess activated sludge production process coupled with ozonation unit in membrane bioreactor. Journal of Environmental Science and Health, Part A 43(11), 1325-1332.
Wei, Y., Van Houten, R.T., Borger, A.R., Eikelboom, D.H., Fan, Y., 2003. Minimization of excess sludge production for biological wastewater treatment. Water Research 37(18), 4453-4467.
Wei, Y., Wang, Y., Guo, X., Liu, J., 2009. Sludge reduction potential of the activated sludge process by integrating an oligochaete reactor. Journal of Hazardous Materials 163(1), 87-91.
Whittaker, M., Bergmann, D., Arciero, D., Hooper, A.B., 2000. Electron transfer during the oxidation of ammonia by the chemolithotrophic bacterium Nitrosomonas europaea. Biochimica et Biophysica Acta (BBA) - Bioenergetics 1459(2–3), 346-355.

Winkler, M.K., Bassin, J.P., Kleerebezem, R., Sorokin, D.Y., van Loosdrecht, M.C., 2012. Unravelling the reasons for disproportion in the ratio of AOB and NOB in aerobic granular sludge. Applied Microbiology and Biotechnology 94(6), 1657-1666.
Xia, Y., Kong, Y., Nielsen, P.H., 2007. In situ detection of protein-hydrolysing microorganisms in activated sludge. FEMS Microbiology Ecology 60(1), 156-165.
Yan, S.-T., Chu, L.-B., Xing, X.-H., Yu, A.-F., Sun, X.-L., Jurcik, B., 2009. Analysis of the mechanism of sludge ozonation by a combination of biological and chemical approaches. Water Research 43(1), 195-203.
Yang, X.-F., Xie, M.-L., Liu, Y., 2003. Metabolic uncouplers reduce excess sludge production in an activated sludge process. Process Biochemistry 38(9), 1373-1377.
Yasui, H., Shibata, M., 1994. An innovative approach to reduce excess sludge production in the activated sludge process. Water Science and Technology 30(9), 11-20.
Zhang, G., Zhang, P., Yang, J., Chen, Y., 2007. Ultrasonic reduction of excess sludge from the activated sludge system. Journal of Hazardous Materials 145(3), 515-519.

Chapter 3:

New mechanistically based model for predicting reduction of biosolids waste by ozonation of return activated sludge

Connecting text: In this chapter, the new mathematical model describing the reaction of ozone with the return activated sludge solids is presented. The model is validated by using the first year of pilot-scale operation data and complementary laboratory-scale ozonation experiments with RAS solids and pure cultures. The results of this work have been published in the paper:

Isazadeh, S., Feng, M., Urbina Rivas, L.E., Frigon, D., 2014. New mechanistically based model for predicting reduction of biosolids waste by ozonation of return activated sludge. Journal of Hazardous Materials 270, 160-168.

3.1. INTRODUCTION

Biosolids are the inevitable by-products of wastewater treatment, and their management imposes an important operational cost and logistic burden on treatment plants. As a result, significant efforts have been recently dedicated to the development of technologies that minimize the production of waste biosolids. One promising technology is the ozonation of return activated sludge (RAS), which uses the oxidation capacity of ozone to break down the biomass and non-degradable constituents of mixed liquor volatile suspended solids (MLVSS) in activated sludge, thus making them bioavailable (Chu et al. 2009b, Foladori et al. 2010a, Paul et al. 2012). Despite the fact that ozonation has proven to be an effective process, so far the ability to predict the level of RAS-ozonation performance for the reduction of biosolids has remained limited due to the lack of proper quantitative parameterization of ozone reactions. In this paper, we propose a model that is capable of solving this problem.

Modelling is one of the tools available for predicting the efficiency of ozonation at reducing waste biosolids. Initial models describing RAS-ozonated activated sludge systems used either global model constants or first-order reaction kinetics to parameterize the effect of ozonation on active biomass and non-degradable MLVSS fractions (Mines et al. 2008, Wang et al. 2008, 1994). However, these models could not easily incorporate changes in influent chemical oxygen demand (COD) fractionations (e.g., variations in non-degradable particulate fractions of MLVSS) or variations in operational conditions such as SRT and temperature with ozone effects on biosolids reduction (Paul et al. 2012). Furthermore, they were incapable of clearly describing the effects of ozone on the biomass, which precludes any direct model prediction of the evolution of biological activities in the systems after the installation of new RAS-ozonation units.

Building models based on the International Water Association (IWA) consensus Activated Sludge Models (ASM) can overcome these limitations by taking the specific characteristics of a wastewater treatment plant (WWTP) like changes in SRT, temperature, and influent COD fractions into account. To our knowledge, Salhi (2003) was the first one to suggest an extension to the IWA-ASM1 model describing RAS-ozonation. For the purpose of model development, it was assumed that ozone only attacks the non-active part of the biosolids if the ozone dose is kept under 0.01 g O_3 transferred g^{-1} suspended solids COD. Although this assumption was justified with some experiments measuring the reduction in specific oxygen uptake rates (SOUR) (Chu et al. 2009b, Paul and Debellefontaine 2007), it has been rarely questioned in the literature. In another study using the IWA-ASM3 model (Frigon and Isazadeh 2011), the comparison of simulation results from several modeling scenarios with experimental data on MLVSS concentrations, ATP concentrations, and nitrification activity data suggested that the biomass inactivation rate constants due to ozone were higher than the non-biomass (i.e., particulate non-degradable and particulate substrate COD) transformation rate constants. This result contrasts drastically with previous modelling assumptions used by Salhi (2003), and further work is necessary to resolve the discrepancies.

In the current study, a mechanistically based model was developed following our previous work (Frigon and Isazadeh 2011) and used to simulate the dynamic behaviour of pilot-scale reactors. For model parameterization and calibration, we specifically examined with independent laboratory experiments the effect of RAS-ozonation on biomass by characterizing inactivation constants and COD solubilization efficiencies from four pure bacterial strains grown at high solids densities. We contrasted these results with those obtained from fresh and sonicated MLVSS samples. Then, we compared three modelling approaches with increasing precision in

the description of biomass inactivation using the results from two pilot-scale (1.7 m^3) reactors (control vs. RAS-ozonated) operated for 98 days.

3.2. MATERIALS AND METHODS

3.2.1 Pilot-scale reactors and operation

We operated two pilot-scale activated sludge reactors (RAS-ozonated and control) in parallel on the site of a full-scale municipal wastewater treatment plant. Approximately 45% of the wastewater COD load was from industrial sources, mainly paper production, food processing, and biodiesel production plants. A schematic of the pilot-scale set-up is presented in Fig. 3.1. The influent flow, dissolved oxygen concentrations, and temperatures were monitored online. Both reactors where inoculated with full-scale plant biosolids 60 days before the beginning of the experimental period reported here.

The RAS-ozone contactor was comprised of two pumps: one centrifugal pump to mix the content of the ozone contactor with ozone gas through a venturi and a peristaltic pump to feed the ozone contactor from the RAS line. The ozone concentrations in the feed gas and in the vent gas were checked manually using online ozone analyzer (model IN2000-L2-LC; INUSA Inc., Norwood, MA, USA). The gas flow rate was varied to adjust the ozone dosage. The experimental period was divided into four phases corresponding to the four ozone dosages used in the ozone contactor: Phase I no-ozone (Day 1-Day 23), Phase II low ozone dose (22 mg/L or 2.1 mg-O_3 g^{-1}-$MLVSS_{inventory}$ d^{-1}, Day 33-Day 52), Phase III medium ozone dose (60 mg/L or 4.0 mg-O_3 g^{-1}-$MLVSS_{inventory}$ d^{-1}, Day 53-Day 76), and Phase IV high ozone dose (98 mg/L or 8.3 mg-O_3 g^{-1}-$MLVSS_{inventory}$ d^{-1}, Day 77-Day 98).

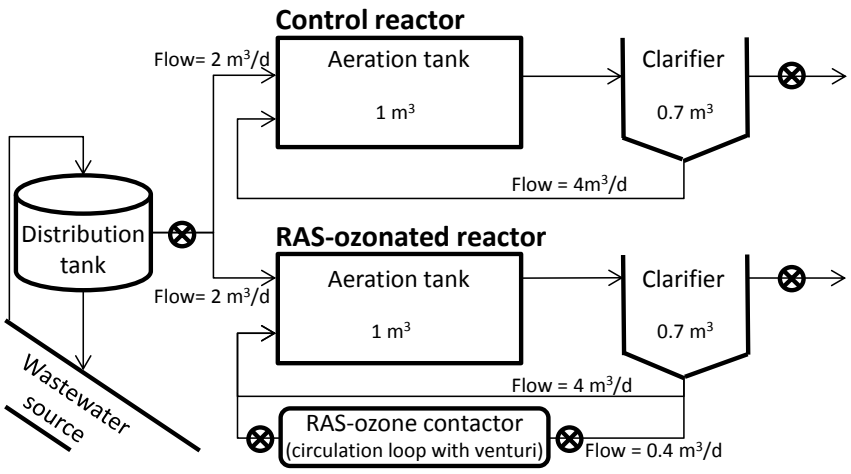

Fig. 3.1. Schematics of the control and RAS-ozonated pilot-scale activated sludge reactors. Arrows indicate water flows. Target flow rates, size of the units, and the autosampler locations (⊗) are indicated.

3.2.2 Sampling and analytical methods

Five auto-samplers obtained 24 h-composite samples from each of the influents and effluents of the activated sludge reactors and the RAS-ozone contactor. Daily samples were kept frozen at −20 °C (except for suspended solids which were kept at 4 °C), and subsequently combined with samples from adjacent days to get two-day or three-day (week-ends) composite samples (i.e., 48 and 72 sub-samples respectively) for analysis. The analysis of total and volatile suspended solids (TSS,VSS; method 2540), total and soluble (filtered through 0.45-µm membrane) COD (method 5220D), and soluble carbonaceous BOD_5 (method 5210B), ammonium (NH_4^+; method 4500-NH_3-F), nitrite (NO_2^-; method 4500-NO_2^--B), and nitrate (NO_3^-; method 4500-NO_3^--H) were performed following standard methods (APHA et al. 2005). The latter nutrients (NH_4^+, NO_2^- and NO_3^-) were measured in a microplate-scale version of the colorimetric methods using a SpectraMax M5 microplate reader (Molecular device, USA).

Grab samples from the aeration tanks, clarifiers, and wasted biosolids were obtained three times a week and processed the same day for analysis of TSS and VSS. Periodically, grab MLSS samples were obtained to determine the active biomass fraction by measuring cellular adenosine triphosphate (ATP) using the Quench Gone 21 Wastewater ATP bioluminescence kit (LuminUltra, Fredericton, New Brunswick, Canada).

3.2.3 Biomass inactivation and COD solubilisation at pilot and laboratory scales

Biomass inactivation constants and COD solubilization efficiencies were examined using specific experiments in two different RAS-ozone contactors: a pilot-scale continuous contactor (Section 3.2.1) and a laboratory-scale 2-L batch contactor. The normal operation of the pilot-scale contactor was interrupted periodically to perform *ad hoc* experiments on the RAS from both the control and the RAS-ozonated reactors. During these experiments, the RAS flow rates were the same as those during normal operation, but the ozone gas flow rate (10% [v/v] ozone) was adjusted every two hours. The ozone concentrations in the feed and vent-gas were measured online to determine the dosage as described above.

Samples were collected from the influent and effluent of the RAS-ozone contactor, immediately stored on ice to minimize additional reactions, and processed in the laboratory within a few hours of sampling to measure the soluble COD and VSS concentrations (Section 3.2.2). COD solubilization efficiency was calculated by plotting measured soluble COD versus ozone doses and regressing a linear model. For heterotrophic biomass activity in each dose, solids suspensions were centrifuged, washed twice with filtered pilot-scale control activated sludge reactor effluent to ensure the removal of possible soluble COD release after ozonation, and re-suspended in 250 mL of the same effluent used for washing. Then, suspensions were mixed with 250 mL of Tris buffer (0.025 M, pH 7.8) giving a final solids concentration of

~1,000-1,500 mg/L, and introduced in the 550-mL-bottle respirometer (AER-208, Challenge Technology, AR, USA). Finally, the maximum heterotrophic biomass activity was measured as the increase in oxygen uptake rates (OUR) upon the injection of sodium acetate (400 mg/L final concentration).

The laboratory-scale ozone contactor was a 2-L conical glass container, and the reactor content was continuously mixed during ozonation to enhance gas transfer and prevent foaming. Ozone was produced using a model-Ozo 2VTT ozone generator (Ozomax, Inc., Sherbrooke, Canada), and injected into the reactor through a glass bubble diffuser. Ozone dosage was determined by measuring the ozone concentrations of the feed and vent-gas streams using a Mini-HiCon O_3 analyzer (INUSA Inc., Norwood, MA, USA). Laboratory-scale ozone contactor experiments proceeded in a similar fashion to the pilot-scale ozone contactor except that ozone dose was controlled by exposure time.

The biomass inactivation coefficients ($\eta_{OHO,O3,inact}$) were calculated by regression of the SOUR vs. $O_{3,dose}$ following an exponential function, and the COD solubilization efficiencies were calculated by regression of the increased soluble COD vs. $O_{3,dose}$ following a linear model. The values of these constants obtained in the laboratory-scale ozonator were compared between fresh RAS samples, sonicated RAS samples, and bacterial pure cultures to determine the effects of particle size and the floc matrix on the ozone reactions, and to better describe the biomass inactivation process. For fresh vs. sonicated RAS solids, the samples were split into two portions, and one of them was dispersed using a Cole-Parmer model 8892 Ultrasonic Cleaner sonication bath for 3 min (Cole-Parmer, Montreal, Canada). For estimation of biomass inactivation, biosolids washed twice prior to the respirometric test with same buffer solution to remove the potential soluble COD increase. Particle size distributions were determined using a Lasentec

model M100 F laser scanning particle size analyzer (Lasentec FBRM, Redmond, WA, USA). Four bacterial species were used to characterize the ozone inactivation reaction: *Escherichia coli* strain K12*, Rhodococcus jostii* strain RHA1, *Cupriavidus necator* strain DSM428 (wild-type), and *Cupriavidus necator* strain DSM541 (a mutant of strain DMS428 that is incapable of accumulating poly-β-hydrohybutyrate). All strains were cultured individually in a Luria-Bertani medium (Sambrook and Russell 2001) up to the stationary phase and concentrated by centrifugation prior to ozonation.

3.2.4 Mathematical model of ozone reactions

The model relies on the separation of the ozone reaction efficiency (due to ozone reacting with the biosolids), and the biosolids reduction efficiency (due to the biosolids composition and bioreactor operations). The model assumes that two groups of processes represent the effect of ozone on the biosolids: (i) the ***transformation/mineralization*** of non-biomass solids (which includes direct oxidation of the solids COD by ozone) and (ii) the ***inactivation*** of biomass. Unlike the previously presented model (Frigon and Isazadeh 2011), the process rates were separated in this version such that the inactivation can be evaluated separately.

The main process input variables for the simulation of the RAS-ozone contactor were the fraction of the MLVSS inventory (expressed as COD) solubilized per day ($q_{X\text{tot,O3sol}}$), the ozone dose (mg/L) and the fraction of MLVSS inventory exposed to ozone per day ($q_{\text{MLVSS treated}}$) to calculate the fraction of biomass inactivated. Note that MLVSS inventory is a mass of accumulated biosloids in the activated sludge aeration tank at a given time. The non-biomass solid transformation rate constant and biomass inactivation rate constant were linked to $q_{X\text{tot,O3,sol}}$ through eq.1.

$q_{Xtot,O3,sol} = q_{XU\_XCB,O3,trans} \times (1 - f_{Bio,storage}) \times (f_{SU\_O3,trans} + f_{SB\_O3,trans}) + b_{Bio,O3,inact} \times f_{Bio} \times (f_{SU\_O3,inact} + f_{SB\_O3,inact})$ **(eq. 1)**

where $f_{Bio,storage}$ and f_{Bio} are biomass fractions including storage compounds (eq. 2 and eq. 3, respectively). Non-biomass solid transformation rate can be calculated by subtracting two other terms in eq.1

$f_{Bio,storage} = (X_{OHO}+X_{ANO}+X_{STO})/(X_{OHO}+X_{ANO}+X_{STO}+X_{CB}+X_{U})$ **(eq 2)**

$f_{Bio} = (X_{OHO}+X_{ANO})/(X_{OHO}+X_{ANO}+X_{STO}+X_{CB}+X_{U})$ **(eq. 3)**

$f_{SU\_O3,trans}$ and $f_{SU\_O3,inact}$ are the fractions of solubilized undegradable COD, $f_{SB\_O3,trans}$ and $f_{SB\_O3,inact}$ are the fractions of solubilized biodegradable COD, and $f_{XU\_Bio,lys}$ is the fraction of biomass debris ($X_{U\_Bio,lys}$) generated by decay. The biomass inactivation rates ($b_{Bio,O3,inact} = b_{OHO,O3,inact} = b_{ANO,O3,inact}$) are obtained from eq.4.

$b_{OHO,O3,inact} = \exp(-\eta_{OHO,O3,inact} \times O_{3,dose}) \times q_{MLVSS\ treated}$ **(eq. 4)**

where $\eta_{OHO,O3,inact}$ is the inactivation constant [$m^3.g^{-1}$], which was determined by *ad hoc* inactivation experiments (see Section 3.2.3); $O_{3,dose}$ is the dose of ozone applied in the RAS-ozone contactor [$g.m^{-3}$]; and $q_{MLVSS\ treated}$ is the fraction of biosolids inventory exposed to ozone per day [d^{-1}] (eq.5).

$q_{MLVSS\ treated} = Q_{contactor} \times RAS\text{-}VSS_{contactor} / (MLVSS_{reactor} \times V_{reactor})$ **(eq.5)**

where $Q_{contactor}$ and $RAS\text{-}VSS_{contactor}$ are the biosolids flow rate and concentration, respectively, passing through the ozone contactor per day; $MLVSS_{reactor}$ and $V_{reactor}$ are the volatile suspended solids in the biological reactor and its volume, respectively.

The Gujer matrix of the model extension to IWA-ASM3 is presented in Table 3.1. All model notations follow the proposal of Corominas et al. (2010). Three modelling approaches were compared.

1) Biomass inactivation was assumed linearly related to the ozone dose in the RAS-ozone contactor with a constant ratio between inactivation ($b_{Bio,O3,inact} = b_{OHO,O3,inact} = b_{ANO,O3,inact}$) and transformation ($q_{XU\_XCB,O3,trans}$) rate constants. The solubilisation fractions for inactivation and transformation were assumed equal. Three ozone model parameters were adjusted for model fitting: (i) ratio $b_{Bio,O3,inact} / q_{XU\_XCB,O3,trans}$, (ii) $f_{SU\_O3,inact} = f_{SU\_O3,trans}$, and (iii) $f_{SB\_O3,inact} = f_{SB\_O3,trans}$. This approach is similar to our previous study (Frigon and Isazadeh 2011).
2) Biomass inactivation was assumed exponentially related to the ozone dose and calibrated from experiments that were independent of the model fitting (section 3.2.3). The solubilisation fractions for inactivation and transformation were assumed equal and adjusted as for Approach 1.
3) Biomass inactivation was assumed exponentially related to the ozone dose and calibrated as for Approach 2 along with solubilized COD fractions ($f_{SU\_O3,inact}$ and $f_{SB\_O3,inact}$). Only $f_{SB\_O3,trans}$ and $f_{SU\_O3,trans}$ were adjusted for model fitting.

Table 3.1. Gujer stoichiometry matrix and process rates for the IWA-ASM3 model extension describing ozone conversions.

Process	COD and N pool										Rates
	S_B	S_U	S_{O3}	S_{NH4}[a]	XC_B	XC_{B_Stor}[b]	X_{OHO}	$X_{OHO,Stor}$	X_{ANO}	X_{U_Inf}	$X_{U\_Bio,lys}$	
Transformation												
Undegradable (influent)	$f_{SB\_O3,trans}$	$f_{SU\_O3,trans}$	$f_{mnr,O3}$	$i_{N\_XU\_inf} - (f_{XCB\_O3,inact} \times i_{N\_XCB})$	$f_{XCB\_O3,trans}$					-1		$q_{XU\_XCB,O3,trans} \times X_{U,inf}$
Undegradable (decay residue)	$f_{SB\_O3,trans}$	$f_{SU\_O3,trans}$	$f_{mnr,O3}$	$i_{N\_XU\_Bio,lys} - (f_{XCB\_O3,inact} \times i_{N\_XCB})$	$f_{XCB\_O3,trans}$						-1	$q_{XU\_XCB,O3,trans} \times X_{U\_Bio,lys}$
Biodegradable	$f_{SB\_O3,trans}$	$f_{SU\_O3,trans}$	$f_{mnr,O3}$	$i_{N\_XCB} \times (f_{XCB\_O3,trans} - 1)$	$f_{XCB\_O3,trans} - 1$							$q_{XU\_XCB,O3,trans} \times XC_B$
Inactivation												
Heterotrophs	$f_{SB\_O3,inact}$	$f_{SU\_O3,inact}$		$i_{N\_XBio} - (f_{XU\_Bio,lys} \times i_{N\_XBio,}) - (f_{XCB\_O3,inact} \times i_{N\_XCB})$	$f_{XCB\_O3,inact}$		-1				$f_{XU\_Bio,lys}$	$b_{OHO,O3,inact} \times X_{OHO}$
Storage						$+1$		-1				$b_{OHO,O3,inact} \times X_{OHO,Stor}$
Autotrophs	$f_{SB\_O3,inact}$	$f_{SU\_O3,inact}$		$i_{N\_XBio} - (f_{XU\_Bio,lys} \times i_{N\_XBio}) - (f_{XCB\_O3,inact} \times i_{N\_XCB})$	$f_{XCB\_O3,inact}$				-1		$f_{XU\_Bio,lys}$	$b_{ANO,O3,inact} \times X_{ANO}$[c]

[a] Note that S_B, and S_U, were, at this point, assumed not to contain nitrogen.
[b] XC_{B_Stor} is consumed at the same rate as XC_B but does not contains nitrogen.
[c] Current modelling assumption: $b_{OHO,O3,inact} = b_{ANO,O3,inact} = b_{Bio,O3,inact}$.

3.2.5 Model calibration

The model parameters suggested by Hauduc et al. (2011) were used as default values for the IWA-ASM3 model except for the heterotrophs' S_B and S_{NOx} half-saturation constants ($K_{SB,OHO}$ and $K_{NOx,OHO}$, respectively), and the nitrifier's S_{NH} half-saturation constant ($K_{NHx,ANO}$). These constants, along with the influent COD fractionations, were calibrated (fitted) using the control reactor operation data: MLVSS inventories, ATP levels per MLVSS, and effluent soluble COD and nitrate concentrations. The concentration of biomass (X_{OHO} and X_{ANO}) in the influent was assumed to be zero. The clarifiers were divided in two parts: the top non-reactive and the reactive bottom part for anoxic conditions (i.e., significant denitrification occurrence) to capture the accumulation of solids.

The solubilized daily fraction of MLVSS inventory ($q_{Xtot,O3sol}$) was measured and used as the input process variable. Biomass inactivation rates ($b_{OHO,O3,inact}$ and $b_{ANO,O3,inact}$) and solubilization fractions ($f_{SB\_O3,inact}$ and $f_{SU\_O3,inact}$) were calibrated by *ad hoc* experiments (Section 3.2.3), and the rates were adjusted using the proportion of MLVSS inventory exposed to ozone daily (eq. 4).

The non-biomass transformation rate constant ($q_{XU\_XCB,O3,trans}$) was calculated from $q_{Xtot,O3sol}$ and $b_{Bio,O3,inact}$ (eq. 1). The ozone model parameters (different ones depending on the modeling approach) were calibrated by fitting predictions to the measured ozonated reactor data: MLVSS inventories, ATP levels per MLVSS, and effluent soluble COD, soluble carbonaceous BOD_5 and nitrate concentrations.

Two statistical tests were used to evaluate the goodness-of-fit during calibration (i.e., simulations vs. observations) and narrow down the possible simulated solution space, namely the t-test (min. $P>0.05$) with unequal variance and the major axis (MA) regression analysis test of

Mesple et al (1996) (null hypothesis criteria: slope=1 [P>0.05] and intercept=0 [P>0.05]). The final fitting was done minimizing the relative sum of square errors using the simplex algorithm (Reichert 1998). All dynamic calculations were performed with AQUASIM ver. 2.0 (Reichert 1998).

3.3. RESULTS

3.3.1 Biomass inactivation and COD solubilization

COD solubilization efficiencies and biomass inactivation profiles were determined using RAS from both control (4 experiments) and the RAS-ozonated reactor (5 experiments) while increasing the ozone dose over a few hours. Our results mirrored those of published reports (Foladori et al. 2010b, Paul et al. 2012), in which the amount of soluble COD increased linearly with the ozone dose. The average COD solubilization efficiencies for the RAS samples from the control or the RAS-ozonated reactors were not significantly different (P>0.05) from each other (Table 3.2); and they were within the range of observed efficiencies compiled from other studies (Labelle et al. 2011). Analyzing inactivation data, it was noticed that the average heterotrophic SOUR significantly increased (P<0.05) after the ozone contactor when ozone was not added to the contactor (Fig. 3.2). Microscopic examinations suggested that the floc structure had been broken during the passage through the ozone contactor. Considering only contactor effluent samples, the SOUR decreased exponentially when the ozone dose increased (Fig. 3.3).

To investigate further the impact of the floc structure on the inactivation and solubilization constants, RAS samples were obtained from the same full-scale activated sludge wastewater treatment plant where the pilot-scale study was conducted, and they were ozonated in a laboratory-scale batch contactor. Unexpectedly, the SOUR increased slightly when the RAS was

exposed to low ozone doses (Fig. 3.2 and 3.3). However, the SOUR increase associated with low ozone doses was completely eliminated by slight sonication (Fig. 3. 2 and 3.3). As it was expected, sonication changed the observed floc structure microscopically (Fig. 3.S1), and decreased the average particle diameter by approximately 60 μm (Fig. 3.S2). Once the initial SOUR increases due to low ozone doses were accounted for, the inactivation constants for the fresh and sonicated RAS samples were not significantly different ($P>0.05$; Table 3.2). In contrast, the COD solubilization efficiency for the sonicated RAS samples was 48% higher than for the fresh samples. However, this increase was not significant ($P>0.05$) due to the high variability of the solubilization efficiencies after sonication (Table 3.2).

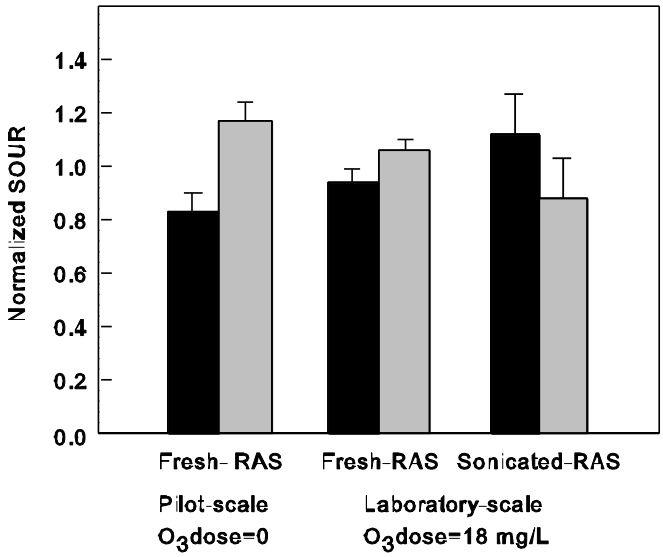

Fig. 3.2. Change in maximum heterotrophic SOUR for RAS samples treated in the pilot-scale ozone contactor without ozone dosed (n=9 experiments) and in laboratory-scale contactor with an average ozone dose of 18 mg/L (n=3 experiments) before and after sonication. Average SOURs of each experimental set were normalized to 1. Black bar: before treatment; grey bar after treatment.

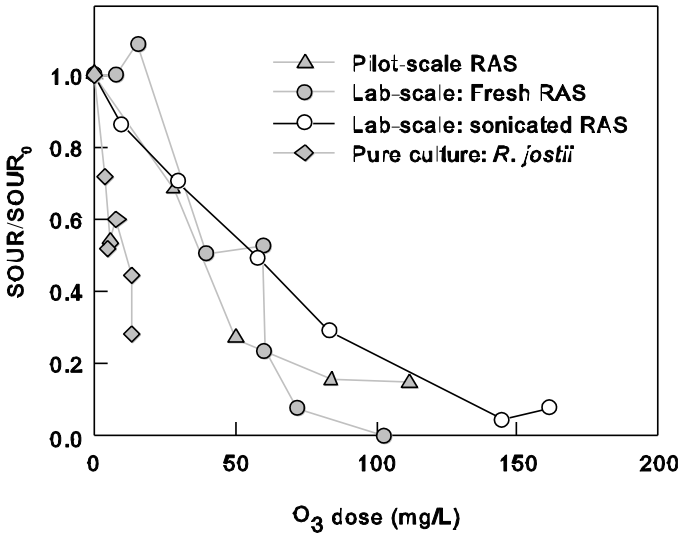

Fig. 3.3. Representative profiles of heterotrophic SOUR as a function of ozone dose for pilot-scale experiments (solid grey triangles), and for laboratory-scale experiments on fresh (solid grey circles) and sonicated (open white circles) RAS samples and pure culture (*Rhodococcus jostii stain* RHA1, solid grey diamonds).

Table 3.2. Average biomass inactivation rate after ozone exposure measured during pilot-scale and laboratory experiments.

Experimental studies	Sample	Inactivation constant ($mg\ O_3/L)^{-1}$	COD solubilization efficiency (mg COD/mg O_3)
Pilot-scale ozonated			
RAS of control reactor	4	0.015±0.003	2.29±0.27
RAS of ozonated reactor	5	0.013±0.001	2.04±0.25
Laboratory-scale ozonated			
Fresh RAS	3	0.020±0.005	2.47±0.03
Sonicated RAS	3	0.021±0.001	3.34±0.40
Laboratory-scale on pure culture			
Average of four pure cultures [a]	4	0.063±0.011	1.48±0.37

[a] *Escherichia coli* strain K12, *Rhodococcus jostii* stain RHA1, *Cupriavidus necator* strain DSM428, *Cupriavidus necator* strain DSM541

To substantiate our description of the biomass inactivation reaction in the model, we performed similar laboratory-scale ozonation experiments with four pure bacterial strains. The

fours strains behaved similarly exhibiting a rapid decrease in SOUR upon exposure to low ozone doses (Fig. 3.3). Although their average inactivation constant was more than 3 times higher ($P<0.05$) than the one of the fresh RAS samples treated in the same ozone contactor, their average COD solubilization efficiency was 40% lower ($P<0.05$; Table 3.2). This suggests that biomass inactivation does not immediately release soluble COD. In fact, at the dose sufficient to cause 50% inactivation of the pure cultures, only 8.2 ± 3.5% (± standard error, n=4 strains) of the biomass COD was solubilized.

3.3.2 Pilot-scale reactor operation

The pilot-scale reactors were operated for 98 days separated in four phases of 3-4 weeks. Phase 1 (no ozone) measured the steady-state conditions before the start of ozonation. Ten days of operation separated Phase 1 and Phase 2 to solve a number of technical issues related to the installation and start-up of the RAS-ozone contactor. Then, in Phases 2 to 4, the ozone dosage was progressively increased, which resulted in an increase in COD solubilization as measured daily and biomass inactivation (Fig. 3.4a) as calculated from the ozone dose and the calibrated inactivation constants reported in Section 3.1.

Since the COD loadings were the same for both control and RAS-ozonated reactors (Fig. 3.4b) and the goal was to keep the inventories of solids same in both reactors, the SRT in the RAS-ozonated reactor progressively increased above the target SRT for the control reactor that was set at ~ 6 days (Fig. 3.4b). In line with literature observations (Chu et al. 2009b), the fraction of MLVSS/MLSS decreased due to ozonation (Fig. 3.4c), while the solids inventories increased in both reactors during the experiment due to the gradual accumulation of solids in the clarifiers (Fig. 3.4d). RAS-ozonation also caused an increase in the ozonated reactor effluent soluble COD

(Fig. 3.4e). Finally, since the study took place between the month of September and December the temperature dropped from 22 °C at the beginning to 15 °C at the end of the experiment (Fig. 3.4c). The observed reduction in waste biosolids increased with increasing ozone dose to reach approximately 46% during the final phase (Fig. 3.5). Additional operation parameters are presented in supplementary materials (Fig. 3.S3).

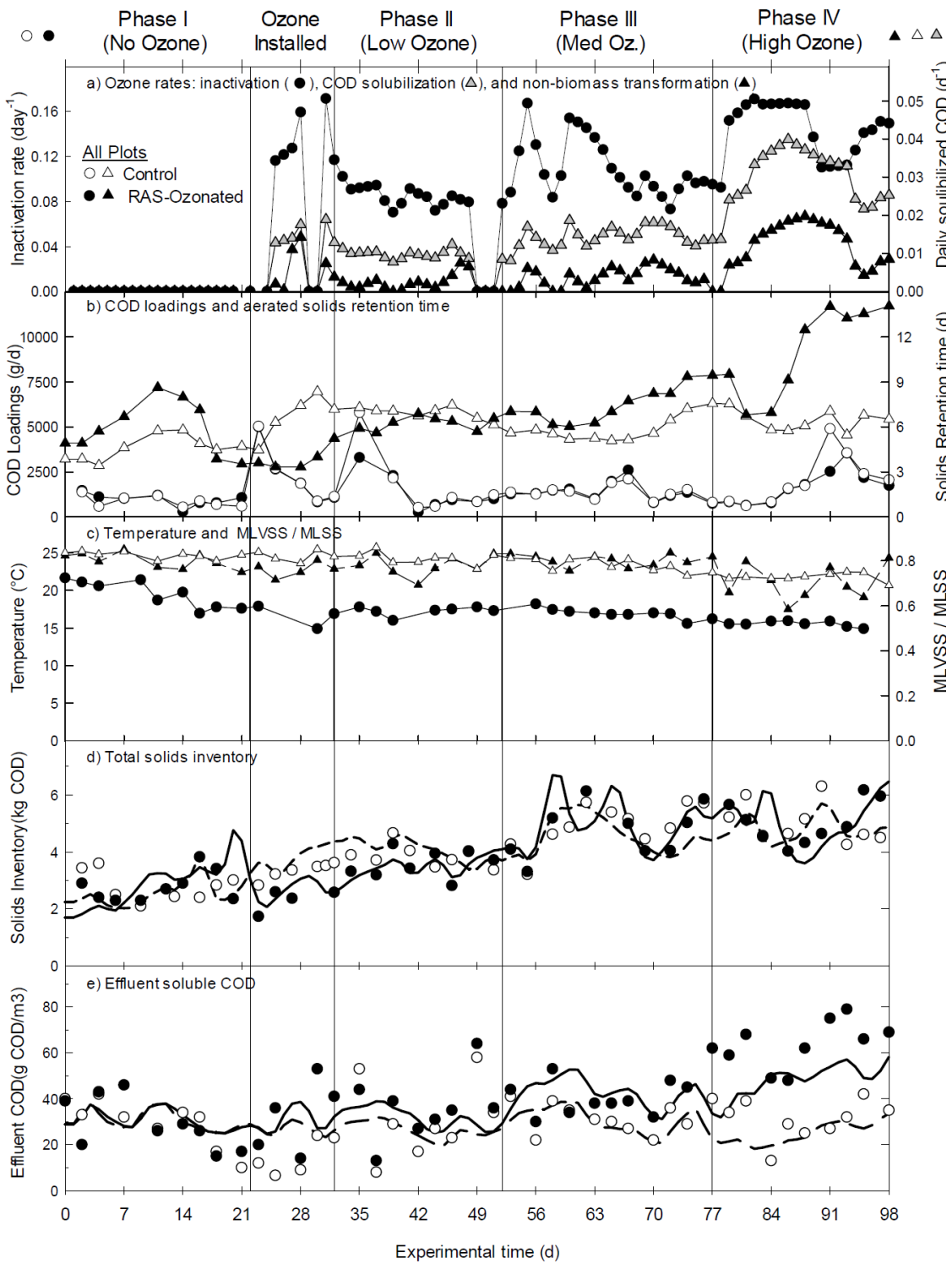

Fig. 3.4. Operational data and simulation results for pilot-scale control and RAS-ozonated reactors. Circles should be read with the left-side axes, while triangles with the right-side axes. In all plots, symbols represent measured data and thick continuous lines shows model predictions (control: open symbols and dashed lines; RAS-ozonated: solid symbols and solid lines).

3.3.3 Model calibration and validation

The data from the RAS-ozonated reactors were fitted by adjusting the ozone reaction parameters using the three modeling approaches with increasing precision in the description of the biomass inactivation. (1) Inactivation linearly related to ozone dose, and all ozone parameters adjusted for the model state-variables to best fit the observed data. (2) Inactivation exponentially related to ozone dose calibrated with Section 3.1 data, and ozone inactivation and transformation fractions adjusted by fitting. (3) Inactivation exponentially related to ozone dose with both rate constant and solubilisation fractions calibrated with Section 3.1 data ($f_{SB\_O3,inact} + f_{SU\_O3,inact} = 8.2\%$, and for simplicity $f_{SU\_O3,inact} / [f_{SB\_O3,inact} + f_{SU\_O3,inact}] = f_{XU\_Bio,lys}$). Table 3.S1 presents the values of the calibrated ozone model parameters. Improving the description accuracy of the biomass inactivation process improved substantially the best fits obtained for the four different observed variables used in fitting, with Approach 3 providing the best results (Table 3.3; note: because the SRT is a model input variable, improvement of the solids inventories predictions result in improvements in biosolids reductions predictions also). This increased model accuracy occurred despite a reduction in the number of ozone parameters used in the fitting exercise. The details of the model prediction quality for the variable profiles obtained with Approach 3 is also presented visually in Fig. 3.4d, 3.4e, Fig. 3.S3e, and Fig. 3.5.

Table 3.3. Relative mean squared error for the best fits between observations and predictions in three modelling approaches with increasing precision in the description of the biomass inactivation process.

Fitted state-variables	Linear inactivation Transformation fractions adjusted	Exponential inactivation Transformation fractions adjusted	Exponential inactivation Inactivation fractions from experiments
Adjusted ozone model parameters for fitting	• $b_{Bio,O3,inact}/q_{XU\_XCB,O3,trans}$ • $f_{SU\_O3,trans} = f_{SU\_O3,inact}$ • $f_{SB\_O3,trans} = f_{SB\_O3,inact}$	• $f_{SU\_O3,\ trans} = f_{SU\_O3,inact}$ • $f_{SB\_O3,\ trans} = f_{SB\_O3,inact}$	• $f_{SU\_O3,trans}$ • $f_{SB\_O3,trans}$
Biosolids inventory [a] [%]	23.3	22.0	21.8
Soluble undegradable (S_U)[b] [%]	19.5	14.0	12.0
Soluble biodegradable (S_B)[b] [%]	27.9	25.9	20.5
Nitrate (S_{NO3}) [%]	23.8	21.8	20.1

[a] Since SRT is a model input parameter, errors on the solids inventory and on biosolids production rate are equivalent.
[b] S_B fitted against effluent soluble carbonaceous BOD_5 with a conversion factor of 0.65, and S_U fitted against effluent soluble COD minus soluble BOD_5.

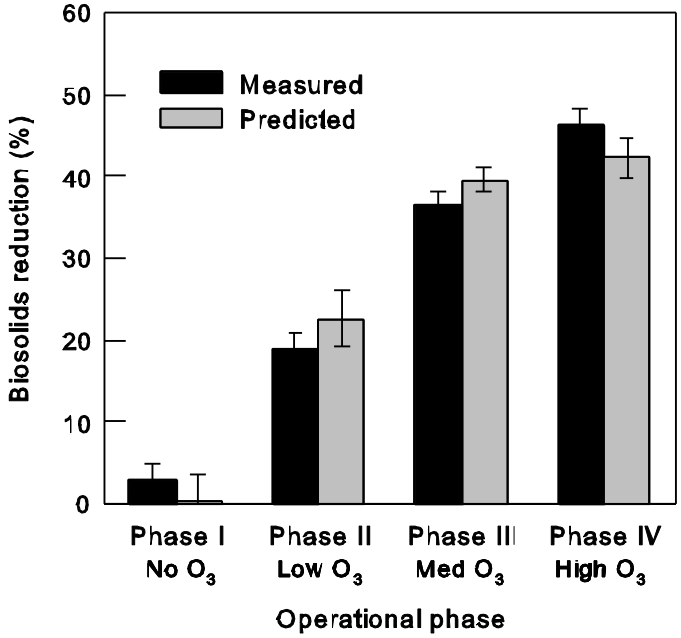

Fig. 3.5. Predicted vs. measured average percent reduction in excess biosolids production for each phase; ozone was not dosed in Phase I and then progressively increased from Phase II to Phase IV.

3.4. DISCUSSION

Variety of techniques such as heterotrophic plate count, heterotrophic maximum specific OUR (SOUR), solids ATP concentrations and enzymatic (e.g., protease) activities (Chu et al. 2008, Chu et al. 2009a, Labelle et al. 2011, Paul and Debellefontaine 2007, Yan et al. 2009, Yasui and Shibata 1994) can be used to measure biomass inactivation during ozonation. In general, several authors disagree on the dose-response model for RAS biomass inactivation by ozone, and on the existence of an ozone dose threshold before the onset of inactivation. In our data, we did not find evidence supporting the use of another model other than the widely accepted Chick-Watson-type model (Crittenden et al. 2005) This model showed an exponential decrease in active biomass with increase in ozone doses (Fig. 3. 3). For the reported thresholds, which contradicts with our finding, it appears that they were observed when using activity (SOUR and enzymatic) data (Chu et al. 2009a, Dziurla et al. 2005, Paul and Debellefontaine 2007), but were not observed with other data (Chu et al. 2008, Labelle et al. 2011, Yan et al. 2009, Yasui and Shibata 1994). The data obtained in the current study may offer an explanation for these contrasting observations. The SOURs increased through the pilot-scale ozone contactor while no ozone dose was applied (Fig. 3. 2). This was the result of important mechanical shear that was likely developed by the pump and the venturi, which disrupted the floc structure as observed microscopically. The SOURs also increased upon exposure to low ozone doses in the laboratory-scale contactor (Fig. 3. 2). This is not an expected outcome because ozone is a strong oxidant capable of inactivation at low doses for pure cultures (Fig. 3. 3). However, exposure to low ozone doses did not increase the SOURs after the floc size had been reduced by sonication (Fig. 3. 2). Therefore, these results together suggest that the SOUR increase in the laboratory-scale contactor after a low-ozone dose

treatment is likely due to a disruption of the floc allowing for a better substrate uptake by the biomass.

The ozone doses at which the SOUR increases were observed (<20 mg O_3/L equivalent to <0.006 mg O_3/mg TSS) were lower than the reported threshold by other groups (0.01 mg O_3/mg TSS) (Paul and Debellefontaine 2007). For the same ozone dose range, other studies that measured cell inactivation using flow cytometry and the live/dead stain also found a rapid decrease in intact cell upon exposure of RAS to even the smallest dose of ozone (Foladori et al. 2010c). Therefore, it is possible that the inactivation threshold observed in the literature is the result of an undetected modification of the floc structure causing an increase of activity at low ozone doses; which should be interpreted as an artifact of the experimental approach.

The results presented here also suggest that the inactivation of biomass cause little direct solubilization. Work with pure cultures showed much lower solubilization efficiencies than with RAS (Table 3.2). This has also been reported by others in previous studies (Paul and Debellefontaine 2007). In fact, once the pure cultures were 50% inactivated, only 8.2% of the initial solids COD had been solubilized. This result is similar to results from the previous flow cytometry in which 3% of the initial COD was reported solubilized while 50% of the cells had lost their energized membrane, a sign of cell inactivation (Foladori et al. 2010c). Thus, it appears that the common way to describe the effect of ozone on activated sludge solids "solubilization of biomass content" is somewhat inaccurate. The more plausible description seems to be the one adopted here for model purposes: (1) biomass is rapidly inactivated at low ozone doses with little release (8.2%) of soluble COD, (2) ozone reacting with influent non-degradable particulate COD, biomass debris and exopolymeric substances (EPS) cause the observed COD solubilization. Future work could elucidate the exact reactions leading to COD solubilisation.

3.5. CONCLUSIONS

Our extension to IWA-ASM3 with the most accurate description of biomass inactivation during RAS-ozonation successfully predicts the solids inventory, the reduction of waste biosolids production, and the effluent characteristics in a pilot-scale reactor. Biomass inactivation rate constant ($b_{OHO,O3,inact}$) was higher than the non-biomass transformation rate constants ($q_{XU\_XCB,O3,trans}$), suggesting that biomass is more sensitive to ozone exposure than non-biomass solids even at low ozone doses. However, biomass inactivation caused little COD solubilization. Delays in biomass inactivation upon exposure of RAS to low ozone doses observed in this study and in the literature are likely connected to the floc structure. This can hinder the ability to measure the inactivation constants at using SOUR or other activity based measurements.

3.6. ACKNOWLEDGMENTS

This work was funded by the Natural Sciences and Engineering Research Council of Canada's Collaboration Research and Development program (NSRC-CRD) in collaboration with Air Liquide Canada and the Régie de l'Assainissement des Eaux du Bassin LaPrairie (RAEBL). The authors thank Michel Épiney of Air Liquide, the technical staff of the RAEBL, John Bartczak of McGill University, for providing technical advice and several undergraduate and MEng students for their assistance in the construction and operation of the pilot-scale units. Dr. Pinar Ozcer and Hala Jawlakh are thanked for reviewing earlier versions of this manuscript.

3.7. REFERENCES

APHA, AWWA, WEF, 2005. Standard Methods for the Examination of Water and Wastewater, American Public Health Association, Washington, DC, USA.

Chu, L.-B., Yan, S.-T., Xing, X.-H., Yu, A.-F., Sun, X.-L., Jurcik, B., 2008. Enhanced sludge solubilization by microbubble ozonation. Chemosphere 72(2), 205-212.

Chu, L., Wang, J., Wang, B., Xing, X.-H., Yan, S., Sun, X., Jurcik, B., 2009a. Changes in biomass activity and characteristics of activated sludge exposed to low ozone dose. Chemosphere 77(2), 269-272.

Chu, L., Yan, S., Xing, X.-H., Sun, X., Jurcik, B., 2009b. Progress and perspectives of sludge ozonation as a powerful pretreatment method for minimization of excess sludge production. Water Research 43(7), 1811-1822.

Corominas, L., Rieger, L., Takacs, I., Ekama, G., Hauduc, H., Vanrolleghem, P.A., Oehmen, A., Gernaey, K.V., van Loosdrecht, M.C.M., Comeau, Y., 2010. New framework for standardized notation in wastewater treatment modelling. Water Science and Technology 61(4), 841-857.

Crittenden, J.C., Trussell, R.R., Hand, D.W., Howe, K.J., Tchobanoglous, G., 2005. Water Treatment - Principles and Design (2nd Edition), John Wiley & Sons.

Dziurla, M.A., Salhi, M., Leroy, P., Paul, E., Ginestet, P., Block, J.C., 2005. Variations of respiratory activity and glutathione in activated sludges exposed to low ozone doses. Water Research 39(12), 2591-2598.

Foladori, P., Andreottola, G., Ziglio, G., 2010a. Sludge Reduction Technologies in Wastewater Treatment Plants, IWA Publishing, London, UK.

Foladori, P., Andreottola, G., Ziglio, G., 2010b. Sludge Reduction Technologies in Wastewater Treatment Plants, IWA Publishing, London, UK.

Foladori, P., Tamburini, S., Bruni, L., 2010c. Bacteria permeabilization and disruption caused by sludge reduction technologies evaluated by flow cytometry. Water Research 44(17), 4888-4899.

Frigon, D., Isazadeh, S., 2011. Evaluation of a new model for the reduction of excess sludge production by ozonation of return activated sludge: what solids COD fraction is affected? Water Science and Technology 63(1), 156-163.

Hauduc, H., Rieger, L., Ohtsuki, T., Shaw, A., Takacs, I., Winkler, S., Heduit, A., Vanrolleghem, P.A., Gillot, S., 2011. Activated sludge modelling: development and potential use of a practical applications database. Water Science and Technology 63(10), 2164-2182.

Labelle, M.A., Ramdani, A., Deleris, S., Gadbois, A., Dold, P., Comeau, Y., 2011. Ozonation of endogenous residue and active biomass from a synthetic activated sludge. Water Science and Technology 63(2), 297-302.

Mesplé, F., Troussellier, M., Casellas, C., Legendre, P., 1996. Evaluation of simple statistical criteria to qualify a simulation. Ecological Modelling 88(1–3), 9-18.

Mines, R.O., Northenor, C.B., Murchison, M., 2008. Oxidation and ozonation of waste activated sludge. Journal of Environmental Science and Health, Part A 43(6), 610-618.

Paul, E., Debellefontaine, H., 2007. Reduction of excess sludge produced by biological treatment processes: effect of ozonation on biomass and on sludge. Ozone-Science & Engineering 29(6), 415-427.

Paul, E., Liu, Q.-S., Liu, Y., 2012. Biological Sludge Minimization and Biomaterials/Bioenergy Recovery Technologies. Paul, E. and Liu, Y. (eds), p. 209, John Wiley & Sons, Inc, Hoboken, New Jersey.

Reichert, P., 1998. AQUASIM 2.0: computer program for the identification and simulation of aquatic systems, Swiss Federal Institute for Environmental Science and Technology (EAWAG).

Salhi, M., 2003. Procédés couplés boues activées - ozonation pour la réduction de la production de boues, Toulouse, INSA.

Sambrook, J., Russell, D., 2001. Molecular Cloning: A Laboratory Manual, Cold Spring Harbor Laboratory Press.

Wang, Z., Wang, L., Wang, B.Z., Jiang, Y.F., Liu, S., 2008. Bench-scale study on zero excess activated sludge production process coupled with ozonation unit in membrane bioreactor. Journal of Environmental Science and Health, Part A 43(11), 1325-1332.

Yan, S.-T., Chu, L.-B., Xing, X.-H., Yu, A.-F., Sun, X.-L., Jurcik, B., 2009. Analysis of the mechanism of sludge ozonation by a combination of biological and chemical approaches. Water Research 43(1), 195-203.

Yasui, H., Shibata, M., 1994. An innovative approach to reduce excess sludge production in the activated sludge process. Water Science and Technology 30(9), 11-20.

3.8. SUPPLEMENTARY MATERIALS

Abbreviations and Symbols

COD pools of ASM3		[units]
$f_{SB,Inf}$	Soluble biodegradable COD fraction in the influent	[none]
S_B	Soluble biodegradable COD	[g-COD.m^{-3}]
S_U	Soluble undegradable COD	[g-COD.m^{-3}]
X_{ANO}	Autotrophic nitrifying organism biomass COD	[g-COD.m^{-3}]
X_{OHO}	Ordinary heterotrophic organism biomass COD	[g-COD.m^{-3}]
$X_{OHO,Stor}$	Storage compound COD in ordinary heterotrophic organisms	[g-COD.m^{-3}]
X_U	Particulate undegradable COD from the influent	[g-COD.m^{-3}]
$X_{U\_bio,lys}$	Biomass debris	[g-COD.m^{-3}]
XC_B	Particulate/colloidal biodegradable COD	[g-COD.m^{-3}]
XC_{B_Stor}	Particulate/colloidal biodegradable COD from storage	[g-COD.m^{-3}]
Model parameters of ASM3 used in the text		
$K_{SB,OHO}$	Half saturation constant for soluble biodegradable COD	[g-COD.m^{-3}]
$K_{NHx,ANO}$	Half saturation constant for soluble ammonium	[g-S_{NH4}. m^{-3}]

Model parameters describing ozone transformation of solids

Stoichiometric solids transformation and inactivation fractions

f_{Bio}	Fraction of biomass in particulate COD excluding storage	[none]
$f_{Bio,storage}$	Fraction of biomass in particulate COD including storage	[none]
$f_{mnr,O3}$	Fraction of transformed COD that is mineralized	[none]
$f_{SB\_O3,inact}$	Soluble biodegradable COD fraction of inactivated biomass soluble	[none]
$f_{SU\_O3,inact}$	undegradable COD fraction of inactivated biomass	[none]
$f_{XCB\_O3,inact}$	Particulate biodegradable COD fraction of inactivated biomass	[none]
$f_{SB\_O3,trans}$	Soluble biodegradable COD fraction of transformed non-biomass	[none]
$f_{SU\_O3,trans}$	Soluble undegradableCOD fraction of transformed non-biomass	[none]
$f_{XCB\_O3,trans}$	Particulate biodegradable COD fraction of transformed non-biomass	[none]

Transformation and inactivation rate constants		
$b_{Bio,O3,inact}$	Average inactivation rate of biomass due to ozone	[d^{-1}]
$b_{ANO,O3,inact}$	Inactivation rate of autotrophic nitrifying organisms due to ozone	[d^{-1}]
$b_{OHO,O3,inact}$	Inactivation rate of ordinary heterotrophic organisms due to ozone	[d^{-1}]
$q_{Xtot,O3,sol}$	Overall solids COD solubilization by ozone rate constant normalized to the aerated solids COD inventory	[d^{-1}]
$q_{XU\_XCB,O3,trans}$	Non-biomass solids transformation rate due to ozone	[d^{-1}]
Inactivation coefficient and exposed inventory fraction		
$\eta_{OHO,O3,inact}$	first-order inactivation coefficient with respect to O_3 *dose*	[m^3.g^{-1}]
$q_{MLVSS\ treated}$	fraction of biosolids inventory exposed to ozone per day	[d^{-1}]

Table 3.S1. Adjusted model parameters by model fitting using the control reactor data for the influent COD fractions and the biological parameters, and using the RAS-ozonated reactor data for the ozone model parameters.

Parameter	Unit	Value[a]
Influent COD fractions (all modeling approaches)		
Soluble biodegradable organics (f_{SB})	g-COD_{SB}/ g-COD_{total}	0.39 ± 0.04
Soluble undegradable organics (f_{Su})	g-$COD_{SU}.m^{-3}$	0.05 ± 0.02
Particulate undegradable organics (f_{XU})	g-$COD_{XU}.m^{-3}$	0.25 ± 0.03
Particulate biodegradable organics(f_{XCB})	g-$COD_{XCB}.m^{-3}$	0.31 ± 0.06
Biomass (f_{XOHO} and f_{XANO})	g-$COD_{biomass}.m^{-3}$	0[b]
Biological parameters (all modeling approaches)		
Half saturation constant for S_B($K_{SB,\ OHO}$)	g-$COD_{SB}.m^{-3}$	9.8 ± 1.2
Half saturation constant for S_{NH4}($K_{NH4,\ OHO}$)	g-$S_{NHx}.m^{-3}$	0.35 ± 0.10
Half saturation parameter for S_{NOx} ($K_{NOx,OHO}$)	g-$S_{NHx}.m^{-3}$	0.10 ± 0.02
Ozone parameters from Approach 1		
Inactivation		
Soluble undegradable COD ($f_{SU\_O3,inact}$)	g-COD_{SU}.g-COD_X^{-1}	0.225 ± 0.028
Soluble biodegradable COD ($f_{SB\_O3,inact}$)	g-COD_{SB}.g-COD_X^{-1}	0.150 ± 0.070
Inactivation /transformation ($b_{Bio,O3,inact}/q_{XU\_XCB,O3,trans}$)		2.2
Transformation		
Soluble undegradable COD ($f_{SU\_O3,trans}$)	g-COD_{SU}.g-COD_X^{-1}	0.225 ± 0.028
Soluble biodegradable COD ($f_{SB\_O3,trans}$)	g-COD_{SB}.g-COD_X^{-1}	0.150 ± 0.070
Particulate biodegradable COD ($f_{XCB,O3,trans}$)	g-COD_{XCB}.g-COD_X^{-1}	0.601 ± 0.080
Oxidized COD ($f_{mnr,O3}$)	g-COD_{mnr}.g-COD_X^{-1}	0.0237[c]
Ozone parameters from Approach 2		
Inactivation		
Soluble undegradable COD ($f_{SU\_O3,inact}$)	g-COD_{SU}.g-COD_X^{-1}	0.216 ± 0.031
Soluble biodegradable COD ($f_{SB\_O3,inact}$)	g-COD_{SB}.g-COD_X^{-1}	0.418 ± 0.065
Transformation		
Soluble undegradable COD ($f_{SU\_O3,trans}$)	g-COD_{SU}.g-COD_X^{-1}	0.216 ± 0.031
Soluble biodegradable COD ($f_{SB\_O3,trans}$)	g-COD_{SB}.g-COD_X^{-1}	0.418 ± 0.065
Particulate biodegradable COD ($f_{XCB,O3,trans}$)	g-COD_{XCB}.g-COD_X^{-1}	0.366 ± 0.072
Oxidized COD ($f_{mnr,O3}$)	g-COD_{mnr}.g-COD_X^{-1}	0.0402[c]
Ozone parameters from Approach 3		
Inactivation		
Soluble undegradable COD ($f_{SU\_O3,inact}$)	g-COD_{SU}.g-COD_X^{-1}	0.016±0.007
Soluble biodegradable COD ($f_{SB\_O3,inact}$)	g-COD_{SB}.g-COD_X^{-1}	0.066±0.028
Transformation		
Soluble undegradable COD ($f_{SU\_O3,trans}$)	g-COD_{SU}.g-COD_X^{-1}	0.303 ± 0.031
Soluble biodegradable COD ($f_{SB\_O3,trans}$)	g-COD_{SB}.g-COD_X^{-1}	0.273 ± 0.065
Particulate biodegradable COD ($f_{XCB,O3,trans}$)	g-COD_{XCB}.g-COD_X^{-1}	0.390 ± 0.072
Oxidized COD ($f_{mnr,O3}$)	g-COD_{mnr}.g-COD_X^{-1}	0.0306[c]

a ± standard error

b assumed value

c calculated value from theoretical considerations. It is influence by the calibrated value of $f_{XCB,O3,trans}$.

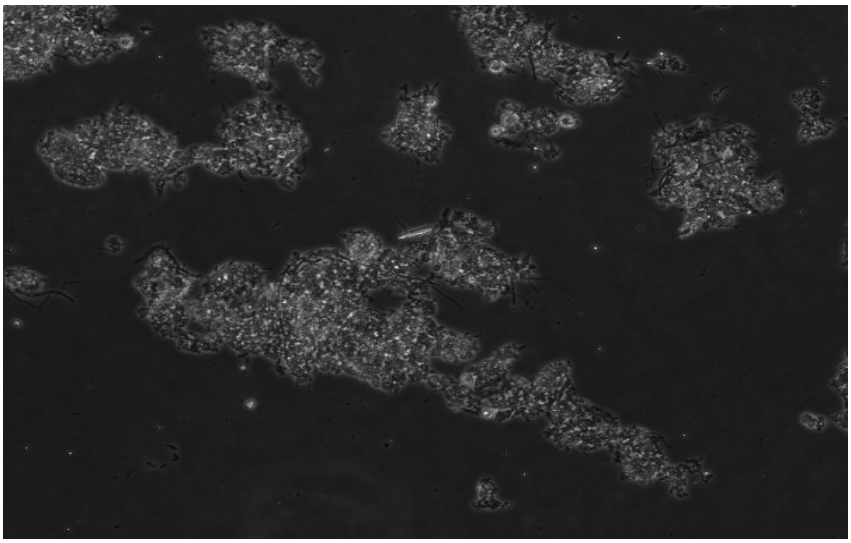

(a)

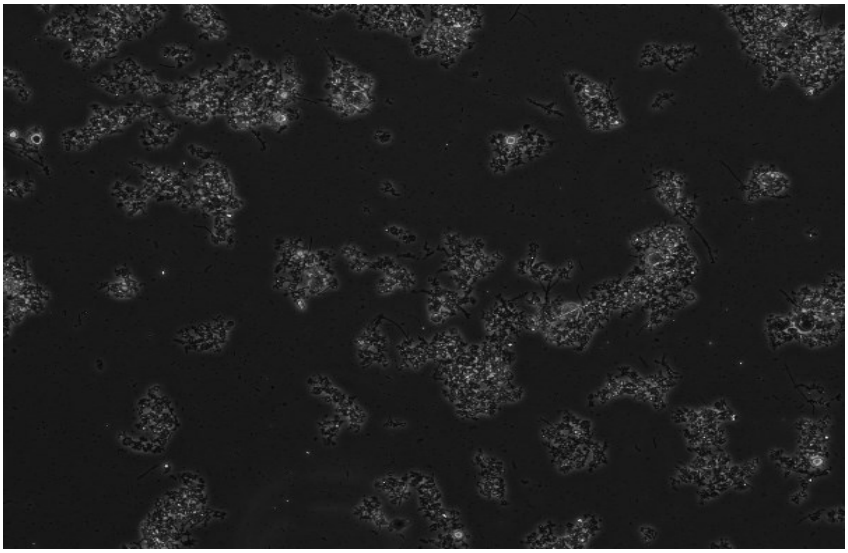

(b)

Fig. 3.S1. Mincorscopic image, in phase contrast (100x magnification), of biosolids floc structure before (a) and after (b) sonication.

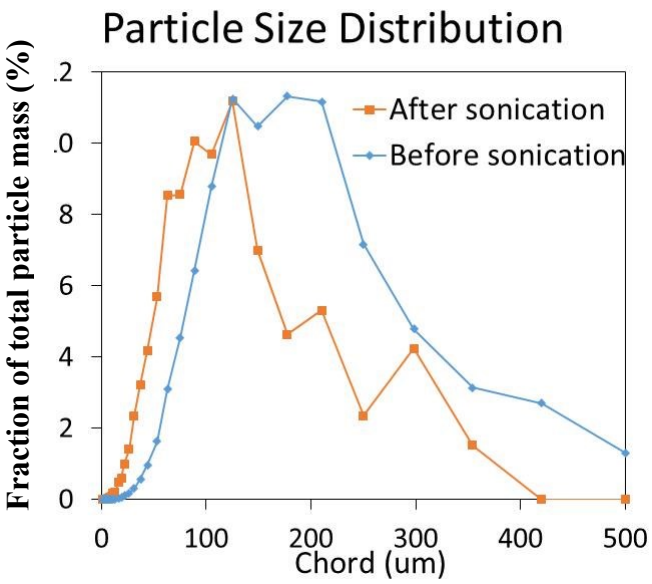

Fig. 3.S2. Particle size distribution before and after sonication. The fractions were calculated from the measured diameters assuming ideal spherical particles of uniform densities.

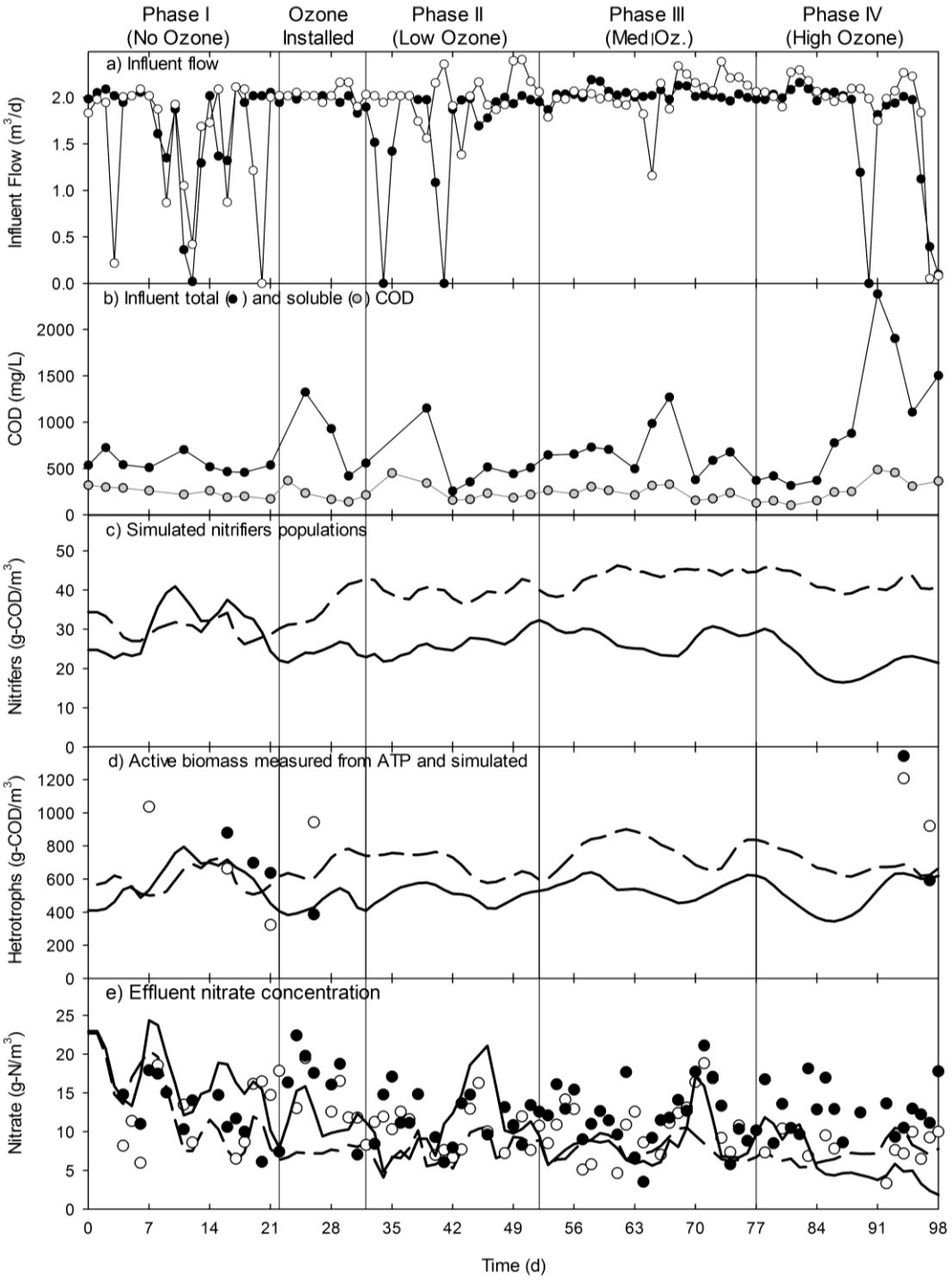

Fig. 3.S3. Operational data and simulation results for pilot-scale control and RAS-ozonated reactors. Circles should be read with the left-side axes, while triangle with the right-side axes. In all plots, symbols represent measured data and thick continuous lines show model predictions (control: open symbols and dashed lines; RAS-ozonated: solid symbols and solid lines). Conversion of ATP per biomass used the conversion constant suggested by the manufacturer.

Chapter 4:

Reduction of waste biosolids by RAS ozonation: model validation and sensitivity analysis for biosolids reduction and nitrification process

Connecting text: In the previous chapter, the accuracy of new model for predicting the reduction of biosolids production and effluent soluble COD concentrations verified. In the current chapter, the model is further validated by showing that the model calibrated against the first year pilot-scale operation data can satisfactorily simulate the second year operation data. Furthermore, the model validity for predicting nitrification activity is verified through a scenario analysis showing that the model can reproduce a wide range of observations from our own pilot-scale experiments and the literature. Finally, a global sensitivity analysis of biosolids reduction efficiency, specific nitrification activity and nitrification stability is presented to obtain insights on the treatment reactor conditions that most influence the practical outcomes of the use of RAS-ozonation for biosolids reduction. The results of this work have been submitted for publication:

Isazadeh, S., Ozcer, P. and Frigon, D., Modelling the behaviour of nitrifiers in activated sludge systems subjected to ozonation for the reduction of biosolids production. *Journal of Environmental Modelling & Software*:

4.1. INTRODUCTION

Management of waste biosolids is one of the main operational costs at wastewater treatment plants (WWTPs), and drives facilities to adopt new technologies to reduce biosolids production. Partial ozonation of return activated sludge (RAS-ozonation) is one of these technologies. During RAS-ozonation, chemical oxygen demand (COD) is solubilized, microbes are inactivated, and non-biodegradable particulate organics are transformed to biodegradable substrates (soluble and particulate) and non-degradable soluble COD (Foladori et al. 2010a). The resulting COD pools are either re-consumed by the biomass or leave the system with the effluent. Therefore, biosolids reduction is achieved by the synergy between the ozone reactions and the biological processes (Paul et al. 2012).

The wide range of biosolids reduction performance reported in the literature (from 3.7 to 10.4 g-$TSS_{reduced}$/g-$O_{3,dosed}$ (Foladori et al. 2010a)) makes it difficult to predict the outcome of new installations. Such disparity in performance stems from variable RAS-ozone contactor characteristics (e.g., ozone transfer efficiency and contactor configurations) (Chu et al. 2008), and variable wastewater treatment operational conditions (e.g., wastewater composition, treatment process, and solids retention time [SRT]). Therefore, reported performance values mix two distinct aspects of process modeling: RAS-ozone contactor performance and biological treatment characteristics (Fig. 4.1). Alternatively, in this study we model these two types of components separately.

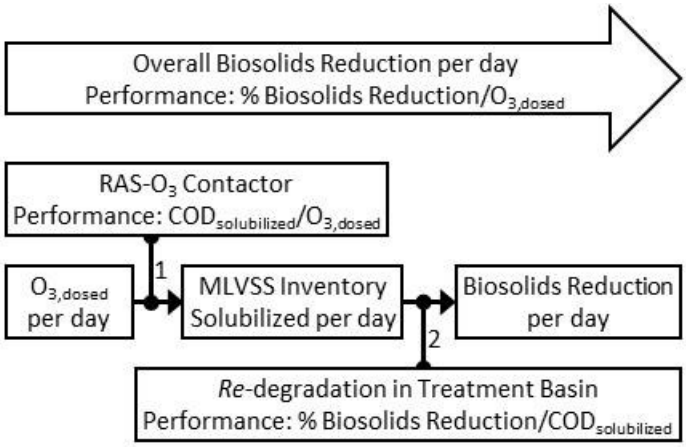

Fig. 4.1. Overall performance of biosolids reduction by RAS-ozonationprocess. Segregation of the accepted concept into the two underlying performance: extant of ozone reaction in RAS-O3 contactor and impact of treatment condition in biosolids COD loss.

We recently introduced an extension of the International Water Association Activated Sludge Model 3 (IWA-ASM3) to describe ozone reactions with suspended solids ((Isazadeh et al. 2014),chapter 3). In this extension, instead of modeling the extent of ozone reactions in the RAS-ozone contactor which widely range between 0.7-9.6 g-COD/g-$O_{3,dosed}$ (Labelle et al. 2011), the model directly uses the amount of COD solubilized *in lieu* of the ozone dose. A major goal of the current study is to conduct a global sensitivity analysis (GSA) of the biosolids reduction performance to better understand how the local wastewater treatment conditions affect biosolids reduction performances.

In addition, we provide a better understanding of the impact of RAS-ozonation on the nitrification process. The vulnerability of nitrifiers to partial RAS-ozonation has been evaluated in long-term monitoring of (i) nitrification process efficiency and (ii) specific nitrification activity (SNA) studies. However, a number of inconsistencies arose from these studies. First, while the nitrification process efficiency (measured as the residual ammonia in the bioreactor effluent) was typically not affected by RAS-ozonation (Böhler and Siegrist 2004, Deleris et al.

2002, Dytczak et al. 2007, Sakai 1997), SNA (measured as the maximum nitrification rate per mixed liquor volatile suspended solids, MLVSS in batch test (mg O_2/g.VSS.day)) was typically reduced with the addition of ozone (Böhler and Siegrist 2004, Dytczak et al. 2007, Vergine et al. 2007). This reduction in SNA suggests a degradation of the treatment process' robustness. Second, although SNA was typically reduced, a number of papers report increases in SNA upon installation of an RAS-ozonation processes. Finally, the combined effect of low temperature and RAS-ozonation on nitrification was never directly investigated. Consequently, a significant knowledge gap still remains with respect to the impact of RAS-ozonation on nitrifiers. This gap is addressed here by first validating our model using data from pilot-scale experiments, and performing a scenario analysis to try to reproduce observed trends reported in the literature followed by a GSA of nitrification activity and stability.

4.2. MATERIALS AND METHODS

4.2.1 Pilot-scale study

Two pilot-scale systems (RAS-ozonated and control) each comprising 1 m^3 reactor and 0.7 m^3 clarifier respectively, were operated in the summers and falls of three consecutive years at a full-scale WWTP. The reactors received diverted municipal wastewater (~2 m^3/d) with ~50% of COD loads (25,000kg/day) originating from industrial sources. Details of the design and operation of the pilot-scale reactors have been described previously (Isazadeh et al. 2014,chapter 3), and the operational phases over the three-years of operation are summarized in Table 4.1.

Table 4.1. Summary of pilot-scale reactors operation and experimental phases over 3 years.

Operation Phase	Length (days)	Operation[b]	Control Reactor Target SRT (days)	Ozone Dose ($mg\text{-}O_3/g\text{-}VSSd^{-1}$)	Biosolids Reduction (%)
Year 1: Single operation and variable ozone dose (Isazadeh et al. 2014. chapter 3)					
Start-up	60			0	NA[a]
Phase 1	21			0	0
Phase 2	28	O	6	2.3±0.3	19±4
Phase 3	26			3.1±0.1	37±3
Phase 4	21			6.5±0.3	46±2
Year 2: Single operation and high ozone dose (presented here)					
Start-up	47			0	NA
Phase 1	40	O	6	5.9±0.4	13±1
Phase 2	34			10.3±0.7	53±6
Year 3: Variable operation and single ozone dose (Isazadeh et al. in prep.)					
Start-up	60	A/O	12	0	NA
Phase 1	100	A/O	12	7.3±0.2	22±2[c]
Phase 2	36	O	12	8.9±0.1	19±2
Phase 3	40	O	6	11.4±0.2	18±2

a NA: Not applicable

b O:Fully Aerobic and A/O: Anoxic/Fully Aerobic

c The recirculation pump of the RAS-ozone contactor caused a decrease in the COD solubilization efficiency between Years 1/2 (5.26 g-COD/g-O3) and Year 3 (2.13 g-COD/g-O3).

4.2.2 Specific nitrification activity

During Year 1 of the study, SNA was measured by a low food/microorganism (F/M) bioassay (Melcer 2004). Concisely, a 2-liter MLSS sample (~2,000 mg/L) was placed in an aerated container and spiked with NH_4Cl (15 mg-N/L) and $NaHCO_3$ (150 mg/L). The concentrations of residual NH_4^+, and NO_3^-) were measured over 6 hours by Method 4500-F and H (APHA et al. 2005) and using a microplate spectrophotometer (model SpectraMax M5, Molecular Devices, LLC, USA). In Years 2 and 3, SNA measurements of ammonia and nitrite oxidizing organisms (AOO and NOO) were performed (Moussa et al. 2003) using batch respirometry (model AER-200, Challenge Technology, USA). Twenty-four-hour aerated MLSS samples (~2,000 mg/L) were subjected to respirometric analysis in 500-mL bottles. The endogenous oxygen uptake rate (Endogenous-OUR) was measured followed by the sequential injection of $NaHCO_3$ (150 mg/L), $NaNO_2$ (10 mg-N/L) and NH_4Cl (15 mg-N/L) to determine NOO-OUR and AOO-OUR profiles,

respectively. The specific OUR (SOUR) of AOO and NOO were obtained by subtraction of OURs in the appropriate incubation phases and dividing by the concentration of MLVSS (eq.1 &2).

$$\text{AOO} - \text{SOUR} = [\text{AOO} - \text{OUR} - \text{NOO} - \text{OUR}]/\text{MLVSS} \qquad \textbf{eq.1}$$

$$\text{NOO} - \text{SOUR} = [\text{NOO} - \text{OUR} - \text{Endogenous} - \text{OUR}]/\text{MLVSS} \qquad \textbf{eq.2}$$

4.2.3 Model description

The proposed model extension describing the fate of the solids COD pools resulting from exposure to ozone is explicitly detailed in (Isazadeh et al. 2014, chapter 3). The model is based on two groups of ozone reactions: (i) the ***transformation/mineralization*** of non-biomass solids and (ii) the ***inactivation*** of biomass. Both of these processes produce degradable soluble substrates (S_B), particulate substrates (XC_B) and non-degradable soluble COD (S_U) (Fig. 4.2; Table 4.S1).

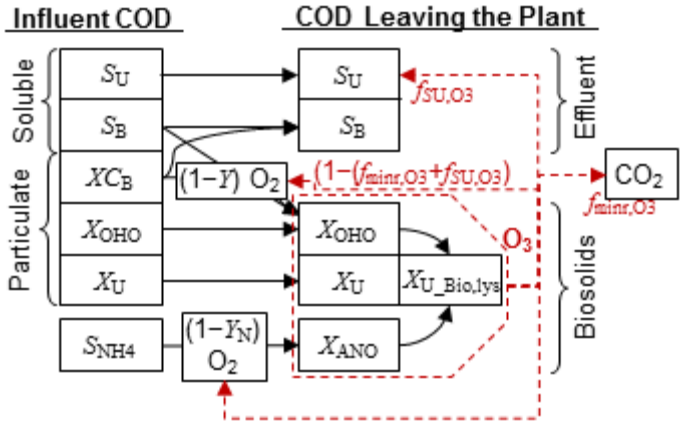

Fig. 4.2. COD flow according to the IWA-ASM3 model and the proposed extension describing ozone reactions with VSS. Solid lines represent biochemical conversions, dashed lines represent conversions due to ozonation of RAS. COD pools: degradable (S_B) and undegradable (S_U) soluble COD, biodegradable (XC_B) and undegradable (X_U) particulate COD, heterotrophic

(X_{OHO}) and nitrifying (X_{ANO}) biomass, biomass debris ($X_{U\_bio,lys}$), and ammonium (S_{NH4}). Ozone reaction fractions: undegradable soluble COD ($f_{SU,O3}$), and mineralized COD ($f_{minr,O3}$).

4.2.4 Model validation and scenario analysis for nitrification

A ***validation study*** was conducted by comparing the observed and simulated solids inventories and SNA in the pilot-scale experiment. The model was calibrated with Year 1 pilot-scale data (Isazadeh et al. 2014, chapter 3), and dynamically simulated the results of Year 2 data. The values of model parameters are presented in Table 4.S2. The differences between model predictions and observations were tested by a paired *t*-test (Sokal and Rohlf 1995).

A ***scenario analysis study*** was conducted to generalize the validity of the model with respect to SNA. Trends were generated through 1,500 Monte Carlo simulations and compared to compiled observations from our pilot-scale and literature studies. The ranges of input variables for model parameters are presented in Table 4.S3. The simulations in this section and in Section 2.5 were performed with AQUASIM software (Reichert 1998).

4.2.5 Global sensitivity analysis

GSA was performed to investigate how the model outputs are influenced by the simultaneous variation of the input parameters when MLVSS is kept constant for the control and RAS-ozonated reactors. The input parameters were categorized into three types: biochemical (B), ozone reaction (Oz) and wastewater treatment operation (Op) parameters. The sensitivity of three model outputs was examined: (1) biosolids reduction efficiency, (2) SNA (evaluated as X_{ANO} $/X_{MLVSS}$ for modeling purposes), and (3) nitrification safety factor (SF_{ANO}; eq. 4&5; the SF_{ANO} measures the relative expected process stability based on the absolute minimum SRT to maintain nitrifiers ($SRT_{ANO,min}$) (Rittmann and McCarty 2001).

BR-Efficiency; for a constant $q_{X\text{tot,O3sol}}$, *BR-Efficiency* = 100% − biosolids production of RAS-ozonated reactor/biosolids production of control reactor × 100% **(eq. 4)**

$$SF_{ANO} = SRT_{operation}/SRT_{ANO,min} \quad \textbf{(eq. 4)}$$

$$SRT_{ANO,min} = (\mu_{ANO,max} - b_{ANO} - b_{ANO,O3,inact})^{-1} \quad \textbf{(eq. 5)}$$

where $\mu_{ANO,max}$ is the maximum growth rate of nitrifiers; b_{ANO} is the endogenous respiration rate constant for nitrifiers at the temperature of operation and $b_{ANO,O3,inact}$ is the inactivation rate constant of nitrifiers due to ozone. The log–transformation of the ratios between RAS-ozonated and non-ozonated reactors for the last two outputs were used to ensure that values of ratios above 1 are in the same scale as values below 1.

The range for each input parameter was adjusted from our pilot-scale data (Isazadeh et al. 2014, chapter 3) for ozone transformation parameters and based on literature for biochemical and operational parameters (Table 4.S3). The parameter "Anoxic vs. Aerobic Systems" was defined by adjusting the range of heterotrophic yields to span values for anoxic (minimum) to aerobic (maximum) yields. The influent COD composition was simplified to only account for two pools: biodegradable soluble substrate ($f_{SB,Inf}$) and non-degradable particulate COD ($f_{XU,Inf}$=1−$f_{SB,Inf}$).

Standardized regression coefficients (*SRCs*) were obtained by first running 500 simulations with random sampling of parameter values following a Latin hypercube sampling method, and then by performing standardized multivariate linear regression between the model outputs and parameters (Sin et al. 2011). The reproducibility of the results was demonstrated by performing the studies three times, and the *SRCs* were tested to be significantly different from zero using a Student's *t*-test (Sokal and Rohlf 1995). Three possible biosolids reduction scenarios including,

variable and constant reduction of 40 and 60% were used to conduct the GSA on SNA and nitrification stability.

4.3. RESULTS and DISCUSSION

4.3.1 Model validation: dynamic simulation of Year 2 pilot-scale data

A pilot-scale study was conducted in the summers/falls of three consecutive years for periods of four to six months each year. Previously, it has been shown that the calibrated model satisfactorily simulated the waste biosolids reductions and the effluent COD concentrations for Year 1 (Isazadeh et al. 2014, chapter 3). Here, we show that when the COD solubilisation rates were considered (Fig. 4.3a), the Year 1 model calibration (Table 4.S2) also properly predicted the Year 2 VSS reactor inventories ($p>0.05$; Fig. 4.3b) despite the highly variable operational conditions of the RAS-ozonated reactor during Year 2.

During the Year 2 operation, ozone dosage started on Day 35 with a dose of 5.9±0.4 (mg-O_3 g^{-1}-$VSS_{inventory}$ d^{-1}) aiming at 50% of waste biosolids reduction. The erroneous calibration of a gas flow meter starting on Day 81, however, resulted in a much higher average ozone dose than expected (10.3±0.7 (mg-O_3 g^{-1}-$VSS_{inventory}$ d^{-1}) which was translated by a higher measured COD solubilization rate (Fig. 4.3a). The data bias was corrected with the recalibration of the faulty meter. The SRT in the RAS-ozonated reactor was increased on Day 85 from an average of 5.0 d before the increase to an average of 10.5 d (the average control reactor SRT was 5.8 d throughout the experiment) (Fig. 4.3a). Despite the higher SRT, the high ozone dose caused a rapid deterioration of the SNA (Fig. 4.3c), which culminated in the complete loss of nitrification activities (ammonia and nitrite oxidation) by Day 100 (Fig. 4.S1). On Day 108, the RAS-

ozonation experiment was halted and nitrification fully recovered by Day 119 (Fig. 4.3c). Other relevant operation data are presented in supplementary materials (Fig. 4.S2).

These data strongly suggest that increasing the apparent SRT upon the introduction of RAS-ozonation (i.e., keeping MLVSS constant) plays a critical role to maintain a healthy nitrification performance. The highly dynamic variations in SNA also provided an opportunity to test the model's ability to predict the nitrification process. The nitrifiers-to-MLVSS ratio (X_{ANO}/X_{MLVSS}) followed the same trend as the SNA (Fig. 4.3c) in cognizance that the SNA is proportional to the nitrifiers' biomass level, X_{ANO}. With these two successful modeling results (solids inventory and SNA), we conclude that the model satisfactorily captures the dynamics of nitrifiers, and define this as our ***Validating Observation 1*** (Table 4.2).

Table 4.2. Summary of validating observations describing RAS-ozonation effects on the SNA.

Observations	Studies
1) High ozone doses with an unadjusted SRT cause a rapid deterioration of the nitrification activity	this study (Year 2)
2) *Linear* change in specific SNA with increasing sludge reduction.	(Böhler and Siegrist 2004, Dytczak et al. 2007)
3) Fully aerobic systems: SNA generally decrease	this study (Years 1 and 3); (Böhler and Siegrist 2004, Dytczak et al. 2007, Gardoni et al. 2011, Vergine et al. 2007)
4) Anoxic/Aerobic systems: Increase or decrease in SNA	this study (Year 3); (Deleris et al. 2002, Dytczak et al. 2007)

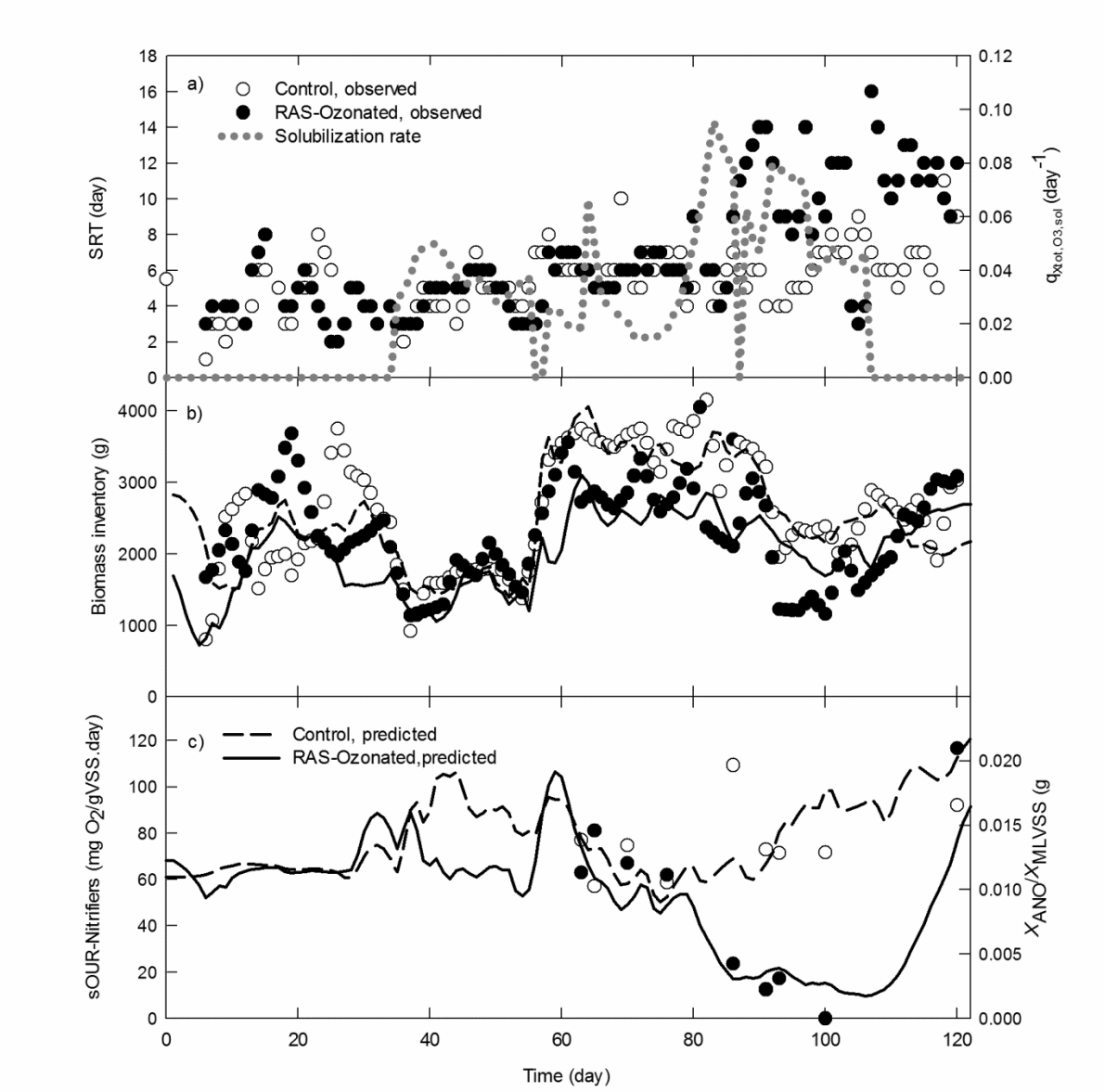

Fig. 4.3. Observed and simulated operation data in RAS-ozonated and control pilot-scale reactors during Year 2. (a) SRT and solids inventory COD solubilization rate ($q_{Xtot,O3,sol}$); (b) volatile solids inventory expresses as COD (assuming 1.42 g-COD/g-VSS). Symbols: measurements in control (open circles) and RAS-ozonated reactors (solid black circles), and ozone solubilization (grey circles); lines: model predictions for control (dashed) and RAS-ozonated (solid) reactors; and (c) observed (right axis) and predicted (left axis) SNA (Oxygen uptake rate with ammonium/nitrite additions minus endogenous, average of duplicates).

4.3.2 Scenario analysis: observations on specific nitrification activity

Between studies the trends in the behaviour of nitrifiers in RAS-ozonated system are less consistent than those for biosolids reduction. Therefore, a comprehensive simulation of the X_{ANO}/X_{MLVSS} was adopted to reproduce the range of trends observed in the literature and in our three-year pilot-scale study. These trends are presented as ***validation observations*** that will be compared to the scenario analysis results.

Throughout the fully aerated operation phases of the pilot-scale reactors (Years 1 and 3), RAS-ozonation caused a significant decrease (*t-test, $p<0.05$*) in SNA compared to the non-ozonated reactor (Fig. 4.4). These observations were true for phases with average SRTs of 6 d (Year 1) and 12 d (Year 3) for the control reactor (Fig 4). Other groups reported similar observations for fully aerobic activated sludge (AS) systems (Böhler and Siegrist 2004, Dytczak et al. 2007, Gardoni et al. 2011, Vergine et al. 2007). Two studies showed that the decrease in SNA was linear with the increase in sludge reduction (Böhler and Siegrist 2004, Dytczak et al. 2007). Based on these findings we define two other validation observations (Table 4.2). ***Validation observation 2***: RAS-ozonation induces a ***linear*** change (increase or decrease) in SNA with increasing sludge reduction, and ***validation observation 3***: SNA generally decreases in fully aerobic systems upon the introduction of RAS-ozonation.

For anoxic/aerobic reactors, the situation does not seem to be as clear. In our pilot-scale study, a significantly higher ($p<0.05$) SNA was observed during the anoxic/aerobic phase of operation (Year 3; Fig. 4.4) for the RAS-ozonated reactor. This is similar to observations made by Deleris et al. (2002), but contrary to observations by Dytczak et al. (2007) for anoxic/aerobic reactors. However, the point of agreement between Dytczak et al. (2007) and our study (Fig. 4.4) is that the "negative" effects of RAS-ozonation on the SNA were more pronounced in fully

aerated systems than in anoxic/aerobic systems studied in parallel. In other words, the SNA decreased in the fully aerobic systems of both studies, but it either decreased less (Dytczak et al. 2007) or even increased (Year 3, Fig 4) in anoxic/aerobic systems. Thus, we define ***validation observation 4***: SNA can either increase or decrease in anoxic/aerobic systems due to RAS-ozonation (Table 4.2).

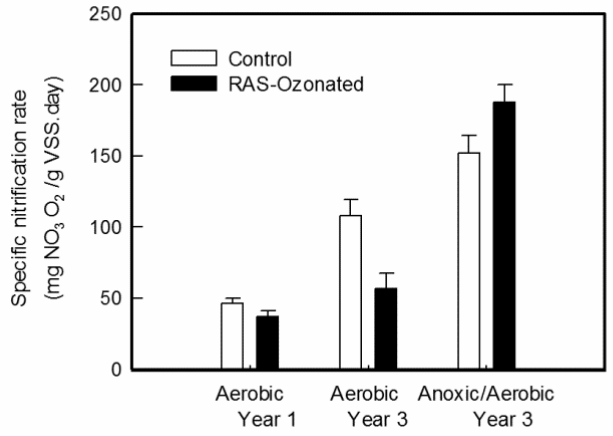

Fig. 4.4. Average specific nitrification rates in pilot-scale reactors in Year 1 (last phase with highest ozone dose, average control SRT≈6 days) and Year 3 (aerobic and anoxic/aerobic phases, average control SRT≈12 days). Nitrification rates in Year 1: NO_3^- production rate (n=5 weekly measurements). Nitrification rates in Year 3: ammonium-oxidation + nitrite oxidation SOURs (n=8 weekly measurements). Error bars indicate standard errors.

A detailed modeling of all literature experiments is difficult since the exact conditions of each study are uncertain. Therefore, we compared the observations with trends seen in the scenario analysis. For constant MLVSS after introduction of RAS-ozonation, the model successfully reproduces the linear change in X_{ANO}/X_{MLVSS} with increasing COD solubilisation (e.g., Fig. 4.5a), showing conformity with validation observation 2 (Table 4.2). To reproduce validation observation 3 (decrease of SNA in aerobic systems), however, scenario analysis results suggest that the ozone inactivation rate constant of nitrifiers ($b_{ANO,O3,inact}$) must be higher

than the ozone non-biomass transformation rate constant ($q_{XU\_XCB,O3,trans}$). If $b_{ANO,O3,inact}$ was equal or lower than $q_{XU\_XCB,O3,trans}$, the SNA would only increase (an increase is plotted above 0 on the y-axis in Fig. 4.5b). This range for $b_{ANO,O3,inact}$ also corroborates validation observation 4 (increase or decrease of SNA in anoxic/aerobic systems, Table 4.2). This finding along with experimental results from Foladori et al. (2010b) and Isazadeh et al (2014, chaptr 3) are opposite to the modeling assumption adopted by other groups, that nitrifying biomass (Deleris et al. 2002), and more generally heterotrophic biomass (Gardoni et al. 2011, Paul et al. 2012), is not inactivated at low ozone doses. For the model presented here, a decrease in biomass proportion (either nitrifiers or heterotrophs) can only occur for $b_{ANO,O3,inact}$ or $b_{OHO,O3,inact}$ (inactivation of heterotrophs) larger than $q_{XU\_XCB,O3,trans}$. Therefore, we restricted the range of the $b_{ANO,O3,inact}/q_{XU\_XCB,O3,trans}$ ratio to above 1 for all other simulations. Finally, validation observation 4 (Table 4.2) was also reproduced by the model scenario analysis as a decrease in the heterotrophic biomass yields varying between anoxic (minimum) and aerobic (maximum), resulting in a decrease in the negative effect of RAS-ozonation on SNAs (Fig. 4.5c).

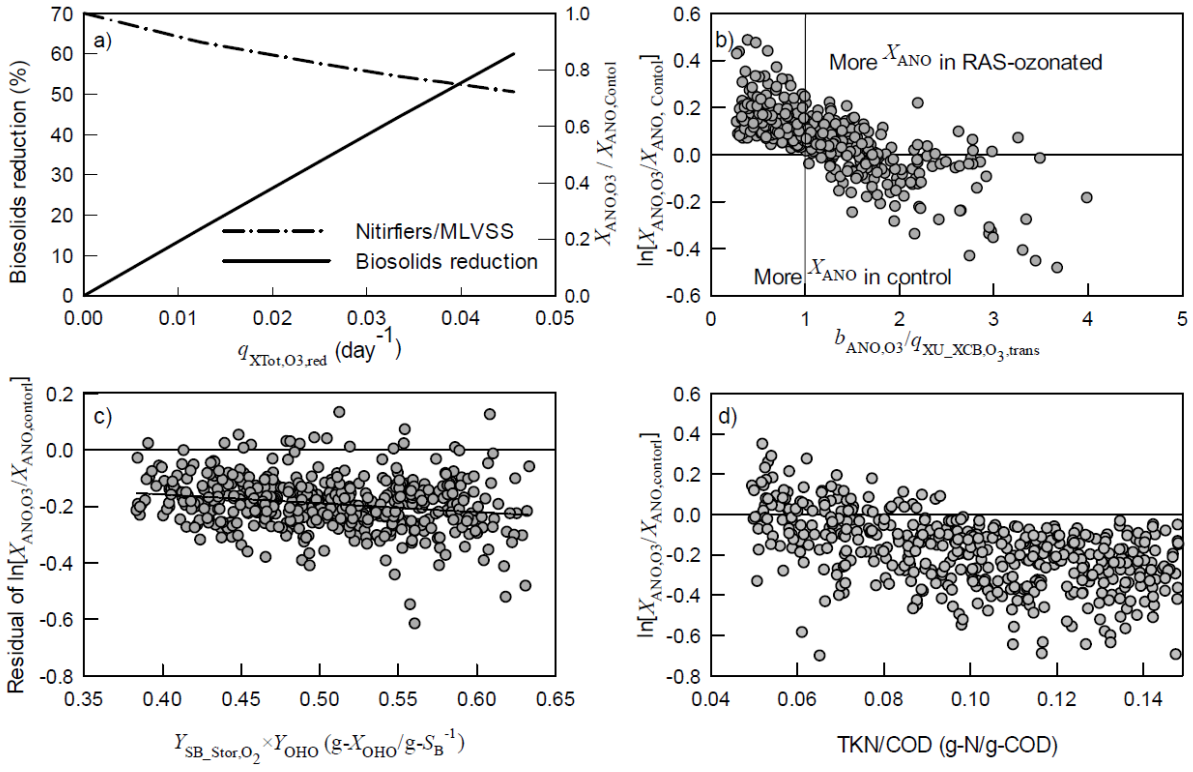

Fig. 4.5. Model predictions of the changes in the proportion of nitrifying biomass in MLVSS (y-axis subscripts: O_3, RAS-ozonated reactor; Ctrl, Control [non-ozonated] reactor). (a) Changes vs. COD solubilisation rate ($q_{XTot,O3,sol}$, a proxy for ozone utilization) and relation with sludge reduction for a specific parameter set (SRT=10 d, $b_{ANO,O3,inact}/q_{XU\_XCB,O3,trans}$=2, Y_{SB_Stor}=0.5,Y_{OHO}=0.63), (b) changes vs. the nitrifier inactivation rate over non-biomass solids transformation rate ratio , distribution in a 40% sludge reduction, (c) changes vs. combined heterotrophic yield after removing the effect of variation in all other model parameters by linear regression, and (d) distribution of changes in the proportion of nitrifying biomass in MLVSS vs. the influent TKN/COD ratio found in the GSA study.

4.3.3 Model sensitivity: biosolids reduction efficiency

In this section we examine the sensitivity of waste biosolids reduction and nitrifiers' activities and stabilities (section 4.3.4) to establish input model parameters and reactor conditions. The high R^2 values (>0.7) obtained for the biosolids reduction efficiency (*BR-Efficiency*) in the GSA study (Table 4.3) indicates that standardized regression coefficients (*SRC*s) are good measurements of the sensitivities (Saltelli et al. 2008). The absolute values of *SRC*s represent the influence of the parameters, and their sign indicates the direction of changes in *BR-Efficiency*;

positive *SRC*s mean higher *BR-Efficiency* with increasing values of the parameter tested. The *BR-Efficiency* was found to be significantly ($p<0.05$) sensitive to eight of the sixteen model test parameters (Table 4.3). The parameters with *SRC,* significantly different from zero, were operational (Op) and ozone reaction (Oz) parameters, while the non-significant parameters were mainly the biochemical (B). The accurate prediction of waste biosolids reduction by RAS-ozonation requires an accurate characterization of the operational parameters (typically measured by WWTPs), and a good calibration of the RAS-ozone reaction parameters (to be done for each WWTP).

BR-Efficiency was found to be most influenced (absolute *SRC*) by SRT of the non-ozonated reactor (i.e., control reactor or before installation of RAS-ozonation), with an enhanced efficiency with increasing non-ozonated SRT (Table 4.3). Two phenomena may explain this sensitivity. First, the portion of non-degradable materials (X_U) in the biosolids increases with SRT and making them bio-degradable assures the greatest reduction gains. Second, longer SRT induces a longer decay of the newly formed biomass leading to lower biosolids production (i.e., similar mechanism as for extended aeration). The next most influential operational parameter is the biodegradable COD fraction of the influent ($f_{SB,Inf}$; Table 4.3); only two fractions were assumed for the influent: $f_{SB,Inf}$ and $f_{XU,Inf}$. The negative *SRC* for $f_{SB,Inf}$ suggests that WWTPs receiving fairly non-degradable influent particulate COD have a higher potential for reduction in biosolids production. Finally, the sensitivity to *temperature* and *decay rate* can probably be understood in the same way as for the SRT.

Changes between *anoxic vs. aerobic system* (tested using heterotrophic biomass yields) are the other operational parameter to which the *BR-Efficiency* is sensitive (Table 4.3). The negative

SRC suggests that systems with lower biomass yields (i.e., anoxic/aerobic) have a greater potential for waste biosolids reduction by ozone.

Table 4.3. GSA of the biosolids production efficiency to various model parameters.

Parameters	Parameter Type[a]	*SRC*[b] (R^2= 0.89±0.02[c])
Significant Parameters ($p<0.05$)		
SRT	Op	+ 0.782±0.03[c]
$1-(f_{SB\_O3,trans}+f_{SU\_O3,trans}+f_{mnr,O3})$	Oz	+ 0.432±0.03
$f_{SB,Inf}$	Op	− 0.138±0.03
Temperature	Op	+ 0.105±0.03
$b_{OHO,O3,inact}/q_{XU\_XCB,O3,trans}$	Oz	− 0.097±0.03
$f'_{SU,O3}$[d]	Oz	+ 0.062±0.03
Anoxic vs. Aerobic systems[e]	Op	− 0.058±0.03
$b_{OHO,O2,20}$	B	+ 0.042±0.03
Non-Significant Parameters ($p>0.05$)		
$K_{XCB,hyd}$	B	− 0.021±0.03
$K_{SB,OHO}$	B	+ 0.018±0.03
HRT	Op	− 0.014±0.03
Volumetric COD loading	Op	+ 0.008±0.03
$\mu_{OHO,Max}$	B	− 0.005±0.03
q_{SB_Stor}	B	+ 0.004±0.03
$q_{XCB\_SB,hyd}$	B	− 0.002±0.03

a Parameter types: Oz, ozone transformation; Op, reactor operation; B, biochemical
b SRC: standardized regression coefficients
c ± standard error of three sampling sets
d $f'_{SU,O3}=f_{SU,O3}/(1-f_{SB\_O3trans})$
e Aerobic vs Anoxic systems was tested by adjusting yields: $Y_{SB\_Stor}\times Y_{OHO}$

4.3.4 Model sensitivity nitrification specific activity and stability

Stability of nitrification should not be adversely affected by the implementation of partial RAS ozonation despite a reduction in SNA because the SRT is allowed to increase to keep the MLVSS constant (Böhler and Siegrist 2004, Dytczak et al. 2008, Vergine et al. 2007). To investigate this, a GSA study on the change in SNA (i.e., change in nitrifier biomass per MLVSS: $[X_{ANO,O3}/X_{MLVSS,O3}]/[X_{ANO,Ctrl}/X_{MLVSS,Ctrl}]$) and nitrification stability was conducted.

Three different sludge reductions scenarios; variable (10-97%) and constant at 40% and 60% were investigated with sensitivity studies. We present here only the results for the varying reduction; the 40% and 60% reduction studies gave similar results and can be seen in the supplementary materials (Tables 4.S4 and S5). The changes in SNA were generally influenced by the reactor operation (Op) and the ozone reaction (Oz) parameters, but not by the biochemical stoichiometry and kinetic (B) parameters (Table 4.4). Focusing on the absolute values of the *SRCs*, one can distinguish four parameters to which the change in the proportion of nitrifiers is most sensitive: relative rates of nitrifier inactivation ($b_{OHO,O3,inact}/q_{XU\_XCB,O3trans}$ and $b_{OHO,O3,inact}/b_{ANO,O3,inact}$), relative total Kjeldahl nitrogen in the influent (TKN_{Inf}/COD_{Inf}), and *temperature*.

The sensitivities of the SNA to *temperature* and TKN_{Inf}/COD_{Inf} (Table 4.4) need to be understood in context. First, the BR-efficiency is lower at low temperature (Table 4.3). Thus, higher ozone doses (and hence biomass inactivation) are necessary for the same biosolids reduction at lower temperature. Consequently, the SNA would be more affected as the operation temperature is lowered. Second, as the initial proportion of nitrifiers in the MLVSS of the control (non-ozonated) reactor is proportional to the TKN_{Inf}/COD_{Inf} ratio, the effect of ozonation will be felt more strongly by nitrifiers at high TKN_{Inf}/COD_{Inf} ratios than at low ratios (Table 4.4).

Table 4.4. Sensitivity of the changes in nitrifying biomass[a] upon introduction of RAS-ozonation with respect to changes in model parameters for variable waste biosolids reductions.

Parameters	Parameter Type[b]		*SRC*[c] (R^2= 0.71 ±0.01[d])
Significant parameters($p<0.05$)			
$b_{OHO,O3,inact}/q_{XU\_XCB,O3,trans}$	Oz	+	0.554 ±0.003[d]
TKN_{Inf}/COD_{Inf}	Op	+	0.504±0.000
Temperature	Op	–	0.445±0.009
$b_{OHO,O3,inact}/b_{ANO,O3,inact}$	Oz	–	0.441±0.009
$q_{XU\_XCB,O3,trans}$	Oz	+	0.304±0.003
$f_{SU,O3}$	Oz	–	0.248±0.000
SRT	Op	+	0.128±0.000
i_{N_XU}	Op	–	0.127±0.017
Anoxic vs. Aerobic systems[e]	Op	+	0.088±0.015
$f_{SB,Inf}$	Op	+	0.051±0.009
$b_{ANO,O2,20}$	B	–	0.022±0.001
Non-significant parameters ($p>0.05$)			
$K_{NHx,ANO}$	B	+	0.024±0.020
$\mu_{ANO,max,20}$	B	–	0.050±0.042
Y_{ANO}	B	+	0.017±0.016
$b_{OHO,O2,20}$	B	+	0.007±0.003

a changes in nitrifying biomass: $(X_{ANO,O3}/X_{MLVSS,O3})/(X_{ANO,Ctrl}/X_{MLVSS,Ctrl})$
b Parameter types: Oz, ozone transformation; Op, reactor operation; B, biochemical
c SRC: standardized regression coefficients
d ± standard error of three sampling sets
e Aerobic vs Anoxic systems was tested by adjusting yields: $Y_{SB\_Stor} \times Y_{OHO}$

A closer look at the distribution of the GSA simulations revealed that the proportion of nitrifiers in the RAS-ozonated reactors will always be lower than in control reactors (i.e., lower than 0 on the y-axis in Fig. 4.5) when the TKN_{Inf}/COD_{Inf} ratio is higher than 0.1. Conversely, when the TKN_{Inf}/COD_{Inf} ratio is lower than 0.1, the proportion of nitrifiers was found to be higher in the RAS-ozonated reactor in 30% of the cases. This provides an explanation for why the SNA increased in the anoxic/aerobic RAS-ozonated reaction for our pilot-scale experiment

(Year 3, Fig. 4.4) and decreased for Dytczak et al. (2007). In our study, the TKN_{Inf}/COD_{Inf} ratio was approximately 0.08 g-N/g-COD, while, for Dytczak et al. (2007), this ratio was at least 0.17 g-N/g-COD (considering the N content of beef and yeast extracts around10% [w/w]; (Acumedia Manufacturers Inc. 2011). Therefore, the model predicted that the reactor conditions in Dytczak et al. (2007) always lead to a decrease in the proportion of nitrifiers, while the different combination of conditions led to an increase for our pilot-scale reactor.

GSA studies have showed that the nitrification stability (i.e., safety factor: SF_{ANO}) is typically enhanced by the RAS-ozonation process (i.e., above 0 on the y-axis in Fig. 4.6a). However, for all the GSA studies, a portion of the simulations resulted in a lower stability of nitrifiers (SF_{ANO}) for the RAS-ozonated systems (i.e., below 0 on the y-axis in Fig. 4.6) than for the non-ozonated one, suggesting that a range of the possible parameter values may lead to a decrease in nitrification process stability upon the installation of new RAS-ozonation systems.

Similar to the two other model outputs, the GSA study found the change in SF_{ANO} significantly sensitive to eight operational (Op) and ozone reaction (Oz) parameters, but not to biochemical (B) model parameters to the exception $\mu_{ANO,max,20}$ (Table 4.5). Notably, SF_{ANO} was not sensitive to the TKN_{Inf}/COD_{Inf} ratio (Table 4.5), contrary to the sensitivity of the SNA (Table 4.4).

SRT and *temperature* were the most influential operational parameters on nitrification stability (Table 4.5). Analysis of simulation results for the 40% sludge reduction study, showed that, in 9% to 11% of the simulations, the $SF_{ANO,ozonated}$ was lower than the $SF_{ANO,control}$ when the $SRT_{control}$ and temperatures were below 10 d (Fig. 4.6b) and 12 °C (Fig. 4.6c), respectively. This means that, in colder climates and for AS systems with lower SRTs, approximately 10% of

simulated cases lead to nitrification failure. For AS systems operating at temperatures above 12 °C or SRT above 10 d before the installation of RAS-ozonation, our simulation study suggests that it is virtually impossible for the nitrification process to be worse with RAS-ozonation than without, which may explain why this concern was never raised for European installations. The situation however, is different in North America.

Table 4.5. Sensitivity of the change in nitrification *SF*[a] upon the introduction of RAS-ozonation with changes in model parameters for variable waste biosolids reductions.

Parameters	Parameters Type[b]		*SRC*[c] (R^2= 0.77±0.01[d])
Significant parameters (p<0.05)			
SRT	Op	–	0.825±0.028 [d]
$q_{XU\_XCB,O3,trans}$	Oz	–	0.448±0.021
$b_{OHO,O3,inact}/q_{XU\_XCB,O3,trans}$	Oz	+	0.182±0.012
$f_{SU,O3}$	Oz	+	0.172±0.023
Temperature	Op	–	0.169±0.014
$b_{OHO,O3,inact}/b_{ANO,O3,inact}$	Oz	–	0.080±0.020
Anoxic vs. Aerobic systems systems[e]	Op	+	0.091±0.001
$\mu_{ANO,max,20}$	B	–	0.054±0.008
Non-significant parameters (p >0.05)			
TKN_{Inf}/COD_{Inf}	Op	–	0.036±0.011
$b_{OHO,O2,20}$	B	–	0.032±0.015
i_{N_XU}	Op	+	0.013±0.011
$f_{SB,Inf}$	Op	–	0.013±0.009
$b_{ANO,O2,20}$	B	–	0.009±0.014
$K_{NHx,ANO}$	B	–	0.005±0.008
Y_{ANO}	B	+	0.000±0.010

a change in nitrification *SF*: $\ln(SF_{ANO,O3}/SF_{ANO,control})$
b Parameter types: Oz, ozone transformation; Op, reactor operation; B, biochemical
c SRC: standardized regression coefficients
d ± standard error of three sampling sets
e Aerobic vs Anoxic systems was tested by adjusting yields: $Y_{SB\_Stor} \times Y_{OHO}$

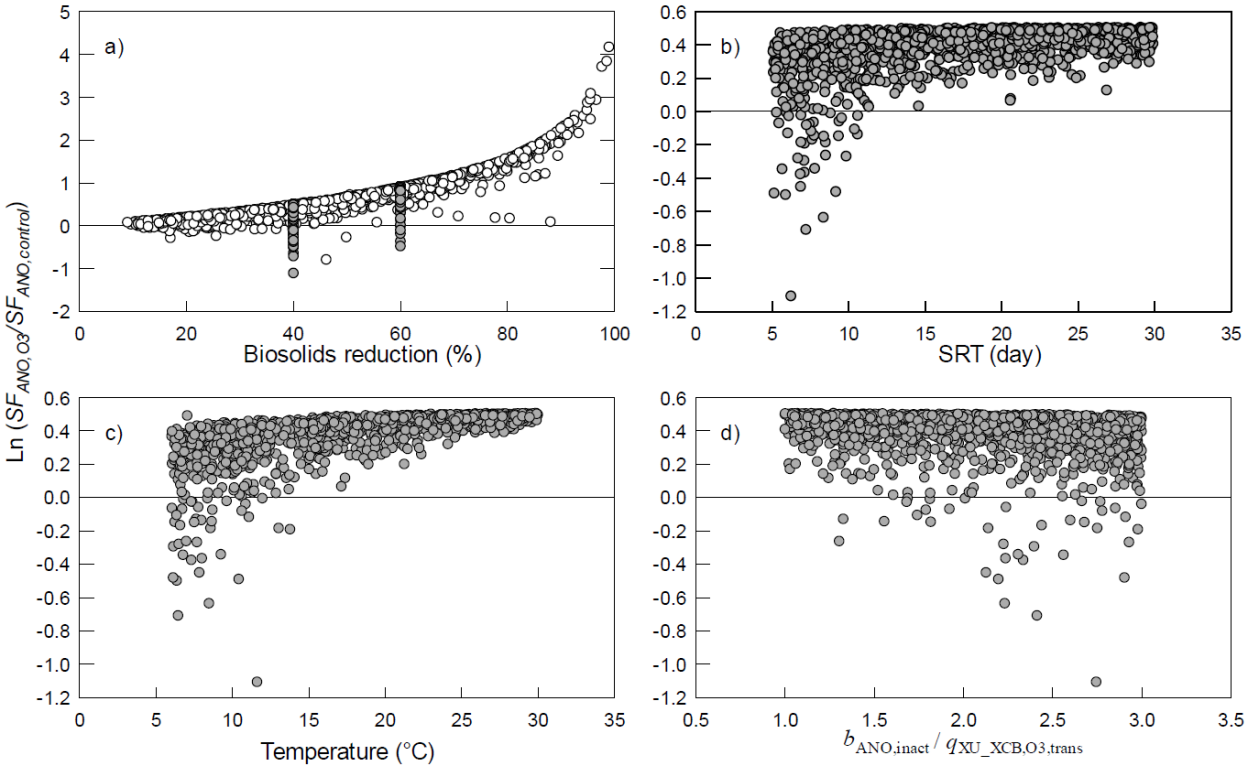

Fig. 4.6. Change in expected nitrification process stability in the GSA study for variable (open white circles) and constant (solid grey circles; 40 and 60%) sludge reduction (a). Changes vs. SRT (b), temperature (c), and nitrifier inactivation rate: non-biomass transformation rate (d) for 40% sludge reduction**.**

4.4. CONCLUSIONS

- The model satisfactorily simulated the Year 2 pilot-scale experiment data with calibrated values from the Year 1. It was also able to simulate validation observations on changes in SNA due to RAS-ozonation compiled from our experiments and the literature.
- GSA on waste biosolids reduction showed the influence of operational and RAS-ozonation related parameters in reducing biosolids production and demonstrated that higher reduction would be achieved in WWTPs with a high non-degradable particulate COD fraction in the influent and a higher process SRT.

- GSA demonstrated that the SNA could either increase or decrease upon the introduction of RAS-ozonation and this variation depends on both ozone transformation and operational parameters.
- GSA suggested that the stability of nitrification in RAS-ozonated systems should be considered carefully in colder climates (temperatures below 12 °C) and in systems with SRTs below 10 d.

4.5. ACKNOWLEDGEMENTS

This work was funded by the Natural Sciences and Engineering Research Council of Canada's Collaboration Research and Development program (NSERC-CRD) in collaboration with Air Liquide Canada.

4.6. REFERENCES

Acumedia Manufacturers Inc., 2011. Yeast Extract (PI 7184), Neogen Corporation, Lansing (MI), USA.

APHA, AWWA, WEF, 2005. Standard Methods for the Examination of Water and Wastewater, American Public Health Association, Washington, DC, USA.

Böhler, M., Siegrist, H., 2004. Partial ozonation of activated sludge to reduce excess sludge, improve denitrification and control scumming and bulking. Water Science and Technology 49(10), 41-49.

Chu, L.-B., Yan, S.-T., Xing, X.-H., Yu, A.-F., Sun, X.-L., Jurcik, B., 2008. Enhanced sludge solubilization by microbubble ozonation. Chemosphere 72(2), 205-212.

Deleris, S., Geauge, V., Camacho, P., Debelletontaine, H., Paul, E., 2002. Minimization of sludge production in biological processes: an alternative solution for the problem of sludge disposal. Water Science and Technology 46(10), 63-70.

Dytczak, M.A., Londry, K.L., Siegrist, H., Oleszkiewicz, J.A., 2007. Ozonation reduces sludge production and improves denitrification. Water Research 41(3), 543-550.

Dytczak, M.A., Londry, K.L., Oleszkiewicz, J.A., 2008. Activated sludge operational regime has significant impact on the type of nitrifying community and its nitrification rates. Water Research 42(8-9), 2320-2328.

Foladori, P., Andreottola, G., Ziglio, G., 2010a. Sludge Reduction Technologies in Wastewater Treatment Plants, IWA Publishing, London, UK.

Foladori, P., Tamburini, S., Bruni, L., 2010b. Bacteria permeabilization and disruption caused by sludge reduction technologies evaluated by flow cytometry. Water Research 44(17), 4888-4899.

Gardoni, D., Ficara, E., Fornarelli, R., Parolini, M., Canziani, R., 2011. Long-term effects of the ozonation of the sludge recycling stream on excess sludge reduction and biomass activity at full-scale. Water Science and Technology 63(9), 2032-2038.

Isazadeh, S., Feng, M., Urbina Rivas, L.E., Frigon, D., 2014. New mechanistically-based model for predicting reduction of biosolids waste by ozonation of return activated sludge. Journal of Hazardous Materials 270, 160-168.

Isazadeh, S., Ozcer, P., Jauffur, S., Frigon, D., in prep. Dynamics and diversity of nitrifiers in activated sludge exposed to ozone for sludge reduction.

Labelle, M.A., Ramdani, A., Deleris, S., Gadbois, A., Dold, P., Comeau, Y., 2011. Ozonation of endogenous residue and active biomass from a synthetic activated sludge. Water Science and Technology 63(2), 297-302.

Melcer, H., 2004. Methods for wastewater characterization in activated sludge modelling, p. 596.

Moussa, M.S., Lubberding, H.J., Hooijmans, C.M., van Loosdrecht, M.C.M., Gijzen, H.J., 2003. Improved method for determination of ammonia and nitrite oxidation activities in mixed bacterial cultures. Applied Microbiology and Biotechnology 63(2), 217-221.

Paul, E., Liu, Q.-S., Liu, Y., 2012. Biological Sludge Minimization and Biomaterials/Bioenergy Recovery Technologies. Paul, E. and Liu, Y. (eds), p. 209, John Wiley & Sons, Inc, Hoboken, New Jersey.

Reichert, P., 1998. AQUASIM 2.0: computer program for the identification and simulation of aquatic systems, Swiss Federal Institute for Environmental Science and Technology (EAWAG).

Rittmann, B., McCarty, P.L., 2001. Environmental Biotechnology : Principles and Applications, McGraw-Hill Science Engineering, New Yourk.

Sakai, Y., 1997. An activated sludge process without excess sludge production. Water Science and Technology, 163-170.

Saltelli, A., Ratto, M., Andres, T., Campolongo, F., Cariboni, J., Gatelli, D., Saisana, M., Tarantola, S., 2008. Global Sensitivity Analysis. The Primer, pp. 237-275, John Wiley & Sons.

Sin, G., Gernaey, K.V., Neumann, M.B., van Loosdrecht, M.C.M., Gujer, W., 2011. Global sensitivity analysis in wastewater treatment plant model applications: Prioritizing sources of uncertainty. Water Research 45(2), 639-651.

Sokal, R., Rohlf, F.J., 1995. Biometry; The Principles and Practice of Statistics in Biological Research.

Vergine, P., Menin, G., Canziani, R., Ficara, E., Fabiyi, M., Novak, R., Sandon, A., Bianchi, A., Bergna, G., 2007. Partial ozonation of activated sludge to reduce excess sludge production: evaluation of effects on biomass activity in a full scale demonstration test, pp. 295-302, Moncton, Canada.

4.7. SUPPLEMENTARY MATERIALS

List of Abbreviations and Symbols

Measured Constituents		Unit
COD	Chemical oxygen demand	[g.m^{-3}]
MLVSS	Mixed liquor volatile suspended solids	[g.m^{-3}]
RAS	Return activated sludge	[g.m^{-3}]
SRT	Solid retention time	[g.m^{-3}]
TKN	Total Kjeldahl Nitrogen	[d]
SF	Safety factor	[g-N.m^{-3}]
LHS	Latin Hypercube Sampling	[g-O_2.g^{-1}-
SOUR	Specific Oxygen uptake rate	VSS .d^{-1}]
BR	Biosolids reduction	
SRC	Standardized regression coefficient	[g NO_3,O_2.g^{-1}-
SNA	Specific nitrification activity	VSS. d^{-1}]
GSA	Global sensitivity analysis	
COD pools of ASM3		
$f_{SB,Inf}$	Soluble biodegradable COD fraction in the influent	[NU][a]
S_B	Soluble biodegradable COD	[g-COD.m^{-3}]
S_U	Soluble undegradable COD	[g-COD.m^{-3}]
X_{ANO}	Autotrophic nitrifying organism biomass COD	[g-COD.m^{-3}]
X_{OHO}	Ordinary heterotrophic organism biomass COD	[g-COD.m^{-3}]
X_{STO}	Storage compound COD in ordinary heterotrophic organisms	[g-COD.m^{-3}]
X_U	Particulate undegradable COD from the influent	[g-COD.m^{-3}]
X_{U_biolys}	Biomass debris	[g-COD.m^{-3}]
XC_B	Particulate/colloidal biodegradable COD	[g-COD.m^{-3}]
Model parameters of ASM3 used in the text		
$K_{SB,OHO}$	Half saturation constant for soluble biodegradable COD Half	[g-COD.m^{-3}]
K_{NH4}	saturation constant for soluble ammonium	[g-S_{NH4}. m^{-3}]

a NU: No Unit

Model parameters describing ozone transformation of solids		
Stoichiometric solids transformation and inactivation fractions		
f_{Bio}	Fraction of biomass in particulate COD excluding storage	[NU]
$f_{Bio,storage}$	Fraction of biomass in particulate COD including storage	[NU]
$f_{mnr,O3}$	Fraction of transformed COD that is mineralized (mnr)	[NU]
$f_{SB\_O3,inact}$	Soluble biodegradable COD fraction of inactivated biomass	[NU]
$f_{SU\_O3,inact}$	Soluble undegradableCOD fraction of inactivated biomass	[NU]
$f_{SB\_O3,trans}$	Soluble biodegradable COD fraction of transformed non-biomass	[NU]
$f_{SU\_O3,trans}$	Soluble undegradableCOD fraction of transformed non-biomass	[NU]
Transformation and inactivation rates and constants		

List of Abbreviations and Symbols

$b_{\text{Bio,O3,inact}}$	Inactivation rate of biomass due to ozone	$[d^{-1}]$
$q_{\text{Xtot,O3,sol}}$	Overall solids COD solubilization by ozone rate constant normalized to the aerated solids COD inventory	$[d^{-1}]$
$q_{\text{XU\_XCB,O3,trans}}$	Non-biomass solids transformation rate due to ozone	$[d^{-1}]$
COD_{sol}	Soluble COD increase through the ozone contactor	$[g.m^{-3}]$
$\eta_{\text{Bio,O3,inact}}$	first-order inactivation coefficient with respect to COD_{sol}	$[m^3.g^{-1}]$
$q_{\text{MLVSS treated}}$	fraction of biosolids inventory exposed to ozone per day	$[d^{-1}]$

Table 4.S1. Gujer stoichiometry matrix and process rates for the IWA-ASM3 model extension describing ozone conversions.

Process	COD and N pool										Rates
	S_B	S_U	S_{O3}	S_{NH4}[a]	XC_B	XC_{B_Stor}[b]	X_{OHO}	$X_{OHO,Stor}$	X_{ANO}	X_{U_Inf}	$X_{U\_Bio,lys}$	
Transformation												
Undegradable (influent)	$f_{SB\_O3,trans}$	$f_{SU\_O3,trans}$	$f_{mnr,O3}$	$i_{N\_XU\_inf} - (f_{XCB\_O3,inact} \times i_{N\_XCB})$	$f_{XCB\_O3,trans}$					−1		$q_{XU\_XCB,O3,trans} \times X_{U,inf}$
Undegradable (decay residue)	$f_{SB\_O3,trans}$	$f_{SU\_O3,trans}$	$f_{mnr,O3}$	$i_{N\_XU\_Bio,lys} - (f_{XCB\_O3,inact} \times i_{N\_XCB})$	$f_{XCB\_O3,trans}$						−1	$q_{XU\_XCB,O3,trans} \times X_{U\_Bio,lys}$
Biodegradable	$f_{SB\_O3,trans}$	$f_{SU\_O3,trans}$	$f_{mnr,O3}$	$i_{N\_XCB} \times (f_{XCB\_O3,trans} - 1)$	$f_{XCB\_O3,trans} - 1$							$q_{XU\_XCB,O3,trans} \times XC_B$
Inactivation												
Heterotrophs	$f_{SB\_O3,inact}$	$f_{SU\_O3,inact}$		$i_{N\_XBio} - (f_{XU\_Bio,lys} \times i_{N\_XBio,})$	$f_{XCB\_O3,inact}$		−1				$f_{XU\_Bio,lys}$	$b_{OHO,O3,inact} \times X_{OHO}$
Storage						+1		−1				$b_{OHO,O3,inact} \times X_{OHO,Stor}$
Autotrophs	$f_{SB\_O3,inact}$	$f_{SU\_O3,inact}$		$i_{N\_XBio} - (f_{XU\_Bio,lys} \times i_{N\_XBio})$	$f_{XCB\_O3,inact}$				−1		$f_{XU\_Bio,lys}$	$b_{ANO,O3,inact} \times X_{ANO}$

[a] Note that S_B, and S_U, were, at this point, assumed not to contain nitrogen.

[b] XC_{B_Stor} is consumed at the same rate as XC_B but does not contains nitrogen.

Table 4.S2. Model parameter values used to simulate the Year 2 operation data from the pilot-scale reactors.

Description	Standard notation	Units	Value	References
Kinetics parameters				
Hydrolysis				
Maximum specific hydrolysis rate	$q_{XCB\_SB,hyd}$	g XC_B.g X_{OHO}^{-1}.d^{-1}	3	[1]
Half saturation parameter for XC_B/X_{OHO}	$K_{XCB,hyd}$	g XC_B.g X_{OHO}^{-1}	1	[1]
Aerobic and Anoxic (storage, growth, and endogenous respiration) of X_{OHO}				
Rate constant for $X_{OHO,Stor}$ storage	q_{SB_Stor}	g XC_B.g X_{OHO}^{-1}.d^{-1}	1	[1]
Maximum growth rate of X_{OHO}	$\mu_{OHO,Max}$	d^{-1}	2.68	[1]
Reduction factor for anoxic growth of	$n_{\mu OHO,Ax}$	_	0.6	[1]
Half saturation parameter for S_B	$K_{SB,OHO}$	g S_B.m^{-3}	9.8	[1]
Half saturation parameter $X_{OHO,Stor}/X_{OHO}$	K_{Stor_OHO}	g X_{Stor}.g X_{OHO}^{-1}	1	[1]
Endogenous respiration rate of X_{OHO}	$b_{OHO,O2,20}$	d^{-1}	0.2	[1]
Endogenous respiration rate of X_{OHO}	$b_{OHO,Ax}$	d^{-1}	0.5	[1]
Endogenous respiration rate of $X_{OHO,Stor}$	$b_{Stor,Ox}$	d^{-1}	0.2	[1]
Endogenous respiration rate of $X_{OHO,Stor}$	$b_{Stor,Ax}$	d^{-1}	0.1	[1]
Half saturation parameter for S_{O2}	$K_{O2,OHO}$	g S_{O2}.m^{-3}	0.2	[1]
Half saturation parameter for S_{NOx}	$K_{NOx,OHO}$	g S_{NOx}.m^{-3}	0.1	[1]
Half saturation parameter for S_{NHx}	$K_{NHx,OHO}$	g S_{NHx}.m^{-3}	0.35	[1]
Half saturation parameter for S_{Alk}	$K_{Alk,OHO}$	mol HCO_3^-.m^{-3}	0.1	[1]
Growth growth, Aerobic and Anoxic endogenous respiration of X_{ANO}				
Endogenous respiration rate for X_{ANO}	$b_{ANO,Ax}$	d^{-1}	0.05	[1]
Maximum growth rate of X_{ANO}	$\mu_{ANO,Max}$	d^{-1}	1	[1]
Endogenous respiration rate for X_{ANO}	$b_{ANO,O2,20}$	d^{-1}	0.15	[1]
Half saturation parameter for S_{O2}	$K_{O2,ANO}$	g S_{O2}.m^{-3}	0.5	[1]
Half saturation parameter for S_{NHx}	$K_{NHx,ANO}$	g S_{NHx}.m^{-3}	0.05	[1]
Half saturation parameter for S_{Alk}	$K_{Alk,ANO}$	mol HCO_3^-.m^{-3}	0.5	[1]
Stoichiometry parameters				
Hydrolysis				
Fraction of inert COD generated in	$f_{SU\_XCB,hyd}$	g S_U.g XC_B^{-1}	0	[1]
Yield for X_{OHO} growth per $X_{OHO,Stor}$	$Y_{Stor\_OHO,Ox}$	g X_{OHO}.g X_{Stor}^{-1}	0.63	[1]
Yield for X_{OHO} growth per $X_{OHO,Stor}$	$Y_{Stor\_OHO,Ax}$	g X_{OHO}.g X_{Stor}^{-1}	0.7	[1]
Yield for $X_{OHO,Stor}$ formation per S_B	$Y_{SB\_Stor,Ox}$	g X_{Stor}.g S_B^{-1}	0.7	[1]
Yield for $X_{OHO,Stor}$ formation per S_B	$Y_{SB\_Stor,Ax}$	g X_{Stor}.g S_B^{-1}	0.33	[1]
Fraction of X_U generated in biomass	$f_{XU\_Bio,lys}$	g X_U.g X_{Bio}^{-1}	0.2	[1]
Yield of X_{ANO} growth per S_{NO3}	Y_{ANO}	g X_{AUT}.g S_{NOx}^{-1}	0.24	[1]
Nitrogen conversion				[1]
N content of S_B	i_{N_SB}	g N.g S_B^{-1}	0	[1]
N content of S_U	i_{N_SU}	g N.g S_U^{-1}	0	[1]
N content of X_U	i_{N_XU}	g N.g X_U^{-1}	0.07	[1]
N content of X_B	i_{N_XCB}	g N.g XC_B^{-1}	0	[1]
N content of biomass (X_{OHO}, X_{PAO}, X_{ANO})	i_{N_XBio}	g N.g X_{Bio}^{-1}	0.0875	[1]
TSS conversion				
Conversion factor X_U in TSS	i_{TSS_XU}	g TSS.g X_U^{-1}	0.75	[1]

Conversion factor X_B in TSS	i_{TSS_XCB}	g TSS.g XC_B^{-1}	0.75	[1]
Conversion factor biomass in TSS	$i_{TSS\_XOHO,Stor}$	g TSS.g X_{Stor}^{-1}	0.8197	[1]
Conversion factor XSTO in TSS	i_{TSS_XBio}	g TSS.g X_{Bio}^{-1}	0.6	[1]
COD and charge conversion				
Conversion factor for NO_3 reduction to	$i_{NOx,N2}$	g COD.g N^{-1}	2.857	[1]
Conversion factor for NO_3 in COD	i_{COD_NOx}	g COD.g N^{-1}	−4.571	[1]
Conversion factor for N_2 in COD	i_{COD_N2}	g COD.g N^{-1}	−1.7143	[1]
Conversion factor for NH_x in charge	i_{Charge_NHx}	Charge.g N^{-1}	0.071	[1]
Conversion factor for NO_3 in charge	i_{Charge_NOx}	Charge.g N^{-1}	−0.0714	[1]
Influent COD fractions				
Soluble biodegradable organics	f_{SB}	g-COD_{SB}/ g-	0.39	[2]
Soluble undegradable organics	f_{Su}	g-COD_{SU}.m^{-3}	0.05	[2]
Particulate undegradable organics	f_{XU}	g-COD_{XU}.m^{-3}	0.25	[2]
Particulate biodegradable organics	f_{XCB}	g-COD_{XCB}.m^{-3}	0.31	[2]
Ordinary heterotrophic organisms	f_{XOHO}	g-COD_{XOHO}.m^{-3}	0	[2]
Ozone transformation parameter (Oz)				
Fraction of undegradable solids COD	$f_{SU\_O3trans}$	g COD_{SU}.g COD_X^{-1}	0.216	[2]
Fraction of biodegradable COD	$f_{SB\_O3trans}$	g COD_{SB}.g COD_X^{-1}	0.418	[2]
Fraction of particulate biodegradable	$f_{XCB,O3\ trans}$	g COD_{XCB}.g COD_X^{-1}	0. 366	[2]
COD fraction mineralized by ozone	$f_{mnr,O3}$	g COD_{mnr}.g COD_X^{-1}	0.0402	[2]

[1] (Hauduc et al. 2011), [2] (Isazadeh et al. 2014, chapter 3)

Table 4.S3. Range of selected variables for sensitivity analysis of BR-efficiency, SNA and stability.

Notation	Description (units)	Values (Min-Max)	References [a]
Biochemical model parameters at 20 °C (B)			
$q_{XCB\_SB,hyd}$	Maximum specific hydrolysis rate (g X_{CB}/g X_{OHO}.d)	3-9	[4]
$K_{SB,OHO}$	Half saturation parameter for S_B (g SB/m^{-3})	2-10	[4]
$K_{XCB,hyd}$	Half saturation parameter for X_{CB}/X_{OHO} (g X_{CB}/g X_{OHO})	0.75-1.25	[5]
$b_{ANO,O2,20}$	Decay coefficient for autotrophs (d^{-1})	0.04-0.15	[1]
$\mu_{OHO,Max}$	Maximum growth rate of X_{OHO} (d^{-1})	2-3	[4]
$b_{OHO,O2,20}$	Decay coefficient for heterotrophs (d^{-1})	0.1-0.3	[4]
$K_{NHx,ANO}$	Ammonia half-saturation coefficient (g-N/m^3)	0.05-1.50	[1]
$\mu_{ANO,max,20}$	Maximum specific growth rate for autotrophs (d^{-1})	1.0-1.3	[1]
Y_{ANO}	Autotrophic yield (g-X_{ANO}/g-N)	0.05-0.35	[1]
Ozone transformation parameter (Oz)			
$b_{OHO,O3}/q_{XU\_XCB,O3,tra}$	Ratio Heterotroph inactivation to non-biomass solid transformation	1-4	[3]
$b_{OHO,O3}/b_{ANO,O3}$	Ratio: heterotroph inactivation to nitrifier inactivation	1-4	[3]
$f_{SU\_O3trans}=f_{SU\_O3\ inact}$	Frac.(Transf& inact) solids COD solubilized and undegradable	0.0-0.3	[3]
$f_{SB\_O3trans}=f_{SB\_O3\ inact}$	Frac. (Transf& inact) solids COD solubilized and biodegradable	0.0-0.3	[3]
$q_{XTot,O3\ sol}$	Overall solids solubilization rate constant (d^{-1})	0.02	Arbitrary
Operational parameters (Op)			
COD	Total chemical oxygen demand (g COD/m^3)	250-900	[1]
i_{N_Xu}	Mass of nitrogen per mass of inertparticulate: COD (g-N/g-CODX_U)	0.00-0.04	[4]
T	Temperature (°C)	6-30	[2]
$f_{SB,Inf}$	Fraction of readily degradable COD on total COD	0.3-1.0	[2]
SRT	Solids Retention Time (d)	5.0-30	[2]
TKN_{Inf}	Mean total Kjeldahl nitrogen inflow concentration (gN-/m^3)	20-60	[2]
$Y_{SB\_Stor,O2}$ [b]	Cell internal storage product yield (g-CODX_{Stor}/g-CODS_B)	0.54-0.80	[4]
$Y_{OHO,O2}$ [b]	Heterotrophic yield (g-CODX_{OHO}/g-CODX_{Stor})	0.7-0.8	[4]
HRT	Hydraulic retention time (d)	0.125-1.25	[2]

[a] Ref: References from which the range were taken. [1] (Rittmann and McCarty 2001)[2] (Tchobanoglous et al. 2003). [3] (Isazadeh et al. 2014, chapter 3) – the results obtained in this paper were multiplied by 2 to get the maximum values, [4] (Hauduc et al. 2011), [5] (Gujer et al. 1999)– 25th and 75th percentiles survey results for minimum and maximum values, respectively.

[b] $Y_{OHO,}$ and $Y_{SB\_Stor,O2}$ have been considered as the operational parameters and the higher values were selected in order to cover the anoxic/aerobic range.

Table 4.S4 Sensitivity of the changes in nitrifying biomass [$\ln(X_{ANO,O3}/X_{ANO,Ctrl})$][a] upon introduction of RAS-ozonation with respect to changes in model parameters.

Constant sludge reduction 40 % (R^2=0.72±0.01 [b])				Constant sludge reduction 60 % (R^2=0.70±0.02)			
Parameters	Types[c]		standardized regression	Parameters	Types		standardized regression coefficients
Significant parameters(p<0.05)				Significant parameters(p<0.05)			
$b_{OHO,O3,inact}/q_{XU\_XCB,O3,trans}$	Oz	+	0.583 ±0.013 [b]	$b_{OHO,O3,inact}/q_{XU\_XCB,O3,trans}$	Oz	+	0.532 ±0.021
TKN_{Inf}/COD_{Inf}	Op	+	0.485±0.006	TKN_{Inf}/COD_{Inf}	Op	+	0.474±0.004
$b_{OHO,O3,inact}/b_{ANO,O3,inact}$	Oz	–	0.462±0.014	$b_{OHO,O3,inact}/b_{ANO,O3,inact}$	Oz	–	0.435±0.021
Temperature	Op	–	0.450±0.023	*Temperature*	Op	–	0.420±0.028
SRT	Op	–	0.248±0.019	*SRT*	Op	–	0.293±0.026
$f_{SU,O3}$	Oz	–	0.132±0.012	$f_{SU,O3}$	Oz	–	0.181±0.021
i_{N_XU}	Op	–	0.101±0.014	i_{N_XU}	Op	–	0.116±0.023
Anoxic vs. Aerobic systems	Op	+	0.091±0.009	*Anoxic vs. Aerobic systems*	Op	+	0.098±0.007
$\mu_{ANO,max,20}$	B	–	0.079±0.004	$\mu_{ANO,max,20}$	B	–	0.083±0.008
$q_{XU\_XCB,O3,trans}$	Oz	+	0.074±0.003	$q_{XU\_XCB,O3,trans}$	Oz	+	0.070±0.002
$b_{ANO,O2,20}$	B	–	0.074±0.021	$b_{ANO,O2,20}$	B	–	0.070±0.015
Non-significant parameters (p >0.05)				Non-significant parameters (p >0.05)			
$K_{NHx,ANO}$	B	–	0.030±0.011	$K_{NHx,ANO}$			0.026±0.009
$f_{SB,Inf}$	Op	+	0.018±0.013	$f_{SB,Inf}$			0.020±0.017
Y_{ANO}	B	+	0.009±0.015	Y_{ANO}			0.008±0.011
$b_{OHO,O2,20}$	B	+	0.008±0.005	$b_{OHO,O2,20}$			0.007±0.006

a For constant MLVSS: $(X_{ANO,O3}/X_{MLVSS,O3})/(X_{ANO,Ctrl}/X_{MLVSS,Ctrl})$ = ratio $(X_{ANO,O3}/X_{ANO,Ctrl})$

b ± standard error of three sampling sets

c Parameter types: Oz, ozone transformation; Op, reactor operation; B, biochemical

Table 4.S5 Sensitivity of the change in nitrification *SF* [interpreted as expected stability; $\ln(SF_{ANO,azonated}/SF_{ANO,control})$] upon the introduction of RAS-ozonation with changes in model parameters.

Constant sludge reduction 40 % (R^2= 0.77±0.01[a])				Constant sludge reduction 60 % (R^2=0.73±0.02)			
Parameters	Types[b]		standardized regression coefficients	Parameters	Types		standardized regression coefficients
Significant parameters(p<0.05)				Significant parameters(p<0.05)			
Temperature	Op	–	0.663±0.024	*Temperature*	Op	–	0.680±0.018
SRT	Op	–	0.475±0.021	*SRT*	Op	–	0.432±0.033
$b_{OHO,O3,inact}/q_{XU\_XCB,O3,trans}$	Oz	+	0.317±0.013	$b_{OHO,O3,inact}/q_{XU\_XCB,O3,trans}$	Oz	+	0.299±0.021
$b_{OHO,O3,inact}/b_{ANO,O3,inact}$	Oz	–	0.268±0.005	$b_{OHO,O3,inact}/b_{ANO,O3,inact}$	Oz	–	0.283±0.011
$\mu_{ANO,max,20}$	B	–	0.091±0.005	$\mu_{ANO,max,20}$	B	–	0.103±0.004
Non-significant parameters (p >0.05)				Non-significant parameters (p >0.05)			
Anoxic vs. Aerobic systems	Op	+	0.067±0.024	*Anoxic vs. Aerobic systems*	Op	+	0.075±0.015
$f_{SU,O3}$	Oz	–	0.060±0.017	$f_{SU,O3}$	Oz	–	0.066±0.027
$q_{XU\_XCB,O3,trans}$	Oz	+	0.060±0.017	$q_{XU\_XCB,O3,trans}$	Oz	+	0.066±0.023
TKN_{Inf}/COD_{Inf}	Op	–	0.029±0.008	TKN_{Inf}/COD_{Inf}	Op	–	0.038±0.006
$K_{NHx,ANO}$	B	–	0.019±0.014	$K_{NHx,ANO}$	B	–	0.024±0.019
i_{N_XU}	Op	+	0.012±0.015	i_{N_XU}	Op	+	0.020±0.020
$f_{SB,Inf}$	Op	+	0.011±0.008	$f_{SB,Inf}$	Op	+	0.017±0.011
$b_{ANO,O2,20}$	B	–	0.010±0.026	$b_{ANO,O2,20}$	B	–	0.013±0.031
Y_{ANO}	B	+	0.008±0.023	Y_{ANO}	B	+	0.009±0.015
$b_{OHO,O2,20}$	B	+	0.001±0.010	$b_{OHO,O2,20}$	B	+	0.001±0.009

a ± standard error of three sampling sets

b Parameter types: Oz, ozone transformation; Op, reactor operation; B, biochemical

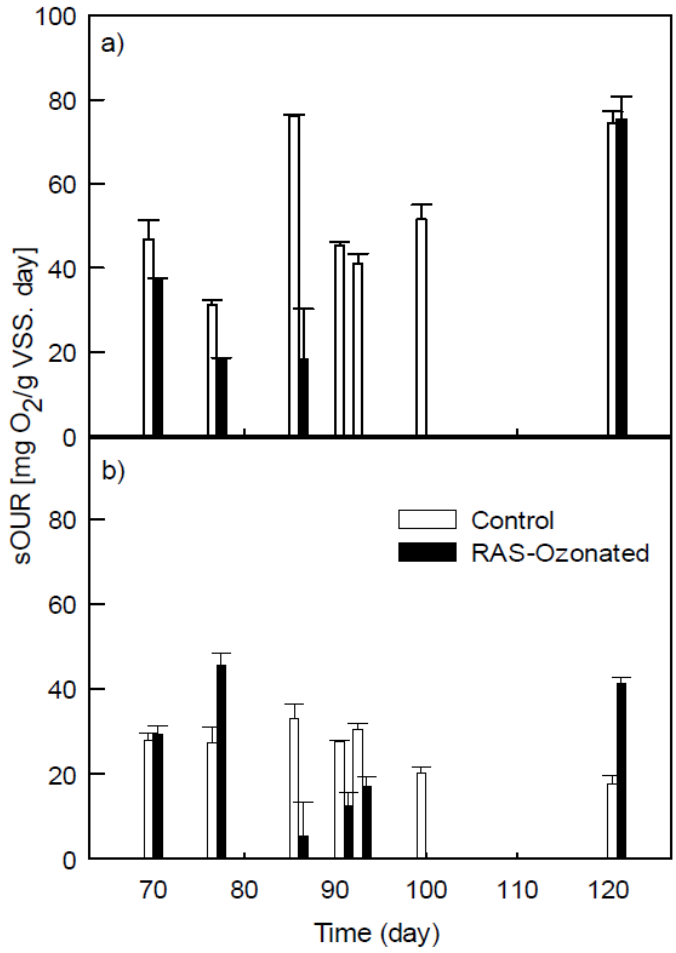

Fig. 4.S1. Specific oxygen uptake rate by: (a) ammonia-oxidizing organisms (AOO) and, (b) nitrite oxidizing (NOO) during the Year 2 of pilot-scale experiment.

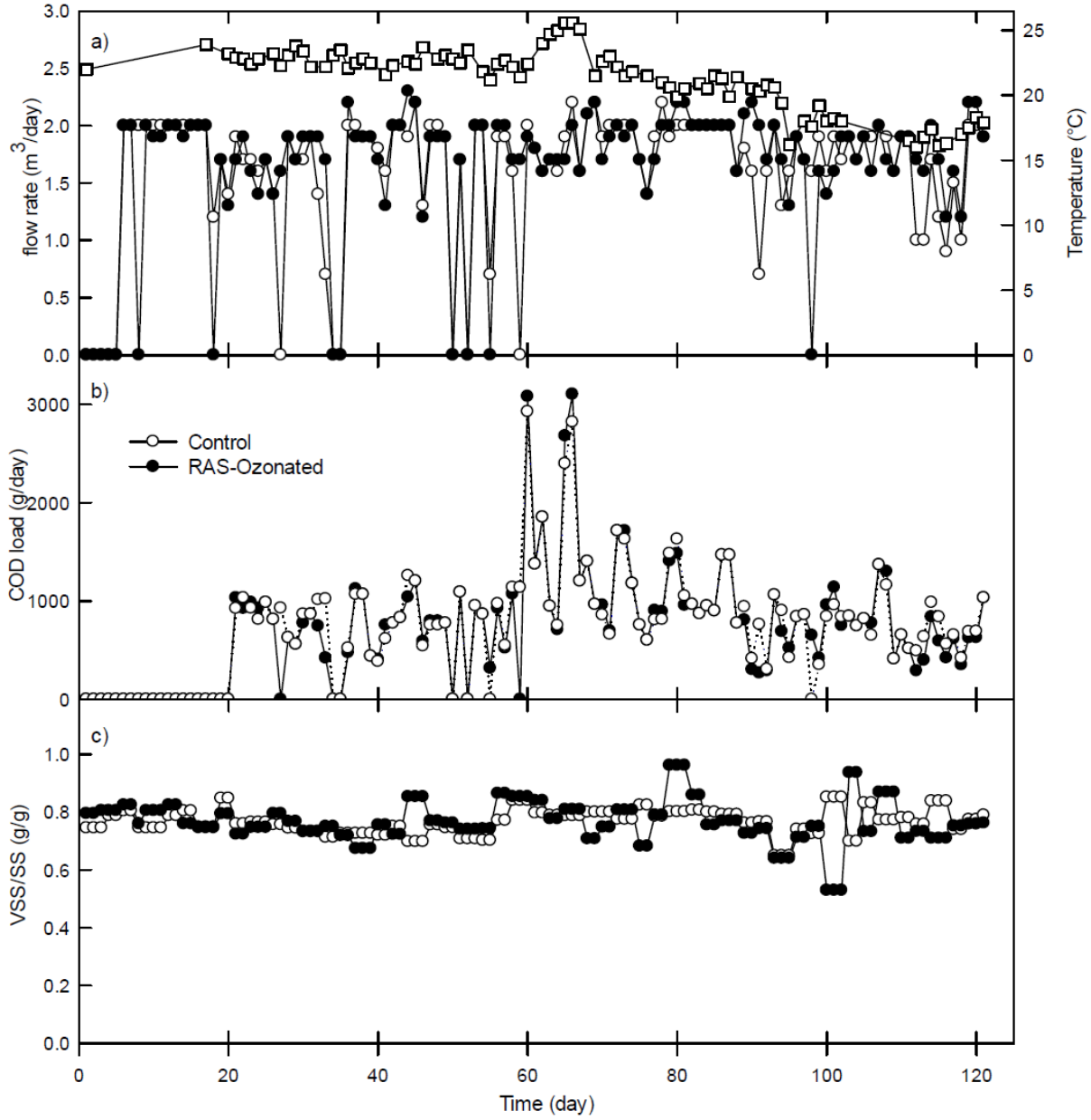

Fig. 4.S2. Influent wastewater characteristics at Year 2 of pilot-scale experiment in control (open circle) and RAS-ozonated (black circle) reactors: (a) Influent flow rate (m^3/day) and temperature (°C) (open square- read with right axis), (b) COD load (g/day) and (c) MLVSS/MLSS ratio in control ad RAS-ozonated reactor.

References of supplementray materials

Gujer, W., Henze, M., Mino, T., van Loosdrecht, M.C.M., 1999. Activated sludge model No. 3. Water Science and Technology 39(1), 183-193.

Hauduc, H., Rieger, L., Ohtsuki, T., Shaw, A., Takacs, I., Winkler, S., Heduit, A., Vanrolleghem, P.A., Gillot, S., 2011. Activated sludge modelling: development and potential use of a practical applications database. Water Science and Technology 63(10), 2164-2182.

Isazadeh, S., Feng, M., Urbina Rivas, L.E., Frigon, D., 2014. New mechanistically based model for predicting reduction of biosolids waste by ozonation of return activated sludge. Journal of Hazardous Materials 270, 160-168.

Rittmann, B., McCarty, P.L., 2001. Environmental Biotechnology : Principles and Applications, McGraw-Hill Science Engineering, New Yourk.

Tchobanoglous, G., Burton, F.L., Metcalf, Eddy, 2003. Wastewater Engineering : Treatment, Disposal, and Reuse, McGraw-Hill, New York.

Chapter 5:

Microbial community structure of wastewater treatment subjected to high mortality rate due to ozonation of return activated sludge

Connecting text: In the current chapter, we turn our attention to the long-term dynamics of the community structure when the solids are subjected to RAS-ozonation. Since 16S rRNA gene PCR amplicon pyrosequencing with primers targeting nearly all bacteria was used, the ordinary heterotrophic microorganisms dominate the community structure data. The data suggest that RAS-ozonation does not really affect the dynamics of the community structure. However, the analysis showed that specific populations occurred in the pilot-scale and full-scale reactors because of specific treatment conditions. Finally, the comparison of community structures from 16S rRNA gene amplicon pyrosequencing and fluorescence *in situ* hybridization (FISH) showed that the biases could occur between the two techniques, and care should be exercised in interpreting the data. The results of this research have been presented in the paper:

Isazadeh, S., Ozcer, P. and Frigon. D,. Microbial community structure of wastewater treatment subjected to high mortality rate due to ozonation of return activated sludge. *Journal of Applied Microbiology*. 2014, 117 (2), 586-596.

5.1. INTRODUCTION

Excess biosolids handling and disposal is one of the main operational burdens of large activated sludge wastewater treatment plants (AS-WWTPs). Besides the environmental risks associated with disposal of biosolids, its cost can account for up to 60% of the total operational budget of a plant (Horan 1990). The ever increasing disposal costs and the continuous tightening of environmental regulations for biosolids reuse and land application are driving many wastewater treatment plant operators to seek new technologies to minimize biosolids production. One such technology that has received increasing attention in recent decades is ozone integration with a portion of the return activated sludge (RAS) flow in ASWTP (Foladori et al. 2010).

RAS-ozonation has been used for biosolids minimization at a number of full-scale wastewater treatment plants in Europe and Asia (Böhler and Siegrist 2004, Cesbron et al. 2003, Huysmans et al. 2001, Yasui and Shibata 1994). However, besides economical reason, resistance to the technology exists in North America in part (i) due to imprecise predictions on the level of reduction in biosolids production to be achieved, and (ii) due to the lack of understanding on the changes that the microbial community will undergo after the installation of RAS-ozonation units. The goal of this paper is to understand the impact of high bacterial mortality by RAS-ozonation on the microbial community structure of activated sludge systems.

Ozone is a strong oxidant that reacts rapidly with suspended solids in the RAS. The immediate effect of this reaction is the solubilisation of a variety of organic compounds measured together as chemical oxygen demand (COD) (Chu et al. 2009). This observed COD solubilisation is the result of two classes of reactions. First, ozone rapidly inactivates microorganisms present in the RAS solids (Foladori et al. 2010). Second, ozone also transforms the non-biomass portion of the volatile solids (e.g., non-degradable cell debris, exopolymeric

substances (EPS), and non-degradable particulate organic compounds) into soluble and particulate degradable organics (Frigon and Isazadeh 2011, Paul et al. 2012). This second class of reactions is likely to be the main contributor to COD solubilisation observed during RAS-ozonation (Isazadeh et al. 2014). The reduction of waste biosolids production is a result of the consumption of ozone reaction products (inactivated biomass and transformed previously non-degradable compounds) by microorganisms in the aeration basin upon return of the treated RAS.

The impact of RAS-ozonation on the microbial community structure of activated sludge remains largely unexplored despite increasing research work on applications of the process. It has been suggested that RAS-ozonation may kill different bacterial populations at different rates depending on their locations in the floc or their capacity for adaptation (Böhler and Siegrist 2004, Deleris et al. 2002). In a study involving PCR/DGGE of 16S rRNA gene, it was found that DNA bands disappeared from activated sludge samples subjected to ozonation of the RAS, and that different bands disappeared at different rates (Yan et al. 2009a), supporting to some extent this hypothesis. If this is the case, then such differential inactivation should lead to restructuring of the microbial community. Additionally, the RAS-ozonation process affects the total solids and biomass turn-over rates. In one hand, the solids retention time (SRT) is typically increased by RAS-ozonation because the total solids inventory is kept constant after its installation. On the other hand, the higher mortality imposed by ozonation induces the microbes to grow faster than what would be expected at steady-state for the measured SRT. These two factors typically affect the abundance of certain microbial populations in activated sludge systems (Rittmann and McCarty 2001). Finally, the transformation of non-degradable particulates into degradable compounds may impact the phylogenetic composition of microbial communities by supplying

new substrates to the biomass. Together, these conjectures suggest that the RAS-ozonation process would likely change the microbial community composition of activated sludge systems.

To our knowledge, only one study ,using synthetic wastewater, investigated the microbial community structures in two lab-scale activated sludge reactors (control and ozonated) using molecular techniques (Yan et al. 2009b). During the experiment, the dissimilarities between the PCR/DGGE profiles of the two reactors increased during the first 60 days of operation and then remained stable until the end, suggesting that the communities in both reactors had acclimatized to the imposed operational conditions. However, with the use of a synthetic wastewater medium it is hard to judge and make any inference about whether ozonation could cause a similar effect in a full-scale system treating more complex real wastewaters. The current work aims at answering this question.

For the current study, two pilot-scale reactors (RAS-ozonated vs. control) treating real wastewater were operated for 98 days. The operation period was divided in four phases, and the ozone doses were increased during the experimental period. The details of the reactor operation and the mathematical modeling of the results are presented elsewhere (Isazadeh et al. 2014). In that previous analysis, it was found that the production of waste biosolids was reduced by approximately 48% in the last phase with the highest ozone dose. In the same phase, it was estimated that 85% of the microbial biomass was inactivated, raising questions on variations in the phylogenetic composition of the community. To address these questions high-throughput 454-pyrosequencing was applied to obtain a deep-sampling of the microbial diversity, and fluorescence *in situ* hybridization (FISH) was performed to detect any possible biases that may occur in the quantitative structures of the communities.

5.2. MATERIALS AND METHODS

5.2.1 Experimental setup

A control activated sludge wastewater treatment reactor and a parallel one equipped with a RAS-ozone contactor (Air Liquide Canada) were operated to treat real municipal wastewater for a total period of 158 days: a 60-day period for start-up and a 98-day period for generation of experimental data. The pilot-scale reactors had a total volume of 1.7 m^3 including clarifier. Each reactor was fed with 2 m^3/day of fresh municipal wastewater. Details of pilot-scale reactor configurations and operation are described elsewhere (Frigon and Isazadeh 2011, Isazadeh et al. 2014). For the RAS-ozonated reactor, approximately 18% of the total inventory was treated in the ozone contactor on a daily basis. The ozone concentrations in the feed and vent gas were measured online using an ozone analyzer (model IN2000-L2-LC; INUSA Inc., Norwood, MA, USA), and all the ozone was transferred to the RAS mixture. The gas flow rate was varied to adjust the ozone dosage. Ozone is a very unstable gas and decomposes within seconds in water in the presence of high concentrations of soluble and particulate organic materials. Furthermore, organic materials in wastewater efficiently scavenge molecular ozone and hydroxyl radicals (potentially generated by the decomposition of ozone), which leaves no detectable ozone residual in the RAS flow in the RAS-ozone reactor outlet. The experimental period was divided into four phases corresponding to four ozone doses in the ozone contactor: Phase I (Day 1-Day 23) with no-ozone, Phase II (Day 23-Day 52) with low ozone dose (22 mg/L or 2.1 mg-O_3 g^{-1}-MLVSS inventory d^{-1}), Phase III (Day 51-Day 76) with medium ozone dose (60 mg/L or 4.0 mg-O_3 g^{-1}-MLVSS inventory d^{-1}) and Phase IV, Day 77-Day 98, with high ozone dose (98 mg/L or 8.3 mg-O_3 g^{-1}-MLVSS inventory d^{-1}). In order to have a similar bacterial population composition at the

startup of the ozonation experiment, the two reactors were mixed and homogenized on Day 27 (i.e., at the beginning of the ozonation).

5.2.2 Process modeling of experimental setup

The effects of RAS-ozonation on the inactivation and growth rates of Ordinary Heterotrophic Organisms (OHO) were evaluated using a mathematical model extension of the International Water Association (IWA) consensus Activated Sludge Modeling 3 (ASM3) to describe ozone reactions with RAS (Isazadeh et al. 2014). ASM3 describes the growth and decay of OHO in activated sludge aeration basins, while the extension describes the transformation of non-degradable solids COD and the inactivation of biomass that result from ozone exposure. Biomass inactivation was modeled as an exponential decrease in OHO activity with increasing ozone doses. Details of model description, and its calibration and verification are presented elsewhere (Isazadeh et al. 2014). The calibrated model has been used herein to quantify the inactivation and growth rates of OHO in each phase of the experiment.

5.2.3 Sampling and analytical methods

Routine operational parameters: total and volatile suspended solids (TSS, VSS; method 2540), total and soluble COD (method 5220D), and BOD_5 (method 5210B), ammonium (NH_4^+; method 4500-NH_3-F), nitrite (NO_2^-; method 4500-NO_2^--B), and nitrate (NO_3^-; method 4500-NO_3^--H) were measured by Standard methods (APHA et al. 2005) by monitoring the influent and effluent characteristics of the activated sludge systems and of the RAS-ozone contactor (for details see Isazadeh et al. (2014)). In addition, two influent grab samples were collected to determine the concentration of alcohol and methane. The concentration of ethanol, isobutanol, isopropanol,

methanol and propanol was measured by GC/FID using the EPA method 8015D (US-EPA 2003) and methane using the Standard method 6211B (APHA et al. 2005).

The solids inventory was monitored by collecting grab samples from the aeration tanks, clarifiers (using a coliwasa), and waste biosolids, and performing TSS and VSS analyses. From a 15-mL portion of these grab samples, the solids were spun by centrifugation and stored at −80 °C until analysis. Twice a week, portions of grab samples taken from aeration basin were also fixed for 3 hours on ice with 4% paraformaldehyde/phosphate buffered saline (PFA/PBS) for FISH analysis. After fixation the solids were washed twice with PBS and re-suspended in 50% ethanol/PBS for storage at −20 °C until analysis (Nielsen and Daims 2009).

5.2.4 DNA extraction, 16S rRNA gene PCR amplification and sequencing

Three samples of aeration basin from Days 20, 60, and 94 (corresponding to periods of no-ozone, medium ozone, and high ozone doses) were selected for pyrosequencing. DNA was extracted using the Ultra Clean Fecal DNA Isolation Kit (MO BIO Laboratories, Inc., Carlsbad, CA, USA) according to the manufacturer's instructions. This kit is optimized for samples from stool, gut material and biosolids and in a comparative study of DNA extraction kit used in permafrost samples (Vishnivetskaya et al. 2014) showed a good yield of genomic DNA similar to other kits. The integrity of the extracted DNA was confirmed by 1% agarose gel electrophoresis in TAE buffer, and the purity of extractions was quantified by UV spectrophotometry (Sambrook et al. 2001). Extracted DNA samples were then submitted to Research and Testing Laboratory (Lubbock, TX, USA) for 16S rRNA gene PCR amplification using universal bacterial primers targeting the V3–V5 variable region (Table 5.S2), and amplicon sequencing using the Roche 454 FLX Genome Sequencer.

To ascertain the phylogenetic affiliation of the *Methylophilaceae* family sequences, a *Methylophilaceae* specific PCR amplification (Table 5.S2) was performed, and resulting amplicons were cloned using the GE p*MOSBlue* kit following the manufacturer's instructions. Colony PCR was performed to generate inserts for eventual sequencing using the T7/M13 universal sequencing primers (Table 5.S2 by the ABI PRISM 3100 genetic analyzer (Applied Biosystems, Foster City, CA, USA); sequences were deposited in Genbank with accession No: KC819805-KC819813. All PCR reactions were subjected to the following program: 5 min at 94 °C, and 35 cycles of 94 °C for 30 s, 54 °C for 30 s, 72 °C for 1 min, and a final extension at 72 °C for 8.5 min.

5.2.5 Pyrosequencing data analysis

Sequences with lengths < 200 bp and quality scores < 25 were excluded from subsequent analyses. The Quantitative Insights Into Microbial Ecology (QIIME) software package (Caporaso et al. 2010) was used for the following sequential analyses: sequence reads de-noising using the Reeder and Knight's algorithm, sequence clustering into Operational Taxonomic Units (OTUs; 97% similarity and 99% minimum coverage) using the CD-HIT algorithm and taxonomic assignation of OTU consensus sequences using the Ribosomal Database Project (RDP) naive Bayesian classifier. Finally, a phylogenetic tree of the aligned consensus sequences was constructed in QIIME using the Fast Tree algorithm (Caporaso et al. 2010).

5.2.6 Fluorescence *in situ* hybridization (FISH)

FISH was used to quantify the abundance of specific phyla and sub-phyla in samples obtained on Days 60 and 94 based on the protocol described by Nielsen and Daims (2009). Briefly, each sample was homogenized using an Ultra-turrax disperser (IKA Works Inc, Wilmington, NC,

USA) prior to application on poly-L-lysine coated slides. Hybridization was conducted at 46 °C in a formamide containing hybridization buffer using a Slide Booster (Advalytix, Brunnthal, Germany), and stringent wash was performed at 48 °C in a washing buffer with NaCl concentration adjusted to provide the appropriate stringency (Table 5.S2). After hybridization, 20 fields of view were chosen randomly and images were acquired using an Olympus BX51 epifluorescence microscope equipped with z-stack motorization (Olympus Optical, Tokyo, Japan). Acquired images were de-convoluted using the AutoDeblur program (AutoQuant, Troy, NY, USA) to obtain near confocal images. The biovolume of probe-defined populations was determined by the image analysis software DAIME (Daims et al. 2006).

5.2.7 Statistical analysis

To investigate differences in microbial community structure, exploratory data analysis (including species richness, diversity indices, shared OTUs and principal coordinates analysis [PCoA]) was carried out using the Vegan package of the R statistical software (Oksanen et al. 2011). Weighted UniFrac distance calculated in QIIME was used to determine the phylogenetic dissimilarity between samples. The Weighted UniFrac matrix was imported into R and ordinated by PCoA. Presented statistics for community structure in the results and discussion part are all reported as a % of bacterial mass.

5.3. RESULTS

5.3.1 Pilot-scale reactor operation and mathematical simulation measured data

The influent flows were kept as constant and similar as possible for both control and RAS-ozonated reactors throughout the experiment, while the influent COD concentrations varied slightly mainly due to variation in solids concentrations (Fig. 5.1a and b). The net yields of

biosolids production for both reactors (control and RAS-ozonated) were about the same before the onset of RAS-ozonation installation (Phase I, Fig. 5.1c). However, biosolids yields in the RAS-ozonated reactor progressively decreased as the ozone dose increased (Phases II-IV, Fig 5.1c). Average measured yield reductions in the RAS-ozonated reactor were 19%, 36%, and 46% for Phases II, III, and IV, respectively. This demonstrates the potential of ozone for biosolids reduction and also indicates that more biosolids reduction is attainable by applying higher ozone dosage.

The application of RAS-ozonation would normally decrease the mixed liquor volatile suspended solids (MLVSS) concentrations if the solid retention time (SRT) was kept constant. However, it is typical practice to keep the MLVSS concentration similar in both reactors (control and RAS-ozonated) by increasing the SRT of the RAS-ozonated reactor. In the current experiment, while the target SRT of the control reactor was ~ 6 days, the SRT of the RAS-ozonated reactor was increased up to 14 days at the end of Phase IV (Fig. 5.1d). Finally, a noticeable change during the operation stemmed from a temperature drop from 22 °C (September) at the beginning to 15 °C (December) at the end of the experiment (Fig. 5.1d).

Mathematical model simulations of the reactor operation data revealed OHO ozone inactivation rates of approximately 0.12 d^{-1} in Phase II, which increased to 0.20 d^{-1} in Phase IV (Fig. 5.1e). This clearly shows the effect of ozone in increasing the microbial mortality. The simulations also showed that the growth rates of OHO were higher in the RAS-ozonated reactor than in the control reactor despite the higher SRT by 25%, 31%, and 40% in Phases II, III, and IV, respectively. This increased in OHO growth rate is due to the increased mortality and is linked partly to the increase in the concentration of biodegradable organic materials produced by RAS-ozonation.

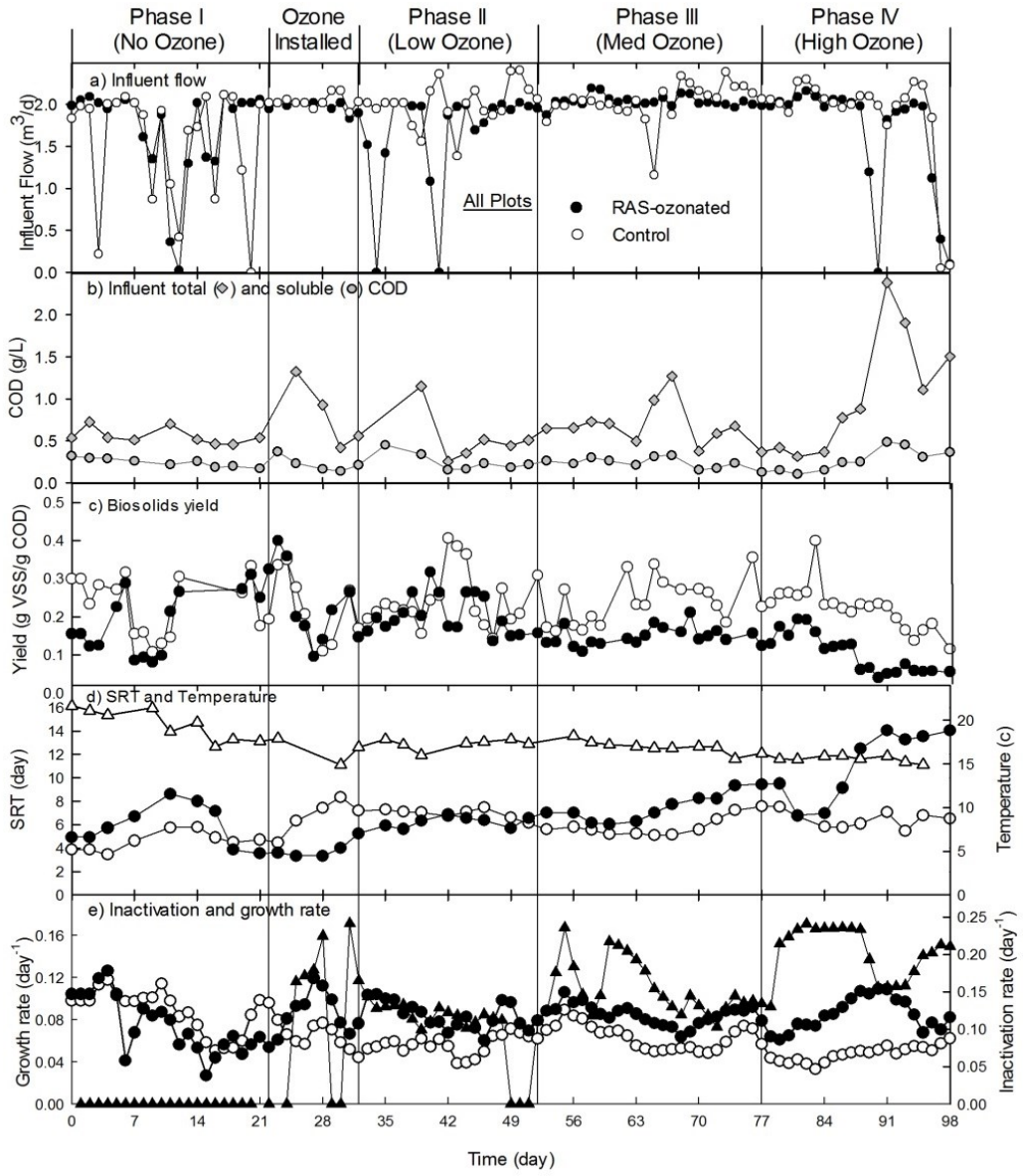

Fig. 5.1. Operational results for pilot-scale control (open circles) and RAS-ozonated (solid circles) reactors. Circles should be read with the left-side axes, while triangles with the right-side axes.

5.3.2 Bacterial community structure

The impact of RAS-ozonation on the composition of microbial populations was evaluated by the pyrosequencing of 16S rRNA PCR generated amplicons of biomass samples from each reactor

collected on Days 20, 60, and 94 representing Phase I, III and IV of experiment respectively. A total of 67,732 sequence reads of ~ 450 bp length on average were obtained, which yielded 9,412 "de-noised" sequence reads that were clustered in 1,074 operational taxonomic units (OTUs) based on 97% sequence identity (Table 5.1). Rarefaction curve analysis did not show saturation despite the large number of reads and de-noising (Fig. 5.2). The communities were highly uneven (i.e., low evenness, Table 5.1); however, when considering the OTUs observed in the two reactors on more than one day, the evenness increased as only the most abundant OTUs were considered (Table 5.1). Finally, consistent with this pattern, the 20 most abundant OTUs accounted for 72% of the reads.

Table 5.1. Summary of number of sequenced amplicons and observed operational taxonomic units (OTUs), and of related Shannon diversity indices for the control and RAS-ozonated reactors.

OTU Observations	Number of reads		OTUs Richness	Shannon Diversity		
	Trimmed	De-noised Number (%)		Diversity Number[a]	Entropy (nat)[b]	Evenness (Hill's ratio)[c]
Control + RAS-ozonated reactor						
Combined samples		9,412 (100%)	1,074	153	5.03	0.142
Both reactors any time		7,878 (84%)	237	74	4.03	0.313
Both reactors all the time		3,587 (38%)	23	15	2.68	0.501
Control reactor						
Combined samples		3,582 (100%)	549	129	4.86	0.235
Day 20	10,188	1,490 (39%)	304	116	4.75	0.382
Day 60	10,486	1,640 (43%)	263	69	4.23	0.263
Day 94	5,912	722 (19%)	168	64	4.17	0.385
Present in 2 days		1,241 (32%)	100	49	3.89	0.492
Present in 3 days		1,861 (48%)	43	23	3.17	0.535
RAS-ozonated reactor						
Combined samples		5,560 (100%)	762	120	4.78	0.157
Day 20	19,994	3,012 (54%)	447	58	4.06	0.130
Day 60	7,814	1,059 (19%)	232	77	4.35	0.335
Day 94	11,338	1,489 (27%)	262	69	4.23	0.263
Present in 2 days		1,405 (25%)	101	46	3.83	0.460
Present in 3 days		2,685 (48%)	39	15	2.75	0.403

a Shannon Diversity Number = exp(Shannon Entropy)

b Shannon Entropy = $-\sum p_i \bullet \ln(p_i)$; where p_i is the proportion of ith OTU.

c Evenness (Hill's ratio) = Shannon Diversity Number / OTU Richness

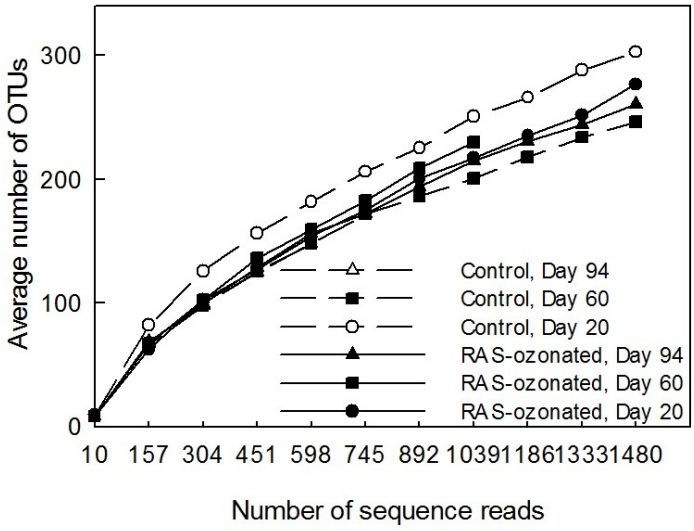

Fig. 5.2. Rarefaction curves obtained from sequenced samples on Days 20, 60 and 94 from the control (open symbols) and RAS-ozonated (solid symbols) pilot-scale reactors.

The bacterial community structures were comprised of sixteen phyla, with *Bacteroidetes*, *Proteobacteria*, *Chloroflexi*, and *Firmicutes* accounting for more than 95% of the 16S rRNA gene amplicon reads (Table 5.2). It is known that microbial community structures obtained by PCR-based methods such as pyrosequencing may exhibit biases incurred by DNA extraction or PCR amplification (Pinto and Raskin 2012). To investigate this possibility, samples from Days 60 and 94 were also analysed by quantitative FISH. The main quantitative discrepancies between the FISH and pyrosequencing results were the higher proportions of *Actinobacteria and Alphaproteobacteria* and the lower proportion of *Flavobacteria* (Table 5.2) found by FISH.

The most abundant family as determined by pyrosequencing was the *Methylophilaceae*, which accounted for ~14% of the sequence reads (Table 5.2). This particularly drew our attention because the members of this family are known to be specialists for methane and methanol consumption. To ascertain the genus identity of the organisms related to the *Methylophilaceae* family, specific PCR amplicons were cloned and sequenced; the seven

sequences obtained were related to the genus *Methylotenera*. Additionally, methanol and methane concentrations were determined in two wastewater influent samples (one week apart), and only methanol was detected at an average concentration of 33.5 ± 5.3 mg/L. Considering the theoretical COD value of methanol (1.5 mg COD/mg CH_4O), this concentration represents, on average, 11% of the average total influent COD.

Table 5.2. Relative frequency of major bacterial taxa in control and RAS-ozonated.

Phylum	Relative frequency of bacterial taxa in percentage (%)[a]			
	Pyrosequencing		FISH	
Class	Control	RAS-ozonated	Control	RAS-ozonated
Bacteroidetes	49.0±1.6	44.6±11.0		
Flavobacteria	12.5±5.9	21.1±14.9	4.2±0.4	1.2±0.1[b]
Sphingobacteria	21.9±1.5	16.3±8.5		
Unaffiliated *Bacteroidetes*	14.5±4.4	7.2±5.3		
Proteobacteria	42.7±1.2	49.4±10.3		
Alphaproteobacteria	5.4±2.4	6.3±2.2	18.3±1.3	16.1±1.8
Sphingomonadales	1.2±0.9	1.4±1.0		
Betaproteobacteria	17.4±5.3	30.2±12.3	17.7±1.0	23.2±1.7
Methylophilaceae	15.0±2.7	13.2±3.7		
Gammaproteobacteria	4.9±2.6	6.5±4.7	10.8±0.5	12.0±1.6
Thiotrichaceae	1.3±1.0	1.7±0.6		
Deltaproteobacteria	14.3±3.6	12.5±2.4	6.8±0.6	12.7±1.5
Nannocystaceae	6.4 1.9 ±	5.7 2.2 ±		
Unaffiliated *Protobacteria*	0.8±0.2	0.8±0.1		
Chloroflexi	2.1±0.8	0.9±1.9		
Firmicutes	0.9±0.1	0.7±0.3	1.8±0.3	0.7±0.1
Actinobacteria	0.2±0.1	0.2±0.1	9.1±0.6	10.8±0.9
Verrucomicrobia	0.2±0.1	<0.1		
Acidobacteria	0.2±0.1	0.3±0.1		
Planctomycetes	~0.1	<0.1		
WS3	~0.1	<0.1		
Fusobacteria	<0.1	~0.1		
OP10	<0.1	<0.1		
Gemmatimonadetes	0.1	0.2±0.1		
Nitrospira	<0.1	<0.1		
Thermotogae	~0.1	~0.1		
Unaffiliated *Bacteria*	3.7±0.	2.7±0.9		

a biomass

b values ± standard error

5.3.3 Variations in bacterial community structures

Variations in the microbial community structures were analyzed by principal coordinate analysis (PCoA) (Legendre and Legendre 2012), which is a Euclidean representation in 2D of the pair wise weighted UniFrac dissimilarity between samples. On Day 20, the communities in the two reactors were the most dissimilar as a result of the two month of operation before the start of the experimental period (i.e., Day 1) (Fig. 5.3). In order to homogenize the community compositions between reactors before starting the ozonation process (Phase II), the MLSS of both reactors were mixed on Day 27. As a result, the pyrosequencing community profiles of both reactors were much more similar on Day 60 than on Day 27 despite the RAS-ozonation treatment. This similarity was maintained until Day 94 owing to a parallel drift in community compositions (Fig. 5.3). Therefore, RAS-ozonation did not promote a significant divergence from the natural shift in the microbial compositions observed in the control reactor.

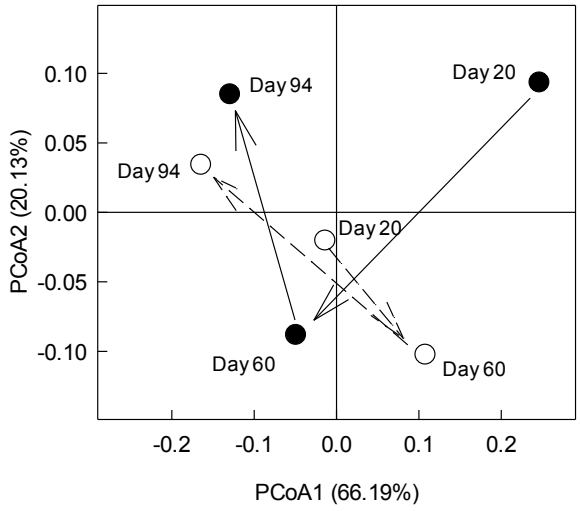

Fig. 5.3. Principal coordinate analysis (PCoA) of weighted UniFrac dissimilarities between pyrosequencing bacterial community structures of mixed liquor samples obtained on Days 20, 60 and 94 from the control (open circle) and RAS-ozonated (solid-circle) pilot-scale reactors.

5.4. DISCUSSION

5.4.1 Bacterial community structures and dynamics

The pyrosequencing results showed that the community structures of the two reactors after day 20 (mixing reactor content) were highly similar in composition and drifted in parallel between day 60 and day 94 (Fig. 5.3), pointing to factors other than RAS-ozonation as a major force structuring microbial community (e.g., influent wastewater composition or temperature) (Fig. 5.1c). These findings contrast somewhat from a similar study based on 16S rRNA gene PCR/DGGE, which found the community structures in a RAS-ozonated and a control laboratory-scale reactor to diverge during the first 60 days (Yan et al. 2009b). Unfortunately, the aforementioned study did not replicate their reactors; and it is known that replicated laboratory-scale reactors will exhibit a certain amount of divergence in community structure after inoculation (Kaewpipat and Grady 2002). This was observed in the current study during the first 80 days of operation (including 2-month start-up) before the onset of ozonation (Day 20 samples, Fig. 5.3). The laboratory-scale experiment on replicated reactors (Kaewpipat and Grady 2002) also suggested that the structure of bacterial communities would not diverge further after they were acclimatized and intermixed between reactors, in a way similar to the MLVSS mixing that occurred on Day 27 of our experiment. Although the observed increase in OHO mortality and growth rates along with the increase in SRTs of the RAS-ozonated reactor has been initially thought to be likely driving forces for restructuring the community, it seems that they had a minor effect on the population composition of the activated sludge community. It appears that changes in community structure are more influenced by factors that are common to both reactors such as a decrease in operation temperature and variations in the concentration and composition of the influent.

5.4.2 Discrepancies between structures determined by pyrosequencing and FISH

The FISH results obtained herein (Table 5.2) are fairly similar to the ones obtained previously for full-scale activated sludge treatment plants (Seviour and Nielsen 2010). This also supports the minimal impact of RAS-ozonation on microbial community structures. The main discrepancies between pyrosequencing and FISH results concern the abundance of the phyla *Actinobacteria* and the class of *Flavobacteria* and *Alphaproteobacteria* (Table 5.2). The under-representation of *Actinobacteria* in high-throughput sequence libraries has been reported in gastrointestinal ecology studies (Zoetendal et al. 2008). The higher GC content of *Alphaproteobacteria* (Lightfield et al. 2011) and *Actinobacteria* (formerly known as the high GC-Gram positive phylum) and the difficulties in extracting its DNA may partially explain these discrepancies. Finally, the lower observed percentage of *Flavobacteria* by FISH than by pyrosequencing (Table 5.2) is due to the lack of hybridization of the Flavobacteria FISH probe (CFB563) to the taxa detected by pyrosequencing.

5.4.3 Significance of the abundance of some taxa

With the ultimate goal to understand the forces structuring the microbial community, it is noteworthy to scrutinize the most abundant populations and to try to link their high abundance to specific conditions governing the operation of the reactors. The most abundant family observed was the *Methylophylacea*, with *Methylotenera* being the most prevalent genus. The high abundance of the *Methylotenera* would be expected if methanol as well as nitrate were present in the wastewater (Kalyuhznaya et al. 2009). Specific testing of the influent wastewater and reviewing the operation data of the wastewater treatment plant under study revealed high methanol (~11% of influent COD) and nitrate concentrations (on average 2.7 ± 0.4 mg-N/L; data not shown). These compounds are derived from industrial sources. These conditions seem to

correspond to the methanol/nitrate utilizing niche described for the genus *Methylotenera* (Kalyuhznaya et al. 2009).

Another intriguing observation for a fully aerated activated sludge systems was the observation, among the 20 most abundant genera in both reactors, of known denitrifying bacterial genera such as *Azonexus*, *Thauera* (both *Betaproteobacteria*), and *Clostridium* (*Firmicutes*). Their presence in high abundance may be due to the clarifier's configuration in which the lower part had to be mixed to avoid deposition and accumulation of solids on the inclined walls resulting in anoxic conditions and promoting growth of anoxic denitrifiers. The progressive accumulation of solids in the clarifier, which combined with the nitrate present in the system, would have likely provided a favorable environment for denitrification.

Given the suggested direct link between *Methylotenera* and influent methanol concentration and the presence of denitrifying bacteria resulting from the clarifier condition, it seems that influent wastewater composition and the reactor operational conditions (i.e., anoxic vs aerobic) were playing a more important role in shaping the bacterial community structure than the ozone induced mortality. It is also believed that the influent wastewater may have also seeded the two reactors with microbial constituents and contributed in shaping the population structure.

5.5. ACKNOWLEDGMENTS

This work was funded by the Natural Sciences and Engineering Research Council of Canada's Collaboration Research and Development program (NSRC-CRD) in collaboration with Air Liquide Canada and the Régie de l'Assainissement des Eaux du Bassin LaPrairie (RAEBL). The authors also thank Michel Épiney of Air Liquide, director and technical staffs of the RAEBL,

John Bartczak of McGill University, and several undergraduate and MEng students for their assistance in the construction and operation of the pilot-scale units.

Conflict of interest

No conflict of interest declared.

5.6. REFERENCES

APHA, AWWA, WEF, 2005. Standard Methods for the Examination of Water and Wastewater, American Public Health Association, Washington, DC, USA.

Böhler, M., Siegrist, H., 2004. Partial ozonation of activated sludge to reduce excess sludge, improve denitrification and control scumming and bulking. Water Science and Technology 49(10), 41-49.

Caporaso, J.G., Kuczynski, J., Stombaugh, J., Bittinger, K., Bushman, F.D., Costello, E.K., Fierer, N., Pena, A.G., Goodrich, J.K., Gordon, J.I., Huttley, G.A., Kelley, S.T., Knights, D., Koenig, J.E., Ley, R.E., Lozupone, C.A., McDonald, D., Muegge, B.D., Pirrung, M., Reeder, J., Sevinsky, J.R., Turnbaugh, P.J., Walters, W.A., Widmann, J., Yatsunenko, T., Zaneveld, J., Knight, R., 2010. QIIME allows analysis of high-throughput community sequencing data. Nat Meth 7(5), 335-336.

Cesbron, D., Déléris, S., Debellefontaine, H., Roustan, M., Paul, E., 2003. Study of Competition for Ozone Between Soluble and Particulate Matter During Activated Sludge Ozonation. Chemical Engineering Research and Design 81(9), 1165-1170.

Chu, L., Yan, S., Xing, X.-H., Sun, X., Jurcik, B., 2009. Progress and perspectives of sludge ozonation as a powerful pretreatment method for minimization of excess sludge production. Water Research 43(7), 1811-1822.

Daims, H., Lücker, S., Wagner, M., 2006. Daime, a novel image analysis program for microbial ecology and biofilm research. Environmental Microbiology 8(2), 200-213.

Deleris, S., Geauge, V., Camacho, P., Debelletontaine, H., Paul, E., 2002. Minimization of sludge production in biological processes: an alternative solution for the problem of sludge disposal. Water Science and Technology 46(10), 63-70.

Foladori, P., Andreottola, G., Ziglio, G., 2010. Sludge Reduction Technologies in Wastewater Treatment Plants, IWA Publishing, London, UK.

Frigon, D., Isazadeh, S., 2011. Evaluation of a new model for the reduction of excess sludge production by ozonation of return activated sludge: what solids COD fraction is affected? Water Science and Technology 63(1), 156-163.

Horan, N.J., 1990. Biological wastewater treatment systems : theory and operation, John Wiley & Sons. Ltd, Canada.

Huysmans, A., Weemaes, M., Fonseca, P A., Verstraete, W., 2001. Ozonation of activated sludge in the recycle stream. Journal of Chemical Technology and Biotechnology 76(3), 321-324.

Isazadeh, S., Feng, M., Urbina Rivas, L.E., Frigon, D., 2014. New mechanistically-based model for predicting reduction of biosolids waste by ozonation of return activated sludge. Journal of Hazardous Materials 270, 160-168.

Kaewpipat, K., Grady, C.P., 2002. Microbial population dynamics in laboratory-scale activated sludge reactors. Water Science and Technology 46(1-2), 19-27.

Kalyuhznaya, M.G., Martens-Habbena, W., Wang, T., Hackett, M., Stolyar, S.M., Stahl, D.A., Lidstrom, M.E., Chistoserdova, L., 2009. *Methylophilaceae* link methanol oxidation to denitrification in freshwater lake sediment as suggested by stable isotope probing and pure culture analysis. Environmental Microbiology Reports 1(5), 385-392.

Legendre, P., Legendre, L., 2012. Numerical ecology, Elsevier, Amsterdam, The Netherlands.

Lightfield, J., Fram, N.R., Ely, B., 2011. Across bacterial phyla, distantly-related genomes with similar genomic GC content have similar patterns of amino acid usage. PloS One 6(3), e17677.

Nielsen, P.H., Daims, H., 2009. FISH handbook for biological wastewater treatment: identification and quantification of microorganisms in activated sludge and biofilms by FISH, IWA Publishing, London, UK.

Oksanen, J., Blanchet, F.G., Kindt, R., Legendre, P., Minchin, P.R., O'Hara, R.B., Simpson, G.L., Solymos, P., Stevens, M.H.H., Wagner, H., 2011. Vegan: Community Ecology Package. R package version 2.0-2.

Paul, E., Liu, Q.-S., Liu, Y., 2012. Biological Sludge Minimization and Biomaterials/Bioenergy Recovery Technologies. Paul, E. and Liu, Y. (eds), p. 209, John Wiley & Sons, Inc, Hoboken, New Jersey.

Pinto, A.J., Raskin, L., 2012. PCR biases distort Bacterial and Archaeal community structure in Pyrosequencing datasets. PloS One 7(8), 1-16.

Rittmann, B., McCarty, P.L., 2001. Environmental Biotechnology : Principles and Applications, McGraw-Hill Science Engineering, New Yourk.

Sambrook, J., Russell, D.W., Janssen, K., Argentine, J., 2001. Molecular cloning: A laboratory manual on the web, Cold Spring Harbor Laboratory, New York.

Seviour, R.J., Nielsen, P.H., 2010. Microbial ecology of activated sludge, IWA Publishing, London, UK.

US-EPA, 2003. Method 8015D, Nonhalogenated Organics using GC/FID , Revision 4, US-EPA, online.

Vishnivetskaya, T.A., Layton, A.C., Lau, M.C.Y., Chauhan, A., Cheng, K.R., Meyers, A.J., Murphy, J.R., Rogers, A.W., Saarunya, G.S., Williams, D.E., Pfiffner, S.M., Biggerstaff, J.P., Stackhouse, B.T., Phelps, T.J., Whyte, L., Sayler, G.S., Onstott, T.C., 2014. Commercial DNA extraction kits impact observed microbial community composition in permafrost samples. FEMS Microbiology Ecology 87(1), 217-230.

Yan, S.-T., Chu, L.-B., Xing, X.-H., Yu, A.-F., Sun, X.-L., Jurcik, B., 2009a. Analysis of the mechanism of sludge ozonation by a combination of biological and chemical approaches. Water Research 43(1), 195-203.

Yan, S.T., Zheng, H., Li, A., Zhang, X., Xing, X.H., Chu, L.B., Ding, G., Sun, X.L., Jurcik, B., 2009b. Systematic analysis of biochemical performance and the microbial community of an activated sludge process using ozone-treated sludge for sludge reduction. Bioresource Technology 100(21), 5002-5009.

Yasui, H., Shibata, M., 1994. An innovative approach to reduce excess sludge production in the activated sludge process. Water Science and Technology 30(9), 11-20.

Zoetendal, E.G., Rajilić-Stojanović, M., de Vos, W.M., 2008. High-throughput diversity and functionality analysis of the gastrointestinal tract microbiota. Gut 57(11), 1605-1615.

5.7. SUPPLEMENTARY MATERIAL

Table 5.S1. Physical and operational characteristic of two pilot-scale reactor.

Parameters	**Control**	**RAS-Ozonated**
Influent Flow (m^3/day)	1.81±0.09	1.89±0.11
Volume of aeration tank (m^3)	1.045	1.015
Volume of clarifier (m^3)	0.705	0.697
Aerated SRT (d)	6.06	7.17
RAS Flow/Influent Flow	1.5	1.3
RAS suspended solids (mg/L)	3,040	3,040
Ozone contact time (min)	-	45
Ozone flow rate (L/h)	-	2-6

Table 5.S2. PCR primers and FISH probes used in this study.

Probes and primers	Label	Sequence (5'–3')	Binding position [b]	Target Group	FA %[c]	Annealing temperature	References
FISH							
EUB338[a]	FITC	GCTGCCTCCCGTAGGAGT	16S (338–355)	Most Bacteria	0 – 50	NA[d]	(Amann 1990)
EUB338-II[a]	FITC	GCAGCCACCCGTAGGTGT	16S (338–355)	Other Bacteria not detected by EUB338	0 – 50	NA	(Daims 1999)
EUB338-III[a]	FITC	GCTGCCACCCGTAGGTGT	16S (338–355)	Other Bacteria not detected by EUB338	0 – 50	NA	(Daims 1999)
ALF968	Cy3	GGTAAGGTTCTGCGCGTT	16S (968 - 985)	*Alphaproteobacteria*	35	NA	(Neef 1997)
BET42a	Cy5	GCCTTCCCACTTCGTTT	23S (1027–1043)	*Betaroteobacteria*	35	NA	(Manz 1992)
-		GCCTTCCCACATCGTTT		Competitor for BET42a	35	NA	
GAM42a	Cy3	GCCTTCCCACATCGTTT	23S (1027–1043)	*Gamaproteobacteria*	35	NA	(Manz 1992)
-		GCCTTCCCACTTCGTTT		Competitor for GAM42a	35	NA	
DELTA495a	Cy5	AGTTAGCCGGTGCTTCCT	16S (495–512)	*Deltaproteobacteria*	35	NA	(Lucker et al. 2007)
-		AGTTAGCCGGTGCTTCTT		Competitor for DELTA495a	35	NA	
CFB563	Cy5	GGACCCTTTAAACCCAAT	16S (563–580)	*Flavobacteria*	20	NA	
LGC354a	Cy5	TGGAAGATTCCCTACTGC	16S (354–371)	*Firmicutes*		NA	(Meier et al. 1999)
HGC69a	Cy3	TATAGTTACCACCGCCGT	23S (1901–1918)	*Actinobacteria*	20	NA	(Roller 1994)
Pyrosequencing							
341F	NA	CCTACGGGAGGCAGCAG	16S (341-357)	Most Bacteria	NA	NA	(Muyzer et al. 1993)
907R	NA	CCGTCAATTCCTTTGAGTTT	16S (891-907)	Most Bacteria	NA	NA	(Lane et al. 1985)
Cloning							
Non-EUB338F	NA	ACTCCTACGGGAGGCAGCAC	16S (338-354)	Most Bacteria	NA	56	(Amann 1990)
Meth1215R[e]	NA	TACGTGTGAAGCCCTGGC	16S (-1199-1215)	*Methylophilaceae*	NA	56	this study
T7 Universal Primer	NA	AATACGACTCACTATAG					
M13 Universal primer	NA	GTTTTCCCAGTCACGAC	16S (20-41)				

a EUB338, EUB338-II, EUB338-III were used in the mixture called EUB_{mix}

b rRNA target site (*Escherichia coli* numbering)

c FA, formamide concentration in the hybridization buffer. For salt concentration in wash buffer see(Nielsen and Daims 2009)

References of supplementary materials

Amann, R.I., 1990. Combination of 16S rRNA-targeted oligonucleotide probes with flow cytometry for analyzing mixed microbial populations. Applied and Environmental Microbiology 56(6), 1919.

Daims, H., 1999. The domain-specific probe EUB338 is insufficient for the detection of all bacteria: Development and evaluation of a more comprehensive probe set. Systematic and Applied Microbiology 22(3), 434.

Lane, D.J., Pace, B., Olsen, G.J., Stahl, D.A., Sogin, M.L., Pace, N.R., 1985. Rapid determination of 16S ribosomal RNA sequences for phylogenetic analyses. Proceedings of the National Academy of Sciences 82(20), 6955-6959.

Lucker, S., Steger, D., Kjeldsen, K.U., MacGregor, B.J., Wagner, M., Loy, A., 2007. Improved 16S rRNA-targeted probe set for analysis of sulfate-reducing bacteria by fluorescence in situ hybridization. Journal of Microbiological Methods 69(3), 523-528.

Manz, W., 1992. Phylogenetic oligodeoxynucleotide probes for the major subclasses of proteobacteria: problems and solutions. Systematic and Applied Microbiology 15(4), 593.

Meier, H., Amann, R., Ludwig, W., Schleifer, K.H., 1999. Specific Oligonucleotide Probes for in situ Detection of a Major Group of Gram-positive Bacteria with low DNA G+C Content. Systematic and Applied Microbiology 22(2), 186-196.

Muyzer, G., de Waal, E.C., Uitterlinden, A.G., 1993. Profiling of complex microbial populations by denaturing gradient gel electrophoresis analysis of polymerase chain reaction-amplified genes coding for 16S rRNA. Applied and Environmental Microbiology 59(3), 695-700.

Neef, A., 1997. Anwendung der in situ Einzelzell-Identifizierung von Bakterien zur Populationsanalyse in komplexen mikrobiellen Biozönosen, Technische Universität München Munich, Germany.

Nielsen, P.H., Daims, H., 2009. FISH handbook for biological wastewater treatment: identification and quantification of microorganisms in activated sludge and biofilms by FISH, IWA Publishing, London, UK.

Roller, C., 1994. In situ probing of Gram-positive bacteria with high DNA G+ C content using 23S rRNA-targeted oligonucleotides. Microbiology 140(10), 2849.

Chapter 6:

Bacterial community assembly in activated sludge: mapping beta diversity across environmental variables

Connecting text: Chapter 5 demonstrated that the bacterial community structure was unaffected by the RAS-ozonation process. Therefore, we wanted to put these results in the larger context of the bacterial diversity observed at 8 full-scale WWTPs around Montreal. It was observed that a number of bacterial families were observed at all the plants, and that these families accounted for most of the biomass. Thus, the beta diversity between plants is relatively small. However, it was also observed that some families were only abundant at some of the plants, which is likely due to specificities in influent characteristics. In fact, when it was attempted to explain the beta diversity by environmental factors (influent characteristics, reactor configuration, temperature, SRT, organic load, and geographic locations), only the influent characteristics and the geographic location could explain an appreciable amount of the variance in community structure between plants. Overall all the presented factors could not explain more than 26% of the variance, which left most of the variance unexplained. Note that Year 1 and 2 in this chapter represent population data from Year 2 and 3 of the pilot-scale reactor, respectively. The results of this work are prepared to be submitted to:

Isazadeh, S., Jauffur, M.S. and Frigon, D., Bacterial community assembly in activated sludge: mapping beta diversity across environmental variables. *ISME Journal*:

6.1. INTRODUCTION

Activated sludge (AS) employed in wastewater treatment plant (WWTP) is one of the world's largest biotechnological processes. Over the last century, AS process has experienced continuous modifications in design and operation to improve its efficiency (Seviour and Nielsen 2010). In the core of AS processes consortium of heterotrophic microorganisms transform incoming organic compounds, through specific metabolisms, into biomass and CO_2. Engineering and modifying the AS process is usually aimed at promoting or controlling specific eco-physiological characteristics in the microbial community. One of the central aspects to achieve further success in process modification lies in the recognition of the key significant abiotic factors governing community assembly within AS systems. Therefore, understanding how the variations in the environmental or operational conditions influence the microbial community composition remains a fundamental goal.

Investigating the assembly of microbial communities in terms of presence and abundance of species has been of prime importance to microbial ecologists over the last two decades (Curtis et al. 2009). Ongoing progress in molecular biology techniques (e.g., FISH, T-RFLP, DGGE, and amplicon cloning) used to study the diversity of 16S rRNA or functional genes have provided new opportunities to better understand the complexity of microbial ecosystems. Recently, high-throughput next generation PCR amplicon sequencing techniques have expanded considerably the depth of description of microbial diversities in wastewater treatments plants with AS process (AS-WWTPs) (Pinto and Raskin 2012). Yet, the challenge remains to ascertain the effect of abiotic variations (e.g., operational, spatial and temporal) on the structure of biotic systems (i.e., the assembly of bacterial communities).

Several lines of evidence link bacterial community compositions and performance of biological wastewater treatment processes to operational variations such as: influent composition (Akarsubasi et al. 2005, Lee et al. 2009), reactor configuration (Rowan et al. 2003), temperature variation (Siripong and Rittmann 2007), and solids retention time (SRT) (Akarsubasi et al. 2009). In addition, ecosystem size has been found to positively influence the observed distances in community composition (called beta diversity) over time (Soininen 2010) and reactor scale can affect species selection based on cellular morphology (Martins et al. 2004). In a comprehensive laboratory-scale study, Pholchan et al. (2010) found that the microbial community of AS reactors was affected by different operational conditions and reactor configurations, however the relationship between the performance and community diversity was not explicitly associated. Zhang et al. (2012) studied the effects of geographical variation on population structure of AS-WWTPs and demonstrated that some core genera were shared between samples in spite of large geographical distances. Valentín-Vargas et al. (2012) scrutinized the bacterial profiles of two geographically distinct AS wastewater treatment systems of different sizes and showed that the larger bioreactor has less dynamic but more efficient and diverse bacterial community. Although these studies highlighted the importance of environmental factors on bacterial community assembly, a systematic quantification of the abiotic parameters contribution on the species composition and distribution of bacterial communities remained to be performed.

In the current study, bacterial community assemblies at 8 full-scale AS-WWTPs and two pilot-scales AS-WWTPs were determined by analyzing 39 samples using high-throughput pyrosequencing of 16S rRNA gene amplicon. Observed variations in beta diversity were partitioned to obtain the relative magnitude of contribution for hypothesized environmental

variables. Environmental variables covering *chemical stress, reactor scale,* and *temporal variations* (inter-annual) were studied based on samples collected from pilot-scale and full-scale reactors of LaPrairie-WWTP's over 2 years. For one of the pilot-scale reactors, ozone was applied to the RAS, which provided a chemical stress by enhancing bacterial mortality (decay) and modified the substrate composition in the system. In turn, ozone effects on the RAS are likely to modify the AS community structure, a hypothesis that was tested by comparing the communities of two pilot-scale reactors: RAS-ozonated vs. non-ozonated. The reactor scale variable was studied at the same location by comparing pilot vs. full-scale reactors. Inter-annual variations in the bacterial population assembly of full-scale reactor were studied over a period of 3 years. In addition to LaPrairie-WWTP, seven other full-scale AS-WWTPs were sampled in different seasons (during the same year) and once more after 4 years to study the effects of other variables such as: influent characteristics, seasonal variations (winter vs. summer), treatment processes (conventional, oxidation ditch and sequence batch reactor[SBR]) on community assemblies of hetrotrophs. The results generated from these two studies enabled us to explore a range of environmental variables which could explain observed bacterial population assemblies and their response to abiotic changes.

6.2. MATERIALS AND METHODS

6.2.1 LaPrairie-WWTP pilot-scale and full-scale study

In order to assess the impact of high mortality due to RAS-ozonation on the microbial community composition, two pilot-scale reactors (a control and a RAS-ozonated test reactor, each with a total volume of 1.7 m^3 including the secondary clarifier) were operated over two years with two experimental periods performed over 6-8 months at the LaPrairie-WWTP. The

reactors were fed with the same sewage entered the full-scale plant, and the hydraulic residence time (HRT) in the AS reactors was adjusted to 12 h. The operational conditions and ozone dosages were varied in order to assess the potential of RAS-ozonation to reduce the excess biosolids production. In Year 1, both pilot-scale reactors were operated under fully aerobic conditions with a target SRT of around 6 days for the non-ozonated control reactor. The ozone dosage varied from medium (5.9±0.4 mg-O_3/[g-$VSS_{inventory}$.d]) in Phase I to high (10.3±0.7 mg-O_3/[g-$VSS_{inventory}$.d]) in Phase 2. In Year 2, the ozone dosage was kept constant (average of 9.2±0.2 mg-O_3/[g-$VSS_{inventory}$.d]) throughout the experiment and the operational conditions were varied through three experimental phases. In Phase 1 with a SRT of ~12 d, the reactor was split into an anoxic section and an aerobic compartment with a recirculation rates equaled to ~4 times of the influent flow between the section which provided for denitrification/nitrification activities to occur in the reactor. In Phase 2, the two reactor sections were operated under aerobic conditions with a SRT of ~12 d. Finally, in Phase 3, aerobic conditions were maintained, but the SRT was reduced to ~6 d. Each phase lasted for a minimum of 3 SRTs to reach steady-state conditions (Table 6.S1). Eleven biomass samples (5-6 samples per reactor) were collected periodically from the reactors at the end of each phase and stored at −80 °C for molecular analysis were performed. In parallel, six samples were also collected from the full-scale AS reactor [16,000 m^3, SRT ≈ 6 d] to investigate the effect of scale (control pilot-scale reactor samples vs. full-scale reactor samples) and temporal variation on the bacterial community assembly. Details of design and operational conditions along with influent characteristics for pilot-scale reactors were presented elsewhere (Isazadeh et al. 2014a, Isazadeh et al. submitted.).

6.2.2 Regional full-scale AS-WWTPs

Seven full-scale regional AS-WWTPs, located within a 68-km radius of the LaPrairie-WWTP were monitored to assess the community assembly and dynamics of bacterial populations growing in their respective aeration basins. The selected plants had influent flow rates ranging from 5,000 to 65,000 m^3/d, and employed mainly the conventional AS, oxidation ditch, and sequence batch reactor (SBR) treatment type processes (Fig 6.S1). The characteristic features of each treatment plant and details of operational data are provided in the supplementary materials (Table 6.S2). The sampling campaign was conducted during two different time frames to evaluate seasonal variations (summer and winter seasons) and inter-annual differences in bacterial population structures. Samples were collected during the summer (August/September) 2008 and winter (February) 2009, while inter-annual variations were based on samples collected during winter (February) 2013. Weekly variations in the community structures were studied at the Granby-WWTP over a period of three consecutive weeks in August 2008. Mixed liquor samples from each WWTP were collected and rapidly transported to the laboratory in ice, where the solids were centrifuged and frozen at −80 °C until conducting molecular analysis.

6.2.3 DNA extraction, PCR amplification and pyrosequencing

Genomic DNA was extracted from the mixed liquor samples using DNA extraction kit (*MoBio* UltraClean™ Fecal DNA Kit, Mo Bio Laboratories Inc., Carlsbad, CA, USA). The DNA was amplified by PCR using a mixture of 3 forward primers (5'-CCTACGGGRGGCAGCAG-3', 5'-ACWYCTACGGRWGGCTGC-3' and 5'-CACCTACGGGTGGCAGC-3') targeting the hypervariable V3 region (*E.coli* position: 338) and 1 reverse primer (5'-TACNVGGGTHTCTAATCC-3') targeting the hypervariable region V4 (*E.coli* position:802). The primers sequences were tagged with pyrosequencing emulsion PCR adaptors (24 bp) and the

reverse primer contained a specific barcode (14 bp). The PCR thermocycling conditions were as follows: 94 °C for 5 min, 30 cycles of 94°C for 1 min, 55 °C for 30 s, 72 °C for 1.5 min followed by a final extended elongation at 72°C for 8.5 min. The PCR amplicons were purified using PCR purification kit (*MoBio* UltraClean PCR Clean-UP Kit, Mo Bio Laboratories Inc., Carlsbad, CA, USA). The amplicon concentration of each sample was determined using the Quant-iT™ PicoGreen kit (Invitrogen, USA) and normalized to a concentration of 50 ng/µl. The PCR products were then pooled and their quality assessed by the Bioanalyzer 2100 (Agilent Technologies, Montreal, Quebec, Canada) to ensure the purity of the amplicons. Purified amplicons were subjected to emulsion PCR, based on the Roche-454 Life Science Protocol and eventually sequenced by the GS FLX Titanium Sequencing machine (Roche Diagnostics, Hoffmann-La Roche Ltd, Montreal, Canada).

6.2.4 Sequence processing and statistical analysis

Post-sequencing analysis was performed using the Qiime pipeline (Caporaso et al. 2010b). Sequences reads first trimmed for barcodes and primers, and the ones with quality scores lower than 25 and length shorter than 200 bp were excluded from downstream analyses. Sequences were clustered at 97% sequence similarity with Uclust (Edgar 2010) and taxonomic assignment was performed using the RDP classifier (Wang et al. 2007). Sequence reads were aligned to the Greengenes core reference alignment (DeSantis et al. 2006) using PyNAST (Caporaso et al. 2010a) to capture the beta diversity (i.e., between communities) based on phylogenetic distances in Unifrac (Lozupone and Knight 2005). A number of other descriptive and statistical methods inside the Qiime pipeline including, alpha diversity (i.e., within a community), diversity indices, and core microbial analysis were applied to acquire better understanding of the bacterial community structure and dynamics. Detailed exploratory data analyses were carried out in the R

software using the Vegan (Oksanen et al. 2011) and cluster packages (Maechler and Hornik 2011). Principal coordinate analyses (PCoA) were performed using operational taxonomic unit (OUT) abundances based on weighted Unifrac and Hellinger distances (Legendre and Legendre 2012). Since both distances resulted in similar ordination plots, the Hellinger distance is presented herein.

6.2.5 Variation partitioning of beta diversity

The relative importance of environmental variables shaping the community assembly was estimated by using redundancy analysis (RDA) (Legendre and Legendre 2012). For LaPrairie-WWTP, two explanatory matrices (containing either environmental or temporal explanatory variables) were used to investigate the variation in beta diversity (Table 6.S3). The environmental matrix included reactors scale (control pilot-scale vs. full-scale), RAS-ozonation (control vs. RAS-ozonated pilot-scale reactors), and season (summer vs. winter); while temporal matrix included the inter-annual variations (2008-2009 vs. 2013).

For the 8 full-scale AS-WWTPs, three explanatory matrices covering; influent characteristics, environmental, and spatial variations were used (Table 6.S4&5). The environmental explanatory matrix included the differences in processes (SRT, MLVSS, and HRT), seasons (winter vs. summer), and inter-annual (2008-2009 vs. 2013) variations. Analyses were performed based on community data transformed by the Hellinger distance. Influent characteristic data were log-transformed and spatial distances measured with latitude-longitude coordinates were converted into principal coordinates of neighbour matrices (PCNM) eigenfunctions. The PCNMs were then used as explanatory variables to analyze the geographic location. The outcome of this approach relates to the fractions explained uniquely by each matrix and their combination. Unexplained fractions represented the parts which were not attributable to any of the applied explanatory

matrix. The abovementioned analyses were performed by using the *varpart* function of the Vegan Package (Oksanen et al. 2011).

6.3. RESULTS

6.3.1 Bacterial community assembly in pilot-scale and full-scale reactors at LaPrairie-WWTP

The 18 samples from the pilot-scale and full-scale reactors yielded a total of 57,316 for 16S rRNA sequence reads, out of which 4,059 were found to be unique OTU. The numbers of reads in all samples ranged between 1,060 and 3,950 with an average of 3,371 (Table 6.1). Nineteen distinct OTUs accounting for 17% of the all the sequence reads were shared among all the samples. Among the full-scale WWTP samples, 40% of the reads belonged to 83 OTUs that appeared in all samples (Table 6.1). The level of shared OTUs was also relatively high between the two pilot-scale reactors (control and RAS-ozonated) with 29 OTUs representing 20% of the sequence reads that were detected in all the pilot-scale reactor samples; while the numbers of shared OTUs among all samples from the same reactor reached 64 and 42 for the control and RAS-ozonated reactors, respectively (Table 6.1). Comparisons between the reactors with regard to the observed number of OTUs (i.e., OTU richness), Shannon diversity numbers (which can be interpreted as the number of abundant OTUs) or the Simpson diversity numbers (which can be interpreted as the number of dominant OTUs) did not reveal any significant difference (Table 6.1), suggesting that the scale or the RAS-ozonation process do not significantly affect the diversity found in the samples from each reactor (i.e., alpha diversity).

Principal coordinate analysis (PCoA) was performed to visualize the differences in community composition between reactors and between sampling times (i.e., beta-diversity). In

the full-scale reactor, the community composition did not vary much over the three sampling years as all the points appear close to each other in the PCoA plot (Fig 6.1a). Conversely, the community composition in the pilot-scale reactors exhibited a much higher degree of variation (Fig 6.1a); however, the communities in the control and RAS-ozonated reactors seemed to have drifted in the same direction keeping the similarity between reactors high for most of the experimental periods. Considering the variations in community composition during Year 2 (changes from anoxic/aerobic conditions to fully aerobic conditions and from ~12 d SRT to ~6 d SRT), it appears that the community composition was affected by the changes in operation implemented throughout the experiment (Fig 6.1a). Finally, comparison of the PCoA coordinates of the samples from the full-scale and pilot-scale reactors suggests that the reactor scale may have influenced the community composition and increased the beta diversity (Fig 6.1a).

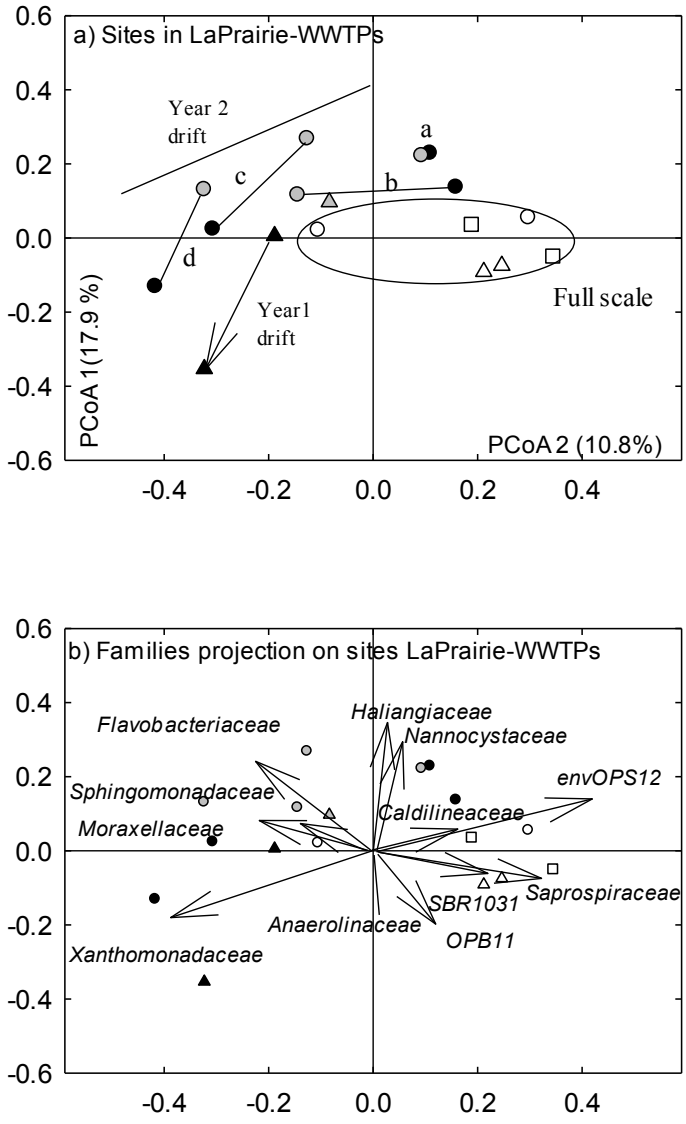

Fig 6.1. Panel a: PCoA of the Hellinger distances between community composition obtained by 16S rRNA gene amplicon sequencing of mixed liquor samples from the LaPrairie-WWTP reactors: full-scale [open symbols], control pilot-scale [grey symbols] and RAS-ozonated [black symbols]. Symbols represent sampling years: triangle for Year 1 and circle for Year 2 pilot-scale experiment; square for sample before pilot-scale experiment. Lines between symbols represents samples obtained at the same times from both pilot-scale reactors and arrows indicate temporal drifts in community composition. For Year 2 pilot-scale experiment, (Samples a) beginning of the experiment after 1-month start-up [May, same operations as Samples b but without ozonation], (Samples b) end of the anoxic/oxic with SRT=12 d phase [Phase I-July], (c) end of the fully aerobic with SRT=12 d phase [Phase II-September], and (d) end of the fully aerobic with SRT=6 d [Phase III-November]. **Panel b:** Projection of major bacterial families marking differences between samples.

The previous observations suggest a high level of similarity among the community assemblies of the three reactors. The average community composition comprised of 8 phyla with relative abundances among the sequences reads higher than 1%. The most abundant phylum was the *Proteobacteria* (38.5% of reads), with the classes *Alpha-*, *Beta-*, *Gamma-*, and *Delta-proteobacteria* accounting for 8.5%, 14.4%, 8.6%, and 6.6% of the reads , respectively. The phylum *Bacteroidetes* (19.8%) was mainly represented by the *Sphingobacteria* (15.0%) and *Flavobacteria* (3.9%) classes. *Chloroflexi* (12.9%) members almost entirely belonged to the class *Anaerolineae* (12.2%); while the phylum *Verrucomicrobia* (7.6%) was dominated by the genus *Prosthecobacter* (5.3%). Finally, the phyla *TM7* (3.7%), *Planctomycetes* (3.6%), *Acidobacteria* (2.3%), and *OP11* (1.3%) were also found amongst the most abundant ones (Table 6.S3). Similarities at the family level were also observed; most notably were the high abundance of two *Betaproteobacteria* families: the *Comamonadaceae* (6% of reads) and *Methylophilaceae,* (5%). These families were among the top 10 most abundant families in all the reactors.

Highlighted differences in community OTU compositions by the PCoA plot (Fig 6.1) could also be related to variations in the abundance of specific families. Fig. 6.S2 and Table 6.S6 show the bacterial population heat map of sites and most abundant families observed in the pilot-scale WWTPs. The main differences between the full-scale WWTP and pilot-scale reactors were the higher abundances of the families *envOPS12*, *OPB11*, *Caldilineaceae*, *Anaerolinaceae*, and *SBR1031* all from the *Anaerolineae* class (phylum *Chloroflexi*) and *Saprospiraceae* belonging to *Sphingobacteriales* order (phylum *Bacteroidetes*) in the full-scale treatment system (Table 6.S6). It appeared that a decrease in the abundances of the *Anaerolineae* population in both pilot-scale reactors (RAS-ozonated and control) occurred when the treatment systems were changed from anoxic/oxic conditions to completely aerobic conditions and this could explain in part the drift in

community compositions observed during Year 2 of the pilot-scale study (Fig 6.1b). Reviewing the full-scale WWTP operation data suggested that the front-end of the aerobic plug-flow reactor was deficient in aeration, and that significant denitrification occurred (data not shown). Thus, the class *Anaerolineae* may be involved in denitrification in these systems, and that variations in treatment process conditions and aeration efficiencies as opposed to specifically reactor scale may be the source of enhanced beta diversity between the full-scale and pilot-scale reactors.

Another population significantly changed through the Year 2 pilot-scale experiment. The family *Xanthomonadaceae* increased in abundance in both pilot-scale reactors when the SRTs decreased from ~12 d to ~6 d. Higher abundances of *Xanthomonadaceae* at 6 d SRT was also observed in a previous pilot-scale study at the same site (Isazadeh et al. 2014b). Thus, low SRTs (i.e., high growth and dilution rates) favored the growth of *Xanthomonadaceae* family in this system.

Table 6.1. Sequence reads, OTUs (total and shared), biodiversity numbers for LaPrairie AS-WWTP.

LaPrairie-WWTP	Sequence reads and OTU richness				Simpson diversity number	Shannon diversity		
	reads	OTUs	shared OTUs	% reads for shared OTUs		number	entropy (nat)	evenness
Full-scale								
1 years before pilot-scale study								
December	3,570	664	83	40	73	222	5.40	0.34
September	3,950	705			74	215	5.37	0.31
Year 1								
August	3,857	688			57	196	5.28	0.29
September	3,866	740			69	212	5.36	0.29
Year 2								
May	3,743	594			63	177	5.18	0.30
September	3,651	638			53	162	5.09	0.25
Pilot-scale reactors								
Control (non Ozonated)								
Year 1								
Phase I-August	3,057	554	64	31	38	154	5.04	0.28
Phase II -September	N.A							
Year 2								
Start-up-May	3,408	659			106	253	5.54	0.38
Phase I-July	3,109	547			46	156	5.06	0.29
Phase II-September	3,714	753			88	262	5.57	0.35
Phase III-November	3,571	651			53	174	5.16	0.27
RAS-Ozonated								
Year 1								
Phase I-August	3,485	673	42	24	102	240	5.48	0.36
Phase II -September	2,503	484			55	164	5.10	0.34
Year 2								
Start-up-May	3,878	689			110	255	5.54	0.37
Phase I-July	3,281	618			90	223	5.41	0.36
Phase II-September	1,060	330			89	175	5.17	0.53
Phase III-November	3,613	594			63	160	5.07	0.27

6.3.2 Bacterial community assemblies among full-scale AS-WWTPs

The lack of difference in bacterial community compositions between the control and RAS-ozonated pilot-scale reactors prompted questions about such observation over a higher scale magnitude. To evaluate this question, a total of 23 mixed liquor samples were obtained from 8 full-scale WWTPs. Temporal sampling in addition to differences in process types and influent characteristics that can be observed between plants allowed the evaluation of seasonal and inter-annual differences for each treatment plant. From these samples, 83,248 of 16S rRNA gene amplicon sequence reads were obtained with the number of reads per sample ranging between 1,505-4,262 (average of 3,619 reads/sample). Unique OTUs were defined by grouping together sequence reads with ≥97% identities, which resulted in 5,610 OTUs. The average OTU richness within a sample was 643 with a range between 420-823 (Table 6.2).

Comparison of the observed OTU alpha diversities (i.e., within sites) between samples obtained in summer 2008 and winter 2009 (only a few months apart) showed significantly higher diversity in the winter than in the summer (paired student t-test, $P<0.05$; Table 6.2). In general, this result is attributable to both higher OTU richness and evenness. The only noticeable counter example is the case of Cowansville WWTP where the community diversity was observed to be much lower in the winter than in the summer; however, this may be due to a lower number of sequence reads recovered for the Cowansville winter 2009 sample (Table 6.2). On average, the temperature drop at these WWTPs between the summer and winter season was about 8 °C (averages for summer being 23 °C and winter being15 °C). Based on these data, it was not possible to conclude whether this represented absolute seasonal differences in temperatures or the level of summer/winter temperatures themselves that influenced the alpha diversities.

Differences in community compositions between samples obtained from the 8 AS-WWTPs were visualized using a PCoA of the Hellinger distances (Fig 6.2a). For comparison of the scales of PCoA projections in Figs. 6.1 and 6.2, it should be noted that the LaPrairie samples in Fig 6.2a represented the same extent of beta diversity as the samples shown in Fig 6.1a for the full-scale WWTP; thus the beta diversity presented in Fig. 6.2 was much higher than in Fig. 6.1.

The reproducibility of the 16S rRNA gene pyrosequencing approach coupled with the small temporal-scale variations (within 1 week) can be visualized with the Granby samples. In summer 2008, 3 samples were obtained on successive weeks; these samples appeared close to each other in Fig 6.2a, suggesting a high technical reproducibility and a slow community turnover. Possibly the most noticeable observation is that samples from the same WWTP remain in the vicinity of each other in Fig 6.2a, indicative of minimal variations in community compositions over time compared to variations between plants. Another important observation is that the seasonal variations (summer 2008 vs. winter 2009) in community compositions within a plant appeared smaller than the inter-annual variations (2008-2009 vs. 2013) drifts for most of the sites (Fig 6.2a).

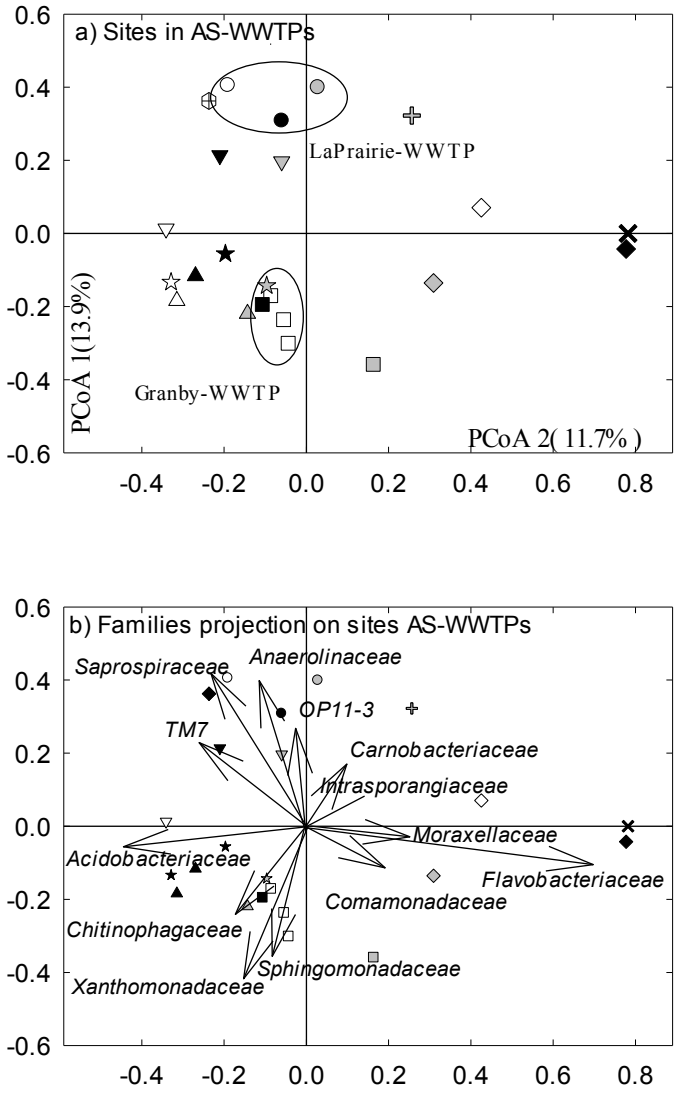

Fig 6.2. Panel a: PCoA plot representing Hellinger distances between community compositions for samples from 8 AS-WWTPs obtained in summer 2008 (open symbols), winter 2009 (black symbols), and winter 2013 (grey symbols). Each plant is indicated by a different symbol: Marieville (triangle-down), Farnham (star), LaPrairie (circle), Cowansville (triangle-up), Granby (rectangular), Pincourt (diamond), Vaudreuil (multiple), and Salaberry (plus). **Panel b:** Projection of major bacterial families which contributed to differences between the sites.

The observed community compositions at the various plants had a relatively high degree of similarities. The relative abundances of sequence reads for the main phyla were similar from

plant to plant and averaged: 36.1% for the *Proteobacteria* (with *Alpha-, Beta-, Gamma-,* and *Delta-proteobactria* classes accounting for 10.8%, 11.5%, 6.4% and 2.4% of the reads, respectively), 27.6% for *Bacteroidetes* (with *Sphingobacteria*, *Flavobacteria* and *Bacteroidia* accounting for 14.1%, 8.9%, and 1.8% of the reads, respectively) 9.0% for *Chloroflexi* (with the *Anaerolinea* class accounting for 8.4% of reads), 8.3% for *Acidobacteria*, 6.1% for *TM7*, 4.4% for *Actinobacteria*, and 3.7% for *Firmicutes*.

Observations at the family levels also revealed high similarities, but also important differences. On the one hand, a group of common families could be defined as those present in at least 50% of the samples. Some of the most abundant of these families on average were identified (Fig. 6.S3 and Table 6.S7), with the most abundant of them being: *Flavobacteriaceae* and *Saprospiraceae* from *Flavobacteriales* and *Sphingobacteriale* class, respectively (both from the phylum *Bacteroidetes*), *Rhodobacteriaceae* and *Sphingomonadaceae* belonging to the *Rhodobacteriales* and *Sphingomonadales* orders (class *Alphaproteobacteria*), respectively, and *Comamonadaceae* belonging to *Burkholderiales* order (class *Betaproteobacteria*). On the other hand, a group of rare families could also be identified by defining families with high abundance, but present in less than 50% of the samples. The main rare families observed were *Methylophilaceae* (at LaPrarie WWTP), *Flexibacteriaceae* (at Farnham WWTP), *Flavobacteriaceae* (at Salaberry, Vaudreuil and Pincourt WWTPs), *Carnobacteriaceae* (at Pincourt WWTP), and *Chitinophagaceae* (at Marieville WWTP).

Table 6.2. Sequence reads, number of OTUs (total and shared), and biodiversity numbers in 8 AS-WWTPs.

AS-WWTPs	Sequence reads and OTU richness				Simpson	Shannon diversity			
Sampling period	No. of reads	OTUs	shared OTUs	% reads for shared OTUs	diversity number	number	entropy (nat)	evenness	Abundant taxa [a]
Marieville									
2008 Summer [b]	3,591	561	140	47	36	123	4.81	0.22	*TM7-1*,
2009 Winter [c]	3,617	834			167	376	5.93	0.45	*Chloracidobacteria,*
2013 Winter [c]	4,261	718			103	243	5.49	0.34	*Chitinophagaceae,*
Farnham									
2008 Summer	3,458	549	123	50	42	137	4.92	0.25	*Rhodobacter,*
2009 Winter	3,285	788			167	345	5.84	0.44	*Saprospiraceae,*
2013 Winter	3,882	715			42	185	5.22	0.26	*Chloracidobacteria*
LaPrairie									
2008 Summer	4,190	663	105	50	36	153	5.03	0.23	*OP11,*
2009 Winter	3,400	656			39	155	5.04	0.24	*TM7* ,
2013 Winter	3,311	717			16	98	4.58	0.14	*Methylotenera,*
Cowansville									
2008 Summer	3,365	687	136	50	87	235	5.46	0.34	*Chloracidobacteria,,*
2009 Winter	1,505	429			120	225	5.41	0.52	*Acidobacteria,*
2013 Winter	4,089	665			98	215	5.37	0.32	*Caldilineaceae,*
Granby									
2008 Summer W1	3,215	704	187	47	82	238	5.47	0.34	*Caldilineaceae,*
2008 Summer W2	3,679	773			90	269	5.60	0.35	*Rhodobacteraceae,*
2008 Summer W3	3,310	727			108	281	5.64	0.39	*Rubrivivax,*[d]
2009 Winter	3,690	755			42	262	5.57	0.35	
2013 Winter	3,669	530			31	107	4.67	0.20	
Pincourt									
2008 Summer	3,699	488	80	35	15	77	4.34	0.16	*Flavobacterium,*
2009 Winter	3,564	571			42	144	4.97	0.25	*Variovorax,*
2013 Winter	4,262	568			69	158	5.07	0.28	*Trichococcus*
Vaudreuil									
2013 Winter	3,882	463			28	82	4.41	0.18	*Flavobacterium, Arcobacter, Moraxellaceae*
Salaberry									
2008 Summer	4,249	641	185	50	27	134	4.90	0.21	*TM71,TM713*, and
2013 Winter	4,075	618			69	171	5.14	0.28	*Flavobacteriaceae*

a; family level is reported unless the rank is not specified,
b; August/September,
c; February
b; class *Burkholderiales*

6.3.3 Partitioning of the beta diversity among LaPrairie samples and among the full-scale AS-WWTPs

The first step in understanding the temporal and between treatment plants variations in community compositions is to correlate the state variables describing various WWTPs with the abundance of certain populations. Such correlation would measure the explanatory power of each state variable. Initially, it may be more productive to measure the explanatory power of all available state variables. In this study, the variance in community composition was partitioned over the various explanatory variables (Table 6.3). The variance among the LaPrairie-WWTP community compositions (full-scale and both pilot-scale reactors) was partitioned over two sets of variables; one describing the environmental conditions (namely scale of the reactor, treatment conditions, and seasonal variation), and another describing the sampling year (which took into account the long term drift in species abundances and influent wastewater composition). Together, these two sets of state variables could only explain 13% of the variance in OTU community composition (Table 6.3). The same step was applied to the samples from the various full-scale WWTPs. While the influent characteristics could explain 21% of the variance in community compositions, the environmental conditions (process types and seasons) and the plants' geographic locations could only add 5% and 4%, respectively, to the explanation of the variance in community compositions (Table 6.3); thus, most of the composition variance among plants remained unexplained (74%). Finally, the composition variance partitioning exercise was performed with the Granby WWTP samples. At this plant, weekly and inter-annual variation contributed only to 3% and 21% of the observed variations, respectively. These findings indicate that the environmental factors analyzed during the current study may not be playing a major role in shaping bacterial population assemblies in AS-WWTPs.

Table 6.3. The results of beta-diversity variation partitioning.

Sampling Sites	Explanatory factors	Variance fractions	
		Explained	Unexplained
LaPrairie-WWTP			
	Environmental [a]	0.11	0.89
	Inter-annual [b]	0.07	0.93
	[a] Environmental + [b] Temporal	0.06+0.05+0.02[f]	0.87
8 AS-WWTPs			
	Influent [c]	0.21	0.79
	[a] Influent + [b] Environmental [d]	0.21+0.00+0.05	0.74
	Geographic locations[e]	0.10	0.90
	[a] Geographic locations + [b] Influent	0.04+0.21+0.00	0.75
Granby-WWTP			
	[a] Weekly + [b] Inter-annual	0.03+0.08+0.21	0.74

Details of the explanatory factors

a ; Environmental = scale (full-scale vs. pilot-scale) + treatment (fully aerobic, anoxic/aerobic, SRTs, RAS-ozonated) + season (winter vs. summer)

b ; Inter-annual (pilot-scale study Year 1, pilot-scale study Year 2, Year before pilot-scale study)

c ; Influent = Industrial fraction (%) + flow rate + COD + BOD_5 + VSS concentrations

d ; Environmental = process types (SBR vs. conventional AS vs. Oxidation ditch) and season (winter vs. summer)

e ; Geographic locations defined by PCNM eigenfunctions

Interpretation of the combined explained variance fractions

f; explained fractions are: [explained solely by a] + [shared explanation (a∩b)] + [explained solely by b]

6.4. DISCUSSION

6.4.1 Core bacterial community of conventional activated sludge systems

The OTU structures of the AS-WWTP bacterial communities determined in the current investigation were in line with previously observed studies; the OTU distributions followed a strong power law rank-abundance model in which the top 10 to 20 OTUs (grouped in 10-20 genera) accounted for 70-80% of the sequence reads, and a long tail of OTUs (~150 genera) account for the remaining 20% of the reads (Hoffmann et al. 2007, Xia et al. 2010). The identities and abundances of observed phyla were also highly similar to the previous studies (Seviour and Nielsen 2010, Zhang et al. 2012).

The striking resemblance of the community assemblies observed in this study were high over time and between WWTPs as determined at the OTU, family and phylum levels (Table 6.S3 and S4). Such similarities in bacterial community have been reported by others when comparing bacterial community assemblies at AS-WWTPs in China and in North America (Zhang et al. 2012). In the current study, some common families (Table S4) were identified and we consider these families comprise the core microbial communities of conventional AS. Given the relatively few very abundant taxa due to the power law distribution of OTUs, it appears that the first task on which environmental microbiologists should focus is to explain the mechanisms leading to the formation of this core group of families within the AS community. It is possible that the presence of such core families is the results of similar compositions of municipal wastewaters, which are relatively constant in spite of differences in human municipal sources (rural vs. urban), income levels, and food cultural habits (Tchobanoglous et al. 2003). In addition, the AS microbial communities are subjected to strong seeding by the human gut microbiome released into the sewer systems, which can also influences the community assemblies (Curtis et al. 2009). Answering these questions are at the top most agenda items for the upcoming years in wastewater microbiology.

6.4.2 Variance in community composition the case of rare families

Although the major part of the variation in community composition remained unexplained (74%) by the factors considered in this study, our study provides some evidence to support the role of environmental variables in shaping community assemblies. The noteworthy prevalence of *Methylophilaceae* (main genus: *Methylotenera*) in all the LaPrairie-WWTP samples (full and pilot-scale reactors) highlighted the importance of influent wastewater composition on shaping the bacterial community structure. Analysis of the influent wastewater from LaPrairie-WWTP

revealed a high methanol and nitrate concentrations, compounds derived from industrial sources, which in turn explains the high abundance of the *Methylotenera* genus in this AS-WWTP (Isazadeh et al. 2014b).

In addition, in the full-scale AS-WWTPs study, despite the observed similarities for the highly abundant species, changes in the numbers of OTUs between summer 2008 and winter 2009 and the presence of abundant plant-specific bacterial families like *Methylophilaceae, Flexibacteraceae, OP11,* and *Chitinophagaceae* suggest the importance of specific factors at local WWTPs selecting for specific families or genera in the mixed liquor bacterial community. Additional evidence of this, at the LaPrairie full-scale and pilot-scale reactors, are the dynamics of the *Anaerolinae* class and *Xanthomonadaceae* family populations which seemed to be related to the anoxic/oxic conditions and the reduced SRTs, respectively. Although the links between environmental factors and the higher abundances of *Flexibacteraceae* at the Farnham WWTP, *Trichococcus* at the Pincourt WWTP, and *Chitinophagaceae* at the Marieville WWTP were not investigated in detail, it seems their unusually higher abundances at these treatment plants could be correlated with specific environmental factors such as influent wastewater characteristics or operational conditions. All of these observations demand further investigations of the role of environmental variables in shaping bacterial population structures in AS systems.

6.4.3 Environmental variables in determining microbial community assembly

Even though changes in some populations were linked to variations in environmental variables, the observed variance in obtained community data with higher resolution 16S rRNA gene amplicon pyrosequencing could not be explained at more than 13% for the LaPrairie-WWTP full-scale and pilot-scale reactors. Thus, the major fraction of the community assembly variance remains unexplained, suggesting that the hypothesized variables namely *continuous chemical*

stress, reactor scale, SRT and inter-annual variation were all minor factors in explaining the community structures. This could be surprising in the case of RAS-ozonation (*continuous chemical stress*), which effectively inactivates approximately 25% of the microbial biomass every day (Isazadeh et al. 2014a). Nonetheless, the difficulty of establishing clear relationships between the community composition dynamics and variation in operational factors was also observed by other authors. For example, Saikaly et al. (2005) and Akarsubasi et al. (2009) observed a slight correlation between changes in SRT and bacterial population assemblies, but had difficulty to show statistically meaningful links between them. Consequently, both groups, who worked with earlier fingerprinting techniques, concluded that higher resolution molecular biology techniques (i.e., deeper sequencing) would reveal the link between the community composition and operational changes. The current study was performed by pyrosequencing and it reached the same results. Therefore, it did not support such speculation.

Knowing that the physical scale of treatment plants does not shape the community structure of WWTPs has two practical implications. First, it implies that pilot-scale studies can faithfully represent full-scale treatment plants. Second, it argues against the principle of having larger bioreactors (as opposed to smaller reactors) to stimulate efficient and stable microbial communities (Curtis et al. 2003, Valentín-Vargas et al. 2012). In the current study, the community compositions between the full-scale and pilot-scale reactors at LaPrairie-WWTP were highly similar for the most part, and the diversities was essentially the same at both scales (Table 1) despite a difference of 16,000× in the size of the bioreactors. Therefore, the size-diversity-stability relationship does not seem supported by the data presented herein. Consequently, it appears that the size of treatment plant infrastructures remains an economic decision, and it is not a process stability issue.

Partitioning the variance in community compositions among AS-WWTP revealed that influent compositions and geographic locations influence the most the bacterial community structures among the factors tested, although these variables did not explain more than 25% of the observed variations. It was in general difficult to differentiate these two factors due to the lack of descriptors of the influent composition, and further study will be required to properly establish the relative importance of each factors.

Geographic locations of WWTPs can affect bacterial population assemblies either by local weather effects, or by watershed effects such as soil composition, which may influence the seeding of treatment plants. However, the proximity of the AS-WWTPs in the current study (136 km between the most distant plants) does not seem to argue for local weather effects. Interestingly, the Pincourt and Vaudreuil WWTPs (appearing on the right of the PCoA plot, Fig. 6.2) are both on the north shore of the St-Laurent's River. Also, the Cowansville, Farnham and Grandby WWTPs (appearing in the bottom left quadrant of the PCoA plot, Fig. 6.2) are all located in the Yamaska River watershed (Fig 6.S1). Therefore, it is possible that watersheds influence the community structure at WWTPs.

In spite of the observed importance of influent wastewater characteristics on community composition, traditional characterization of municipal wastewater is likely insufficient to understand WWTP communities. For example, the prevalence of *Methylophilaceae* in the case of LaPrairie-WWTP was linked to the presence of methanol and nitrate in the influent (Isazadeh et al. 2014b). Consequently, wastewater treatment microbial ecologists need to go beyond the conventional influent characterization such as BOD_5, COD, total phosphorus and ortho-phosphate, total Kjeldhal nitrogen, and volatile suspended solids to describe the composition of

incoming wastewater with a high enough precision to understand the community structure and meaningfully explore the structure-functions relationships of heterotrophs.

6.4.4 Theoretical prospects of microbial community assembly in activated sludge

The variance partitioning performed in this study found that environmental variables were not the major factors shaping bacterial population assemblies in wastewater treatment systems. Yet, before concluding, environmental factors should be investigated in more depth than the traditional measures (e.g., COD, BOD_5, and VSS), and the community should be characterized with likely more relevant attributes to improve mapping of the beta diversity in community assembly of AS across any environmental variable. First, domestic wastewater contains: proteins (40-60%), carbohydrates (25-50%), fats and oils (10%), urea and a large number of organic compounds including pesticides and herbicides (Bitton 2011). Therefore, wastewater characterization should reveal the diverse organic content of wastewater. Such characterization would help linking the community assembly and wastewater composition. For example, recent studies showed that members of the *Bacteroidetes* (one of the two dominant bacterial phyla in the human adult gut) exhibit broad glycan-degrading abilities, and they are responsible for the degradation of long chain carbohydrates (Larsbrink et al. 2014).

Second, characterization of microbial community based on functional attributes instead of only 16S rRNA gene diversity could provide a better indication of the relevant diversity related to heterotrophic niches. For instance, Xiaohui et al (2014) were able to explain a total of 53% of microbial community variation based on the presence of functional genes using the GeoChip microarray. Direct sequencing of total mixed community DNA (i.e., metagenomics data) could also be a useful mean to obtain the necessary data to link ecological heterotrophic functions to each community members.

This being said, the results of community composition variance partitioning could also be related to limitations of the approach, namely that communities could be assembled by neutral mechanisms (Hubbell 2001). Curtis and Sloan (2006) used the stochastic approach based on random-assembly to describe autotrophic populations of ammonia oxidizing bacteria (AOB) in wastewater systems. Ofiţerua et al (2010) suggested that neutral community models should form the foundation of any description of open biological system. There are also room for a spectrum of theoretical mechanisms between niche-assembly and random-assembly approaches if one considers that the niche exclusion principle does not absolutely limit community diversity, and that even competition may be compatible with more neutral community assembly models. For example, competition dynamics can generate periodic or chaotic oscillations in the abundances of species that can generate niches with more species than limiting resources (Huisman and Weissing 1999). This last finding was also supported by a modeling approach based on game theory that showed that the diversity in a local niche is more dependent on the meta-community diversity for a given function than the number of limiting resources associated with the niche. These considerations suggest that much more data and theoretical development will be necessary to understand community assemblies in biological wastewater treatment systems.

6.5. CONCLUSIONS

The following conclusions can be drawn from the present study

1. There is a core bacterial community shared by all AS wastewater treatment plants and defined by a common set of families.
2. There are specific variations in the rare families that seemed to be linked to the influent characteristics, operation conditions, and geographic locations.

3. Defined environmental variables explained no more than 26% of the variations in bacterial community structures and compositions. Further studies are required to better understand understand AS microbial diversity through more in-depth characterization of influent wastewaters.
4. Continuous chemical stress, reactor scale, SRT and inter-annual variation were all minor factors and did not significantly contribute to the beta diversity of the bacterial communities.

6.6. ACKNOWLEDGMENTS

This study was funded by an NSERC Collaborative Research and Development Grant in partnership with Air Liquide Canada and Régie d'Assainissement des Eaux du Bassin LaPrairie. We are grateful to our collaborators at 8 WWTPs, who made this study possible by providing us with the wastewater samples. The staff and director of LaPrairie-WWTP are specially thanked for their support during the pilot-scale study.

6.7. REFERENCES

Akarsubasi, A.T., Ince, O., Kirdar, B., Oz, N.A., Orhon, D., Curtis, T.P., Head, I.M., Ince, B.K., 2005. Effect of wastewater composition on archaeal population diversity. Water Research 39(8), 1576-1584.

Akarsubasi, A.T., Eyice, O., Miskin, I., Head, I.M., Curtis, T.P., 2009. Effect of Sludge Age on the Bacterial Diversity of Bench Scale Sequencing Batch Reactors. Environmental Science & Technology 43(8), 2950-2956.

Bitton, G., 2011. Wastewater microbiology, Wiley-Blackwell, Hoboken, N.J.

Caporaso, J.G., Bittinger, K., Bushman, F.D., DeSantis, T.Z., Andersen, G.L., Knight, R., 2010a. PyNAST: a flexible tool for aligning sequences to a template alignment. Bioinformatics 26(2), 266-267.

Caporaso, J.G., Kuczynski, J., Stombaugh, J., Bittinger, K., Bushman, F.D., Costello, E.K., Fierer, N., Pena, A.G., Goodrich, J.K., Gordon, J.I., Huttley, G.A., Kelley, S.T., Knights, D., Koenig, J.E., Ley, R.E., Lozupone, C.A., McDonald, D., Muegge, B.D., Pirrung, M., Reeder, J., Sevinsky, J.R., Turnbaugh, P.J., Walters, W.A., Widmann, J., Yatsunenko, T., Zaneveld, J., Knight, R., 2010b. QIIME allows analysis of high-throughput community sequencing data. Nat Meth 7(5), 335-336.

Curtis, T.P., HEAD, I.M., GRAHAM, D.W., 2003. Peer reviewed: Theoretical ecology for engineering biology. Environmental Science & Technology 37(3), 64A.

Curtis, T.P., Sloan, W.T., 2006. Towards the design of diversity: stochastic models for community assembly in wastewater treatment plants. Water Science & Technology 54(1), 227-236.

Curtis, T.P., Wallbridge, N.C., Sloan, W.T., 2009. Speciation and Patterns of Diversity. Butlin, R., Bridle, J. and Schluter, D. (eds), Cambridge University Press.

DeSantis, T.Z., Hugenholtz, P., Larsen, N., Rojas, M., Brodie, E.L., Keller, K., Huber, T., Dalevi, D., Hu, P., Andersen, G.L., 2006. Greengenes, a chimera-checked 16S rRNA gene database and workbench compatible with ARB. Applied and Environmental Microbiology 72(7), 5069-5072.

Edgar, R.C., 2010. Search and clustering orders of magnitude faster than BLAST. Bioinformatics 26(19), 2460-2461.

Hoffmann, K.H., Rodriguez-Brito, B., Breitbart, M., Bangor, D., Angly, F., Felts, B., Nulton, J., Rohwer, F., Salamon, P., 2007. Power law rank–abundance models for marine phage communities. FEMS Microbiology Letters 273(2), 224-228.

Hubbell, S.P., 2001. The Unified Neutral Theory of Biodiversity and Biogeography, Princeton University Press, NJ.

Huisman, J., Weissing, F.J., 1999. Biodiversity of plankton by species oscillations and chaos. Nature 402(6760), 407-410.

Isazadeh, S., Feng, M., Urbina Rivas, L.E., Frigon, D., 2014a. New mechanistically-based model for predicting reduction of biosolids waste by ozonation of return activated sludge. Journal of Hazardous Materials 270, 160-168.

Isazadeh, S., Ozcer, P., Frigon, D., 2014b. Microbial community structure of wastewater treatment subjected to high mortality rate due to ozonation of return activated sludge. Journal of Applied Microbiology 117(2), 587-596.

Isazadeh, S., Urbana, R.L., Ozcer, P., Frigon, D., submitted. Reduction of waste biosolids by RAS ozonation: model validation and sensitivity analysis for biosolids reduction and nitrification Environmental Modelling & Software.

Larsbrink, J., Rogers, T.E., Hemsworth, G.R., McKee, L.S., Tauzin, A.S., Spadiut, O., Klinter, S., Pudlo, N.A., Urs, K., Koropatkin, N.M., Creagh, A.L., Haynes, C.A., Kelly, A.G., Cederholm, S.N., Davies, G.J., Martens, E.C., Brumer, H., 2014. A discrete genetic locus confers xyloglucan metabolism in select human gut Bacteroidetes. Nature 506(7489), 498-502.

Lee, C., Kim, J., Hwang, K., O'Flaherty, V., Hwang, S., 2009. Quantitative analysis of methanogenic community dynamics in three anaerobic batch digesters treating different wastewaters. Water Research 43(1), 157-165.

Legendre, P., Legendre, L., 2012. Numerical ecology, Science Direct.

Lozupone, C., ., Knight, R., . 2005. UniFrac: a new phylogenetic method for comparing microbial communities. Applied Environmnetal Microbiology 71(12), 8228-8235.

Maechler, M., Rousseeuw, P., Struyf, A., Hubert, M.,, Hornik, K., 2011. luster: Cluster Analysis Basics and Extensions. R package version 1.14.1.

Martins, A.M., Pagilla, K., Heijnen, J.J., van Loosdrecht, M.C., 2004. Filamentous bulking sludge--a critical review. Water Research 38(4), 793-817.

Ofiţeru, I.D., Lunn, M., Curtis, T.P., Wells, G.F., Criddle, C.S., Francis, C.A., Sloan, W.T., 2010. Combined niche and neutral effects in a microbial wastewater treatment community. Proceedings of the National Academy of Sciences 107(35), 15345-15350.

Oksanen, J., Blanchet, F.G., Kindt, R., Legendre, P., Minchin, P.R., O'Hara, R.B., Simpson, G.L., Solymos, P., Stevens, M.H.H., Wagner, H., 2011. Vegan: Community Ecology Package. R package version 2.0-2.

Pholchan, M.K., Baptista, J.d.C., Davenport, R.J., Curtis, T.P., 2010. Systematic study of the effect of operating variables on reactor performance and microbial diversity in laboratory-scale activated sludge reactors. Water Research 44(5), 1341-1352.

Pinto, A.J., Raskin, L., 2012. PCR biases distort Bacterial and Archaeal community structure in Pyrosequencing datasets. PloS One 7(8), 1-16.

Rowan, A.K., Snape, J.R., Fearnside, D., Barer, M.R., Curtis, T.P., Head, I.M., 2003. Composition and diversity of ammonia-oxidising bacterial communities in wastewater treatment reactors of different design treating identical wastewater. FEMS Microbiology Ecology 43(2), 195-206.

Saikaly, P.E., Stroot, P.G., Oerther, D.B., 2005. Use of 16S rRNA Gene Terminal Restriction Fragment Analysis To Assess the Impact of Solids Retention Time on the Bacterial Diversity of Activated Sludge. Applied and Environmental Microbiology 71(10), 5814-5822.

Seviour, R.J., Nielsen, P.H., 2010. Microbial ecology of activated sludge, IWA Publishing, London, UK.

Siripong, S., Rittmann, B.E., 2007. Diversity study of nitrifying bacteria in full-scale municipal wastewater treatment plants. Water Research 41(5), 1110-1120.

Soininen, J., 2010. Species turnover along Abiotic and Biotic gradients: patterns in space equal patterns in time? Bioscience 60(6), 433-439.

Tchobanoglous, G., Burton, F.L., Metcalf, Eddy, 2003. Wastewater Engineering : Treatment, Disposal, and Reuse, McGraw-Hill, New York.

Valentín-Vargas, A., Toro-Labrador, G., Massol-Deyá, A.A., 2012. Bacterial Community Dynamics in Full-Scale Activated Sludge Bioreactors: Operational and Ecological Factors Driving Community Assembly and Performance. PloS One 7(8), e42524.

Wang, Q., Garrity, G.M., Tiedje, J.M., Cole, J.R., 2007. Naive Bayesian classifier for rapid assignment of rRNA sequences into the new bacterial taxonomy. Applied and Environmental Microbiology 73(16), 5261-5267.

Xia, S., Duan, L., Song, Y., Li, J., Piceno, Y.M., Andersen, G.L., Alvarez-Cohen, L., Moreno-Andrade, I., Huang, C.L., Hermanowicz, S.W., 2010. Bacterial community structure in geographically distributed biological wastewater treatment reactors. Environmental Science & Technology 44(19), 7391-7396.

Xiaohui, W., Yu, X., Xianghua, W., Yunfeng, Y., Jizhong, Z., 2014. Microbial Community Functional Structures in Wastewater Treatment Plants as Characterized by GeoChip. PloS One 9(3).

Zhang, T., Shao, M.-F., Ye, L., 2012. 454 Pyrosequencing reveals bacterial diversity of activated sludge from 14 sewage treatment plants. ISME J 6(6).

6.8. SUPPLEMENTARY MATERIALS

Table 6.S1. Summary of pilot-scale reactors operation and experimental phases over 2 years.

Study Year Operation Phase	Length (days)	Operation[b]	Control Reactor Target SRT (days)	Ozone Dose (mg-O3/g-VSS.d^{-1})	Reduction in Biosolids Production (%)
Year 1: Single treatment operation and high ozone dose					
Start-up	47		6	0	NA
Phase 1	40	Aerobic	6	5.9±0.4	13±1
Phase 2	34		6	10.3±0.7	53±6
Year 2: Variable operation and a single ozone dose					
Start-up	60	A/O	12	0	NA
Phase 1	100	A/O	12	7.3±0.2	22±2
Phase 2	36	Aerobic	12	8.9±0.1	19±2
Phase 3	40	Aerobic	6	11.4±0.2	18±2 [c]

a: NA: Not applicable

b: O:Fully Aerobic and A/O: Anoxic/ aerobic

c: The recirculation pump of the RAS-ozone contactor caused a decrease in the COD solubilization efficiency between Years 1 (5.26 g-COD/g-O_3) and Year 2 (2.13 g-COD/g-O_3).

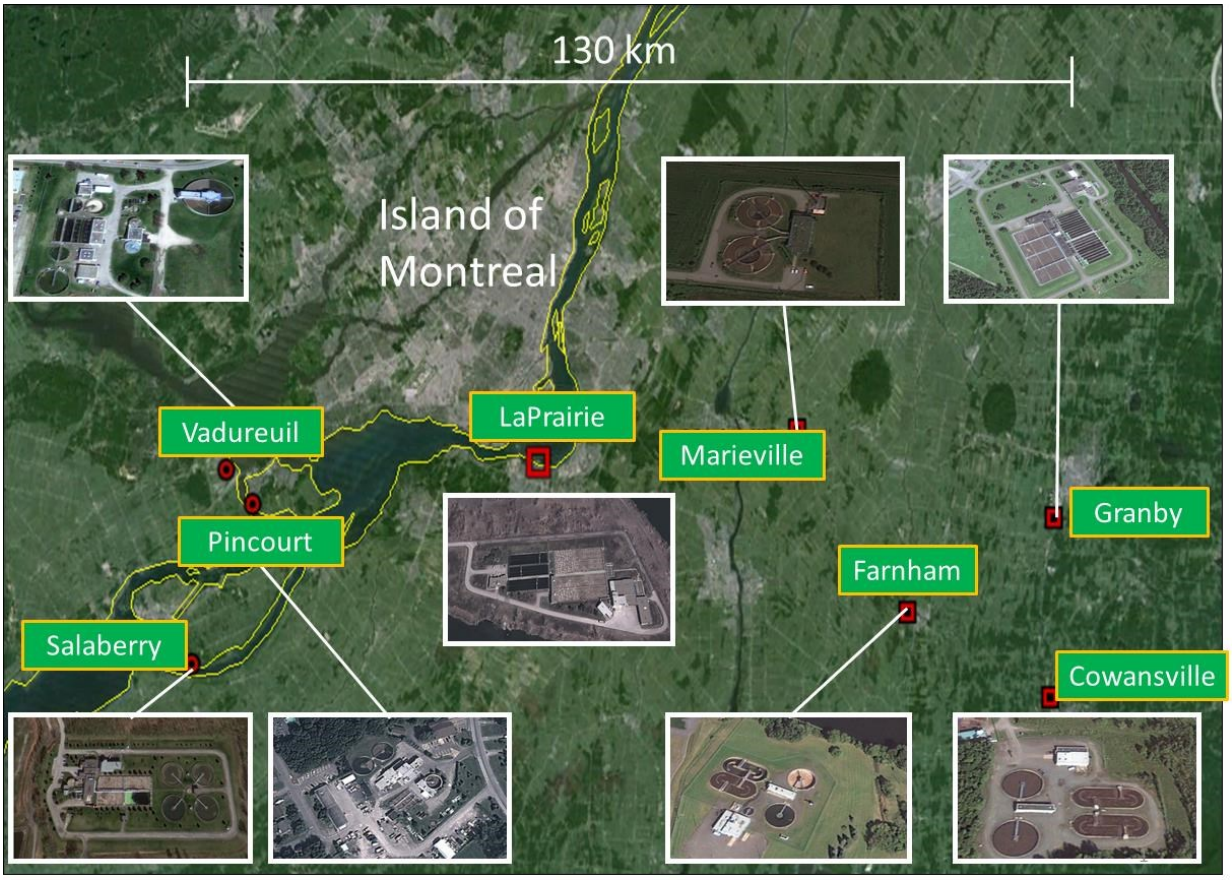

Fig 6S1. Location of 8 AS-WWTPs used in this study. South shore of Montreal island,Canada.

Table 6.S2. Characteristic of AS-WWTPs (full -scale).

AS-WWTPs	Process [a]	# of samples	Operational Parameters				Influent Characteristics			Geographic Position	
			Flow rate (m^3/day)	SRT (day)	HRT (h)	MLVSS (mg/L)	Influent Composition[b] (%)	COD (mg/L)	BOD_5 (mg/L)	Latitude N	Longitude W
Marieville	OD	3	5,000	25	12	3200	80+20	250	128.7	45°26'20.28"	73° 9'51.40"
Farnham	OD	3	6,000	80	48	6080	80+20	206	30	45°17'21.90"	72°59'35.05"
LaPrairie	CA	3	65,000	18	22	1850	45+55	333	143	45°24'16.48"	73°33'22.06"
Cowansville	OD	3	14,000	10	18	4910	90+10	233	46	45°13'16.55"	72°46'30.41"
Granby	CA	4	55,000	7	20	3116	50+50	468	231	45°22'17.45"	72°46'23.98"
Vaudreuil	SBR	1	18,000	5	3	3000	50+50	285	120	45°23'25.30"	74° 1'37.34"
Pincourt	CA	3	6,000	15	8	2121	90+10	316	102	45°23'25.30"	74° 1'37.34"
Salaberry	CA	2	57,000	25	12	2500	27+6+57	245	95	45°13'34.61"	74° 4'20.44"

a:,OD;Oxidation Ditch CA; Conventional Aeration, SBR; Sequence Bach Reactor, Carrousel is a process based on the principals of oxidation ditch

b: Influent Composition in (%) Residential + Industrial +Infiltration

Table 6.S3. Environmental explanatory matrix in for LaPrairie AS-WWTP.

LaPrairie-WWTP	Scale [a]	Treatment [b]	Seasonal [c]
Full-scale			
1 years before pilot-scale study			
December	0	1	0
September	0	1	1
Year 1			
August	0	1	1
September	0	1	1
Year 2			
May	0	1	0
September	0	1	1
Pilot-scale reactors			
Control (non ozonated)			
Year 1			
Phase I-August	1	1	1
Phase II -September	N.A	N.A	N.A
Year 2			
Start-up-May	1	1	0
Phase I-July	1	1	1
Phase II-September	1	1	1
Phase III-November	1	1	0
RAS-ozonated			
Year 1			
Phase I-August	1	0	1
Phase II -September	1	0	1
Year 2			
Start-up-May	1	0	0
Phase I-July	1	0	1
Phase II-September	1	0	1
Phase III-November	1	0	0

a: pilot-scale=0, full-scale=1
b: no ozone exposure =1, ozone exposure = 0
c: winter=0, summer=1

Table 6.S4. Environmental explanatory matrix for the in 8 AS-WWTPs.

	Process [a]	Temperature [b]	Temporal [c]
Marieville			
2008 Summer	2	1	0
2009 Winter	2	0	0
2013 Winter	2	0	1
Farnham			
2008 Summer	2	1	0
2009 Winter	2	0	0
2013 Winter	2	0	1
LaPrairie			
2008 Summer	0	1	0
2009 Winter	0	0	0
2013 Winter	0	0	1
Cowansville			
2008 Summer	2	1	0
2009 Winter	2	0	0
2013 Winter	2	0	1
Granby			
2008 Summer	0	1	0
2009 Winter	0	0	0
2013 Winter	0	0	1
Pincourt			
2008 Summer	0	1	0
2009 Winter	0	0	0
2013 Winter	0	0	1
Vaudreuil			
2013 Winter	1	1	1
Salaberry			
2008 Summer	0	1	0
2013 Winter	0	0	1

a: conventional activated sludge=0, SBR=1, Oxidation ditch=2

Table 6.S5. Environmental explanatory matrix in Granby-WWTP.

Sample	Year	Week	Season
2008 Summer W1	0	1	0
2008 Summer W2	0	1	0
2008 Summer W3	0	1	0
2009 Winter W3	0	0	1
2013 Winter	1	0	1

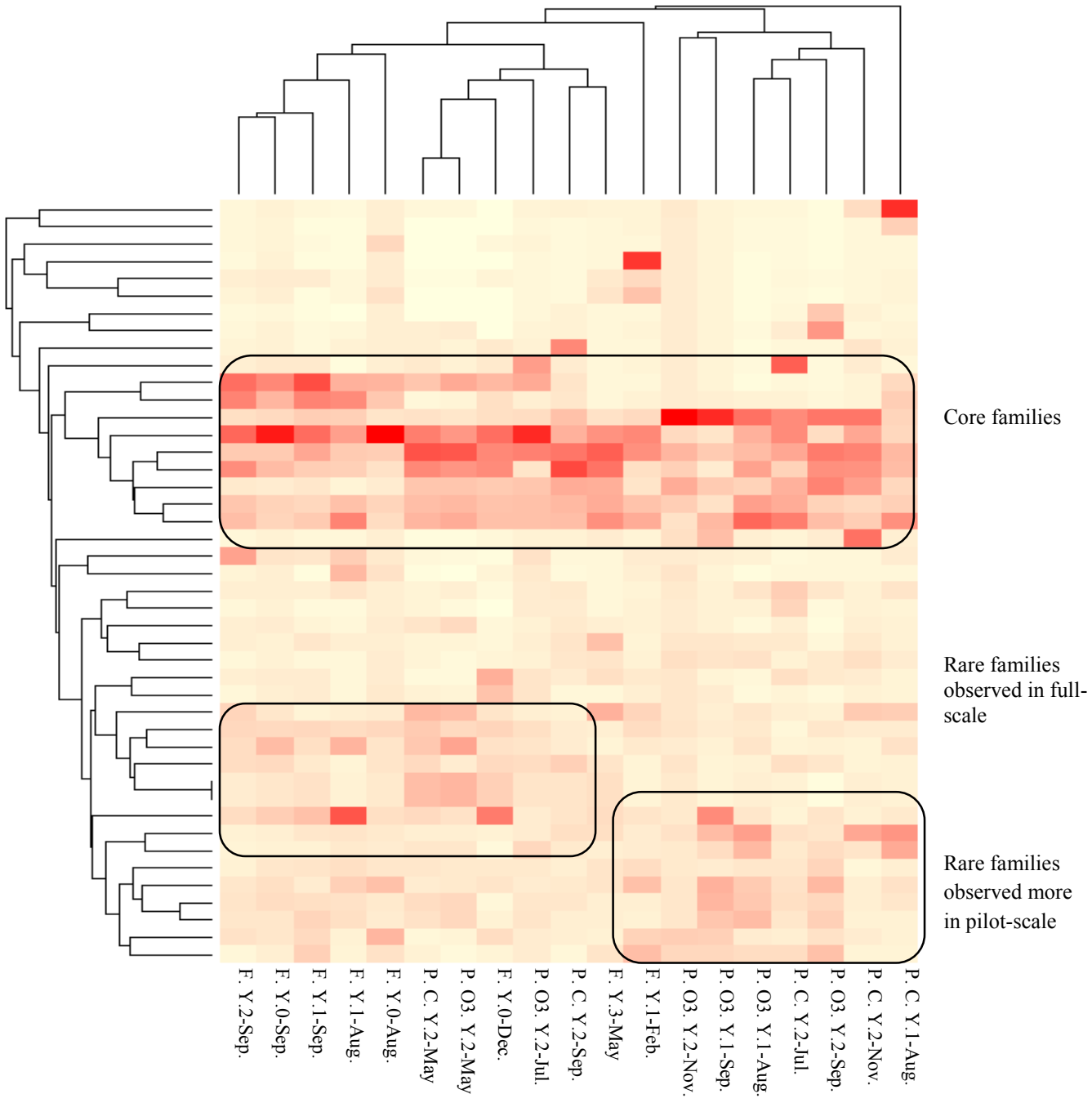

Fig. 6.S2. Heat map of sites and of top 10 highly abundant families observed in LaPrairie-WWTP reactors. For the sample name, F, O3 and C represent; Full-scale, RAS-ozonated, and control reactor, respectively, and Y.0, Y.1 and Y.2 show the sampling time a year before and the first and second year of pilot-scale study, respectively.

Table 6.S6. Observed abundant families in LaPrairie-WWTP reactors.

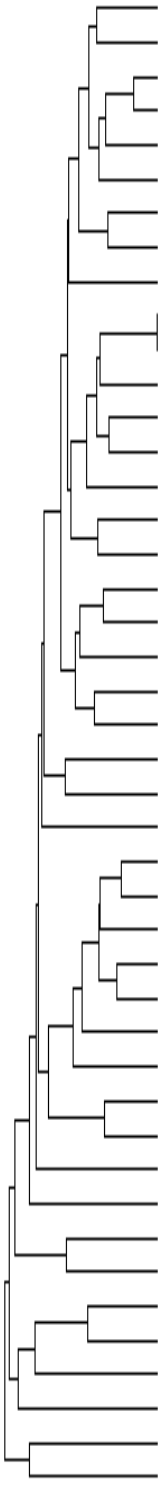

Phylum	Class	Order	Family
Proteobacteria	*Deltaproteobacteria*	*Myxococcales*	*Haliangiaceae*
Proteobacteria	*Gammaproteobacteria*	*Thiotrichales*	*Thiotrichaceae*
OP11	*WCHB1-64*	*d153*	N.A[a]
TM7	*TM7-3*	*I025*	N.A
Actinobacteria	*Actinobacteria*	*Actinomycetales*	*Intrasporangiaceae*
TM7	*TM7-3*	N.A	N.A
Proteobacteria	*Alphaproteobacteria*	*Rhodospirillales*	N.A
Verrucomicrobia	*[Pedosphaerae]*	*[Pedosphaerales]*	*auto67_4W*
Proteobacteria	*Deltaproteobacteria*	*Myxococcales*	*Polyangiaceae*
Proteobacteria	*Deltaproteobacteria*	*Myxococcales*	*Other*
Chloroflexi	*Anaerolineae*	*envOPS12*	N.A
Chloroflexi	*Anaerolineae*	*SBR1031*	*A4b*
Proteobacteria	*Gammaproteobacteria*	*Xanthomonadales*	*Xanthomonadaceae*
Bacteroidetes	*Sphingobacteriia*	*Sphingobacteriales*	*Saprospiraceae*
Proteobacteria	*Betaproteobacteria*	*Burkholderiales*	*Comamonadaceae*
Proteobacteria	*Betaproteobacteria*	*Methylophilales*	*Methylophilaceae*
Bacteroidetes	*Flavobacteriia*	*Flavobacteriales*	*Flavobacteriaceae*
Bacteroidetes	*Sphingobacteriia*	*Sphingobacteriales*	*Chitinophagaceae*
Verrucomicrobia	*Verrucomicrobiae*	*Verrucomicrobiales*	*Verrucomicrobiaceae*
Proteobacteria	*Gammaproteobacteria*	*Pseudomonadales*	*Moraxellaceae*
Acidobacteria	*Chloracidobacteria*	N.A	N.A
Bacteria	*TM7*	N.A	N.A
Acidobacteria	*Acidobacteria-6*	*iii1-15*	*mb2424*
Proteobacteria	*Alphaproteobacteria*	*Other*	*Other*
Proteobacteria	*Betaproteobacteria*	*YCC11*	N.A
Verrucomicrobia	*[Spartobacteria]*	*[Chthoniobacterales]*	*[Chthoniobacteraceae]*
Proteobacteria	*Alphaproteobacteria*	*Sphingomonadales*	*Sphingomonadaceae*
Proteobacteria	*Betaproteobacteria*	*Rhodocyclales*	*Rhodocyclaceae*
SR1	N.A	N.A	N.A
Sphingobacteriia	*Sphingobacteriales*	*Flexibacteraceae*	*Sphingobacteriia*
Other	*Other*	*Other*	*Other*
Chloroflexi	*Anaerolineae*	*Caldilineales*	*Caldilineaceae*
Proteobacteria	*Alphaproteobacteria*	*Sphingomonadales*	*Sphingomonadaceae*
Proteobacteria	*Deltaproteobacteria*	*Myxococcales*	*Haliangiaceae*
Proteobacteria	*Deltaproteobacteria*	*Myxococcales*	*Polyangiaceae*
Chloroflexi	*Anaerolineae*	*OPB11*	N.A
Proteobacteria	*Alphaproteobacteria*	*Rhodobacterales*	*Rhodobacteraceae*
Proteobacteria	*Alphaproteobacteria*	*Rhizobiales*	*Hyphomicrobiaceae*
OP8	*OP8_1*	*OPB95*	N.A
Chloroflexi	*Anaerolineae*	*Anaerolineales*	*Anaerolinaceae*
Planctomycetes	*Planctomycetia*	*Pirellulales*	*Pirellulaceae*
Planctomycetes	*Planctomycetia*	*Planctomycetales*	*Planctomycetaceae*
OP11	*OP11-3*	N.A	N.A
TM7	*TM7-1*	N.A	N.A

a: N.A not assigned

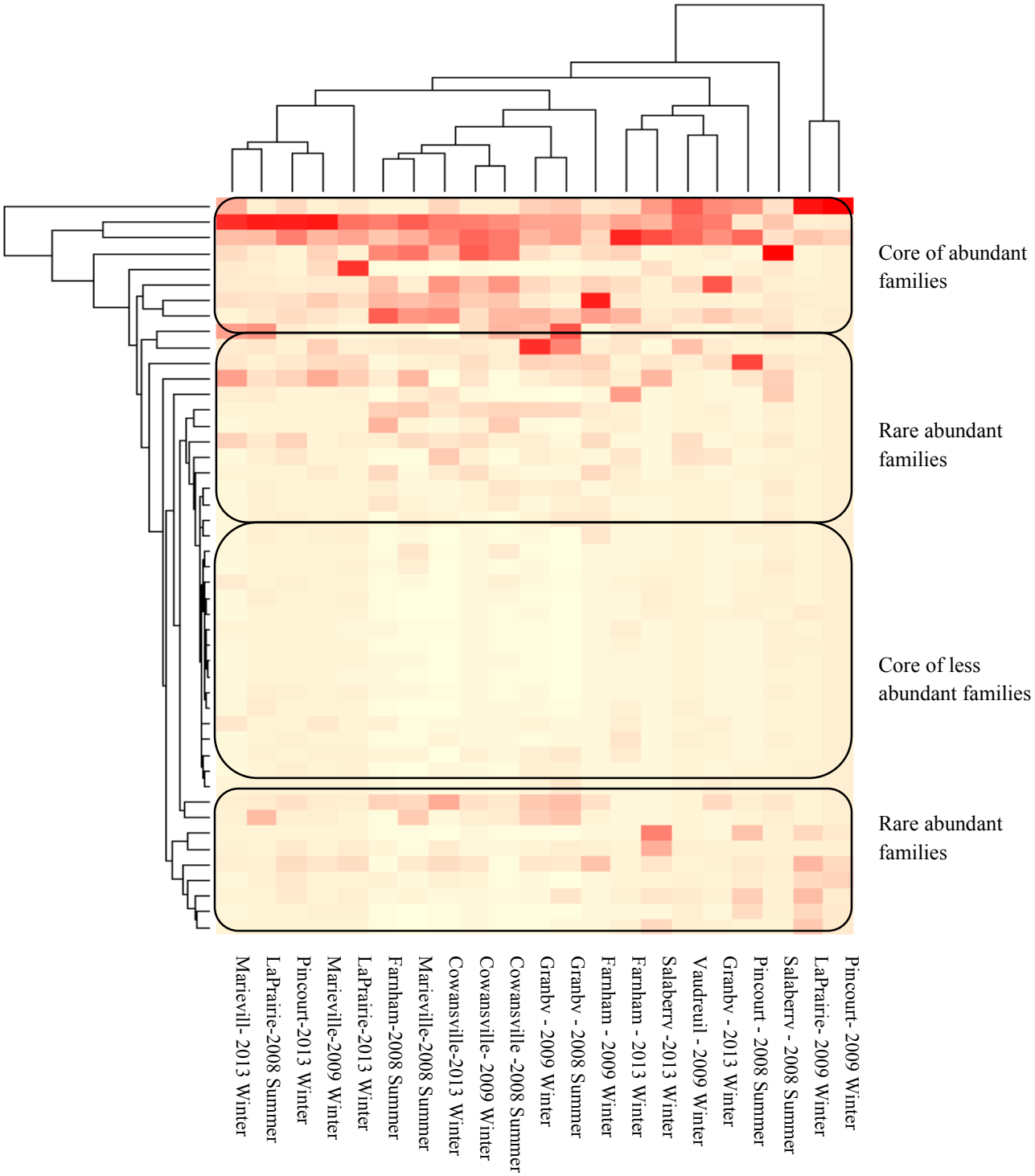

Fig 6.S3 Heat map of sites and top 10 highly abundant families observed in 8 full scale WWTPs.

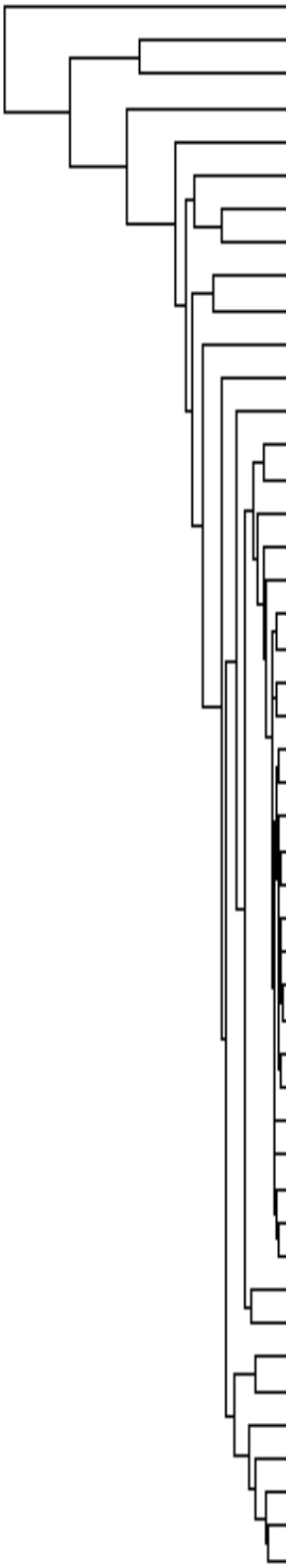

Table 6.S7. Observed top 10 highly abundant families observed in AS-WWTP reactors.

Phylum	Class	Order	Family
Bacteroidetes	*Flavobacteriia*	*Flavobacteriales*	*Flavobacteriaceae*
Bacteroidetes	*Sphingobacteriia*	*Sphingobacteriales*	*Saprospiraceae*
Proteobacteria	*Betaproteobacteria*	*Burkholderiales*	*Comamonadaceae*
Acidobacteria	*Chloracidobacteria*	N.A[a]	N.A
TM7	*TM7.3*	*I025*	N.A
Proteobacteria	*Alphaproteobacteria*	*Sphingomonadales*	*Sphingomonadaceae*
Proteobacteria	*Alphaproteobacteria*	*Rhizobiales*	*Phyllobacteriaceae*
Proteobacteria	*Alphaproteobacteria*	*Rhodobacterales*	*Rhodobacteraceae*
Chloroflexi	*Anaerolineae*	*envOPS12*	N.A
Proteobacteria	*Gammaproteobacteria*	*Xanthomonadales*	*Xanthomonadaceae*
Actinobacteria	*Actinobacteria*	*Actinomycetales*	*Intrasporangiaceae*
TM7	*TM7.1*	N.A	N.A
Chloroflexi	*Anaerolineae*	*WCHB1*	N.A
Acidobacteria	*Acidobacteria.6*	*iii1*	*mb2424*
Proteobacteria	*Alphaproteobacteria*	*Rhodospirillales*	*Rhodospirillaceae*
Verrucomicrobia	*Verrucomicrobiae*	*Verrucomicrobiales*	*Verrucomicrobiaceae*
Proteobacteria	*Betaproteobacteria*	*YCC11*	N.A
Actinobacteria	*Acidimicrobiia*	*Acidimicrobiales*	N.A
Bacteroidetes	*Flavobacteriia*	N.A	N.A
Planctomycetes	*Planctomycetia*	*Pirellulales*	
Planctomycetes	*Planctomycetia*	*Planctomycetales*	
TM7	*SC3*	N.A	N.A
Chlorobi	*SJA*	N.A	N.A
Chloroflexi	*Anaerolineae*	*Anaerolineales*	*Anaerolinaceae*
Verrucomicrobia	*Pedosphaerae*	*Pedosphaerales*	N.A
Proteobacteria	*Alphaproteobacteria*	*Caulobacterales*	
Proteobacteria	*Gammaproteobacteria*	*Aeromonadales*	
Proteobacteria	*Gammaproteobacteria*	*Alteromonadales*	
Proteobacteria	*Gammaproteobacteria*	*FCPT525*	
Actinobacteria	*Thermoleophilia*	*Solirubrobacterales*	
WPS2			
NKB19	*TSBW08*	N.A	N.A
SR1	N.A	N.A	N.A
Proteobacteria	*Betaproteobacteria*	*Ellin6067*	N.A
Proteobacteria	*Deltaproteobacteria*	*Myxococcales*	N.A
Acidobacteria	*Acidobacteria*	N.A	N.A
TM7	*TM7.3*	*Other*	N.A
Verrucomicrobia	*Opitutae*	*Opitutales*	N.A
Chloroflexi	*Anaerolineae*	*Caldilineales*	*Caldilineaceae*
Chloroflexi	*Anaerolineae*	*SBR1031*	N.A
Bacteroidetes	*Bacteroidia*	*Bacteroidales*	N.A
Proteobacteria	*Betaproteobacteria*	*Rhodocyclales*	*Rhodocyclaceae*
Firmicutes	*Bacilli*	*Lactobacillales*	*Carnobacteriaceae*
Firmicutes	*Clostridia*	*Clostridiales*	N.A
Proteobacteria	*Gammaproteobacteria*	*Pseudomonadales*	*Moraxellaceae*
Fusobacteria	*Fusobacteria*	*Fusobacteriales*	*Leptotrichiaceae*
Proteobacteria	*Epsilonproteobacteria*	*Campylobacterales*	*Campylobacteraceae*

Chapter 7:

Dynamics of nitrifying populations in activated sludge wastewater treatment systems subjected to ozonation of return activated sludge for biosolids reduction

Connecting text: In previous chapters (3 and 4), model accuracy in prediction of biosolids reductions and nitrification activities was shown. Additionally, Chapters 5 and 6 demonstrated that the RAS-ozonation process does not affect the bacterial community structures. In this chapter, model validation is further substantiated by satisfactory simulation of the results in Year 3, in which the treatment configuration and the SRT were varied. Furthermore, we used PCR amplicon pyrosequencing of *amoA* and *nxrB* functional genes to take a closer look at the effects of RAS-ozonation on the two nitrifying populations: ammonia oxidizing bacteria (AOB) and *Nitrospira*-related nitrite oxidizing bacteria (NOB). Similarly, the RAS-ozonation process does not seem to affect the structure and composition of these two populations. However, the duration of the aerated SRTs seems to impact the composition of AOBs, while a combination of treatment configuration and SRTs may influence the *Nitrospira*-related NOBs. The results of this work are prepared to be submitted to:

Isazadeh, S., Ozcer, P. and Frigon, D., Nitrification process and Nitrifiers population dynamics in ozone integrated activated sludge for biosolids reduction. *Bioresource Technology*

7.1. INTRODUCTION

Exposing the return activated sludge to ozone (RAS-ozonation) is one of the methods to minimize biosolids production in biological wastewater treatment. Ozone affects the solids chemical oxygen demand (COD) pools through the transformation of non-degradable solids COD and inactivation of biomass (Isazadeh et al. 2014, chapter 3). RAS-ozonation modifies the growth conditions of bacterial populations by increasing the mortality of ordinary heterotrophic organisms (OHO) and autotrophic nitrifying organisms (ANO) and can disrupt the existing ecological relationships between them. It is important to investigate the behavior of nitrifiers population to ascertain the ecological implication of RAS-ozonation on the community compositions and on the stability of biological processes.

Nitrification is a two-step biological oxidation process of ammonium (NH_4^+) to nitrite (NO_2^-) and nitrate (NO_3^-). It is performed in activated sludge wastewater treatment plants (AS-WWTP) by ammonia oxidizing bacteria (AOB) and nitrite oxidizing bacteria (NOB) (Rittmann and McCarty 2001). Nitrification is potentially vulnerable to RAS-ozonation because AOB and NOB have lower maximum specific growth rates than OHO (Rittmann and McCarty 2001). Furthermore, it appears that they may lack the necessary enzymes for the glutathione gated potassium efflux mechanism (GGKE) (Kelly and Love 2004), which make them less resistant to the oxidative stress caused by RAS-ozonation.

The vulnerability of nitrifiers to RAS-ozonation of activated sludge has been evaluated by two approaches: (i) in long-term monitoring of nitrification process efficiency (measured as the transformation of NH_4^+ into NO_3^- through the bioreactor), and (ii) specific nitrification activity (SNA; measured as the maximum nitrification rate per mass unit of mixed liquor volatile

suspended solids [MLVSS] in a batch test). Nitrification process efficiency showed that complete nitrification is typically not affected by RAS-ozonation (Böhler and Siegrist 2004, Deleris et al. 2002, Dytczak et al. 2007, Sakai 1997). However, these observations were made at temperatures above 15 °C, and our own modeling work suggested that the stability of nitrification may decrease with the installation of a RAS-ozonation process at temperatures below 12 °C (Isazadeh et al. submitted.,chapter 4). Furthermore, the SNA was often reduced with the reduction in biosolids production (Böhler and Siegrist 2004, Dytczak et al. 2007, Vergine et al. 2007). Our previous modelling results showed that these reductions were highly dependent on specific operational parameters such as influent total Kjeldahl nitrogen (TKN)/COD ratio, temperature, and fully aerobic vs. anoxic/aerobic reactors (Isazadeh et al. submitted.,chapter 4). Therefore, important questions remain on the changes that could be imposed by RAS-ozonation on the species composition of the ANO populations and on the nitrification process stability.

To answer these questions, the current communication reports on results from a pilot-scale activated sludge reactor study. The study was conducted over three years, and led to the development of a new mathematical model for the prediction of RAS-ozonation performances using the results from Years 1 and 2 of the study (Isazadeh et al. 2014,chapter 3 and Isazadeh et al. submitted.chapter 4). In the current report, the Year 3 results are used to evaluate three outstanding issues with respect to the nitrification process: (i) determination of the ozone inactivation rates of ANOs compared to OHOs in RAS-VSS, (ii) verification of the effects of reactor operations (various solids retention times [SRTs] and anoxic/oxic vs. fully aerobic) on SNA, and (iii) assessment of RAS-ozonation impact on the the ANO populations.

7.2. MATERIALS AND METHODS

7.2.1 Pilot-scale reactors operation

Two pilot-scale activated sludge reactors, RAS-ozonated and non-ozonated (control), were used to study the effects of biosolids minimization by RAS-ozonation over three years of experiment. Effects of ozonation on the nitrification process and on the ANO population structures were studied through the changes in ozone doses (Year 1 and 2) and treatment reactors' operational conditions (variations in SRTs and aeration regimes; Year 3). Prior to the onset of the experiments, the reactors were operated for two months to reach stable conditions, and their mixed liquor were then mixed to assure similar bacterial communities in both reactors at the start of the experiments (Kaewpipat and Grady 2002). After start-ups, these experiments lasted for 98, 120, and 200 days in Year 1, Year 2, and Year 3 of the study, respectively (Table 7.S1). Approximately 10-30% of the RAS flow was exposed to ozone, which corresponded to an exposure of 15-32% of the solids inventory. The volatile suspended solids (VSS) concentrations in both reactors were kept as similar as possible by adjusting the SRTs in the RAS-ozonated reactor. The summary of operation in Year 1 and 2 of the study are presented in Table 7.S1, and the details were discussed previously (Isazadeh et al. 2014, chapter 3 and Isazadeh et al. submitted. chapter 4).

In Year 3, the aeration regime in the two compartments of the biological treatment tank (the tank was separated by a perforated Plexiglas wall) was adjusted to make the first one anoxic and the second one aerobic (Fig. 7.1). Mechanical mixing was added to the first compartment to maintain the solids in suspension. The mixed liquor in the aerobic compartment was recirculated to the anoxic compartment ($R=Flow_{recirculation}/Flow_{influent}=3$) to support the denitrification process. Other details of the flow pattern and operation of the reactors can be seen in Fig. 7.1.

Four operational phases were covered through the study (Fig. 7.2). During the *Start-up* (Days 1 to 29), the reactors were operated in the anoxic/oxic (A/O) configuration with an SRT for the control reactor ~ 12 days (~6 days aerated SRT), and no ozonation occurred (phase description: A/O-No ozone). During *Phase I* (Days 30 to 92), the operation conditions were kept the same as during the Start-up phase, but RAS-ozonation was initiated (phase description: A/O-Long SRT). During *Phase II* (Days 92-160), the anoxic/oxic compartments were continuously aerated, which converted the reactor conditions to fully oxic reactor. The control reactor's SRT remained the same, which increased the aerated SRT to ~12 days (phase description: Oxic-Long SRT). In *Phase III* (Days 160-192), control reactor's SRT was reduced from ~12 to ~6 days (phase description: Oxic-Short SRT).

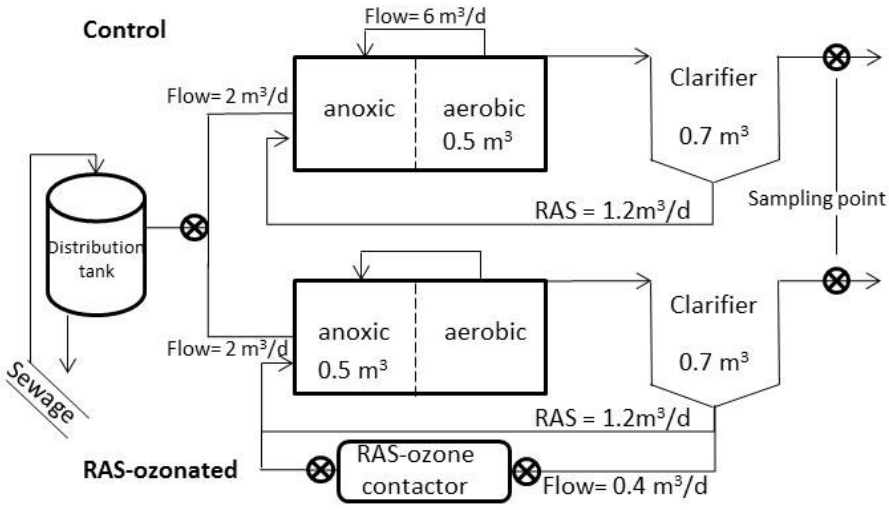

Fig 7.1. Configuration of pilot-scale reactors used in this study. Dashed lines in the aeration tanks depicts the perforated Plexiglas walls used to separate anoxic and oxic chambers.

7.2.2 Sampling and analytical methods

All analytical methods used for the analysis of reactor performance (total and soluble COD, TSS, MLVSS, TKN, NH^{+}_{4}, NO_2^{-}, and NO_3^{-})followed the Standard Methods (APHA et al. 2005) and

have been described in detail elsewhere ((Isazadeh et al. 2014), chapter 3). Total and colloidal Kjeldahl nitrogen (TKN), before and after the ozone contactor were digested in a Hach Digesdahl digestion apparatus (Hach, Loveland, USA).

In total, 12 mixed liquor suspended solids (MLSS) samples were taken from reactors to determine the composition of the ANO populations under different ozone doses and operational conditions. MLSS samples were taken during the last phase of each experiment in Year 1 (progressive increase in ozone dose) and Year 2 (high ozone dose) to compare the RAS-ozonated and control reactor (4 samples). During Year 3, MLSS samples were taken at the end of each experimental phase to compare the effects of operational changes (8 samples). In addition, to compare the ANO population structures between scales, in the middle of the Year 3 experiment two samples were collected from the influent, which fed both the full and pilot-scale reactor, and mixed liquor of the aeration basin in the full-scale reactor (LaPrairie-WWTP).

7.2.3 COD solubilisation and nitrifiers inactivation by ozone

At regular intervals during the Year 3 experiment, the performance of the ozone contactor with respect to COD solubilization, nitrogen release and biomass inactivation (both of heterotrophs and nitrifiers) was measured by 11 independent *ad hoc* experiments as was explained in Isazadeh et al. (2014),chapter 3). In this experiment the ozone doses were raised over a few hours, and RAS-ozone contactor influent and effluent sample were collected. Nitrifying biomass inactivation rate determination followed a similar procedure to the one used for OHO, and used a respirometry method to measure activities. For the respirometric assays, sufficient buffer capacity and inorganic carbon concentration (addition of 4.75 mM of $NaHCO_3$), specific nitrification activities were measured by subtracting the increase in oxygen uptake rates (OUR),

upon the sequential addition of $NaNO_2$ (0.7 mM) and NH_4Cl (1 mM) from the endogenous OUR (Isazadeh et al. submitted., Moussa et al. 2003).

7.2.4 Process simulation

The biological treatment processes were simulated with the IWA-ASM3 model which was previously extended to account for reactions of ozone with RAS solids ((Isazadeh et al. 2014), chapter 3). In this extension, the ozone effects on the solids COD pools included: (i) a transformation/mineralization process for the non-biomass (mainly undegradable) solids, and (ii) an inactivation process for the biomass. The Gujer matrix for the model extension and the calibrated model parameters were presented previously (Isazadeh et al. 2014, Isazadeh et al. (submitted.), chapters 3 and 4). In the current report, the model was used to predict the data from both reactors obtained during Year 3 by using the calibrated parameters obtained by fitting the Year 1 data.

7.2.5 DNA extraction, PCR amplification, and sequencing

DNA extraction was performed on biomass collected and stored at −80 °C, using the *MO BIO* UltraClean™ Fecal DNA Kit (Carlsbad, CA). The DNA of AOB population was analyzed by PCR amplifying a 453-bp fragment of the *amoA* genes using the specific forward (*amoA-1F*: GGGGTT TCTACTGGTGGT) and reverse (*amoA-2R*: CCCCTCTGCAAAGCCTTCTTC) primers (Purkhold et al. 2000). The following thermocycling cycle conditions were used for PCR amplification: 95 °C for 5 min, followed by 35 cycles of denaturation at 95 °C for 40 s, annealing at 56 °C for 30 s and elongation at 72 °C for 1 min, and then a final elongation step at 72 °C for 10 min. tNA from The genus *Nitrospira* one of the phylogenetic groups of NOB were analyzed by PCR amplifying a 447-bp fragment of the *nxrB* gene using the specific forward

(*nxrB-F169*: TACATGTGGTGGAACA) and reverse (*nxrB-638R*: CGGTTCTGGTCRATCA) primers (Pester et al. 2013). The following PCR conditions were used to amplify *nxrB* fragments: 95 °C for 5 min, followed by 30 cycles of denaturation at 95 °C for 40 s, annealing at 62 °C for 40 s and elongation at 72 °C for 1 min, and then a final elongation step at 72 °C for 10 min. All PCR reactions were carried out in 50 µL volumes containing 2.5 µL of forward primer, 2.5 µL of reverse primer, 10 µL of 5x buffer, 2 µL of template DNA (5-10 ng), 0.5 uL of *Taq* DNA polymerase (2.5 units), 0.5 µL of deoxynucleotide triphosphates (250 µM each), 2.75 µL of mM of $MgCl_2$ and 29.25 µl of distilled water. The dsDNA PCR products were purified using the *MOBIO* UltraClean PCR Clean-UP Kit and quantified using the Quant-iT™ PicoGreen reagent (Invitrogen, USA). The concentration of the purified amplicons was normalized to 50 ng/µl. The PCR products were pooled and the quality was checked by the Bioanalyzer 2100 (Agilent Technologies, USA) to ensure the purity of the resulting amplicons. Purified amplicons were subjected to emulsion PCR (ePCR) based on the Roche-454 Life Science protocol and sequenced by the GS FLX Titanium machine (Genome Québec, McGill University).

7.2.6 Pyrosequencing and data analysis

Sequence reads were filtered out using the Qiime pipeline (Caporaso et al. 2010) if they did not match the following criteria: perfect match to the given primer; length of sequences > 200 bp, and a minimum quality score of 25. Subsequently, filtered sequence reads were subjected to the RDP's functional gene and repository pipeline (Fish et al. 2013). This pipeline used the following steps: frameshift corrections of DNA sequences using Frame Bot by finding the most closely related protein reference sequence (Fish et al. 2013), the sequence align using HMMER3, and clustering the sequence reads by using RDP mcClust with the complete-linkage algorithm. All downstream statistical analysis including biodiversity indices, calculation of the Bary-Curtis

distances and principal coordinate analysis (PCoA) were performed using the Vegan package in the R statistical package with a 5% identity cut off. The partial *amoA* and *nxrB* sequences recovered in this study were deposited in the NCBI GeneBank Short Read Archive.

7.3. RESULTS

7.3.1 Ozone effect on COD, organic nitrogen and nitrifiers

The results of *ad hoc* RAS-ozonation experiments used to characterize the effects of RAS-ozonation on ANO activity and nitrogen species show that the exposure of the RAS to ozone caused a linear increase in soluble COD release (regression $P<0.05$; Fig. 7.2a). While the total TKN remained constant (regression $P>0.05$; Fig. 7.2 c), at the same time, the soluble/colloidal TKN increased (regression $P<0.05$; Fig. 7.2d). The increases in the soluble/colloidal TKN demonstrated the transformation of the nitrogen contained in the biosolids by ozone. It was determined that an average ~40% of the generated soluble/colloidal TKN was NH_4^+.

While COD was solubilized and nitrogen species were transformed, RAS-ozonation also inactivated ANO. Comparing the inactivation profiles of ANO and OHO revealed that the two populations followed a very similar exponential inactivation rate in response to soluble COD increase (Fig. 7.2b). This indicates ANO are equally susceptible to ozone as OHO in the pilot-scale RAS-ozone contactor. Consequently ANO are not protected from ozone by floc structure as speculated by Dytczak et al (2008).

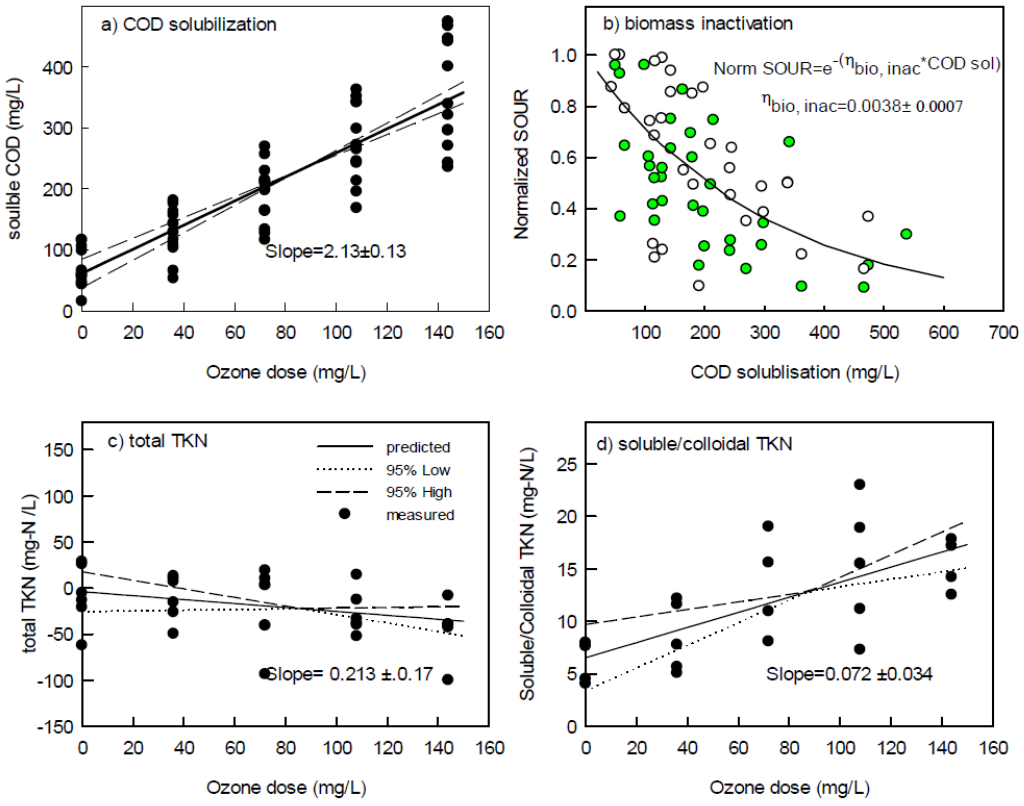

Fig.7. 2. Changes in properties of RAS mixture between the entry and the exit of the RAS-ozone contactor: a) soluble COD, b) biomass inactivation rate (OHO green and nitrifiers white circles), c) total TKN, and d) soluble/colloidal TKN. Note that data points present the different before and after ozonation

7.3.2 Pilot-scale reactor operation data and mathematical process simulation

The pilot-scale experiment in Year 3 during the three years of pilot-scale study intended to examine the RAS-ozonation impact on activated sludge reactors with variable operational conditions. Thus, the experiment was separated in 3 experimental phases after a start-up period: Phase I with anoxic/oxic-long SRT (~12 days) operation, Phase II with fully oxic-long SRT (~12 days) operation, and Phase III with the fully aerobic-short SRT (~6 days) operation. Throughout this experiment, the influent flow rates were kept fairly constant (~2 m^3/day), which resulted in fairly constant COD loading rates of approximately 1 kg/day (Fig. 7. 3a and Fig. 7. S1a). The water temperature varied slowly between 15 °C and 25 °C following a seasonal variation (Fig. 7.

3a). Dissolved oxygen concentration in the anoxic reactor compartment was kept at zero during the start-up and Phase I and increased to 3-4 mg/L during the fully aerobic Phases II and III. The SRT in the control reactor was kept around its target for all the experimental phases, while the SRT in RAS-ozonated reactor was always higher than the control reactor to keep the MLVSS concentrations similar in both reactors (Fig. 7. 3b). Ammonium (NH_4^+) concentration after the RAS-ozone contactor showed an increase by ~10 mg-N.L^{-1} due to ozone reactions with biosolids (Fig. 7. 3c).

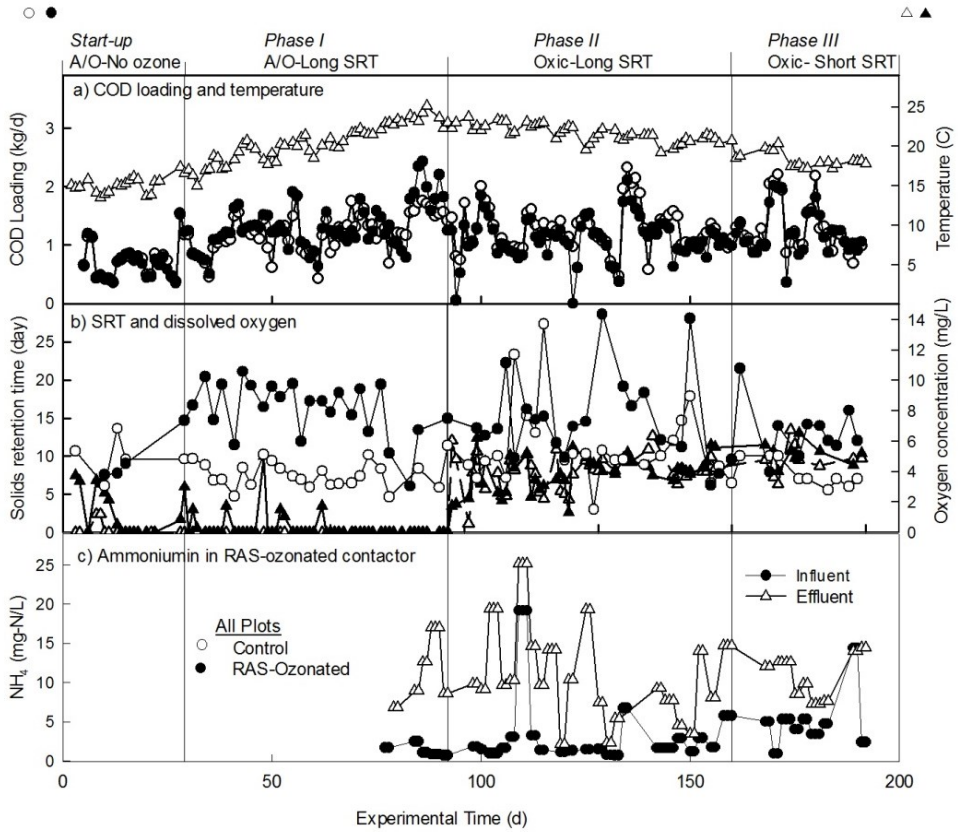

Fig. 7.3. Operation data from the pilot study in Year 3. In all plots open and solid symbols represent control and RAS-ozonated reactor data, respectively. Circles and triangles symbols should be read with left and right side axis, respectively.

With the pilot-scale experiments conducted in Years 1 and 2, a mathematical model extension of IWA-ASM3 was employed to describe the ozone reactions with the RAS solids. This model was calibrated using the Year 1 data and *ad hoc* experiments (Isazadeh et al. 2014, chapter 3), and the calibrated values were used here to predict the observed operational results in both the control and RAS-ozonated reactors. The model simulation results are reported in Fig. 7.4. Ozone-dependent process rates (biomass inactivation, COD solubilization and COD transformation rates) stayed relatively constant during the experimental Phases I and II (Fig. 7. 4a). These rates fluctuated during Phase III when the SRT was reduced due to dynamic changes in the solids inventories. The model satisfactorily simulated the total solids inventories in the control and RAS-ozonated reactor (Fig. 7. 4b) as well as effluent soluble COD concentrations (Fig. 7. 4c). These support the validity of the model and its calibration.

Beyond predicting solids inventories, the model was able to predict changes in the relative activities of heterotrophs and nitrifiers. The activities of these two groups were measured by SOUR upon the addition of acetate (OHO) or ammonium/nitrite (ANO). Differences in SOUR between the control and RAS-ozonated reactors were monitored by the ratio of SOURs from both reactors (i.e., $SOUR_{RAS\text{-}ozonated}/SOUR_{control}$). The model reasonably reproduced the SOUR dynamics observe between the two reactors (Fig. 7. 4e).

The capacity of the model at predicting biosolids inventories, effluent soluble COD concentrations and biomass activities argues for its accuracy. Thus, the model simulations can indicate the trends in the levels of nitrifying biomass within the reactors (Fig. 7. 4d). Based on the model simulations, during Phase I (Anoxic/Oxic-Long SRT), it appears that the levels of nitrifiers per MLVSS in the RAS-ozonated reactor was higher than in the control reactor despite the higher mortality in the RAS-ozonated reactor. With the change to Phase II (Fully Oxic-Long

SRT), the levels of nitrifiers decreased in the RAS-ozonated reactor and the levels of nitrifiers continued to decrease in Phase III (Fully Oxic-Short SRT). Such lower levels of nitrifiers in the RAS-ozonated reactor were also observed in Years 1 and 2 of the pilot-scale study (Isazadeh et al. submitted., chapter 4).

Along with predicted nitrifying biomass levels, the capacity of the model to accurately predict nitrification performance (nitrogen transformations) can be evaluated from the effluent nitrate (NO_3^-) concentrations. During Phase I, the effluent NO_3^- concentrations were very low because of the anoxic/oxic configuration, which supported denitrification/nitrification (Fig. 7. 4f). When the configuration was changed to fully aerobic (Phases II and III), NO_3^- concentrations in the both reactors increased. Although predicted effluent NO_3^- concentrations in the control reactor were in good agreement with the observed data, these values for the RAS-ozonated reactor's effluent were much lower than observed NO_3^- concentrations (Fig. 7. 4f). This is true despite the seemingly accurate prediction of specific nitrification activities in the RAS-ozonated reactor compared to the control reactor (Fig. 7. 4e). Similar discrepancies in effluent NO_3^- concentrations were also observed during Years 1 and 2 of the study (Fig. 7. S2 and 7. S3).

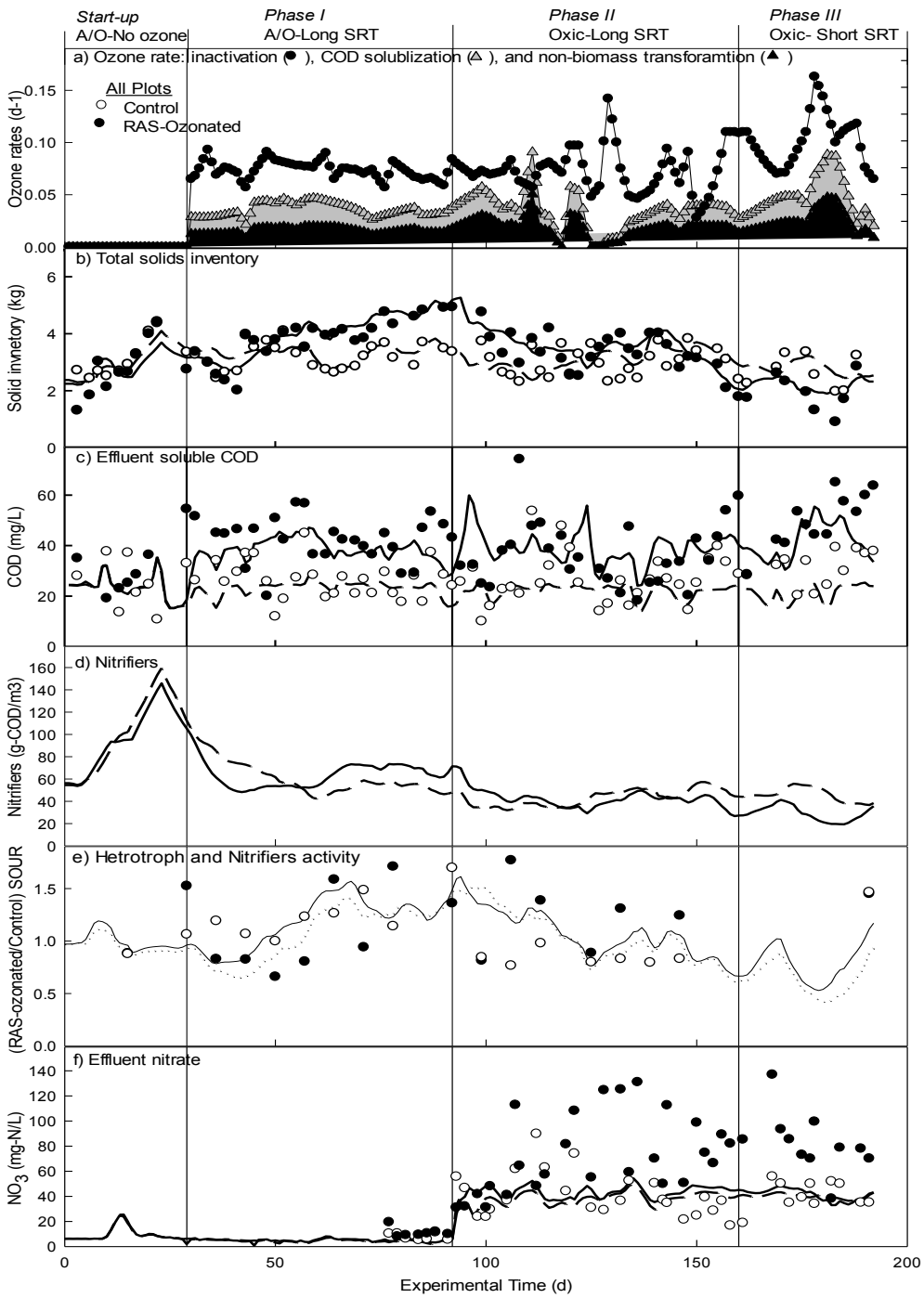

Fig. 7. 4. Operational data and simulation results for control and RAS-ozonated reactors. In all plots, symbols represent measured data and thick continuous lines show predictions (control: open symbols and dashed lines; RAS-ozonated: solid symbols and solid lines).

7.3.3 Nitrifying population structures: ammonia oxidizing and *Nitrospira*-related bacteria

A total of 14 MLVSS samples were analyzed for the study. Samples were obtained at the end of each phase during Year 3 from both pilot-scale reactors (8 samples), samples were obtained from each of the reactors during Year 1 and 2 of the study (4 samples), and an influent and MLSS samples from the full-scale reactor were obtained during Year 3 of the study (2 samples). The *amoA* and *nxrB* gene amplicon sequencing were used to characterize AOBs and *Nitrospira*-related NOBs, respectively. Preliminary semi-quantitative PCR amplification of *Nitrobacter*- and *Nitrospira*-related NOBs by *nxrB* gene showed that *Nitrospira*-related NOBs were dominant in all the samples (Fig. 7.S4). Therefore, the diversity analysis focused on *Nitrospira*-related NOBs.

The *amoA* and *nxrB* gene amplicon sequencing yielded 17,885 and 24,291 sequence reads for AOBs and *Nitrospira*-related NOBs, respectively. From these reads, 1390 AOB unique operational taxonomic units (OTUs) and 564 *Nitrospira*-related NOB OTUs were obtained by clustering sequencing with ≥95% nucleotide identities (Table 7.1). AOBs seemed to have been somewhat more diverse than *Nitrospira*-related NOBs (Table 7.1), but this could have been due to the narrower population targeted by NOB primers for *nxrB* than the AOB primers for *amoA*. Finally, the two populations showed very high dominance of a few OTUs as can be seen from the low evenness numbers and the low Shannon and Simpson diversity numbers compared to the observed numbers of OTUs (Table 7.1). In fact, one of the AOB OTUs accounted for 26% of the *amoA* reads and one of the *Nitrospira*–related NOB OTUs accounted for 67% of the *nxrB* reads.

In Year 3, among AOB species reported in the literature*, Nitrosomonas europaea ATCC 19718*, *Nitrosomonas sp.AL212, Nitrosospira sp.Nsp5* where observed only in the RAS-ozonated reactor while *Nitrosomonas sp.Is79A3* and *Nitrosospira briensis,* were observed only in the control reactor. *Nitrosospira sp.1117* was observed in both reactors. Comparing the number of

OTUs and the diversity indices did not show a substantial difference between the RAS-ozonated and control reactors. This indicates that ozone application does not significantly change the alpha diversity in RAS-ozonated reactors

Table 7.1. Diversity indices for ammonia oxidizing bacteria and Nitrospira-related nitrite oxidizing in pilot and full-scale reactors

Samples	Ammonia Oxidizing Bacteria from *amoA*					*Nitrospira*-related Nitrite Oxidizing Bacteria from *nxrB*				
	Number of Reads	OTU Richness	Shannon Entropy (nat)[a]	Shannon Diversity Number	Simpson Diversity Number.	Number of Reads	OTU Richness	Shannon Entropy (nat)	Shannon Diversity Number	Simpson Diversity Number
Pilot-scales										
Year 1[b]										
Control	839	227	4.02	56	14	2,127	141	1.98	13	7
RAS-ozonated	1,143	263	4.15	64	14	1,196	110	1.97	13	7
Year 2										
Control	1,054	176	4.10	61	14	2,020	111	1.73	13	6
RAS-ozonated	1,843	318	3.78	44	14	2,161	128	1.79	13	6
Year 3										
Control										
Start-up	1,884	348	4.05	58	14	1,595	107	1.35	13	4
Phase I	1,676	325	4.20	67	14	1,522	98	1.42	13	4
Phase II	769	283	5.03	154	14	2,081	124	1.41	13	4
Phase III	1,808	322	4.13	63	14	1,035	109	2.01	13	7
RAS-ozonated										
Start-up	1,282	344	4.45	86	14	1,686	107	1.09	13	3
Phase I	1918	383	4.39	81	14	1,976	125	1.35	13	4
Phase II	963	150	3.25	26	14	2,065	120	2.13	13	8
Phase III	1,780	316	4.15	63	14	1,734	161	2.56	13	13
Full-scale										
Influent	1,493	272	3.82	46	14	1,459	84	2.33	13	10
MLSS	926	207	3.54	35	14	1,634	103	1.36	13	4

Differences in the composition of the AOB and the *Nitrospira*-related NOB populations were visualized by PCoA analysis. The most striking observation is that, except when the reactors' operation configurations were changed during Year 3, most of the samples exhibited very similar structures for both populations as most of the points appear very close on the PCoA plot (Fig. 7.5). This is even true for the sample obtained from the full-scale activated sludge reactor, while the influent samples showed some differences with the MLVSS samples (Fig. 7.5). From these observations, it does not appear that the higher mortality due to RAS-ozonation really affected the structure of the nitrifying populations.

The OTU structures of the nitrifying populations followed interesting behaviors during Year 3 of the experiment when the operations of the reactors were modified over the three experimental phases. For the AOB populations, the drifts have some similarities in both reactors (Fig. 7.5a). During Phase I, the changes in the AOB population structures were small. However, during Phase II, when the configuration was changed from anoxic/oxic to fully oxic, the population structures changed such that the samples at the end of the phase appeared to the right of the main cluster of points (direct right for control reactor and below-right for the RAS-ozonated reactor). During Phase III, the AOB population structures of the two reactors converged back to the main cluster of points (Fig. 7.5a). The main difference between Phase II and the other experimental periods is that the aerated SRTs were doubled (~12 days vs. ~6 days). Therefore, it appears that the aerated SRT influenced the composition of the AOB population at this site.

The population structures of *Nitrospira*-related NOB for the same years showed a common cluster like AOB in the Year 1 and Year 3. However, they showed different behavior in Year 3 of experiment. The AOB population in RAS-ozonated reactor diverged after moving to the Oxic-Long SRT condition, this was not the case with *Nitrospira.* Furthermore, *Nitrospira*-related NOB

population did not converge to the same location when a similar change was made from the Oxic-Long SRT to the Oxic-Short SRT phase.

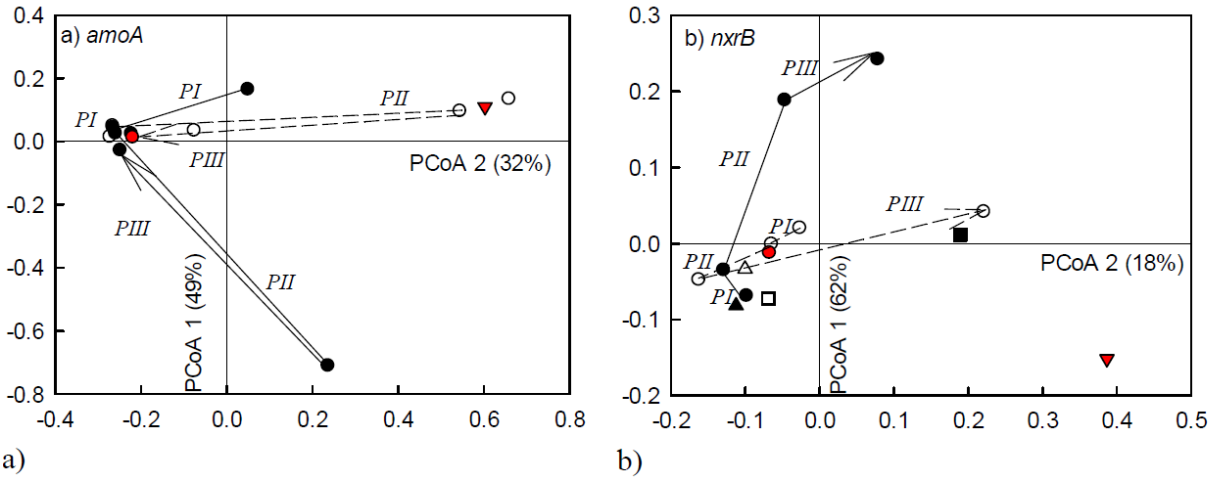

Fig. 7.5. PCoA projection obtained using a Bary-Curtis distance matrix observed over three-year pilot study: a) AOB population and (b) *Nitrospira*. In both graphs symbols with red, black and white represent the full-scale, RAS-ozonated and control reactors, respectively. In pilot-scales reactors triangle, square, and circle symbols represent the results in Year 1, Year 2, and Year 3 of the experiment, respectively. In this graph, red triangle (down) shows influent and red circle shows sample taken from the aeration basin of full-scale LaPrairie WWTP.

7.4. DISCUSSION

7.4.1 Nitrification process simulation

In different operational conditions, we showed that our proposed model is able to capture the dynamic trends in important biological factors: biosolids inventory, effluent COD, and heterotrophs concentration (Isazadeh et al. 2014), (Isazadeh et al. submitted.) chapters 3 and 4. These observations suggested that the model could be used to reliably investigate the nitrification process in detail.

The simulated nitrifier biomass and NO_3^- concentration in the effluent of two reactors were compared with measured SNA and NO_3^- concentrations. Measured SNAs showed lower activity of nitrifiers in the RAS-ozonated reactor than in the control reactor under fully oxic phases with different SRTs. Contrary to these observations the measured SNAs were higher under anoxic/oxic phase in the RAS-ozonated reactor (Fig. 7.4). Similar observations were also made by others (Dytczak et al. 2007). Furthermore, simulated nitrifying biomass in the RAS-ozonated and control reactor followed similar trends (Fig. 7.4e, Fig. 7.S1 and S2). Similar predicted OHO content in both reactors supports the model accuracy in biomass content prediction and indicates that the nitrifiers' biomass was predicted accurately and was the representative of experimental results.

Although the nitrifiers biomass content seems to be accurately modeled, effluent nitrate concentrations in the RAS-ozonated reactors showed some discrepancy. The simulated effluent NO_3^- values for both reactors are presented in the Figs. 7.4 (Year 3), S1 (Year 1), and S2 (Year 2). All these simulations agreed closely with observe NO_3^- data for the control reactor. However, the NO_3^- concentrations for the RAS-ozonated reactor showed significant discrepancies during all the three experiment years. In order to check this problem, a nitrogen mass balance was conducted for both reactors. Although the difference between the input and output nitrogen mass of N in the control reactor was negligible, in the RAS-ozonated reactor the output was higher (60 g-N.d^{-1}) (Fig. 7. S1 b). As the discrepancies are from the high concentrations of NO_3^- in the effluent, it appears that a source of NO_3^- is not accounted for in this analysis. Two possibilities have been considered as a source of NO_3^-. First, NO_3^- might be generated from the reactions of N_2 with O_3 in the ozone generator via NO_X as an intermediate. However, such a reaction would account for only an additional 0.38 g-N.d^{-1}, which is much lower than the estimated additional

60 g-N d^{-1} observed. Second , the reaction of ozone with some organic compounds carrying forms of nitrogen such as: azide, azine, azo, hydrazone, nitrate, nitrite, nitrile, nitro, nitroso, oxime, and semicarbazone that are not detected by the TKN test (method 4500-N_{org}) (APHA et al. 2005). It seems that the second possibility is the most plausible. Therefore, unpredicted NO_3^- could be driven from the non-biological source.

7.4.2 Ozone effects on population structures of ammonia oxidizing and *Nitrospira*-related bacteria

Monitoring nitrifier populations under RAS-ozonation revealed similar inactivation rates between nitrifiers and OHO (Fig. 7.2b). This indicates that nitrifiers, have no specific advantage in the presence of lethal ozone. Therefore, speculated higher nitrifiers content in the RAS-ozonated reactor by Dytczak et al. (2007) is not due to floc protection effect.

In practice, higher biosolids reduction demands more COD solubilisation and thus higher ozone mass transfer. Higher ozone mass transfer without physical perturbation of floc structure is difficult to achieve during successful implementing in full scale plants. Therefore, floc protection cannot conceivably be held responsible for nitrifiers or other OHO protection in full-scale application.

Close monitoring of AOB and *Nitrospira*-related NOB populations showed a compositional similarity in all three reactors during similar operation and influent source. A limited number of core species was observed in all AOB and *Nitrospira* samples, comprising about 80% of each community's structure. This shows that nitrifier populations in activated sludge are rather similar and not very diverse. The main divergence in the population structures happened after operational changes and was not due to ozone. Dytczak et al. (2008) showed the importance of

operational changes on the population dynamics of nitrifiers in activated sludge. Furthermore, the observed dynamics of *Nitrospira,* compared with AOB in Year 3, may indicate that the first one is less resilient to ozone or the combination of ozone and operational changes made them more susceptible for population dynamics.

7.5. CONCLUDING REMARKS

The calibrated model satisfactorily simulated the observed trends in Year 3 of the pilot-scale experiment in RAS-ozonated reactor for the biomass inventories, effluent COD concentrations, and relative heterotrophic and nitrification activities. Nitrifier inactivation was similar to that of other OHO in activated sludge. A higher nitrification efficiency observed in RAS-ozonated reactor in spite of lower nitrifier biomass content during the Oxic process connected to the chemical reaction of ozone with incoming organic nitrogen. This part could not be measured with normal TKN analysis. The population structure of AOB and *Nitrospira* were more influenced by operational changes (A/O to Oxic, and SRT) rather than by RAS-ozonation.

7.6. ACKNOWLEDGMENT

The presented study was supported by NSERC-CRD grant in collaboration with Air Liquid Canada. The authors would like to thank all the graduate and undergraduate students who helped in the operation of these pilot-scale reactors.

7.7. REFERENCES

APHA, AWWA, WEF, 2005. Standard Methods for the Examination of Water and Wastewater, American Public Health Association, Washington, DC, USA.

Böhler, M., Siegrist, H., 2004. Partial ozonation of activated sludge to reduce excess sludge, improve denitrification and control scumming and bulking. Water Science and Technology 49(10), 41-49.

Caporaso, J.G., Kuczynski, J., Stombaugh, J., Bittinger, K., Bushman, F.D., Costello, E.K., Fierer, N., Pena, A.G., Goodrich, J.K., Gordon, J.I., Huttley, G.A., Kelley, S.T., Knights, D., Koenig, J.E., Ley, R.E., Lozupone, C.A., McDonald, D., Muegge, B.D., Pirrung, M., Reeder, J., Sevinsky, J.R., Turnbaugh, P.J., Walters, W.A., Widmann, J., Yatsunenko, T., Zaneveld, J., Knight, R., 2010. QIIME allows analysis of high-throughput community sequencing data. Nat Meth 7(5), 335-336.

Deleris, S., Geauge, V., Camacho, P., Debelletontaine, H., Paul, E., 2002. Minimization of sludge production in biological processes: an alternative solution for the problem of sludge disposal. Water Science and Technology 46(10), 63-70.

Dytczak, M.A., Londry, K.L., Siegrist, H., Oleszkiewicz, J.A., 2007. Ozonation reduces sludge production and improves denitrification. Water Research 41(3), 543-550.

Dytczak, M.A., Londry, K.L., Oleszkiewicz, J.A., 2008. Activated sludge operational regime has significant impact on the type of nitrifying community and its nitrification rates. Water Research 42(8-9), 2320-2328.

Fish, J.A., Chai, B., Wang, Q., Sun, Y., Brown, C.T., Tiedje, J.M., Cole, J.R., 2013. FunGene: the Functional Gene Pipeline and Repository. Frontiers in Microbiology 4.

Isazadeh, S., Feng, M., Urbina Rivas, L.E., Frigon, D., 2014. New mechanistically-based model for predicting reduction of biosolids waste by ozonation of return activated sludge. Journal of Hazardous Materials 270, 160-168.

Isazadeh, S., Urbana, R.L., Ozcer, P., Frigon, D., submitted. Reduction of waste biosolids by RAS ozonation: model validation and sensitivity analysis for biosolids reduction and nitrification Environmental Modelling & Software.

Kaewpipat, K., Grady, C.P., 2002. Microbial population dynamics in laboratory-scale activated sludge reactors. Water Science and Technology 46(1-2), 19-27.

Kelly, R.T., Love, N.G., 2004. Investigating the role of oxidative stress mechanisms in chemically inhibited nitrifiers. Proceedings of the Water Environment Federation 2004(10), 92-112.

Moussa, M.S., Lubberding, H.J., Hooijmans, C.M., van Loosdrecht, M.C.M., Gijzen, H.J., 2003. Improved method for determination of ammonia and nitrite oxidation activities in mixed bacterial cultures. Applied Microbiology and Biotechnology 63(2), 217-221.

Pester, M., Maixner, F., Berry, D., Rattei, T., Koch, H., Lucker, S., Nowka, B., Richter, A., Spieck, E., Lebedeva, E., Loy, A., Wagner, M., Daims, H., 2013. NxrB encoding the beta subunit of nitrite oxidoreductase as functional and phylogenetic marker for nitrite-oxidizing Nitrospira. Environmental Microbiology.

Purkhold, U., Pommerening-Roser, A., Juretschko, S., Schmid, M.C., Koops, H.-P., Wagner, M., 2000. Phylogeny of All Recognized Species of Ammonia Oxidizers Based on Comparative 16S rRNA and amoA Sequence Analysis: Implications for Molecular Diversity Surveys. Applied and Environmental Microbiology 66(12), 5368-5382.

Rittmann, B., McCarty, P.L., 2001. Environmental Biotechnology : Principles and Applications, McGraw-Hill Science Engineering, New Yourk.
Sakai, Y., 1997. An activated sludge process without excess sludge production. Water Science and Technology, 163-170.
Vergine, P., Menin, G., Canziani, R., Ficara, E., Fabiyi, M., Novak, R., Sandon, A., Bianchi, A., Bergna, G., 2007. Partial ozonation of activated sludge to reduce excess sludge production: evaluation of effects on biomass activity in a full scale demonstration test, pp. 295-302, Moncton, Canada.

7.8. SUPPLEMENTARY MATERIALS

Table 7.S1. Summary of pilot-scale reactor operation and experimental phases

Study Year Operation Phase	Length (days)	Operation[b]	Control Reactor Target SRT (days)	Ozone Dose ($mg\text{-}O_3/g\text{-}VSS$)	Biosolids Reduction (%)
Year 1: Single treatment operation and variable ozone dose					
Start-up	60	O	6	0	NA[a]
Phase 1	21	O	6	0	0
Phase 2	28	O	6	2.3±0.3	19±4
Phase 3	26	O	6	3.1±0.1	37±3
Phase 4	21	O	6	6.5±0.3	46±2
Year 2: Single treatment operation and high ozone dose					
Start-up	47	O	6	0	NA
Phase 1	40	O	6	5.9±0.4	13±1
Phase 2	34	O	6	10.3±0.7	53±6
Year 3: Variable operation and a single ozone dose					
Start-up	60	A/O	12	0	NA
Phase 1	100	A/O	12	7.3±0.2	22±2[c]
Phase 2	36	O	12	8.9±0.1	19±2
Phase 3	40	O	6	11.4±0.2	18±2

a NA: Not applicable

b O:Fully Aerobic and A/O: Anoxic/Fully aerobic

c The recirculation pump of the RAS-ozone contactor caused a decrease in the COD solubilization efficiency between Years 1/2 (5.26 $g\text{-}COD/g\text{-}O_3$) and Year 3 (2.13 $g\text{-}COD/g\text{-}O_3$).

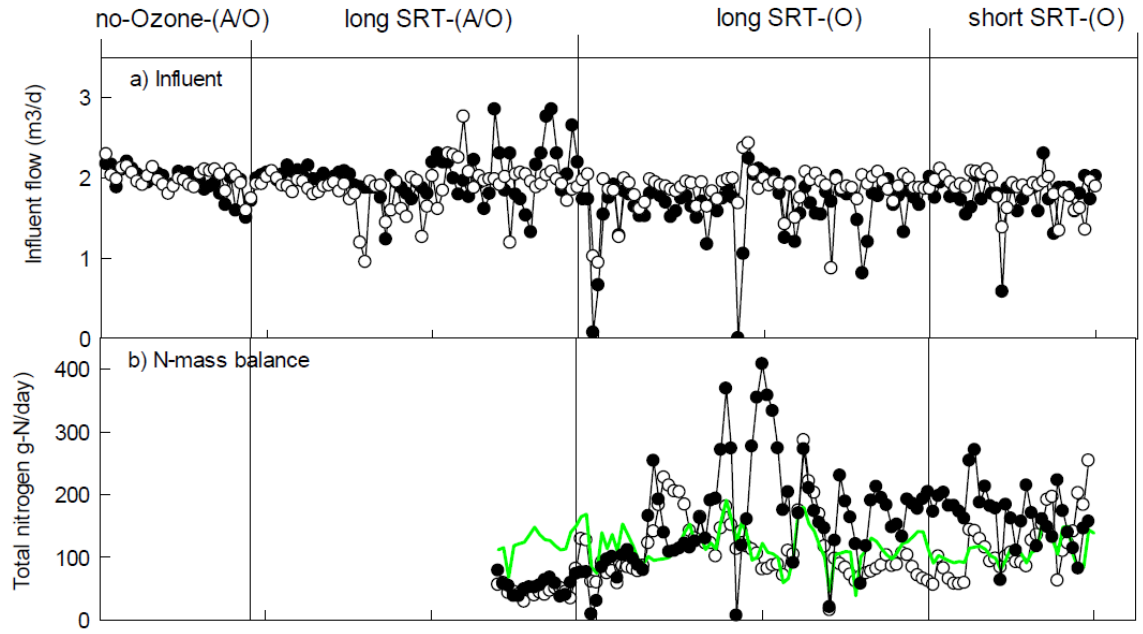

Fig. 7.S1. Influent (a) and nitrogen mas balance (b) in the control (open circles) and RAS-ozonated (black circles). In panel b the grey line represents incoming nitrogen load.

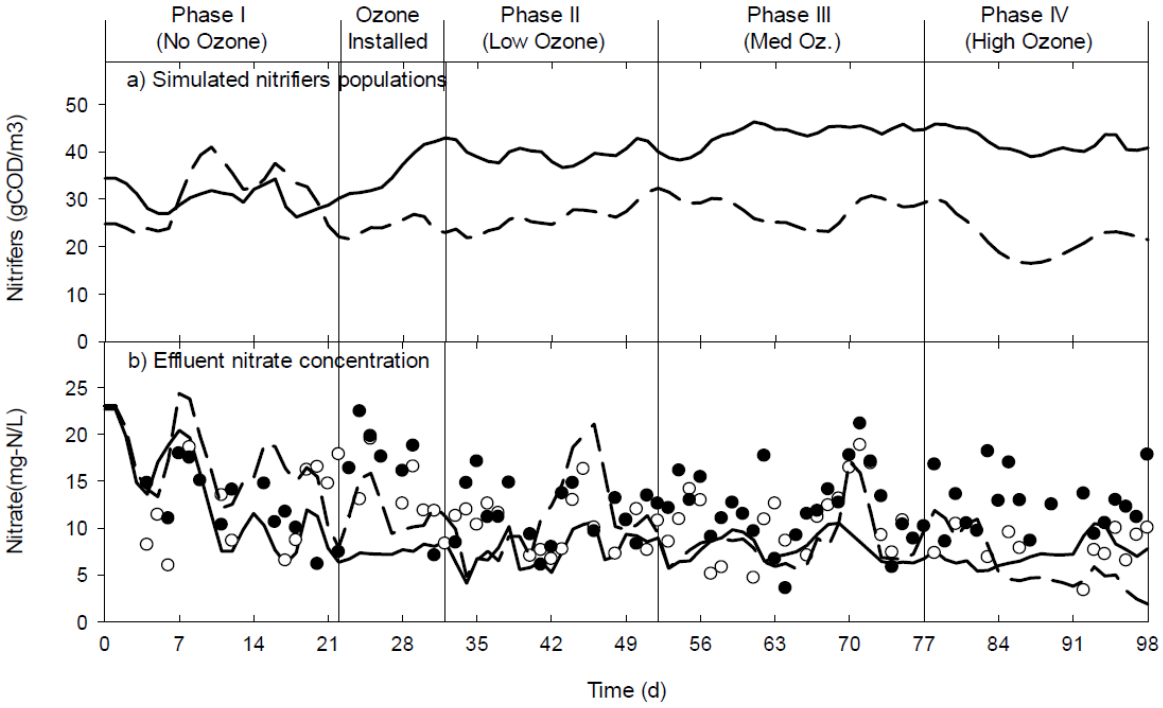

Fig. 7.S2. Simulated and measured data for nitrifier concentration and effluent nitrate concentration in the control and RAS-ozonated reactors in Year 1 of study. In this graph, lines (solid and dashed) represent simulation and symbols (white and black) represent observed data in control and RAS-ozonated reactors, respectively.

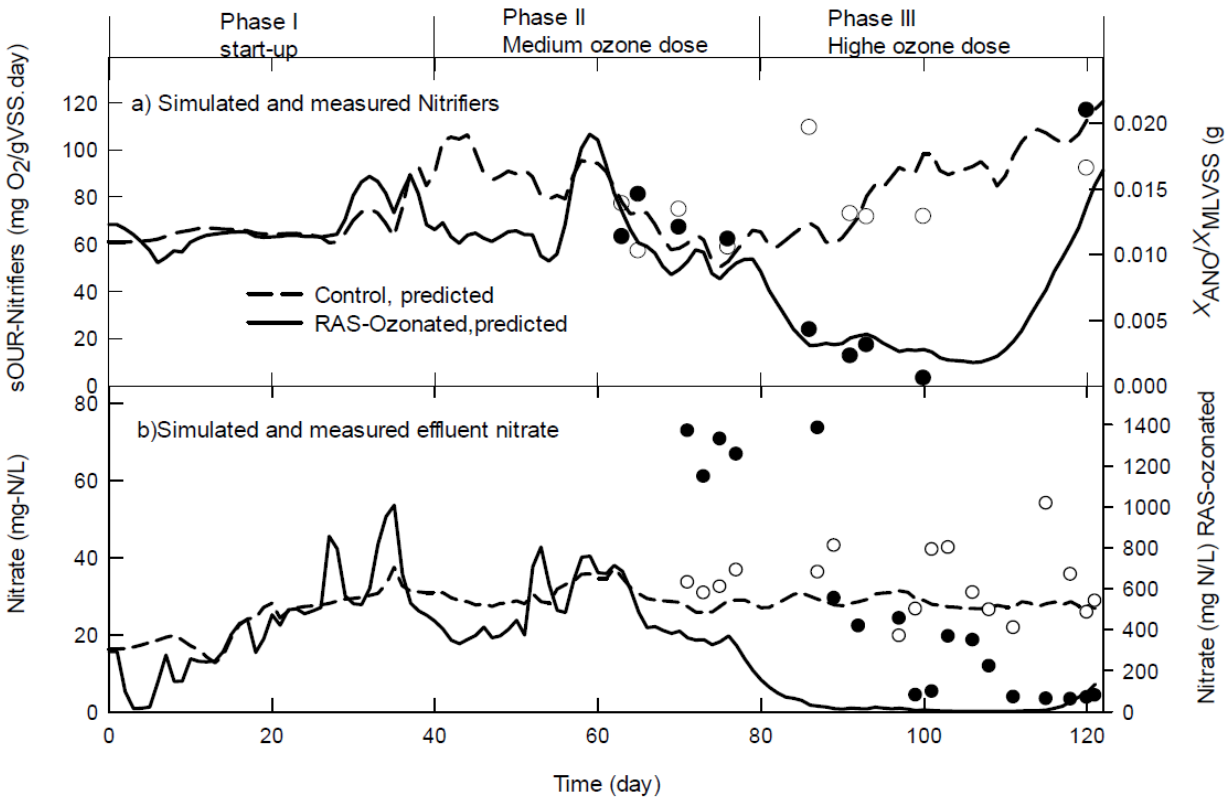

Fig. 7.S3. Simulated and measured data for nitrifier concentration and effluent nitrate concentration in the control and RAS-ozonated reactors for Year 2 of study. In this graph, lines (solid and dashed) represent simulation and symbols (white and black) represent observed data in control and RAS-ozonated reactor respectively.

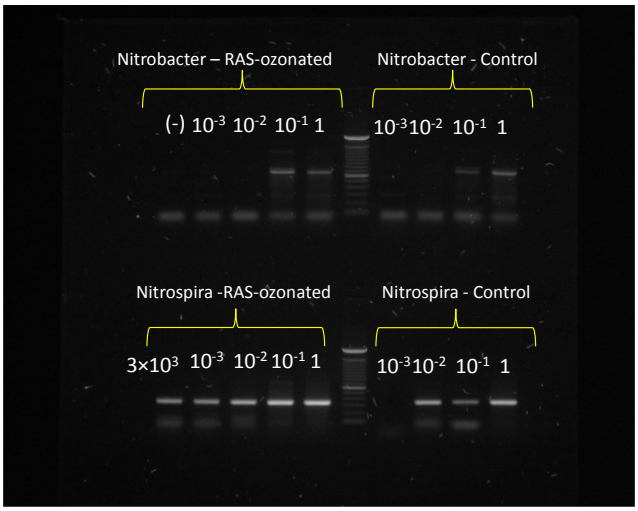

Fig. 7.S4 Semi-quantitative PCR amplification of *Nitrobacter*-related (top) - and *Nitrospira*-related (bottom) NOBs in the two pilot-scale reactors. Lane headings indicate template dilutions; for 1, 1.5 ng of DNA template was added to the PCR mix, and then dilutions of 10. (-) indicate the negative control. In this experiment EUBf (ACTCCTACGGGAGGCAGC) were used as forward primer and NIT3r- CCTGTGCTCCATGCTCCG and Ntspa685r- CGGGAATTCCGCGCTC were used as a reverse primer for *Nitrobacter* and *Nitrospira* respectively.

Chapter 8:

Summary and Conclusions

8.1. CONCLUSIONS AND FUTURE WORK SUMMARY

8.1.1 Summary

The overall goal of this thesis was to better understand and predict the effect of integrating the RAS-ozonation process with activated sludge wastewater treatment to minimize biosolids production. The first task was to develop a mathematical model based on the IWA-ASM3 model to investigate the mechanism of RAS-ozonation. To verify the model, two pilot-scale reactors fed with real municipal wastewater were operated under different conditions over a period of three years. Once the most accurate description of biomass inactivation by ozone was adopted in the model formulation, the model satisfactorily predicted the solids inventories, the reduced biosolids production, and the effluent characteristics of the pilot-scale reactors. Our findings demonstrate that the biomass inactivation rate constant ($b_{OHO,O3,inact}$ and $b_{ANO,O3,inact}$) were higher than the non-biomass (mainly non-degradable) solids COD transformation rate constants ($q_{XU\_XCB,O3,trans}$), suggesting that biomass is more sensitive to ozone than non-biomass solids even at low ozone doses. However, biomass inactivation caused little COD solubilisation, which is contrary to common descriptions in the literature. The ozone dose thresholds, reported in the literature, below which biomass inactivation in RAS does not occur, were also observed in the current study under the specific experimental conditions. However, the data presented herein showed that they were likely due to the disintegration of the floc structure at low ozone doses. Thus, they are an artefact of measuring the biomass inactivation using SOUR or other activity-based assays.

The proposed model`s capabilities at predicting biosolids reduction and specific nitrification activities were further demonstrated by satisfactorily simulating data from the Year 2 and Year 3

pilot-scale experiment using calibration values from Year 1. The model was able to reproduce changes in the specific nitrification activity due to RAS-ozonation observed in pilot-scale experiments and reported in the literature by scenario analysis. All these results clearly argue for the accuracy and the validity of proposed model in the current thesis.

A global sensitivity analysis showed the influence of operational conditions, but not of the biochemical related parameters, on waste biosolids reduction efficiency. The analysis suggested that ozonation would reduce biosolids production in WWTPs with higher non-degradable particulate COD fractions in the influent and higher process SRTs. The global sensitivity analysis also demonstrated that RAS-ozonation could either increase or decrease the specific nitrification activities depending both on the ozone transformation parameters and the influent TKN/COD ratio. Finally, the global sensitivity analysis suggested that the stability of the nitrification process is generally enhanced in the RAS-ozonated systems operated in warmer temperature; it can be unstable in colder climates (temperatures below 12 °C) and in systems with SRTs below 10 d.

Notwithstanding that the simulations of the nitrification process were reasonably predicted by the specific nitrification activities, higher nitrate concentration in the effluent of the RAS-ozonated reactor could not be predicted correctly. It was discovered that for this pilot-scale system, the nitrogen mass was not balanced, and that an additional source of nitrogen occurred in the system. Likely the municipal wastewater influent may have contained a nitrogenous organic compound that is not detected by the TKN test, but that becomes degradable after ozone treatment. Further work will be needed to substantiate this hypothesis and to identify the compound.

In the second part of this project, the effects of RAS-ozonation on the bacterial population structures of heterotrophs, ammonia oxidizing bacteria (NOB) and *Nitrospira*-related nitrite oxidizing bacteria (NOB) were evaluated. The bacterial community structures were investigated under variable ozone doses during the first year of the pilot-scale study by 16S rRNA gene amplicon pyrosequencing and fluorescence *in situ* hybridization (FISH). The structures remained highly similar throughout the experiment despite the ozone treatment. Comparative analyses between the pyrosequencing and FISH data revealed some clear discrepancies in the proportions of some populations. The results suggest that RAS-ozonation does not strongly influence the community composition. Instead, the parallel drifts and slight convergence of the community structures in both reactors indicate that other environmental factors, such as influent wastewater composition and temperature, may be more important than ozonation. Similar results were obtained for the nitrifying AOB and NOB populations studied during Year 3 of the pilot-scale study.

The significance of environmental factors on the shape of the bacterial community in activated sludge was studied by additional sampling and analysis by pyrosequencing, of eight full-scale wastewater treatment plants. The results revealed that the influent characteristics or the geographic location were the major variables explaining most of the variance in the community structures, but that the hypothesized environmental factors could not explain more than 26% of the observed variations. Additional studies will be needed to better understand the activated sludge microbial diversity. Based on the results obtained herein, it appears that an in-depth characterization of influent wastewaters would be a good starting point.

8.1.2 Future work

The results of this thesis suggest that further investigations are necessary at the laboratory-scale to understand the interaction between ozone and nitrogen species, especially organic nitrogen compounds in biosolids. Furthermore, the effects of RAS-ozonation on the production of nitrous oxide (N_2O; a potent greenhouse gas) need to be investigated. Higher doses of ozone may trigger the generation of this compound inside the ozone contactor or biological reactor. These studies will pave the way to modify the presented model to include a two-step representation of the nitrification process, with the possibility of including chemical nitrification. This will provide an opportunity to estimate the rate of chemical nitrification and also to investigate if there is any direct N_2O production. With these capabilities, the model could be used for life cycle analyses and a comparison of the carbon-footprints of a WWTP with or without RAS-ozonation.

Treatment of return activated sludge with ozone can enhance the removal of pharmaceutical compounds, emerging contaminants, and pathogenic species while minimizing biosolids production. These potentials have not been studied in this thesis and should be investigated in the future.

The nitrification process is often considered to be the Achilles heel of wastewater treatment plants. The precise monitoring of community dynamics (AOB and NOB), metabolic activities, and gene expression in these groups is only possible in controlled laboratory-scale studies fed with mineral salt media containing only ammonium as a source of energy. The study of metabolic responses to oxidative stresses such as the presence of ozone will help to discover mechanisms used by nitrifiers.

.